Durham E-Theses

The Aqueous Phosphorylation and Ligation of Nucleoside Analogues and Aqueous Azide Reduction Methodology

CONWAY, LOUIS,PATRICK

University of Durham

A Thesis Entitled

The Aqueous Phosphorylation and Ligation of Nucleoside Analogues

and

Aqueous Azide Reduction Methodology

Submitted by

Louis Conway

Department of Chemistry

A Candidate for the Degree of Doctor of Philosophy

2014

ii

Statement of Copyright

The copyright of this thesis rests with the author. No quotation from it should be published without the author's prior written consent and information derived from it should be acknowledged.

Acknowledgements

This thesis could not have been completed without the assistance of a huge number of people; I would first and foremost like to thank my supervisor, Dr David R W Hodgson for his guidance, advice and enthusiasm throughout the course of my PhD studies. I would also like to express my gratitude for the support and advice provided by the past and present members of the DRWH group.

I would also like to thank all of the departmental staff, especially Catherine Heffernan, Ian Kenwright, and Ian McKeag of the NMR service, Jackie Mosely, David Parker, and, Peter Stokes in Mass Spec., Aileen Congreve, Chris Coxon, Ellie Hurst, and Lenny Lauchlan in HPLC, and Aaron Brown and Malcolm Richardson in Glassblowing. I would especially like to thank AnnMarie O'Donoghue, particularly for her help with the kinetic aspects of my research.

Thanks to Richard Delley, Gemma Freeman, Irene Georgiou, Ricardo Girling, Casey Lam, Vicki Linthwaite, Richard Massey and Garr-Layy Zhou for friendship, support and solidarity throughout my studies.

Finally, I would like to thank my family and friends for support and patience over the course of my P.h.D.

Memorandum

Elements of this work have been presented at:

- RSC Bioorganic Chemistry Group Postgraduate Meeting, 2011, London (Poster)

- RSC Physical Organic Group Meeting, 2011, AstraZeneca Macclesfield (Poster)

- Northern Sustainable Chemistry Meeting, 2011, York (Poster)

- RSC Organic Section North East Regional Meeting, 2011, York (Poster)

- Durham University Gala PG Symposium, 2012 (Poster)

- Nucleic Acids Forum, 2012, Birmingham (Poster)

- 4th EuCheMS Congress, 2012, Prague (Poster)

- 21st IUPAC International Conference on Physical Organic Chemistry, 2012, Durham (Poster)

- Northern Sustainable Chemistry Meeting, 2012, York (Poster)

- Durham University Gala PG Symposium, 2013 (Oral Presentation)

- RSC POC Postgraduate Meeting, 2013, Syngenta, Jealotts Hill (Oral Presentation)

Abbreviations

Ac	acetate
AZT	$3'$-azido-$3'$-deoxythymidine
CMP-Neu5Ac	cytidine-$5'$-monophosphate-N-acetylneuraminic acid
DCM	dichloromethane
DEAD	diethyl azodicarboxylate
DIAD	diisopropyl azodicarboxylate
DMF	dimethylformamide
DMP	2,2-dimethoxypropane
DMSO	dimethylsulphoxide
DMT	$4,4'$-dimethoxytrityl
DNA	deoxyribonucleic acid
dsDNA	double-stranded deoxyribonucleic acid
dsRNA	double-stranded ribonucleic acid
ESR	electron spin resonance
FITC	fluorescein isothiocyanate
GABA	γ-aminobutyric acid
GMP	guanosine monophosphate
GMPS	O-linked guanosine $5'$-monothiophosphate
GNN	$5'$-deoxy-$5'$-hydrazinoguanosine
GSMP	S-linked guanosine $5'$-monothiophosphate
HPLC	high performance liquid chromatography
ICP-AES	inductively coupled plasma atomic emission spectroscopy
IS	ionic strength
MES	2-(N-morpholino)ethanesulphonic acid

MMT	4-monomethoxytrityl
mRNA	messenger ribonucleic acid
NMR	nuclear magnetic resonance
NMP	nucleoside monophosphate
ppm	parts per million
psT	S-5′-deoxy-5′-thiothymidine phosphate
RNA	ribonucleic acid
ssNMR	solid-state nuclear magnetic resonance
TBDMS	*tert*-butyldimethylsilyl ether
TEAB	triethylammonium bicarbonate
TFA	trifluoroacetic acid
TGA	thermogravimetric analysis
THF	tetrahydrofuran
Tnp	N-3′-amino-3′-deoxythymidine phosphate
Tnps	N-3′-amino-3′-deoxythymidine thiophosphate
TnpsT	3′-amino-3′-deoxythymidylyl(3′→5′)-5′-deoxy-5′-thiothymidine
TnpT	3′-amino-3′-deoxythymidylyl(3′→5′)-thymidine
TpT	thymidylyl-3′,5′-thymidine
Ts	toluenesulphonyl

Overview

The research within this thesis is primarily concerned with the synthesis of modified nucleosides, their oxyphosphorylation and thiophosphorylation to form analogues of nucleoside monophosphates and phosphodiester linkages, and the chemistry of the thiophosphoryl group. These families of compounds may have potential in the areas of antisense oligonucleotide agents or nuclease inhibition. The work described here may also provide routes to new glycosyltransferase inhibitors.

This work builds upon previous work in the Hodgson research group, principally the thiophosphorylation and subsequent alkylation of organic amine fragments as a ligation strategy, and the optimisation of the thiophosphorylation procedure as applied to 5′-amino-5′-deoxyguanosine. My role was to extend these techniques to the thiophosphorylation of other nucleoside derivatives and to use the thiophosphorylation procedure to produce potentially biologically active compounds.

This thesis is divided into a number of chapters and appendices, and commences by providing a review of the synthesis, properties, and applications of natural and unnatural phosphodiester compounds in the first chapter.

The second chapter details the work which has already been carried out within this research group on the synthesis, oxyphosphorylation, and thiophosphorylation of aminodeoxynucleosides; this forms the foundation to my own work on optimisation of the oxyphosphorylation procedure, and the application of both the oxyphosphorylation and the thiophosphorylation methodology to other aminodeoxynucleosides.

The third chapter describes the application of the thiophosphorylation procedure to the synthesis of a thiophosphoramidate mimic of a dinucleoside. The following chapter concerns the investigations into the hydrolytic stability of the thiophosphoramidate group, using the dinucleoside thiophosphoramidate analogue as a model.

The fifth chapter is on an aqueous method for the reduction of organic azides using the thiophosphate ion as the reducing agent. The reaction was tested on a number of alkyl and aryl susbstrates, and the mechanism of the reduction was investigated.

Appended to this thesis are some chapters on work related to the main project in their application of modified nucleosides and nucleotides; in the first appendix, modifications were made to the phosphate group of guanosine monophosphate to allow the role of the phosphate group in the formation of G-quadruplex structures to be studied. The second appendix concerns work done in support of a project to incorporate 5′-deoxy-5′-hydrazinoguanosine into the 5′- terminus of RNA strands, which allowed the termini to be labelled with fluorescein isothiocyanate (FITC). Using 5′-deoxy-5′-hydrazinoguanosine as a model for the modified RNA strands, it was shown that within the limits of detection, each hydrazine group reacts with only one molecule of FITC.

Contents

Chapter 1

Introduction

This chapter will provide a general overview of the roles of phosphate containing biomolecules, and the synthesis, properties, and applications of phosphate diester analogues.

1.1 Phosphates in Biological Systems

Phosphate-containing compounds are ubiquitous in living systems. They form the backbone of DNA strands, play roles in cell signalling, and are essential to many metabolic processes. The study of these compounds is therefore of great interest, and it is important to be able to produce naturally occurring phosphates and their mimics for the elucidation of structure and mechanism, as described in section 1.4.

1.1.1 Phosphates in Nucleic Acids

Phosphates play a critical role in linking together nucleosides to form nucleic acids **1** such as DNA and RNA. The phosphodiester backbone can be readily constructed by polymerase enzymes or broken down by nucleases and yet in the absence of catalysis is exceedingly stable.[1] Studies have been conducted
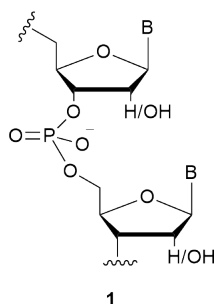
Figure 1.1: The general structure of a nucleic acid.

using model phosphodiester systems, often with difficulty and requiring harsh (relative to physiological) conditions due to the very long half-lives of these compounds. As an example, the observed rate constant for hydrolysis of the deoxyribonucleoside thymidylyl-3′,5′-thymidine (TpT) system at 80 °C in 1 M potassium hydroxide solution has been found to be $6 \times 10^{-7} s^{-1}$.[2] It has been shown that this is likely to be an overestimate of the rate constant, as thymidine itself decomposes at the same rate as TpT, under the same conditions; hydrolytic studies performed on simpler phosphodiester systems show a rate of hydrolysis approximately 10^5 times slower.[3,4] The hydrolysis of the nucleoside may therefore provide alternative routes to hydrolysis rather than the P-O cleavage of the phosphate ester.

A 'pH-rate' profile for the hydrolysis of uridylyl(3′,5′)uridine, a model for RNA, has been determined by Järvinen *et al.*[5] and illustrates the great stability of the phosphodiester linkage at physiological pH (Figure 1.2). At higher pH values the hydrolysis of the UpU system is rapid due to the presence of the 2′-hydroxyl group, which, through deprotonation by hydroxide, can intramolecularly attack the phosphodiester linkage.

1.1.2   Phosphates in Phospholipids

Phosphates are also present as structural elements in cells. Phospholipids (an example of which is shown in Figure 1.3) are not only components in the cell membrane, but play roles in cell signalling and apoptosis.[6]
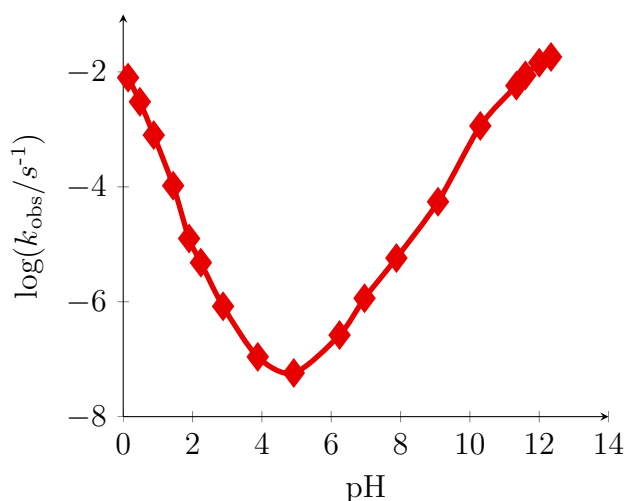
Figure 1.2: The pH-rate profile determined by Järvinen *et al.*[5] for the hydrolysis of uridylyl(3′,5′)uridine at 90 °C.

2
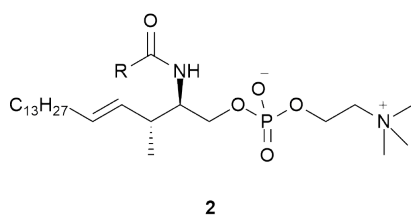
Figure 1.3: A sphingomyelin phospholipid, where R is a fatty acid chain.

1.1.3 Phosphates in Nucleoside Phosphate Sugars

The glycosyltransferases are a family of enzymes, whose role is to transfer a monosaccharide from a glycosyl donor to an acceptor molecule. The acceptor is generally a molecule possessing hydroxyl or amine functionality, such as a protein, lipid, or polysaccharide.

In many cases, glycosyl donors take the form of a monosaccharide joined to a nucleoside via a pyrophosphate or phosphate linkage (Figure 1.4). The glycosyltransferases which utilise these substrates are known as Leloir enzymes. All but one of the substrates of the Leloir enzymes found in mammals possess the pyrophosphate moiety, the exception being CMP-Neu5Ac **4**, a sialyltrasferase, as it transfers a sialic acid unit from a monophosphate donor.[7]
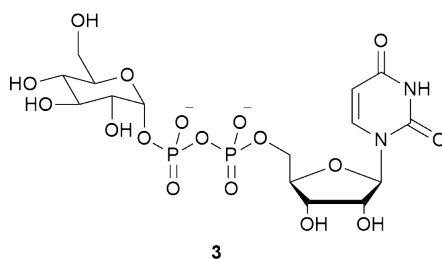
Figure 1.4: Uridine diphosphate glucose, an example of a nucleotide sugar.

The carboxylate on the sialic acid along with the monophosphate linkage play the same role as pyrophosphate in other nucleotide sugars, binding to a metal ion such as Mn^{2+} in the active site of the glycosyl transferase.[8,9]
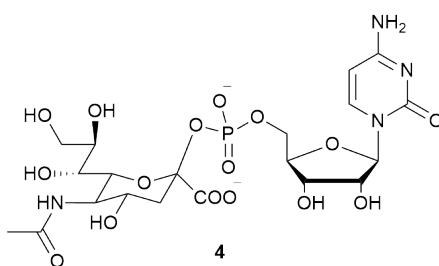
Figure 1.5: CMP-Neu5Ac – a glycosyl donor.

The sugar-nucleotide glycosyl donors, while of interest due to their role in carbohydrate biosynthesis and enzyme inhibition, are often difficult to synthesise due to their polarity, poor stability, and solubility in organic solvents.[10]

1.2 Synthesis of Phosphate-Containing Systems

Phosphorylation has also been used as a solubilisation or a masking strategy both for drug molecules and nucleoside derivatives.
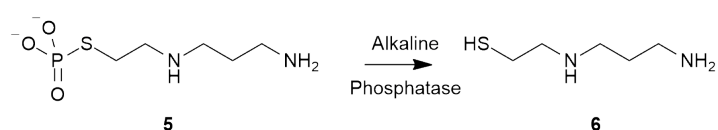
Scheme 1.1: Amifostine **5**, a thiophosphate-containing prodrug, is hydrolysed *in vivo* to liberate the active cytoprotective agent **6**.

One example is the prodrug Amifostine **5**, which possesses an *S*-linked thiophosphate moiety. The thiophosphate is hydrolysed *in vivo* by alkaline phosphatase (which is more highly expressed in healthy cells) to form the cytoprotective active compound **6**.[11]

Another example is the work by Zhang *et al.* on the synthesis of 5′-deoxy-5′-thioguanosine-5′-monophosphate **7** (GSMP) and its incorporation into RNA. Once the phosphorothioate has been incorporated, the thiol functionality can be unmasked through hydrolysis by alkaline phosphatase and ligated (Scheme 1.2).[12,13] See also David Williamson's work,[14,15] described in section 2.1.1.

Given the importance of phosphate-containing systems in nature, they are significant targets for study and so facile methods of synthesis of this class of compound are desirable.
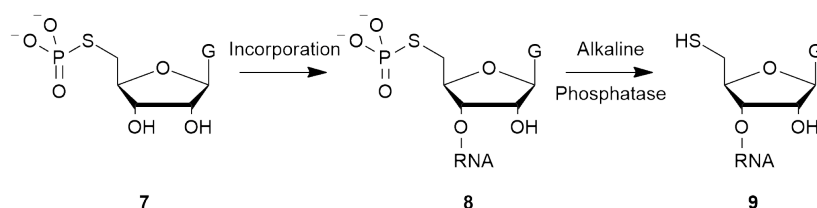
Scheme 1.2: The incorporation of GSMP into RNA and the unmasking of the thiol functionality.

1.2.1 Nucleotide Synthesis

The delocalisation of charge within simple phosphate-based ions and the formation of water clathrate structures makes phosphates poor nucleophiles in Poulter type reactions (Scheme 1.3), in which the pyrophosphate nucleophile displaces the tosylated 5′-hydroxyl group of a nucleoside derivative **10**.[16] The apparatus used must therefore be rigorously dry and even with these precautions, yields tend to be moderate. The tetralkylammonium salts which are typically used tend to be hygroscopic, compounding the problem.[17,18]
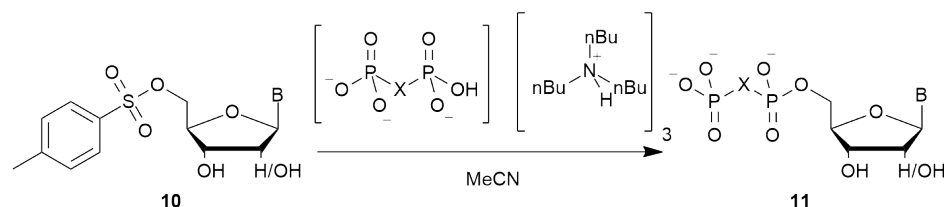
Scheme 1.3: The Poulter reaction, in which X may be O, CH_2, or CF_2[16]

Using the method developed by Yoshikawa and extended by Ludwig, phosphoryl chloride is attacked by the 5′- hydroxyl group of a nucleoside **12** to produce a dichloridate **13**, which then reacts with pyrophosphate, or can be hydrolysed to produce the monophosphate **14**.[19,20] The reaction can also be adapted to produce an α-thiophosphate, by using thiophosphoryl chloride in
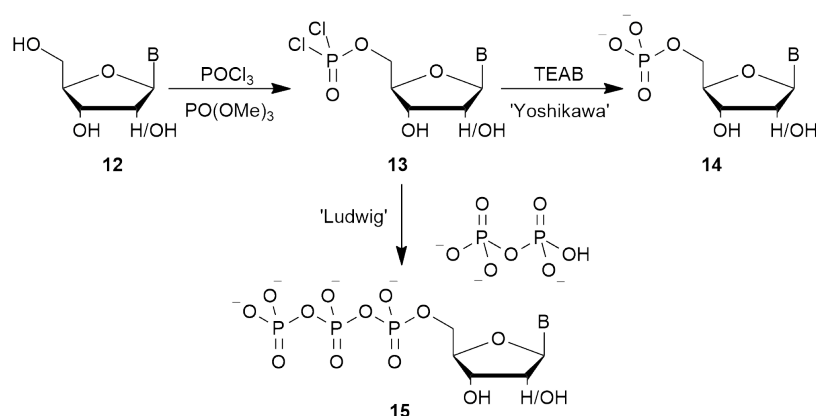
Scheme 1.4: The Yoshikawa procedure for the synthesis of nucleoside monophosphates,[19] and the Ludwig modification to produce a triphosphate.[20]

place of phosphoryl chloride.[21, 22]

There are several drawbacks to the Yoshikawa and Ludwig methods. Both hydroxyl groups and phosphates are very poor nucleophiles. As such, any highly nucleophilic functional groups on the nucleoside must be protected or protonated to ensure that they do not compete. Any water present in the reaction will also compete with the 5′-hydroxyl group, significantly lowering yields. The problems associated with water are exacerbated in the Poulter reaction and the Ludwig modification to the Yoshikawa reaction, in which the trialkylammonium pyrophosphate salts are exceedingly hygroscopic,[17, 18] and so the reagents require rigorous drying before use. In both the Poulter and Yoshikawa reactions certain nucleosides, such as guanosine and its derivatives can be very sparingly soluble. (*cf.* Burgin and Pace,[21] who thiophosphory-lated a suspension of guanosine with thiophosphoryl chloride and achieved yields of approximately 5%.) While the Yoshikawa reaction does phospho-rylate predominantly on the 5′- position, phosphorylation at the 2′- and 3′- (in the case of ribonucleosides) positions is also observed.[23] The products of this reaction typically require purification by ion exchange chromatography which can be difficult to achieve, considering the similarites in the ionisation properties of the 5′- monophosphate product and 2′- and 3′- monophosphate byproducts.

A method which could produce monophosphate or polyphosphate esters, or analogues of these compounds, while avoiding problems relating to reagent solubility or competition with water, would therefore be very synthetically useful.

Other methods, such as those using phosphorus (III) chemistry, are also available. These are based on the protocols developed for the synthesis of oligonucleotides such as the *H*-phosphonate and phosphoramidite methods, described in the next section. (section 1.2.2).

1.2.2   The Synthesis of Phosphodiesters

The synthetic methodology for the chemical synthesis of RNA and DNA strands is well developed, with the *H*-phosphonate and phosphoramidite methods both being widely adopted. Work in this direction was initiated by Todd with the development of the *H*-phosphonate method (Scheme 1.5).[24]
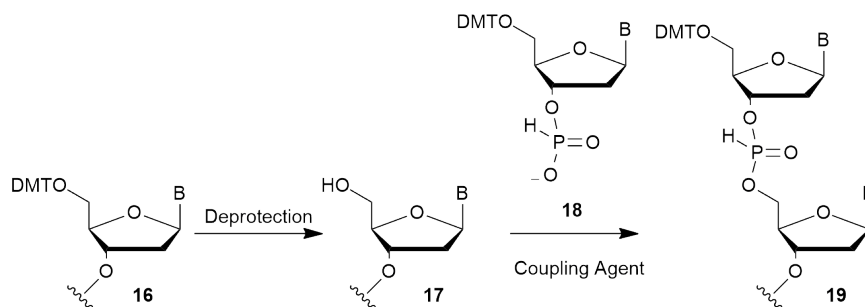
Scheme 1.5: Alexander Todd's *H*-phosphonate method for the synthesis of oligonucleotides.

The nucleotide chain is extended by reaction with a protected *H*-phosphonate nucleotide monoester **18**, using a coupling agent such as 2,4,6-triisopropyl-benzenesulphonyl chloride.
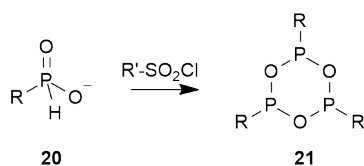
Scheme 1.6: The sulphonyl chloride activating agent reacts with the *H*-phosphonate to produce a more reactive intermediate.[25]

Strömberg *et al.* contend that the sulphonyl chloride compound dehydrates the *H*-phosphonate **20** to form a cyclic trimer of phosphite triesters **21** (Scheme 1.6).[25] The phosphite triester system then reacts with the 5′-hydroxyl group of the growing strand to form a *H*-phosphonate diester linkage **19**. The newly coupled residue is then deprotected, and the cycle is repeated.
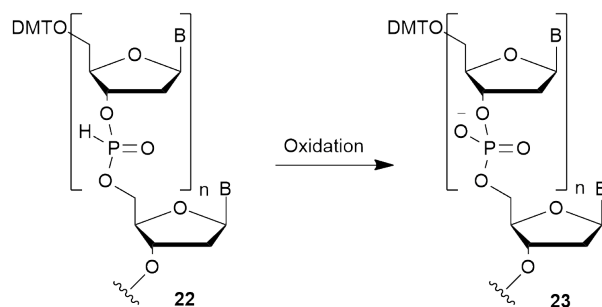
Scheme 1.7: The oxidation step to produce the oligonucleotide.

Once the full chain has been synthesised, the final step is oxidation of the *H*-phosphonate diesters **22** to phosphates **23**, typically using an aqueous iodine / pyridine solution.

Using a methodology bearing similarities to the Poulter method described earlier, Khorana used a protected nucleoside 5′- monophosphate **25** to attack a nucleoside **24** at the 3′- position,[26] using *p*-toluenesulphonyl chloride to activate the phosphate group. The protecting group can then be removed,
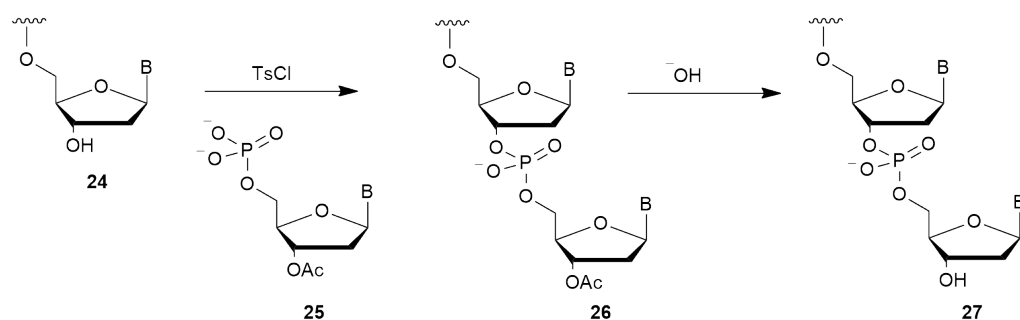
Scheme 1.8: The Khorana method for oligonucleotide synthesis.

and the cycle repeated to elongate the nucleotide chain.

The most widespread way of making oligonucleotides currently is the phosphoramidite method.[27]
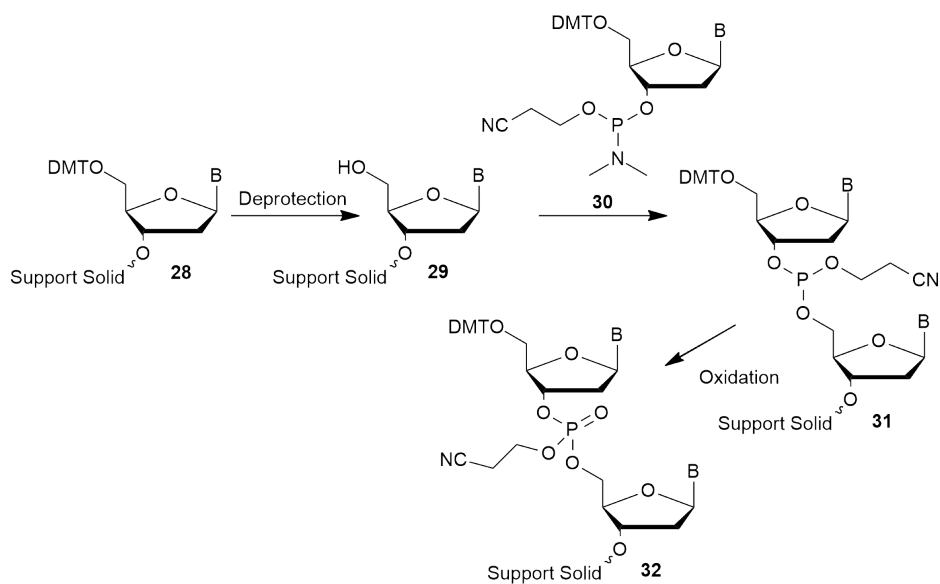
Scheme 1.9: The phosphoramidite method.

Conceptually, this is similar to the Todd's method, but instead of a *H*-phosphonate monoester, a nucleoside with a phosphoramidite on the 3′- po-

sition is used as the monomer **30**, and reacts with a the 5′- terminal hydroxyl group of the oligonucleotide to extend the oligomer. Oxidation of the phosphite **31** to a phosphate triester **32** is carried out using the mild iodine/pyridine reagents with water to effect the transformation. Deprotection of the new 5′- terminus allows the cycle to be repeated until the desired sequence has been synthesised. The oligonucleotide is then deprotected and released from the solid support with ammonia solution. This route is appealing due to its speed and selectivity and is usually automated.

1.2.3 The Synthesis of Phosphodiester Mimics

Morpholino Oligomers

One well studied modification to the phosphate-ribose backbone of a nucleic acid is to replace the ribose sugar with a morpholine, and the anionic oxygen in the linking phosphate is replaced by an amine, rendering the structure uncharged. These compounds are known as morpholino oligomers (see Figure 1.6), and were first developed by Stirchak, Summerton, and Weller.[28,29]
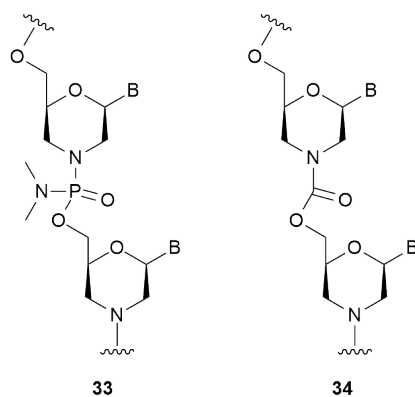
Figure 1.6: Morpholino oligomers, with phosphodiamidate (left) or carbamate (right) linkages.

Morpholino phosphordiamidate compounds **33** are water soluble where other morpholine-based molecules (*e.g.* with a carbamate linkage in place of the phosphordiamidate, **34**) are not; this is posited to be due to their ability to base-stack, reducing exposure of hydrophobic moieties to water.[30] Their unnatural structure makes them poor substrates for nucleases, and so they are much more stable *in vivo* than their natural counterparts.[31] These qualities make these oligomers useful as antisense agents, where a morpholino strand complementary to a nucleic acid sequence of interest is constructed. The morpholino strand binds to the target mRNA strand, preventing it from being translated. In this way, expression of the protein coded by the mRNA is reduced. This is useful as a research tool for eliciting the function of a particular gene, and may also have applications in pharmaceuticals in the future.

Phosphorothioate Analogues
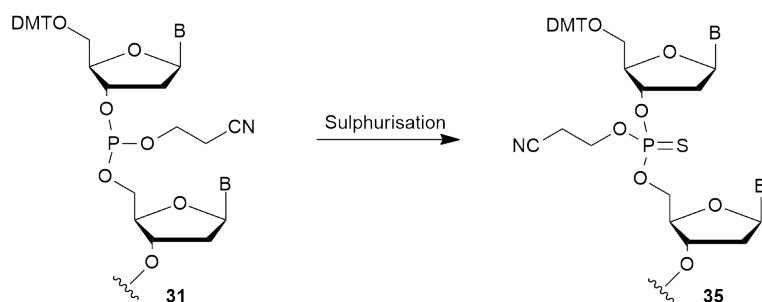
Scheme 1.10: Sulphurisation to produce a phosphorothioate. The introduction of the sulphur atom generates an additional stereogenic centre at phosphorus.

Another common phosphodiester mimic is the phosphorothioate group where one of the non bridging oxygen atoms on the phosphate is replaced by sulphur.[32, 33] The advantage of this procedure is that it can be done very readily

using the standard phosphoramidite method, the only difference being that there is a sulphurisation step in place of the oxidation step (Scheme 1.10). Like the morpholino analogues, the modification to the phosphate groups makes the resulting oligonucleotide more stable to degradation by nucleases and so extends the lifetime of the oligonucleotide analogue in living systems.

Phosphorothioated DNA may also be synthesised enzymatically; deoxynucleoside 5′-O-(1-thiotriphosphate) S_P isomers may be used as substrates by DNA polymerases in place of the natural deoxynucleoside triphosphate with negligible adverse effects.[34]

Phosphorothiolate Analogues
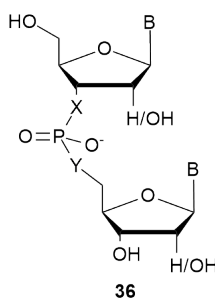
Figure 1.7: The general structure of a dinucleoside analogue in which X or Y can be nitrogen, sulphur, or oxygen. When X=S and Y=O, or *vice versa*, the compound is a phosphorothiolate. When X=N and Y=O, or *vice versa*, the compound is a phosphoramidate.

As has already been shown, phosphorothioate compounds can be synthesised just as readily as a natural oligonucleotide, the only difference is that in place of an oxidation step, there is a sulphurisation reaction. Compounds in which the sulphur is bonded to the ribose sugar (phosphorothiolates), however, present a more difficult synthetic target, as the ribose must be modified to allow the sulphur to be incorporated.
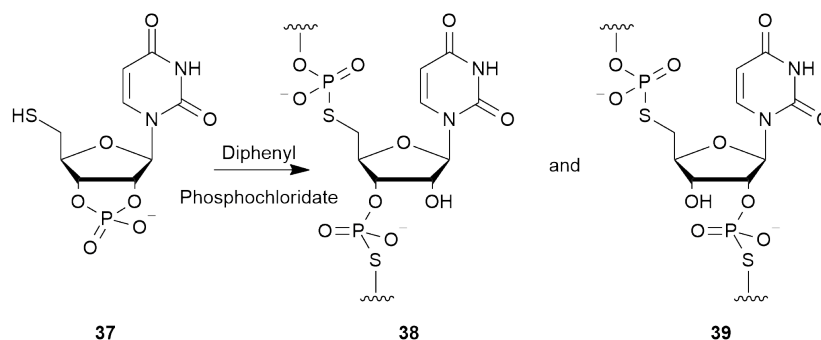
Scheme 1.11: Michelson polymerised 5′-thio-5′-deoxyuridine-2′,3′-cyclic phosphate to produce polynucleotides bearing sulphur at the 5′-position with both 3′→5′ and 2′→5′ linkages.

The first synthesis of an phosphorothiolate-containing nucleic acid was reported in 1962 by Michelson, who synthesised 5′-thio-5′-deoxyuridine-2′,3′-cyclic phosphate **37**. This polymerised with the aid of diphenyl phosphochloridate to give a mixture of 5′-*S*-bearing polynucleotides, with both 3′→5′ (**38**) and 2′→5′ (**39**) linkages.[35] Michelson also showed the phosphorothiolated polynucleotides to be vulnerable to degradation by pancreatic ribonuclease and rattlesnake venom at the 3′→5′ linkages.
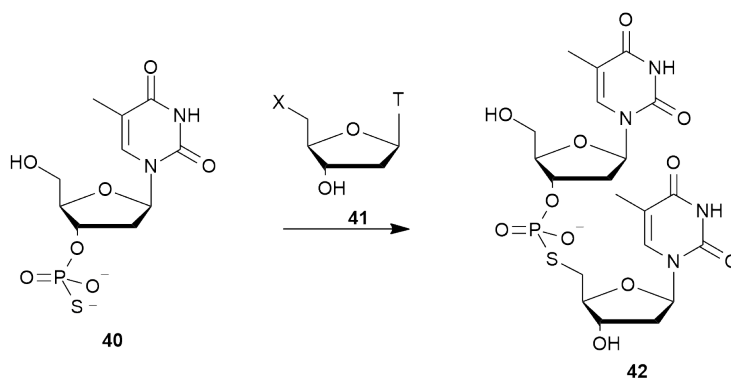
Scheme 1.12: Cook developed a method of synthesising dinucleoside phosphorthiolates through nucleophilic displacement,[36] later elaborated on by Chladek and Nagyvary.[37] X = OTs or I.

A method of synthesising phosphorothiolate dinucleosides in which the 5′-oxygen has been substituted for sulphur was developed by Cook and expanded by Chladek and Nagyvary in which thymidine was thiophosphorylated at the 3′- position, then alkylated with thymidine modified to possess a leaving group at the 5′-position (Scheme 1.12).[36,37] This approach bears similarities to our synthesis of thiophosphoramidates, described in chapter 3. An intramolecular example of this reaction was used more recently by Sintim[38] to synthesise a phosphorothiolate analogue of a cyclic guanosine monophosphate dimer (Figure 1.8).
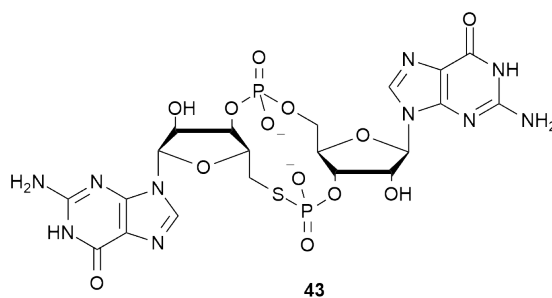
Figure 1.8: The thiophosphate-containing analogue of a cyclic guanosine synthesised by Sintim *et al.*

Cosstick and Vyle pioneered the use of 3′-S substituted phosphorothiolates through the use of phosphorus(III) reagents, as illustrated in Scheme 1.13. Firstly, they synthesised a 3′-S substituted phosphorothiolate analogue of thymidyly-thymidine **47**, reacting a 5′-protected 3′-deoxy-3′-thiothymidine **44** with (tetrazolyl)$_2$,PO(CH$_2$)$_2$CN **45** followed by 3′-acetate-protected thymidine **46**. The resulting molecule was then oxidised and deprotected to yield the 3′-S-phosphorothiolated analogue of a natural dinucleoside.[39,40]

Cosstick and Vyle then extended this methodology to the synthesis of 3′-thiolated nucleoside phosphoramidites required for the thiolates to be incorporated into the standard phosphoramidite synthesis of oligonucleotides
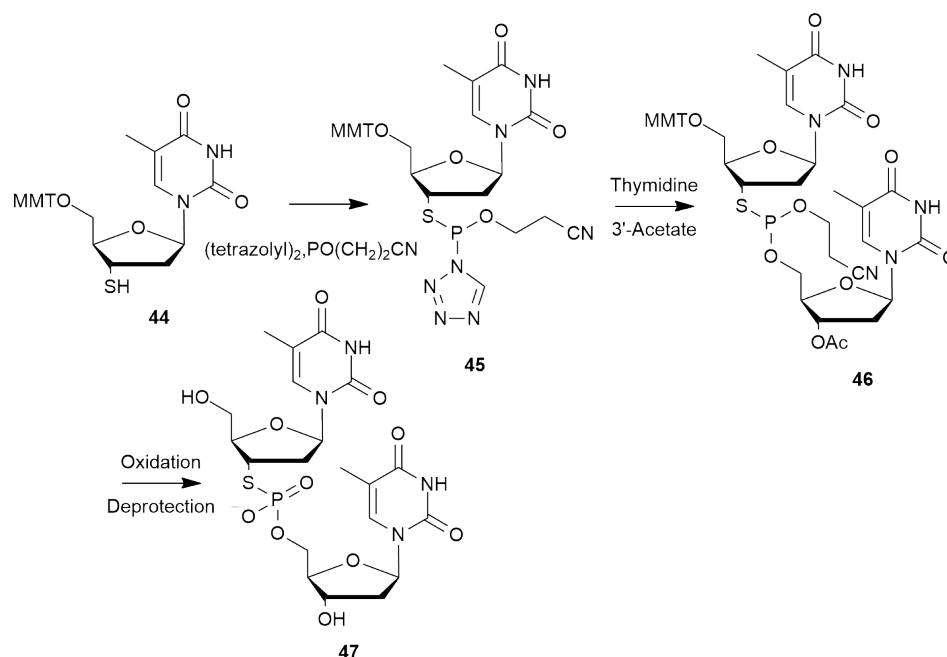
Scheme 1.13: A synthesis of a thymidylyl-3′,5′-thymidine
phosphorothiolate analogue by Cosstick and Vyle.

(Scheme 1.14).[41] This method also allowed the thiophosphoramidite to be
sulphurised in place of the oxidation step, giving access to 3′-*S*-phospho-
rodithioates. These innovations allowed the thiolate group to be placed at
specific locations on the oligonucleotide chain and greatly eased the synthesis
of these molecules.

Phosphoramidate Analogues

The *H*-phosphonate method has been adapted by Gryaznov *et al.* for the
synthesis of phosphoramidate oligonucleotides, through the use of 3′-amino-
3′-deoxynucleosides.[42, 43, 44] The phosphoramidate oligonucleotides have been
shown to bind more strongly to complementary DNA and RNA strands than
their natural counterparts while also being resistant to enzymatic cleavage.[45]

A 3′-*N* linked phosphoramidate analogue of thymidylyl-3′,5′-thymidine simi-
lar to the thiophosphoramidate analogue described later (chapter 3) has been
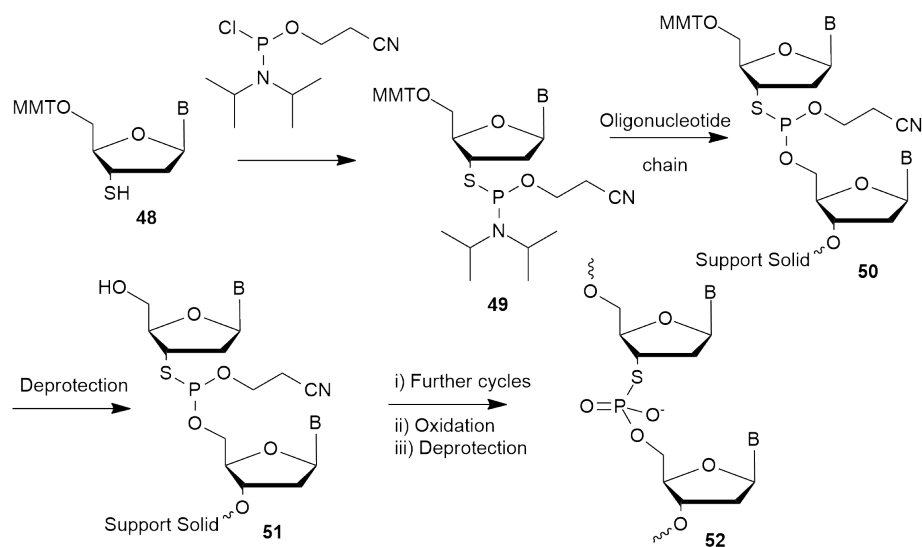
Scheme 1.14: Cosstick and Vyle developed the synthesis of oligonucleotides $3'$-S phosphorothiolated at specific positions.

prepared by Ora *et al.*[46]

The methodology has also been applied to the synthesis of the corresponding uridine system, with appropriate protection of the $2'$-hydroxyl groups.[47]

Oligonucleotide phosphoramidates have been synthesised by adapting the standard phosphoramidite method to use $3'$-amino-$3'$-deoxynucleoside derivatives.[48]

Thiophosphoramidate Analogues
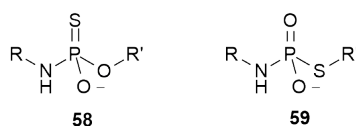
Figure 1.9: An S-non-bridging (left) and an S-bridging (right) thiophosphoramidate.
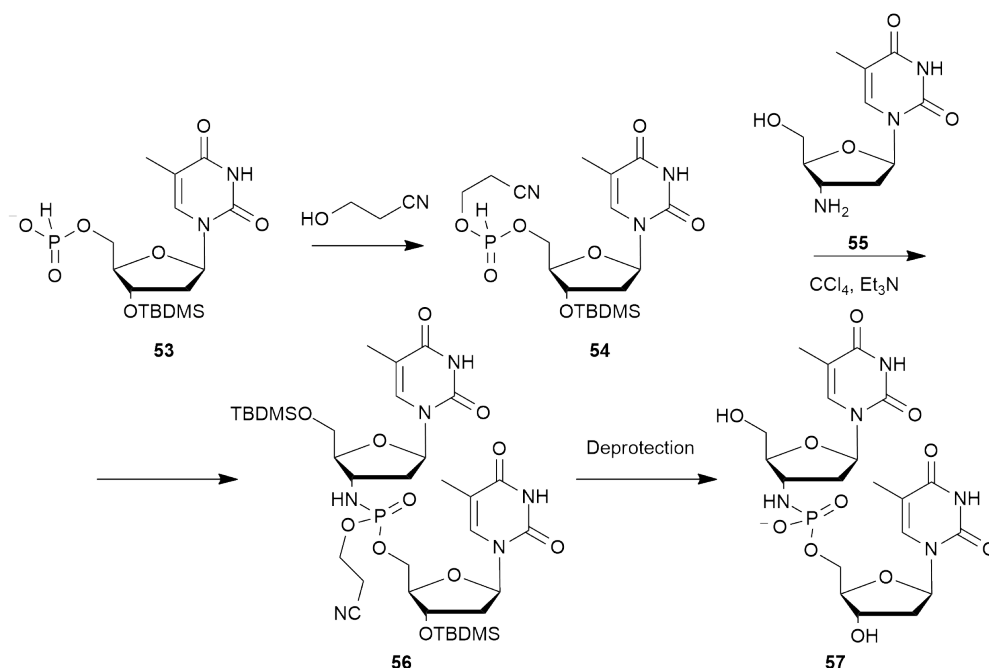
Scheme 1.15: The synthesis of a protected thymidylyl-3′,5′-thymidine
analogue.

Whilst N- and S-linked thiophosphoramidates **59** have been used to link sim-
ple organic fragments by Milena Trmčić[49] (see section 2.1.2), in the context
of nucleic acid mimics, only the N-linked, S-nonbridging analogues **58** have
been reported.[50] These have been developed by Pongracz and Gryaznov
based on the phosphoramidite method referred to in the previous section
(1.2.3). However, instead of the usual oxidation step to produce a phospho-
ramidate, a sulphurisation step is performed in the same manner as that de-
scribed for the synthesis of phosphorothioate oligonucloetides (section 1.2.3).

Alternatively, a variation on the H-phosphonate method can be applied,
in which a nucleoside 5′-H-phosphothionate **61** is synthesised,[51] activated,
and reacted with a protected 3′-amino-3′-deoxynucleoside. Deprotection then
yields the N-linked thiophosphoramidate phosphodiester analogue **64**.[46]
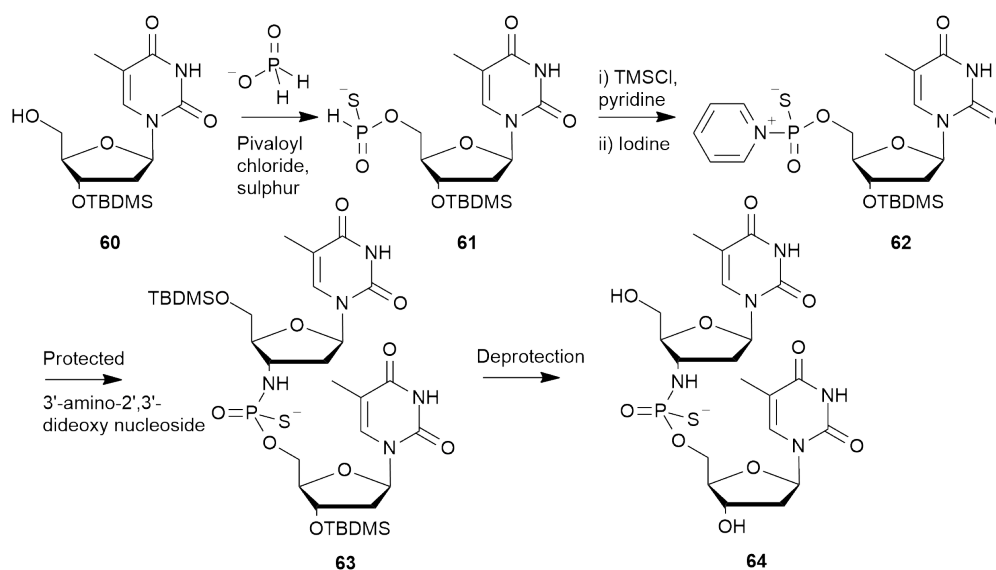
Scheme 1.16: The synthesis of an *N*-linked thiophosphoramidate phosphodiester analogue.

Other Analogues

Oligonucleotide analogues in which the phosphate group has been replaced by a methyl phosphonate have been synthesised.[52] The phosphite chain **65** (as in the phosphoramidite synthesis, before the oxidation step) is allowed to react with methyl iodide in an Arbuzov reaction to produce the phosphonate **67**. The phosphorus atom becomes a stereogenic centre where the ratio of diastereoisomers is approximately 1:1.[53] More recently, more stereocontrolled syntheses have also been reported.[54]
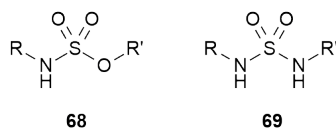
Figure 1.10: The sulphamate (left) and sulphamide (right) analogues of the phosphodiester linkage.
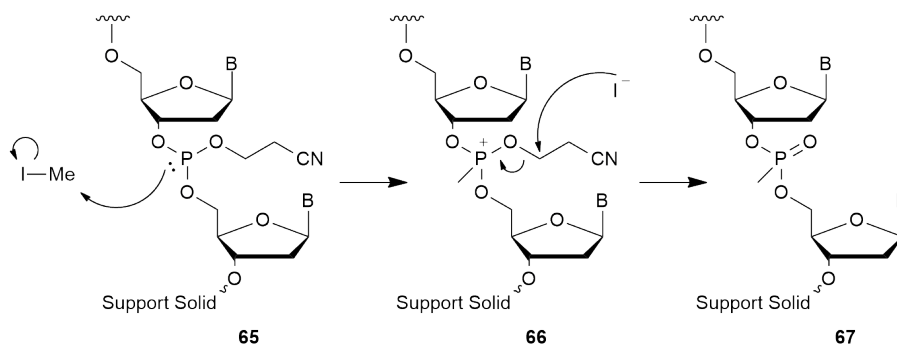
Scheme 1.17: The synthesis of methyl phosphonate oligonucleotide analogues.

The internucleosidic linkages described in the previous sections have all been phosphorus-based, but there are many examples of nucleic acid analogues in which the phosphorus atom has been entirely substituted. Examples include the sulphamates and sulphamides (Figure 1.10), which retain the tetrahedral configuration and general shape of the phosphate group.
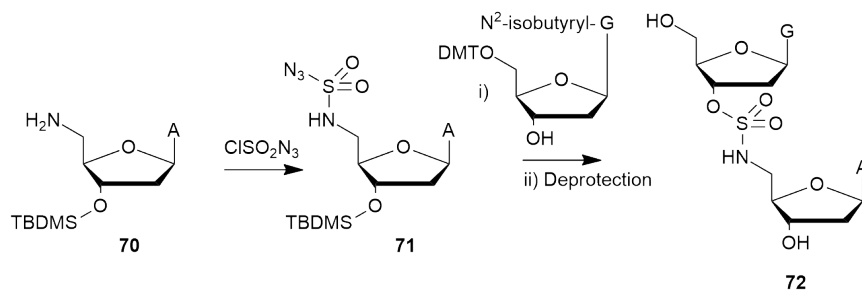
Scheme 1.18: The synthesis of a $5'$-N-sulphamate

The synthesis of $5'$-N-sulphamate linkages was developed by Huie, Kirshenbaum, and Trainor[55] who used sulphuryl chloride azide to couple a $5'$-amino-$5'$-deoxynucleoside to another nucleoside (see Scheme 1.18).

The $3'$-N-sulphamates and sulphamides, developed by Micklefield *et al.*,[56,57,58] were synthesised using a $3'$-amino-$3'$-deoxynucleoside and 4-nitrophenol chloro-
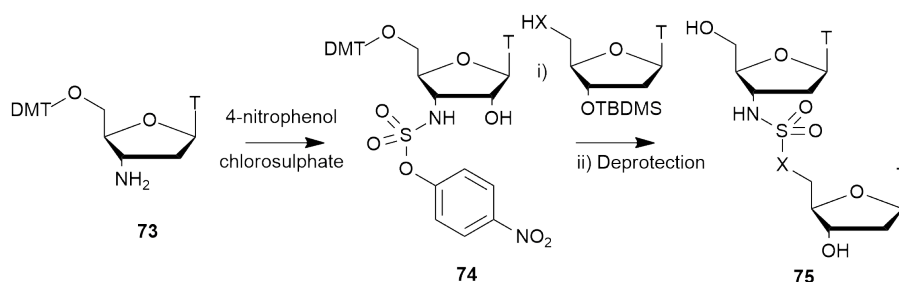
Scheme 1.19: The synthesis of a $3'$-N-sulphamate (when X is O) or a sulphamide (when X is N)

sulphate as the coupling agent (Scheme 1.19).

There are a huge variety of other nucleic acid mimics, such as boron[59] or selenium[60] substitutions to the phosphodiester linkage, or the use of peptide nucleic acids.[61] However, in the interest of brevity, this survey has had to be confined to those analogues which are phosphorus-containing or are isostructural with phosphodiesters, as these are the main focus of this thesis.

1.2.4 Templated Oligonucleotide Ligations

The ligation of oligonucleotides is of interest for the detection of nucleic acids; by using the sequence to be detected as a template, two partially-complementary single strands may be brought together and ligated. The formation or lack of formation of the ligated strand then indicates the presence or absence of the template sequence. While efficient methods exist for the detection and amplification of DNA *in vitro*, they require reagents or conditions which typically cannot be applied *in vivo*.[62] The first templated ligations were performed using natural oligonucleotides.

Shabarova *et al.* found that DNA could act as a template for oligonucleotides, which could then be ligated (Scheme 1.20).[63] This was extended to the synthesis of circular DNA by Kool *et al.*[64,65] Both these methods use cyanogen bromide, a highyl toxic compound, as the coupling agent. Other groups have developed methods of ligation using modified oligonucleotides, for example
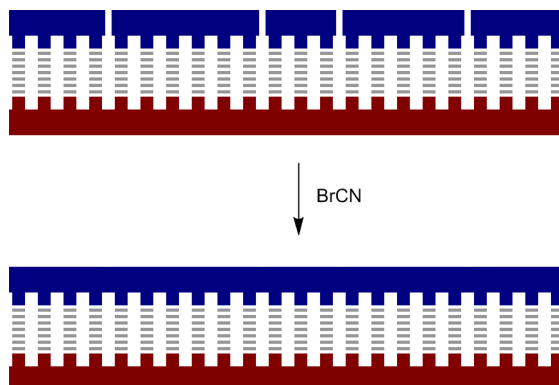
Scheme 1.20: Oligonucleotides may be ligated using a complementary
strand of DNA. DNA template in red, oligonucleotides in blue.

with amine and aldehyde termini (Scheme 1.21).[66] After binding to the DNA
template, the amine and aldehyde react to form an imine, and this linkage
can be made permanent through reduction with sodium cyanoborohydride.
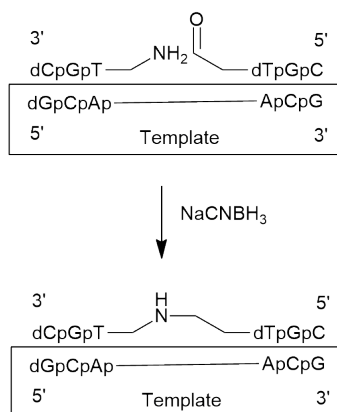
Scheme 1.21: The synthesis by Lynn *et al.* of oligonucleotides linked
by a secondary amine.[66]

All these methods, however, use reagents which are unsuitable for *in vivo*
couplings. The methods could be improved by using oligonucleotides modi-
fied to possess reactive moieties which will require only the template to bring

the reactive functional groups into close proximity, and no other reagents. Such a technique was devised by Herrlein and Letsinger[67] and expanded upon by Kool *et al.*[68, 69] in which one oligonucleotide possesses a terminal 3'- phosphorothioate, while the other has a 5'- leaving group, such as iodide or toluenesulphonate (Scheme 1.22).
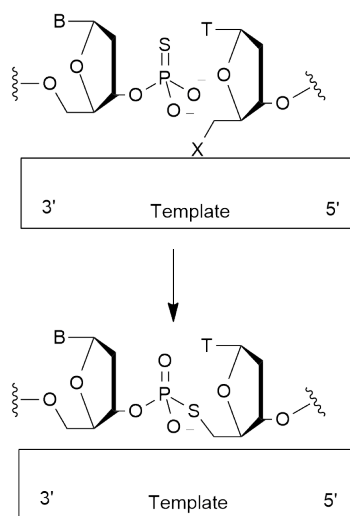
Scheme 1.22: When the oligonucleotides modified to have phosphorothioate and alkylating functionality, no reagents other than the template are required for ligation. X is an iodide, tosyl, or dabsyl (a quencher).

This methodology has been used to create oligonucleotides with a quencher (Scheme 1.22, X = dabsyl) at the 5'- position, and a fluorophore nearby on the same oligonucleotide. When the template is present, attack by phosphorothioate takes place and the loss of the quencher allows fluorescence to be observed, which serves as a signal that the template is present.[70]

1.3   Properties of Phosphate-Containing Systems

1.3.1   Nucleotide Conformation

Modifications to the substituents on a ribose ring may alter its conformation, and this may have implications for the larger-scale structure of a molecule containing a nucleotide analogue. For example, double-stranded nucleic acids can take up a number of conformations; double-stranded DNA (dsDNA) generally exists in solution as the familiar double helical 'B' form, while dsRNA and RNA-DNA hybrids usually take the more compact helical 'A' form (Figure 1.11).[71] In the solid state, other conformations are possible, depending on, amongst other conditions, humidity and the identity of counter cations. The conformation of the double stranded polynucleotide is dictated by the conformation of the ribose units in the ribose-phosphate backbone.

If unnatural phosphodiester compounds are to be prepared as mimics of nucleic acids, it is therefore useful to study the effect that the modification has on the conformation of the ribose ring.

The elucidation of solution-state ribose conformation by means of ^{1}H-NMR J-coupling values was pioneered by Altona and Sundaralingam.[73,74]

The geometry of a ribose ring is similar to that of cyclopentane, which has two important energy minima; the low energy 'envelope' in which all but one of the five members lies in a plane, or the higher energy 'twist' conformation, in which three members lie in a plane, and one of each of the remaining members lies above and below the plane (Figure 1.12). Substituents other than hydrogen on the ring, however, as in a ribose ring, will change the energy profile and may result in energy minima at different conformations. The conformation of the five-membered ring can be described by two parameters; P denotes the position of the deviation from planarity, while r_m indicates the magnitude of the deviation.
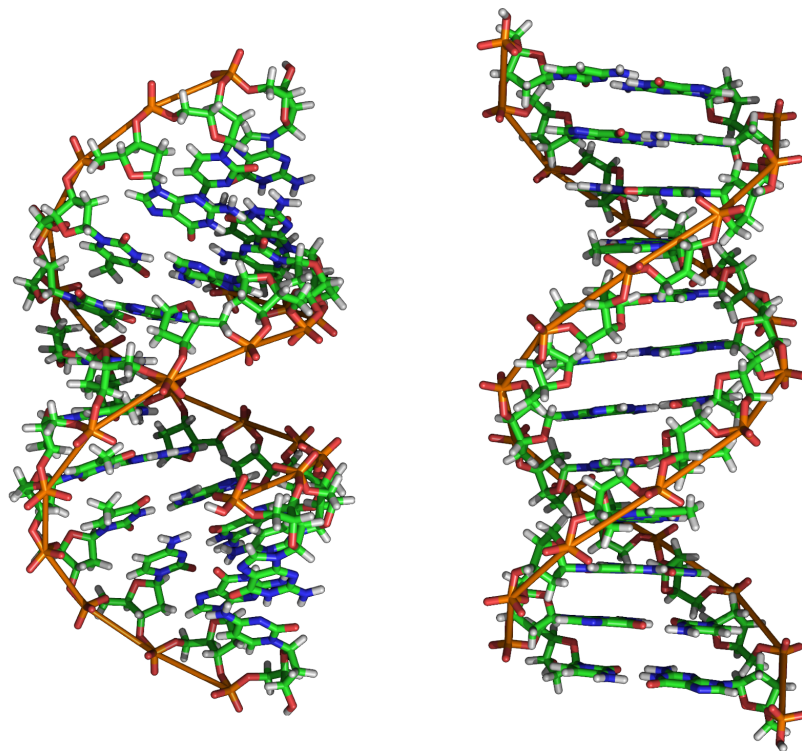
Figure 1.11: A-DNA (left) and B-DNA(right).[72]

Analysing the conformations of a number of nucleoside and nucleotide derivatives, Altona and Sundaralingam found that the rings tended to adopt one of two conformations (see Figure 1.13), one centered around a P value of approximately $10°$ (corresponding to a $3'$-*endo* configuration) and at approximately $160°$ (corresponding to a $2'$-*endo* conformation) labelled 'North' and 'South' respectively (Figure 1.14).

The fact that the vast majority of nucleosides and nucleotides fell into these two categories indicated that these conformations corresponded to minima of similar energy separated by relatively large barriers, as relatively small modifications to the ribose substituents could force a shift from one conformation to the other.

Assuming this small energy difference in the conformations, in the solution
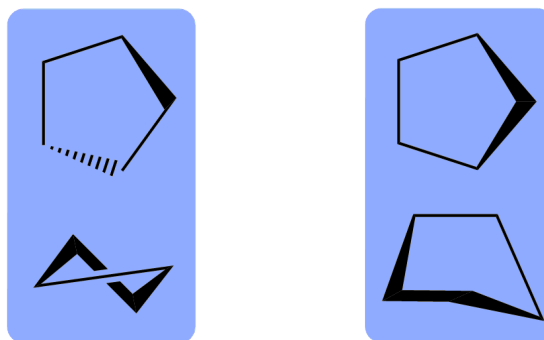
Figure 1.12: The 'twist' (left) and 'envelope' (right) conformations of cyclopentane.
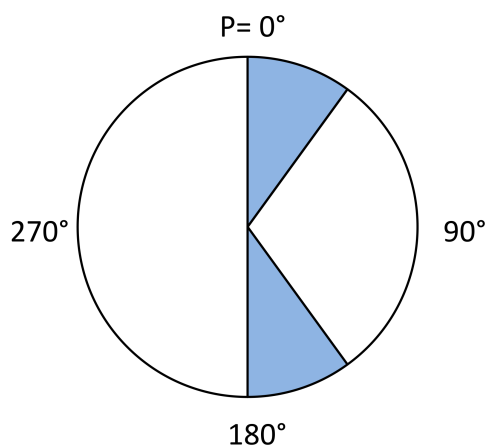
Figure 1.13: Altona and Sundaralingam found that most nucleotides and nucleosides fell into two conformations.

state the ribose ring can be considered, to a first approximation, to be oscillating between these two forms, with an equibilbrium constant being a function of the difference in energy of the two states. If the interconversion between the two conformers is rapid on the NMR timescale, the measured J-coupling is then a time-weighted average of the theoretical J-couplings of the two static conformers. The values of the J-couplings are, through the Karplus equation (equation 1.1), dependent on the dihedral angles (Figure 1.16) between the relevant protons.

P = 0°
North
C(3′) endo

P = 180°
South
C(2′) endo
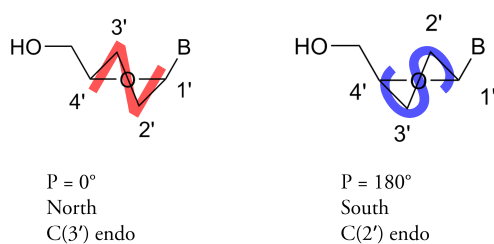
Figure 1.14: An idealised diagram of the two major conformations; in reality the P values of 0°and 180°are extremes.

P / deg
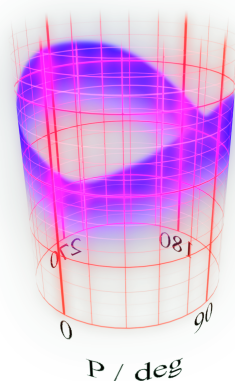
Figure 1.15: The two major conformers represent minima on the energy profile.

$$J(\phi) = A\cos^2\phi + B\cos\phi + C \tag{1.1}$$

Altona and Sundaralingam used the fact that there are coupling constants and sums of coupling constants which are predicted to be weakly dependent on the conformation, specifically the values of $J_{2'3'}$ and $J_{1'2'} + J_{3'4'}$. Observing the *pseudo*-symmetry of the conformations (see Figure 1.17) provides a qualitative justification for this. These values may then be used to derive Karplus parameters which can in turn be used to determine theoretical values for the J-couplings of the static conformers. Comparison of the calculated J-couplings with the observed couplings then allows the position of equilibrium
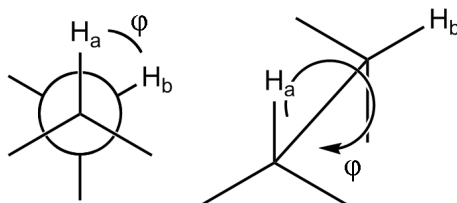
Figure 1.16: The dihedral angle between vicinal protons.
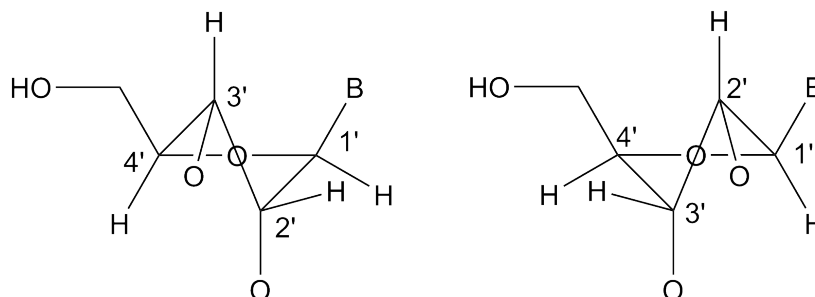
Figure 1.17: The two major conformations, with protons.

between the two conformers to be determined.

Several approximations have been made in this approach; among others, the assumption that the same Karplus parameters can be used for the couplings between different protons on the ring, that only two conformers are present and that they are the same two conformers that have been observed in the solid state.

An additional problem with this method is that in systems containing more than one ribose unit, overlap in the ^{1}H NMR spectrum is likely occur and second-order effects will render the determination of the relevant J-couplings non-trivial; simulation of the spectrum and fitting to the experimental data may be required, as performed by Beevers *et al.* on a $3'$-S-$5'$-O-linked dinu-cleoside thiophosphate.[75]

When approaches such as these have proved impractical, Rinkel and Altona have developed a method of calculating the conformational parameters of ribose rings based on sums of J-coupling constants which are, in practice, the widths of certain ^{1}H NMR multiplets. Since the individual J-coupling

values do not have to be determined, this alleviates some of the problems that second order effects present.[76]

Studies were performed on both the natural thymidylyl-thymidine system, and analogues in which either the 3′- or the 5′- oxygen atoms in the phosphodiester were replaced by sulphur.[75,77] Two deoxynucleosides linked by a 3′→5′ phosphodiester possessed ribose rings which were predominantly in the 'south' conformation (approx. 73% south for Tp, 64% for pT.). When the 3′-substitution for sulphur was made, the proportion of conformers of each ribose ring shifted towards the north, with the 3′-linked fragment taking up the 'north' conformation, predominantly. Very little change, on the other hand, was observed when the 5′- substitution was performed; this more distant modification, unsurprisingly, had a minimal conformational effect. Studies by Nottoli, Lambert, and Letsinger have likewise confirmed that the effect of substitution of nitrogen for oxygen at the 5′- position has little effect on the conformation.[78]

1.3.2 Enzymatic Hydrolysis and its Avoidance

Phosphorothioates have proven resistant to hydrolysis by nucleases, where the resistance depends on the enzyme, and can range from a ten-fold decrease in the rate of hydrolysis in the case of snake venom diesterase to almost complete resistance to *E. coli* DNA polymerase I. Phosphorothioate linkages possess a stereogenic centre at phosphorus, and the rate of hydrolysis by a given phosphodiesterase depends on this configuration. For example, nuclease P1 hydrolyses S_P phosphorothioates but not the R_P counterparts, while for other nucleases the selectivity is reversed.[32]

Both the 3′-S and 5′-S phosphorothiolates have also been shown to be more resistant to enzymatic hydrolysis than their natural counterparts.[79,40]

1.4   Phosphodiester Analogues as Mechanistic Probes

There are a large number of reviews on the synthesis and use in the elucidation of mechanism of phosphodiester analogues. The most common modification made to the nucleotide phosphodiester group is exchange of oxygen for sulphur.[80,81,82,83,84,60,85,54,86] Oxygen and sulphur belong to the same group, so the modified linkage is isoelectronic with the natural phosphodiester. However, the van der Waals radius of sulphur is slightly larger than that of oxygen (1.85 *vs.* 1.44 Å), and the P-S bond is significantly longer than the P-O bond (*circa* 2.0 *vs. circa* 1.6 Å).[82,87] The majority of the literature on applications of unnatural phosphodiesters appears to be on phosphorothioate analogues, probably due to their greater synthetic accessibility, as described in section 1.2.3.

In this section, an overview of the main areas of application is provided, with examples. Some more novel techniques are also covered.

1.4.1   Stereocontrol at Phosphorus in Phosphodiester Linkages

The stereochemistry which substitution of one of the oxygen atoms for sulphur imparts to the molecule is a useful mechanistic probe for the elucidation of the mechanism of enzymes which cleave phosphodiester bonds. The use of a phosphorothioate of known configuration in conjunction with oxygen isotope labelling renders the formerly equivalent non-bridging oxygen atoms of the cleaved phosphodiester distinct, and can thus be used to follow the stereochemical course of a reaction.

An example of this type of methodology is the work by Mizuuchi *et al.*,[88] in which the mechanisms of phosphodiester cleavage by the *Sfi*I and *Hpa*II endonucleases and MuA transposase were investigated. A DNA strand with a phosphothioate linkage of known stereochemistry **76** was cleaved by the
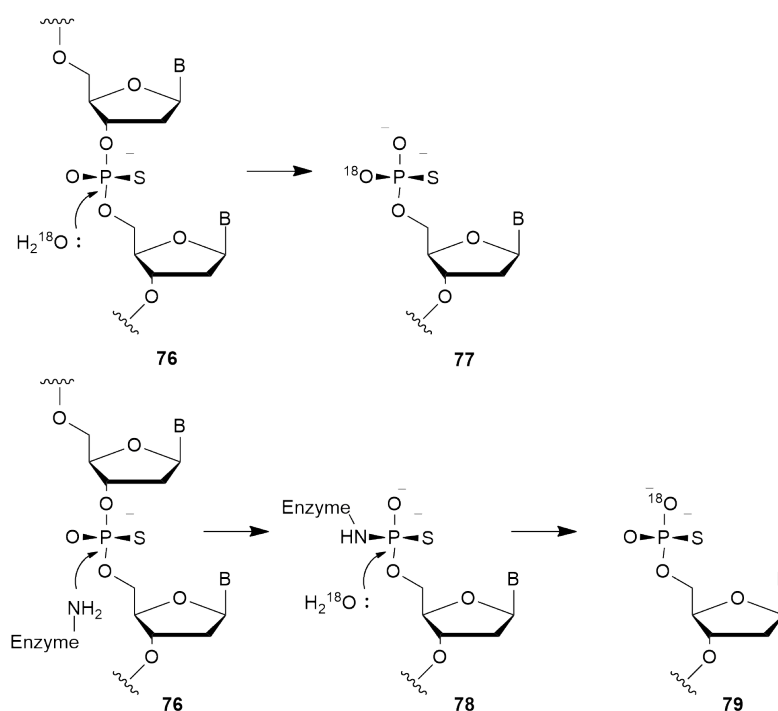
Scheme 1.23: A one-step cleavage (top) and a two-step cleavage (bottom) result in different stereoisomers when performed in ^{18}O-enriched water. These experiments were performed on the *Sfi*I endonuclease and MuA transposase.[88]

enzyme in ^{18}O-labelled water, before being ligated with biotinylated DNA for analysis.

A cleavage involving a single step, *i.e.* attack by a water molecule, would result in the inversion of stereochemistry (to produce **77**), while after two steps, such as attack by an enzyme followed by hydrolysis by water, the original stereochemistry would be retained (producing **79**, see Scheme 1.23). After enzymatic ligation to a biotinylated DNA strand, the stereochemistry of the monophosphate resulting from cleavage can be determined by the loss or retention of oxygen-18 (Scheme 1.24).

Applying a similar methodology, phosphorothioates of known configuration have also been used to study the mechanism of cleavage of phosphodiester linkages in DNA transposition.[89]
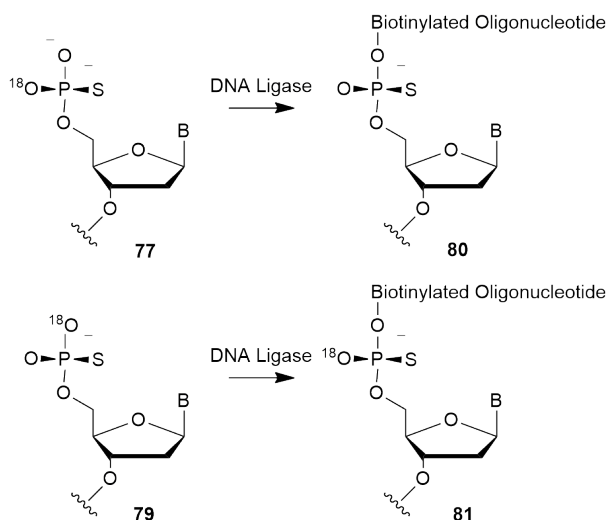
Scheme 1.24: Conjugation by DNA ligase results in the retention or loss of oxygen-18, depending on the stereochemistry of the monothiophosphate.

1.4.2 The Role of Metal Ions in Enzymatic Catalysis

The reduced affinity of sulphur for the hard metal cations bound by phosphates, and conversely, its greater affinity for soft metal cations (Figure 1.18) allows the role of bound metal ions in ribozymatic processes to be investigated: one by one, the phosphate groups of a ribozyme are systematically modified to incorporate sulphur in the non-bridging position. A reduction in the rate of cleavage in the presence of a hard metal cation such as magnesium, followed by recovery of catalytic activity with the substitution of the cation for a 'softer' species such as manganese indicates that the modified phosphate group is involved in metal cation binding which promotes the catalytic activity. This methodology has been applied to a number of species displaying ribozymatic activity.[90, 91, 92, 93, 94]

In a number of studies, the use of the phosphorothiolate is similar to that of the phosphorothioate; while phosphorothioates may be used to determine the identity of mechanistically significant binding by non-bridging oxygen atoms of the phosphate group to metal ions, phosphorothiolate analogues can be used to likewise identify the important bridging positions and the necessity
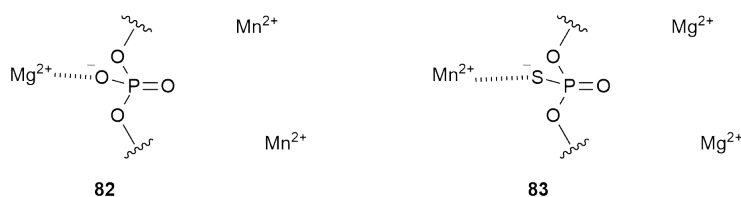
Figure 1.18: Oxygen tends to bind 'hard' metal cations such as magnesium, while sulphur binds softer metal cations *e.g.* manganese

or otherwise of metal cation binding.[95,96,97,98] This analysis has also been performed with simultaneous bridging and non-bridging substitutions.[94,99]

The role of hydrogen bonding to the oxygen atoms of the phosphodiester linkage has been investigated by Lu *et al.* through substitution of the 3′-linked oxygen for sulphur, which does not form hydrogen bonds.[100]

1.4.3 Ligation of Oligonucleotides Through a Modified Phosphodiester Linkage

The phosphorothioate group is highly nucleophilic at sulphur, in contrast to the unmodified phosphate group, which is a poor nucleophile. This quality allows phosphorothioate groups to be ligated in a stereospecific manner, and has been exploited by Popova and Qin to attach a probe containing a stable nitroxide radical to DNA modified to include phosphorothioate groups at specific positions (Scheme 1.25).[101]

The change in the electron spin resonance (ESR) spectrum was then used to report the local environment of the radical probe. Similar methodology, also using ESR techniques, has also been used to determine the distance between pairs of nitroxide radicals within a single DNA strand, and to study the interaction between a spin labelled RNA strand and a protein.[102]
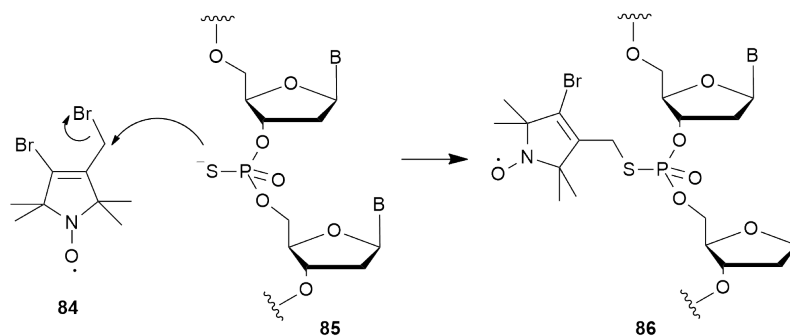
Scheme 1.25: The nucleophilicity of the phosphorothioate group allows
facile ligation to a spin-active molecule.

1.4.4 Role of the Leaving Group in Phosphodiester Hydrolysis

Substitution of the bridging oxygen atoms of the internucleotidic phosphate
group also permits the identification of the role that the leaving group plays
in nucleic acid hydrolysis. Studies in this direction have been performed by
Eckstein *et al.* in which uridine dinucleosides have been modified so that the
5′- bridging position is substituted for sulphur, and the 2′- hydroxyl group
neighbouring the phosphate linkage becomes an amine. The effect of these
changes on the hydrolysis of the compound thus provides information on the
roles of the leaving group and the nucleophilic attack of the 2′- hydroxyl
group.[103, 104, 105]

1.4.5 Other Applications

Williams and Halford have used phosphorothioated DNA to show that the
*Sfi*I endonuclease, which must bind two strands of DNA with the correct
recognition before cleavage can occur, requires both recognition sequences
to have non phosphorothioated backbones; if even one strand possesses a
non-bridging sulphur atom, neither strands are cut, indicating that there is
communication between both DNA binding sites.[106]

Substitution for sulphur at the bridging positions of phosphodiesters have

also been used to distinguish between general acid and base catalysis.[33, 107] Das and Piccirilli have used this phosphorothiolate methodology to distinguish whether a cytosine residue in a ribozyme has a role as a general acid or base catalyst; when the cytosine was substituted for uracil or modified cytosine, the catalytic activity dropped to a much greater degree in the natural substrate compared to the sulphur-substituted analogue. The fact that this occurs, even though the uncatalysed hydrolysis profiles of both substrates are similar, indicates that the effect is due to the the phosphorothiolate having a better leaving group, and that the cytosine residue is increasing the leaving ability of the natural substrate and thus acting as a general acid.[108]

The greater rate of uncatalysed hydrolysis of phosphorothiolate diesters as compared to their natural analogues has also been exploited by Korennykh *et al*. to determine whether the rate determining step of RNA cleavage by the restrictocin ribonuclease is chemical or physical; if the rate determining step is physical, there should be little change when the natural restrictocin substrate is substituted for an analogue bearing a 3′- phosphorothiolate group at the cleavage site, while a chemical rate determining step would result in a significant change in the rate of cleavage. In this case it was found that the phosphorothiolate was cleaved more rapidly than the natural counterpart, indicating that the chemical step is rate limiting.[109]

1.5 Aims and Objectives

A technique has been developed in the Hodgson group for the aqueous phosphorylation or thiophosphorylation of nucleosides modified so that one hydroxyl group on the ribose ring is substituted for an amine (described in more detail in chapter 2). In the case of thiophosphorylation, the reactive thiophosphoramidate may then go on to react with an alkylating agent to form a phosphodiester analogue. The initial aim of the work described in this thesis is to optimise the phosphorylation and alkylation processes. Once this has been achieved, the next step is to apply these procedures to the

synthesis of mimics of biological systems. Potential targets could include oligonucleotides, possibly in templated reactions of the kind described in section 1.2.4. Nucleotide sugars (see section 1.1.3) are another example of potential targets, the analogues of which could act as inhibitors or substrates of biological processes. The properties of the thiophosphoramidate linkage, such as hydrolytic stability and effect on nucleoside ribose conformation, will also be studied, and it is expected that this information will be of use in futher optimising the synthesis of these compounds and in determining their suitability of use in biological applications.

Chapter 2

The Phosphorylation of Aminodeoxynucleosides

2.1 Introduction

This chapter describes the synthesis, and subsequent N-oxyphosphorylation and thiophosphorylation of a number of nucleosides in which a hydroxyl group on the ribose sugar has been replaced by an amine, as illustrated in Scheme 2.1.
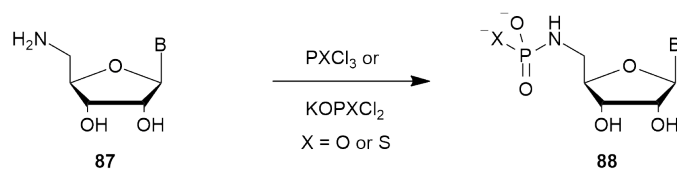
Scheme 2.1: The oxyphosphorylation (X = O) and thiophosphorylation (X = S) of 5′-amino-5′-deoxynucleosides.

The pH of the phosphorylation procedure was optimised using 5′-amino-5′-

deoxyguanosine as the substrate. The optimal conditions were then applied to other aminodeoxynucleoside derivatives.

2.1.1   Aqueous Phosphorylation Methodologies

Within the Hodgson group, work in this area was begun by David Williamson, who wished to use 5′-amino-5′-deoxyguanosine **89** as an initiator in the enzymatic synthesis of RNA sequences so that the RNA strands thus formed could then be labelled selectively at the reactive terminal 5′-amine position. This had been attempted previously by others,[110] however, their attempts resulted in poor levels of incorporation probably because of the very low aqueous solubility of many guanosine derivatives.

Williamson's solution was to phosphorylate the 5′-amino group. This strategy served not only to increase the solubility of the initiator, but the phosphoramidate group is hydrolytically labile under the reaction conditions, allowing the amine functionality to be easily unmasked once it was incorporated into the newly formed RNA sequence.[14, 15]

In contrast to the conditions employed by Yoshikawa *et al.* for the phosphorylation of ribonucleosides,[19] Williamson carried out the *N*-phosphorylation under aqueous conditions, using a solution of 5′-amino-5′-guanosine and sodium hydroxide. The use of a highly basic solution resulted in the deprotonation of the guanine base on the aminodeoxyguanosine substrate (with a pK_a of 9.4, Scheme 2.2),[111] forcing the substrate into solution and thus obviating the problem of solubility. A solution of phosphoryl chloride in THF was then slowly added to the solution.

This approach proved to be successful, with high levels of conversion and good levels of incorporation into RNA transcriptions.

In general, organic reactions requiring the use of water-sensitive reagents are performed with, so far as is possible, the exclusion of all moisture. However, David Williamson's reaction, in an approach somewhat reminiscent of the Schotten-Baumann reaction,[112, 113] reacts phosphoryl chloride (which is
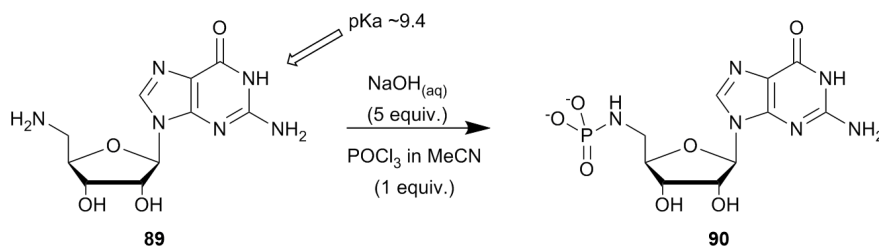
Scheme 2.2: The aqueous phosphorylation of
5′-amino-5′-deoxyguanosine, developed by David Williamson.

highly reactive to water)[114] selectively with an amine in aqueous solution, due to the much greater nucleophilicty of amines compared to water or hydroxide. This allows the phosphoramidate to be formed with high levels of conversion, despite competition with water.

2.1.2 Thiophosphorylation and Alkylation of Amines

The *N*-aminophosphorylation of 5′-amino-5′-deoxyguanosine was then extended and modified by Milena Trmčić to include the *N*-thiophosphorylation of a small library of commercially available alkyl amines, using thiophosphoryl chloride in place of phosphoryl chloride. Trmčić found that the thiophosphoramidates **92** formed through this procedure could then be alkylated at sulphur with an excess of the alkylating agent, to produce analogues of phosphodiesters **93**.
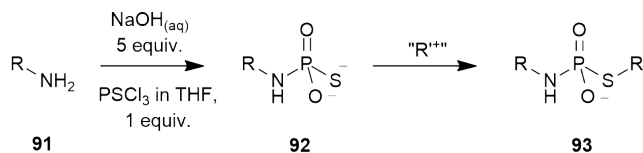
Scheme 2.3: The *N*-thiophosphorylation and *S*-alkylation procedure as
developed by Trmčić.

The procedure worked well, as shown in Table 2.1, frequently displaying very high levels of conversion.[49]

Table 2.1: The conversion levels for the thiophosphorylation and alkylation of a range of amine substrates, as determined by ^{31}P NMR spectroscopy.

Alkylating Agent: / Amine:	Me–I	Br⁀OH	⁀Cl (benzyl)	⁀I (propyl)	⁀I (isopropyl)	acrylate	styrene oxide	epoxide
benzylamine (⁀NH₂)	98%	100%	100%	100%	94%	92%	65% (1-) 30% (2-)	96% (1-)
allylamine (⁀NH₂)	98%	100%	99%	97%	91%	n.d.	n.d.	n.d.
HO⁀NH₂	88%	84%	73%	n.d.	n.d.	n.d.	n.d.	n.d.
morpholine (O⁀NH)	98%	92%	92%	95%	95%	n.d.	n.d.	n.d.
propylamine (⁀NH₂)	n.d.	n.d.	92%	n.d.	n.d.	n.d.	n.d.	n.d.

The procedure was also applied to 5′-amino-5′-deoxyguanosine **89** and the dihydrochloride salt of 5′-amino-5′-deoxyadenosine **122** (with two extra equivalents of sodium hydroxide to compensate for the two equivalents of acid). Methyl iodide was used as the *S*-alkylation agent, and conversion levels of *circa* 70% by ^{31}P NMR spectroscopy were observed.[115, 116]

In order to improve the conversion levels of these reactions, phosphodichloridate **98** and thiophosphordichloridate **100** anions were investigated as alternative phosphorylation reagents. It was hoped that they would prove more water-soluble and thus that they may increase the levels of conversion through improved mixing. Richard Delley studied the hydrolysis kinetics of the phosphodichloridate and thiophosphordichloridate anions, and found that their hydrolyses were relatively slow (oxyphosphodichloridate re-
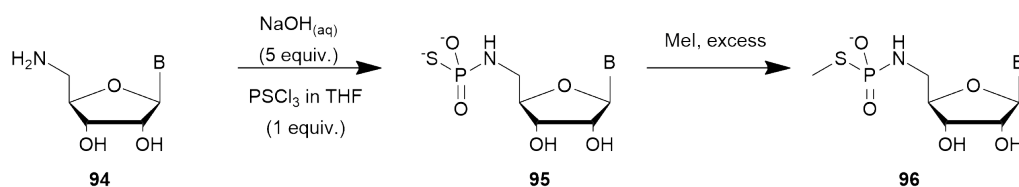
Scheme 2.4: The synthesis of nucleoside methyl thiophosphoramidates, developed by Milena Trmčić.[115, 116]

acts approximately 10^4 fold more slowly than oxyphosphoryl chloride), and independent of pH up to very high pH values.[118]
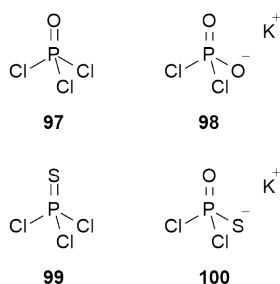
Figure 2.1: Oxyphosphorylating agents phosphoryl chloride (**97**) and potassium phosphodichloridate (**98**), and thiophosphorylating agents thiophosphoryl chloride (**99**) and potassium thiophosphodichloridate (**100**).

These characteristics suggested that they would be suitable for our purposes; a slower reaction time may improve selectivity, and the lack of reactivity with hydroxide is important under the highly alkaline reaction conditions required to stabilise the phosphoramidate and thiophosphoramidate products of the reaction.

The use of the dichloridates **98** and **100** may also reduce the quantity of undesired phosphorodiamidate (see Figure 2.2) side products formed.

Delley also investigated pH control as a route towards improving conversion
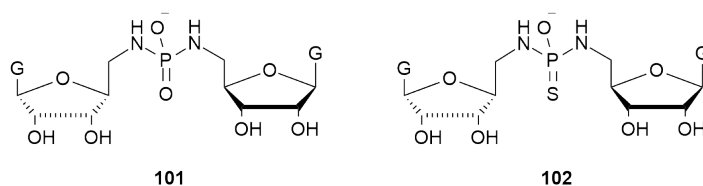
Figure 2.2: Phosphorodiamidates **101** and thiophosphorodiamidates **102** may be formed as side products of the reaction
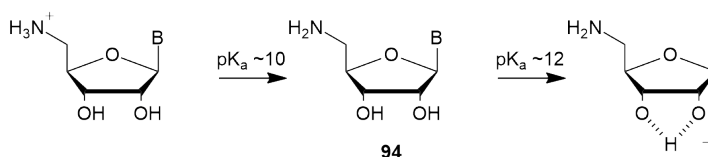
Scheme 2.5: Possible ionisations of a 5′-amino-5′-deoxynucleoside.[117] Amine ionisation estimated from the pK_a of ethanolamine.[119]

levels. There are a number of pH dependent phenomena which may influence the degree of phosphorylation observed – for example, the protonation of the 5′-amine, the deprotonation of the 2′- and 3′- *cis* diols (as shown in Scheme 2.5), and the hydrolysis of the desired product. In order to investigate the effect of pH on reaction outcome, thiophosphorylation reactions were repeated at constant pH, using an autotitrator to add potassium hydroxide solution to maintain a constant, preset pH, with 5′-amino-5′-deoxyguanosine **89** as the substrate. This was done using both thiophosphoryl chloride **99** (Figure 2.4) and potassium thiophosphodichloridate **100** (Figure 2.3) as thiophosphorylating agents.

For both thiophosphorylation agents, there were observed pH optima at *circa* 12, where thiophosphodichloridate gave the greatest levels of conversion to the thiophosphoramidate – 97%, compared to 93% for thiophosphoryl chloride. The pH of the alkylation reaction was then optimised, using guanosine 5′-*S*-thiophosphoramidate synthesised under the conditions determined to be optimal, *i.e.* pH 12, as the model substrate, and thiophosphodichloridate as the phosphorylating agent. Methyl iodide, benzyl chloride, and 2-bromoethanol were used as *S*-alkylating agents, again at a range of pH values but in each case keeping the pH constant. Delley's results are shown
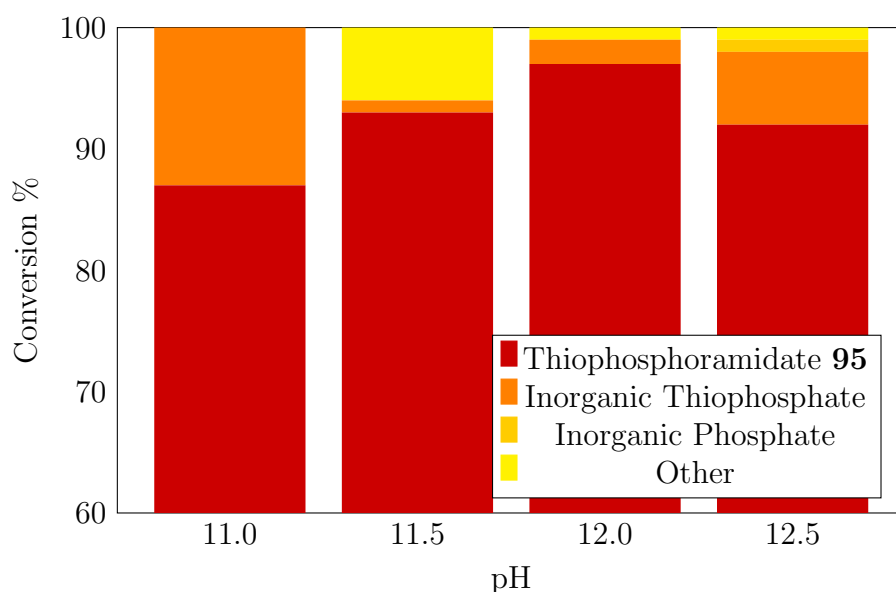
Figure 2.3: The product distribution of the reactions of
5′-amino-5′-deoxyguanosine with thiophosphodichloridate at different pH
values, as determined by ^{31}P NMR spectroscopy by Richard Delley.
Note that the *y*-axis begins at 60%

in Figure 2.5

The trend in the levels of conversion is not clear, however, in all cases the conversions are greater than those achieved though the methodology without pH control. A number of ways in which this work could be built upon could be envisaged:

- The synthesis and use of other aminonucleosides.

- Testing oxyphosphorylating agents **97** and **98** and thiophosphorylating agents **99** and **100** on other aminonucleosides.

- Application of the methodology to the synthesis of biomolecular analogues.

This chapter describes the efforts in pursuit of the first two points; the final point is described in chapter 3.
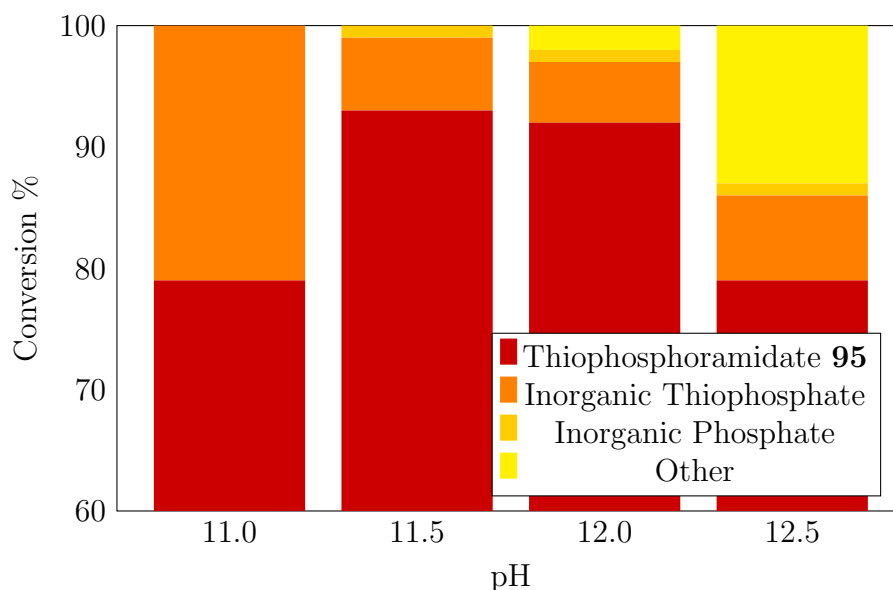
Figure 2.4: The product distribution of the reactions of
5′-amino-5′-deoxyguanosine with thiophosphoryl chloride at different pH
values, as determined by ^{31}P NMR spectroscopy by Richard Delley.
Note that the *y*-axis begins at 60%

2.2   Optimisation of the Oxyphosphorylation of 5′-Amino-5′-deoxyguanosine

With the thiophosphorylation procedure for aminoguanosine having been optimised, the next step was to optimise the oxyphosphorylation, and determine the most favourable pH for this process.

2.2.1   5′-Amino-5′-deoxyguanosine Synthesis

A straightforward method for accessing 5′-amino-5′-deoxyguanosine was described by Dean (as shown in Scheme 2.6),[120] beginning with the conversion of guanosine into the 5′-iodide through an Appel-type reaction. Displacement of the iodide by azide and subsequent Staudinger reaction yielded the amine in good yield, and without any laborious purification procedures. This synthetic route has been repeatedly used by others in the Hodgson group.

(a) Methyl iodide   **(b)** Benzyl chloride   **(c)** 2-Bromoethanol
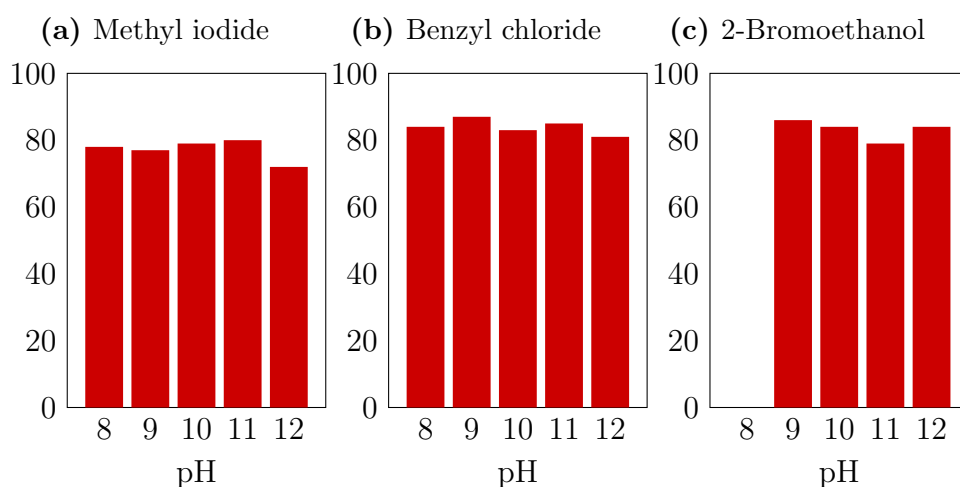
Figure 2.5: The conversion levels for the alkylation of guanosine thiophosphoramidate **95** with a number of alkylating agents, over a range of pH values, as determined by ^{31}P NMR spectroscopy by Richard Delley.
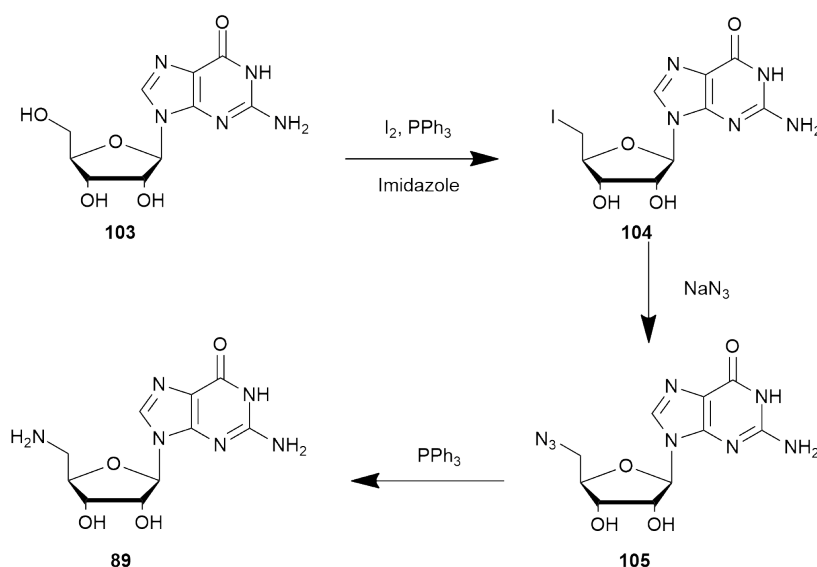
Scheme 2.6: The synthesis of 5′-amino-5′-deoxyguanosine.[120]

2.2.2 Optimisation of the Phosphorylation Procedure Using Phosphoryl Chloride

With the 5′-amino-5′-deoxyguanosine **89** in hand, the phosphorylation was performed at a range of pH values, initially using a solution of phospho-
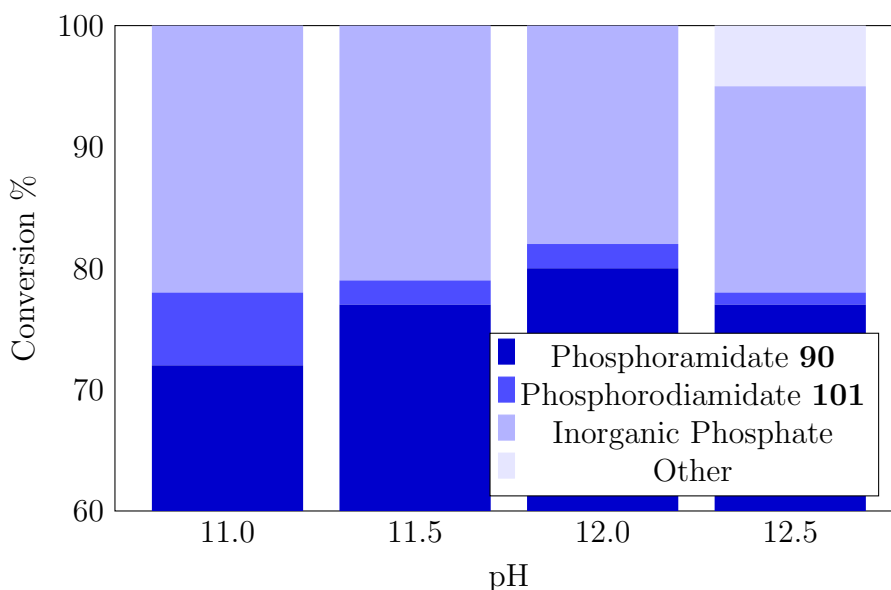
Figure 2.6: The results of the phosphorylation of aminoguanosine with phosphoryl chloride, derived from ^{31}P NMR spectroscopy data. Note that the y-axis begins at 60%.

ryl chloride **97** in acetonitrile as the phosphorylating agent. Experiments were performed at pH 11.0, 11.5, 12.0, and 12.5, in the expectation that the optimum would be found at a similar value to that of the previous (thio)phosphorylations. After the reactions were complete, the solvents were removed, and the crude materials were analysed by ^{31}P NMR spectroscopy.

The conversions were lower than those obtained for the thiophosphorylation of aminoguanosine **89** using thiophosphoryl chloride **99**, but this is perhaps to be expected, due to the greater reactivity of oxyphosphoryl chloride **97**.

The optimum pH for phosphorylation was found to be 12. At higher pH, signals are observed by ^{31}P NMR spectroscopy which cannot be attributed to the diamidate product **101** or inorganic phosphate, and appear likely to be due to hydrolysis of the phosphoramidate product under these basic conditions.

2.2.3 Preparation of Potassium Phosphodichloridate

With phosphorylation using phosphoryl chloride optimised, the next step was to repeat the optimisation process using potassium phosphodichloridate **98**. The phosphodichloridate was prepared according to a literature procedure[118,121] by stirring a solution of phosphoryl chloride in acetonitrile with two equivalents of potassium hydrogen carbonate – one equivalent to react with the phosphoryl chloride, and another to absorb the hydrogen chloride produced. The potassium chloride precipitate is then filtered off to leave the phosphorylating agent in acetonitrile, which is used directly.
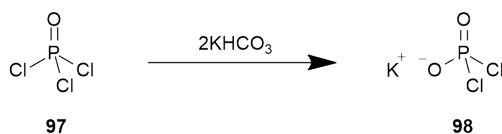
Scheme 2.7: The synthesis of potassium phosphodichloridate.

2.2.4 Optimisation of the Phosphorylation Procedure Using Potassium Phosphodichloridate

The reactions were performed using potassium phosphodichloridate at different pH values with a single equivalent of 5′-amino-5′-deoxyguanosine **89** as the substrate. After the reactions were complete, acetonitrile was removed under reduced pressure, and the aqueous remainder was lyophilised and analysed by ^{31}P NMR spectroscopy. The results are shown in Figure 2.7.

The same trend as the previous optimisation process is apparent; the conversion levels rise with pH up to 12, after which additional phosphorus-containing species begin to appear in the ^{31}P NMR spectrum, likely due to hydrolysis under these basic conditions. Higher conversions are achieved, and
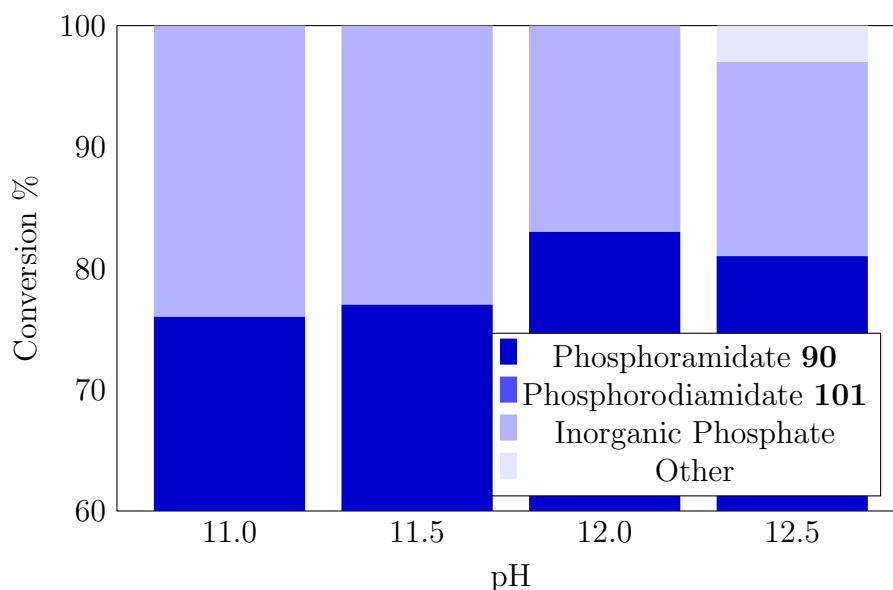
Figure 2.7: The results of the phosphorylation of aminoguanosine with potassium phosphodichloridate, derived from ^{31}P NMR spectroscopy data. Note that the *y*-axis begins at 60%.

no trace of diamidate products **101** are observed when the phosphodichloridate is used as the phosphorylating agent.

2.2.5   Discussion

There are several conclusions which can be drawn from this series of experiments. The first and most obvious comes from the fact that formation of a diamidate product (highlighted in red in Scheme 2.9) was observed when phosphoryl chloride was used as the phosphorylating agent, but not when the dichloridate was used. Formation of phosphorotriamidate was not observed under any conditions.

Crunden and Hudson have proposed that the reaction of the phosphorus-halide bond proceeds through an S_N2-type displacement, and that steric effects dominate.[123] Following this line of reasoning, the phosphorodiamidic chloride **106** would be sterically congested, and attack by another bulky aminodeoxynucleoside to form the *tris* adduct **109** would be difficult. The
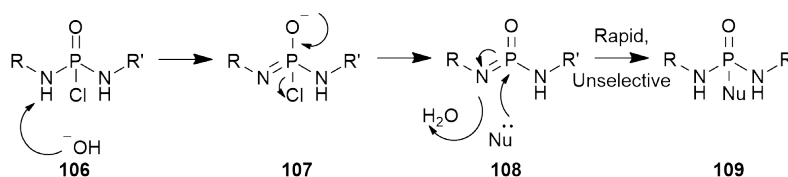
Scheme 2.8: Traylor and Westheimer proposed a monomeric metaphosphate intermediate in the reaction of phosphorodiamidic chlorides.[122]

phosphorodiamidic chloride **106** thus hydrolyses instead, to produce the diamidate product. This does not appear to explain why the reaction with the phosphodichloridate as the phosphorylating agent produces no diamidate; the monochloridate intermediate **114** does not appear to be more sterically hindered than the phosphoramidic dichloridate **110**, which may proceed to form the diamidate.

Traylor and Westheimer, on the other hand, have contended that phosphorodiamidic chlorides which possess primary or secondary phosphoramidates, *i.e.* the neutral amide has a hydrogen bonded to the nitrogen, can be deprotonated, leading to the elimination of chloride to form a monomeric metaphosphate intermediate **108**.[122] This reactive intermediate could then react rapidly with a nucleophile in an S_N1 type reaction, in which the intrinsic nucleophilicity of the nucleophile is of little importance. The reaction thus depends only on the concentrations of the nucleophilic species. Since water is in great excess over the amine, only the hydrolysis product is observed, with negligible quantities of the aminolysis product. This would account for the fact that no *tris* adducts are observed. The hydrolysis of the monochloridate intermediate **114** possibly proceeds *via* a similar mechanism, and would thus explain why no diamidate is observed.

The lack of diamidate **115** formation in the reaction with phosphorodichloridate is a great advantage of this method; not only does the smaller number of products simplify potential purification, but formation of the diamidate product also reduces the availability of amine. In a one to one reaction of phosphorylating agent and amine, for every molecule of the diamidate
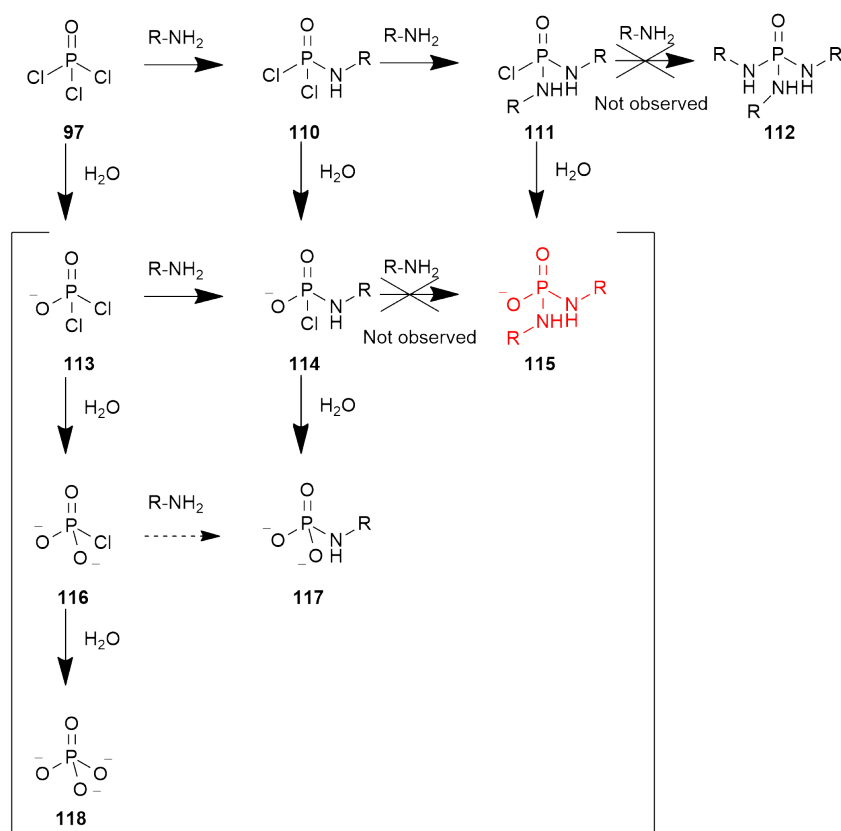
Scheme 2.9: The various pathways the phosphorylation reaction with phosphoryl chloride can take to form the products. The bracketed area illustrates the pathways the reaction with phosphodichloridate can take.

compound formed, there is one less molecule of amine to react, and thus a molecule of inorganic phosphate is formed instead.

2.3   Application to Other Nucleoside Derivatives

With the procedure optimised both for oxyphosphorylation and thiophosphorylation on 5′-amino-5′-deoxyguanosine **89**, the process was applied to other nucleoside derivatives to explore whether similar conversions could be achieved. To this end, a number of 5′-amino-5′-deoxynucleosides were syn-

thesised.

2.3.1   5′-Amino-5′-deoxyadenosine Synthesis

Kolb *et al.*[124] developed a straightforward synthetic route to the dihydrochloride salt of 5′-amino-5′-deoxyadenosine **122**. In this protocol, adenosine was first protected at the 2′- and 3′- positions with an isopropylidene group (this protected adenosine **119** is commercially available, and so can serve as our starting point). The 5′- hydroxyl group was then replaced by phthalimide in a Mitsunobu-type reaction. In analogy with a Gabriel synthesis, the masked amine was liberated by refluxing the compound in hydrazine. The isopropylidene protecting group was removed with formic acid, and the residue was dissolved in ethanol. The dihydrochloride salt **122** was precipitated by bubbling hydrogen chloride gas through the solution, and after filtration the authors claim no further purification was required.
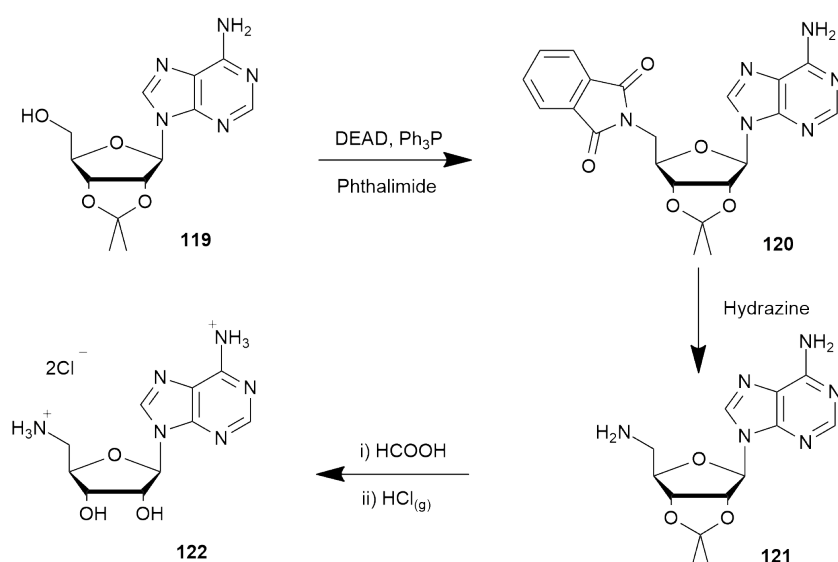
Scheme 2.10: The synthesis of 5′-amino-5′-deoxyadenosine, dihydrochloride salt **122** reported by Kolb *et al.*[124]

The dihydrochloride salt of 5′-amino-5′-deoxyadenosine **122** was synthesised by this method. The route produced the desired compound in a straightforward manner with no laborious purification requirements.

2.3.2   5′-Amino-5′-deoxycytidine Synthesis
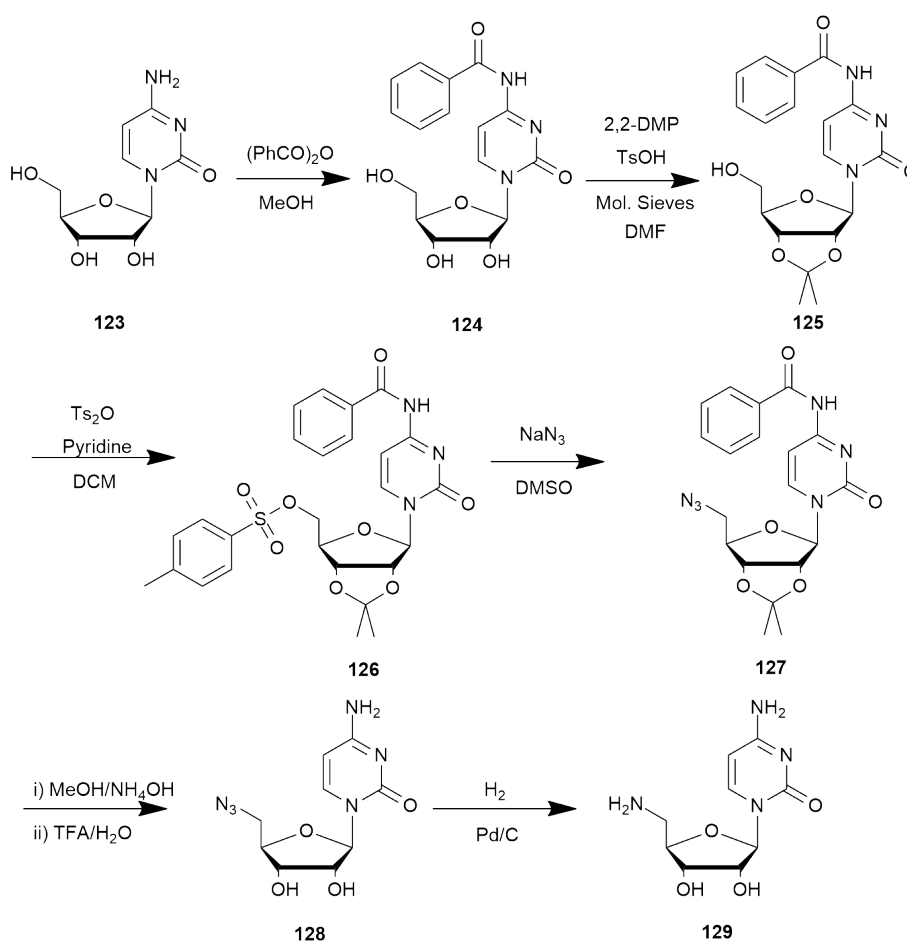
Scheme 2.11: The synthetic pathway to 5′-amino-5′-deoxycytidine **129**, partially developed by Jon Neville.

The method followed for the synthesis of 5′-amino-5′-deoxycytidine **129**, was that partially developed by Jon Neville, within the Hodgson group. The amine on the cytidine nucleobase was first protected by benzoylation. The 2′- and 3′- hydroxyl groups were then protected as an isopropylidene ketal, using 2,2-dimethoxypropane. The 5′- position was activated through tosylation, then substituted for an azide. Deprotection was accomplished by stirring in ammonia solution, followed by trifluoroacetic acid solution. This yields the trifluoroacetate salt of the azide, and ion exchange chromatography was required to produce the free base **128**. Up to this point, the method required no chromatography, and while the ion exchange does present a bottleneck, the fact that it occurs late in the synthesis means that it is not hugely problematic.

The final step is reduction of the azide **128** to an amine **129**. Jon Neville used hydrogenation to accomplish this, however, I encountered problems with overreduction (at the nucleobase carbon-carbon double bond) and the reluctance of the reaction to go to completion.

Reduction of the azide through a Staudinger reduction was therefore attempted, however, this appeared to give two products, and the reaction could not be forced to completion.

The next method tried was reduction by sodium thiophosphate, which was developed within the Hodgson group (see chapter 5 for further details). This reaction is normally performed on rather hydrophobic amines, which can then be extracted into an organic solvent. In contrast to this, both azido- and aminonucleosides are exceedingly hydrophilic, and cannot be separated from the salt byproducts by extraction. Instead, the phosphate and thiophosphate salts were removed by precipitation with methanol. The solution was acidified, which causes polysulphide byproducts to break down into elemental sulphur, which precipitated, and hydrogen sulphide, which was lost to the atmosphere. Finally, the protonated amine was isolated by ion exchange chromatography.

The reaction was first performed on a small scale, in D_2O, and monitored

by ^{1}H NMR spectroscopy to get an idea of the timescale of the reduction (Figure 2.8).
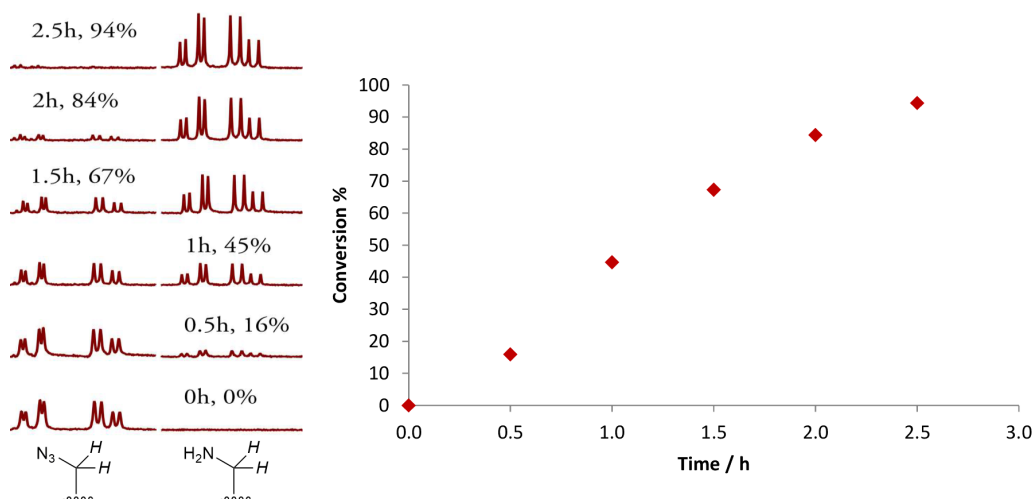
Figure 2.8: The conversion of 5′-azido-5′-deoxycytidine **128** to the 5′-amine **129**, by sodium thiophosphate, determined by monitoring the appearance/disappearance of the 5′- protons. Note the characteristic sigmoid shape of the curve – see chapter 5 for further details.

It can be seen that the reaction was almost complete after three hours, and so a reaction time of four hours was deemed sufficient to ensure full conversion. The free base was isolated as described above. The protonated amine was loaded on to a cation exchange column and washed with water to remove non-cationic impurities. Washing the column with a solution of ammonium hydroxide followed by lyophilisation produced the unprotonated amine. The thiophosphorylation procedure was attempted using this material, however, there appeared to be residual salts in the material, leading to disappointing levels of conversion.

After the failure of these reduction methods, the Staudinger reduction was revisited. It was found that when acid was added to the crude product

of the reaction, the NMR peaks resolved into those of a single compound. This indicated that the reaction was complete, but speciation was occurring. The compound was therefore isolated as the dihydrochloride salt by dissolving it in the minimum quantity of ethanol and bubbling hydrogen chloride though until the product precipitated out. Upon thiophosphorylation, however, this material gave rise to two peaks corresponding to thiophosphoramidates; one appeared to be the desired product, while the other showed no coupling pattern. This led me to believe that residual ammonia from the Staudinger reaction work-up could have been retained, and had reacted with the thiophosphorylating agent under the reaction conditions to produce this side product. Refluxing the crude material in water for several hours before lyophilisation appeared to remove the hypothesised residual ammonia, and the phosphorylation reactions were carried out successfully, as described in section 2.3.5.

2.3.3 3′-Amino-3′-deoxythymidine Synthesis

3′-Amino-3′-deoxythymidine was chosen as a possible test substrate for our aqueous phosphorylation procedure because the 3′-azide **130** (an antiretroviral drug more commonly known as AZT) is readily available. A number of methods for the synthesis of the 3′-amine from this compound are described in the literature, including reduction with triphenylphosphine in pyridine,[125] catalytic hydrogenation,[126, 127] hydrogen sulphide in pyridine,[128] and free radical reactions with silanes and stannanes.[129, 130]

The procedure used by Cano-Soldado *et al.*[125] was adapted for the synthesis of 3′-amino-3′-deoxythymidine. Commercially available 3′-azido-3′-deoxythymidine **130** was reduced with triphenylphosphine in pyridine, followed by the addition of ammonia solution. The mixture was then diluted with water, and extracted with chloroform to remove pyridine, triphenylphosphine oxide, and residual triphenylphosphine. The aqueous remainder was then lyophilised. The product was isolated as the hydrochloride salt **131** by dissolving the crude material in ethanol and bubbling hydrogen chloride gas
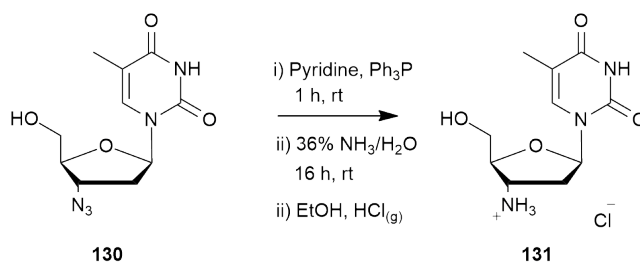
Scheme 2.12: The reduction of AZT to 3′-amino-3′-deoxythymidine and formation of the hydrochloride salt.

through until precipitation occured, then filtering.

2.3.4 5′-Amino-5′-deoxyuridine Synthesis

Two main methods of synthesising 5′-amino-5′-deoxyuridine **135** are reported in the literature.[131,132] Winans and Bertozzi first protected the 2′- and 3′-positions on uridine with an isopropylidene group, then tosylated the 5′-position. The tosyl group was displaced by an azide, and the isopropylidene group was removed using trifluoroacetic acid. The azide **134** was reduced to an amine **135** with hydrogen over a palladium catalyst.[131]

An alternative method for the synthesis of the azide was reported by Yamamoto, Sekine, and Hata, in which the 5′-azide **137** was produced in a single step from unprotected uridine **136** in a variation on the Appel reaction.[132] The azide was then reduced to the amine with hydrogen over a palladium catalyst, as in the method developed by Winans and Bertozzi. There are also reports in the literature of the use of a Staudinger-type reaction to produce the amine.[133]

The method for the synthesis of 5′-azido-5′-deoxyuridine **137** developed by Yamamoto *et al.* was followed, with a minor adaptation. In the original method, triphenylphosphine and triphenylphosphine oxide must be separated from the product by column chromatography. These unwanted compounds were exceedingly difficult to remove completely. However, it was found that the hydrophilic product of the reaction (along with unreacted starting mate-
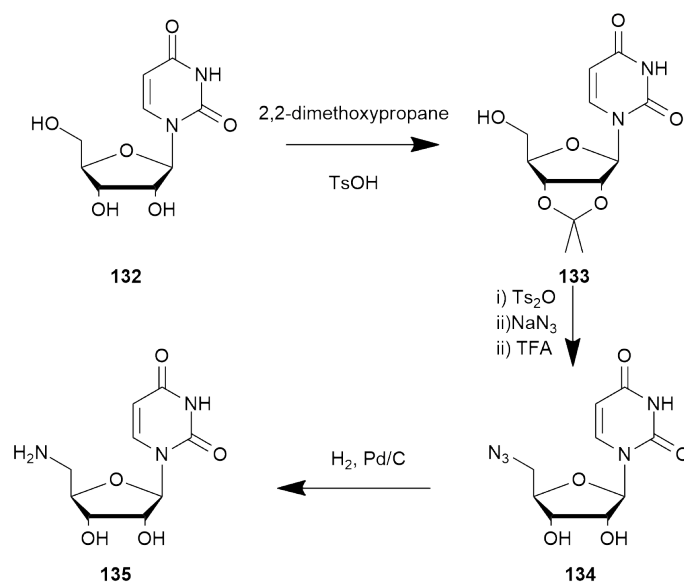
Scheme 2.13: Winans and Bertozzi's synthesis of
5′-amino-5′-deoxyuridine **135**.[131]
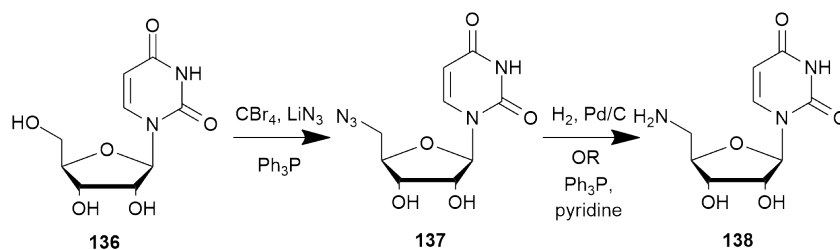
Scheme 2.14: Yamamoto, Sekine, and Hata developed a direct route to
5′-azido-5′-deoxyuridine **137**, which allows access to the amine *via*
reduction.[132]

rial) could be dissolved in water, while the highly hydrophobic triphenylphos-
phine and its oxide could be extracted with chloroform. After the aqueous
layer was lyophilised, chromatography of the crude product was trivial.

The reduction of the azide proved problematic, for the same reasons as de-
scribed in the synthesis of 5′-amino-5′-cytidine **129** (section 2.3.2), *i.e.* what
appears to be speciation of the product. This was solved in the same manner,
and the 5′-amino-5′-deoxyuridine **138** was isolated as the hydrochloride salt.

2.3.5   Aminonucleoside Phosphorylations

The thiophosphorylations were carried out using both thiophosphoryl chloride **99** and thiophosphodichloridate **100** on 5′-amino-5′-deoxyadenosine **122**, 5′-amino-5′-deoxycytidine **129**, 3′-amino-3′-deoxythymidine **131**, and 5′-amino-5′-deoxyuridine **138**. The oxyphosphorylations were performed using both oxyphosphorylating agents on 5′-amino-5′-deoxyadenosine **122** and 3′-amino-3′-deoxythymidine **131**. In every case, one equivalent of phosphorylating agent was used, and the phosphorylations were performed at pH 12, the optimum pH as determined in the optimisation experiments.
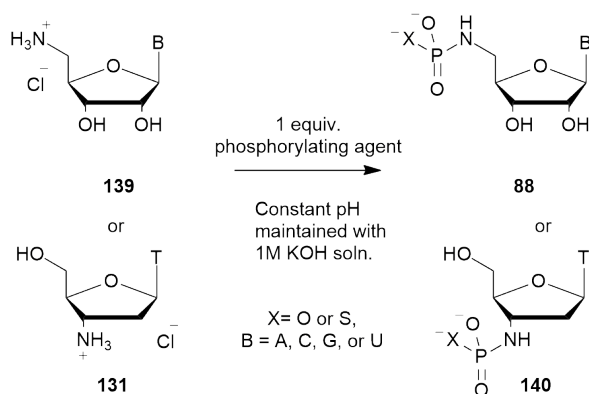
Scheme 2.15: The phosphorylations of the aminonucleosides

The results of the thiophosphorylations and oxyphosphorylations of 5′-amino-5′-deoxyadenosine **122** can be seen in Figure 2.9. Very high levels of conversion were observed for both thiophosphorylating agents; 90% in the case of thiophosphodichloridate **100**, and close to 100% for the reaction with thiophosphoryl chloride **99**. No diamidate products were observed in either case. In the oxyphosphorylation reactions, on the other hand, the conversions were significantly lower at around 73%. The phosphorylation with phosphoryl chloride **97** produced a relatively large quantity of diamidate product.
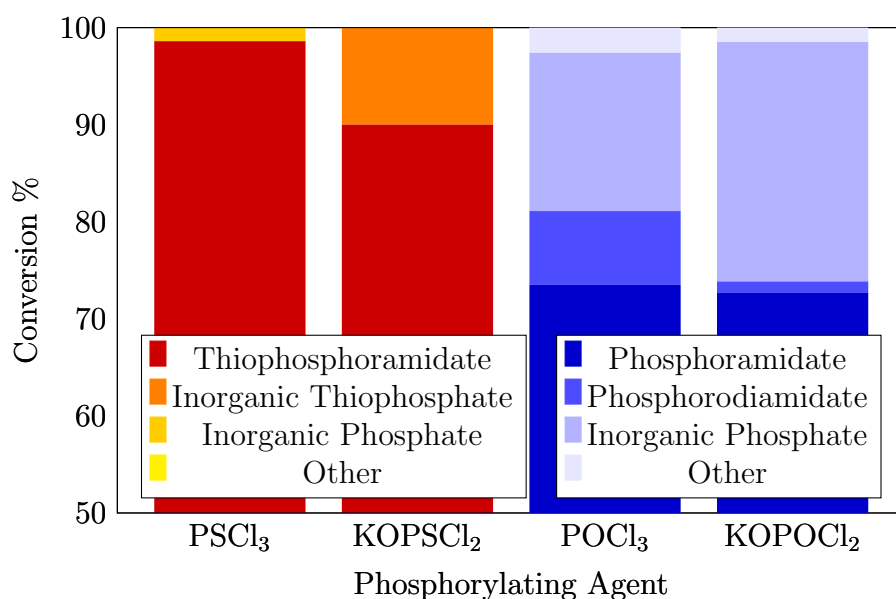
Figure 2.9: The results of the thiophosphorylations and oxyphosphorylations 5′-amino-5′-deoxyadenosine **122**, derived from ^{31}P NMR spectroscopy data. Note that the y-axis begins at 50%.

Unusually, a very small amount, approximately 1%, was also seen in the reaction with phosphodichloridate **98**. This may be due to residual phosphoryl chloride in the phosphorylating agent.

Both the thiophosphorylations and oxyphosphorylations of 3′-amino-3′-deoxythymidine **131** (Figure 2.10) were much less effective than the phosphorylations of the 5′-amino-5′-deoxynucleosides, this was perhaps due to the greater accessibility of the 5′- position. Thiophosphoryl chloride **99** proved to be the most efficient phosphorylating agent, although it did produce small quantities (*circa* 0.5%) of the diamidate side product which was not observed at all when the thiophosphodichloridate **100** was used. For the oxyphosphorylating procedure, meanwhile, oxyphosphoryl chloride **97** gave a lower level of conversion to the phosphoramidate than its phosphodichloridate counterpart **98**.

5′-Amino-5′-deoxycytidine **129** and 5′-amino-5′-deoxyuridine **135** both performed well as substrates for the thiophosphorylation procedure (Figure 2.11).
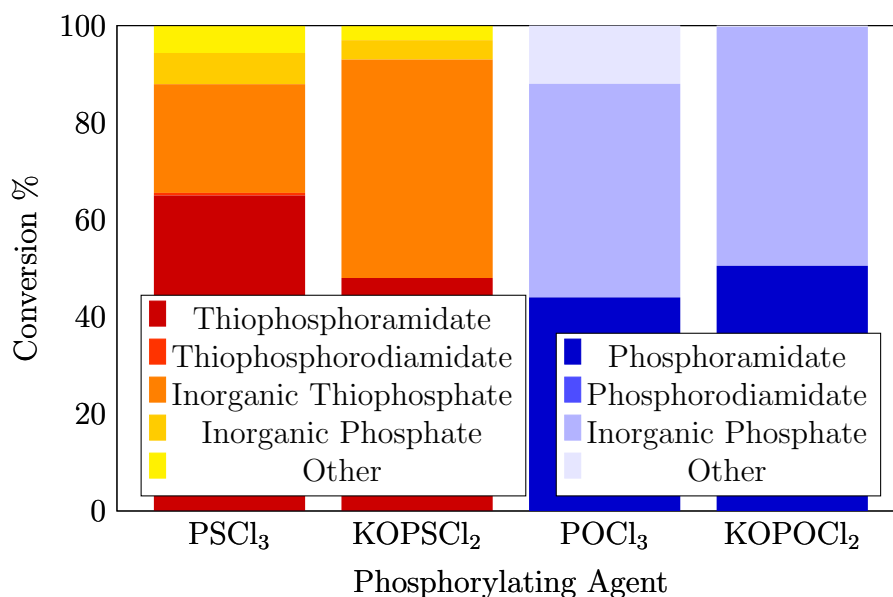
Figure 2.10: The results of the thiophosphorylations and oxyphosphorylations 3′-amino-3′-deoxythymidine **131**, derived from ^{31}P NMR spectroscopy data.

Conversions of over 90% were observed for both amines when phosphoryl chloride **97** was used as the the phosphorylating agent, accompanied in the case of 5′-amino-5′-deoxyuridine **135** by the formation of some diamidate product. The thiophosphodichloridate **100** was again less efficient, with conversions of around 80%.

The collected results of the experiments are shown in Figure 2.12. The conversion levels for the thiophosphorylations of the aminonucleosides were generally high, especially for the reactions of 5′-amino-5′-deoxyguanosine **89** with thiophosphodichloridate **100** and 5′-amino-5′-deoxyadenosine **122** with thiophosphoryl chloride **99**, with conversions of 97% and 99% respectively. A notable exception to the high thiophosphorylation conversions was the reaction with 3′-amino-3′-deoxythymidine **131**; this is likely due to the more sterically hindered environment of the 3′- position.

Use of thiophosphoryl chloride **99** gave greater levels of conversion than the thiophosphodichloridate ion **100**, with the exception of the reaction with 5′-
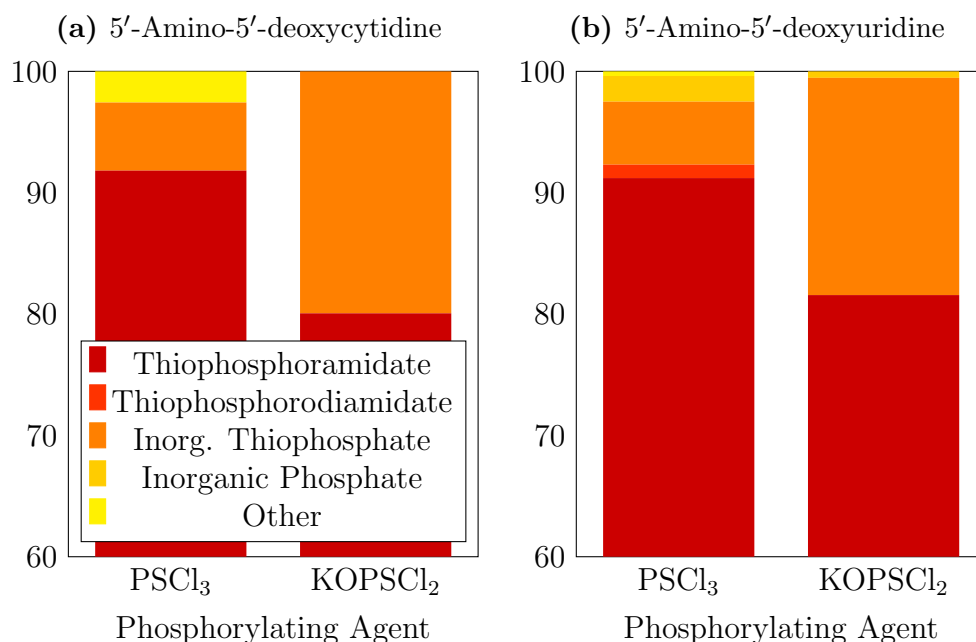
Figure 2.11: The conversion levels for the thiophosphorylations of 5′-amino-5′-deoxycytidine **129** and 5′-amino-5′-deoxyuridine **135**, as determined by ^{31}P NMR spectroscopy. Note that the y-axes begin at 60%.

amino-5′-deoxyguanosine **89**. Unlike the thiophosphodichloridate ion, thiophosphoryl chloride shows very limited solubility in water. This may give rise to the improved selectivity, despite thiophosphoryl chloride's greater reactivity, possibly through reaction at interfaces rather than in homogeneous solution.

In other cases, the advantage of potassium thiophosphodichloridate as a thiophosphorylating agent is that it produces fewer side-products such as the thiophosphorodiamidate. For the oxyphosphorylating agents, the trend appears to be reversed; the phosphodichloridate reactions tended to give the greatest levels of conversion, possibly due to the longer reaction times allowing better mixing and thus greater selectivity than with phosphoryl chloride. In general, the levels of conversion for the oxyphosphorylations are more moderate than those of the thiophosphorylations with a maximum of 83% for the reaction of 5′-amino-5′-deoxyguanosine **89** with phosphodichloridate **98**. 3′-
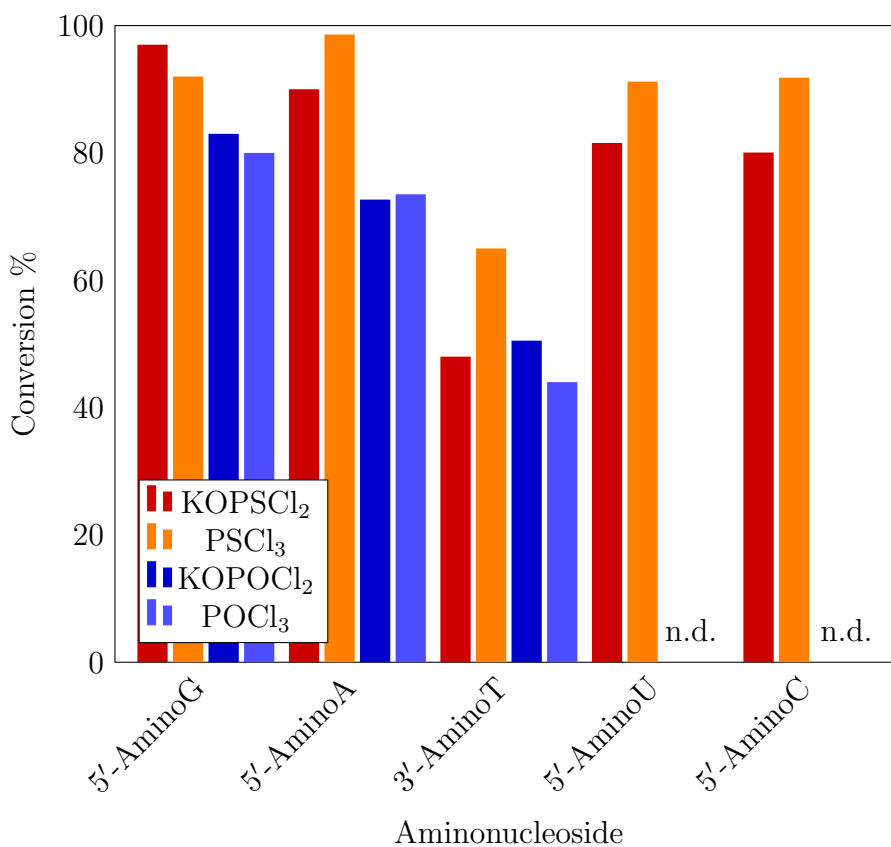
Figure 2.12: Conversion levels for the phosphorylations and thiophosphorylations of the aminonucleosides, including those determined for the thiophosphorylation of 5′-amino-5′-deoxyguanosine **89** by Richard Delley

Amino-3′-deoxythymidine **131** again showed the poorest conversions, at 44% and 51% for the reactions with oxyphosphoryl chloride **97** and oxyphospho-dichloridate **98** respectively.

2.4   Conclusion

The phosphorylation of 5′-amino-5′-deoxyguanosine **89** has been optimised, and the optimum pH has been found to be 12, similar to that of the thiophos-phorylations optimised by Richard Delley, although the variation with pH is

not so pronounced. The 5′-amino-5′-deoxy derivatives of the other natural ribonucleosides (adenosine, cytidine, uridine) and 3′-amino-3′-deoxythymidine have been synthesised, and in the case of the cytidine and uridine derivatives, the syntheses have been improved upon. These 5′-amino-5′-deoxy nucleosides have all been thiophosphorylated and shown high levels of conversion. It has been shown that the use of thiophosphodichloridate is a viable alternative to thiophosphoryl chloride; while the use of the dichloridate tends to decrese the conversion, it does eliminate the formation of undesired diamidate side products.

It had been hoped that the aminonucleosides would be easily prepared, and thus allow a facile synthesis of the nucleoside phosphoramidates and thiophosphoramidates from start to finish. In the case of some of these, such as 5′-amino-5′-deoxyguanosine **89** and 5′-amino-5′-deoxyadenosine **122**, this is the case. With the cytidine, thymidine, and uridine derivatives, however, extensive problems were encountered during their synthesis. However, the improved syntheses described here have made these compounds much more accessible.

Further investigations following on from this work could include methods for the isolation of the phosphoramidates through selective precipitation, or application of this methodology to the synthesis of analogues of natural compounds, such as the NMP sugars described in section 1.1, or the thymidylyl-thymidine analogue described in the following chapter.

Chapter 3

The Synthesis of 3′-Amino-3′-deoxythymidylyl(3′→5′)-5′-deoxy-5′-thiothymidine

3.1 Introduction

With the N-thiophosphorylation of aminodeoxynucleosides in hand and optimised, we sought to apply this knowledge to the synthesis of mimics of biological phosphate systems. The first target was an analogue of thymidylyl-3′,5′-thymidine **141** (TpT), in which the phosphate bridge is replaced by a thiophosphoramidate **142**.

There were several reasons for choosing this compound as a target. The main reason was that it could serve as a model for future experiments using an single stranded nucleic acid template to bring together and ligate two oligonucleotide strands, one possessing a thiophosphorylated terminus, the other having an alkylating agent at its terminus (see section 1.2.4). The analysis of this compound could also provide information on the characteristics of the thiophosphoramidate group such as its effect on the ribose conformation of the nucleosides it is bound to, and its hydrolytic stability.
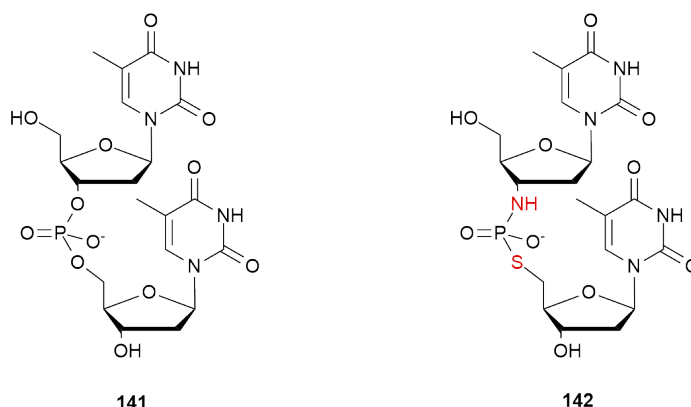
Figure 3.1: Thymidylyl-3′,5′-thymidine **141** and a thiophosphoramidate analogue **142**

Synthetically speaking, this target had several appealing advantages; the starting materials required to synthesise this molecule - 3′-amino-3′-deoxythymidine **55**, and thymidine modified to possess a 5′- leaving group **41** - are relatively easily accessible. Additionally, the use of nucleosides means that the product will possess a good chromophore, the lack of which would render chromatographic purification much more difficult. The UV/vis activity of both organic fragments attached to the thiophosphoramidate will also be very useful in any further studies which might require UV/vis techniques (for example, the HPLC-based kinetic analyses in chapter 4).

3.2   Synthesis

The synthesis of the required amine, 3′-amino-3′-deoxythymidine **55**, was described in 2.3.3. At that time, the pH optimisation described in chapter 2 had not yet been performed, and so the thiophosphorylation was carried out based on the procedure developed by Milena Trmčić,[49] with 1.5 equivalents of thiophosphoryl chloride **99** being used to try to ensure complete thiophosphorylation.

^{31}P NMR analysis of the resulting solution showed a major signal, and a cluster of smaller signals (collectively comprising approximately 60 % of the
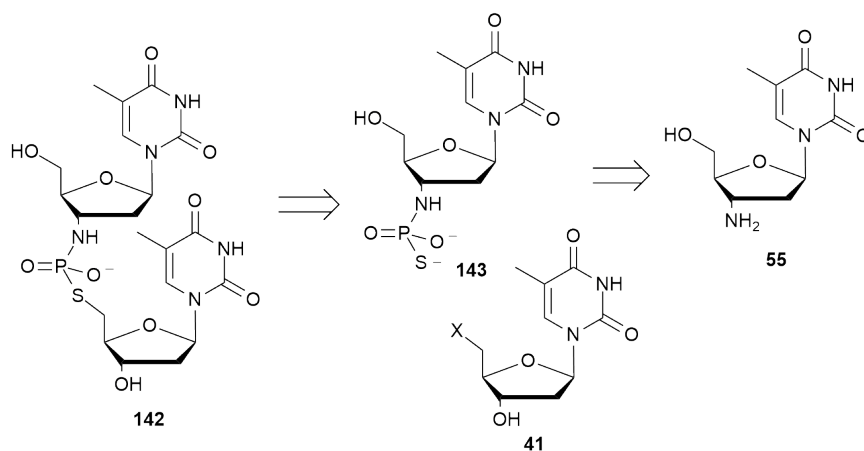
Scheme 3.1: The retrosynthesis of the dinucleoside thiophosphoramidate.
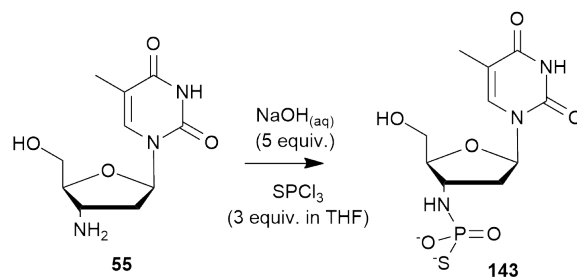
Scheme 3.2: The first attempt at thiophosphorylating 3′-amino-3′-deoxythymidine **55**.

total phosphorus-containing compounds) in the 40 - 45 ppm chemical shift region corresponding to the desired product.

5′-Deoxy-5′-tosylthymidine **145** was initially chosen as the alkylating agent. A literature procedure for the synthesis is available[134] which calls for chromatographic purification of the crude product. As this was quite time consuming and laborious (the crude material was sparingly soluble in the ethanol / chloroform flash chromatography solvent system described) it was found to be more expedient to simply purify the material through recrystallisation from water. This produced a pure product, albeit at the cost of a slightly reduced yield.

The *S*-alkylation of the thiophosphoramidate **143** was then attempted using
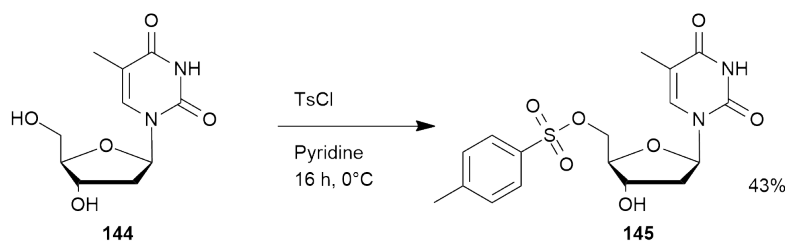
Scheme 3.3: The selective tosylation of thymidine

5′-deoxy-5′-tosylthymidine **145** as the alkylating agent. As the 5′-deoxy-5′-tosylthymidine **145**was found to be very sparingly soluble in water, it was dissolved in THF before being added to the solution of (5:3 water/THF) thiophosphorylated 3′-amino-3′-deoxythymidine. Despite the use of organic solvent, the tosylate did not dissolve fully in the reaction mixture. In spite of this, the mixture was stirred for 20 hours in the hope that if the alkylating agent was at least partly soluble, the reaction could go forward. The precipitate was then removed by centrifugation and the solvents were removed from the remaining solution first under vacuum, then by lyophilisation before the residual solid was analysed by ^{1}H and ^{31}P NMR spectroscopy. The ^{31}P NMR spectrum showed no signals in the 20-25 ppm chemical shift region, indicating that the alkylated thiophosphoramidate **142** was not present. The synthesis was thus unsuccessful, and this was ascribed to the poor solubility of the alkylating agent.

A better solvent was required, and so during the next attempt the residual THF from the thiophosphorylation step was removed under reduced pressure, and the aqueous remainder was freeze-dried. The residue was mixed with tosylated thymidine **145** and dissolved in DMSO-d$_6$. Some undissolved material could still be observed.

This reaction too was unsuccessful, with no product being observed by ^{31}P NMR spectroscopy. Under the reaction conditions, the reactants were again poorly soluble, and the use of organic solvents possibly also destabilised the ionic intermediates and product (phosphoramidates have been shown to hydrolyse more quickly in dioxane/water mixtures than in water).[135] Based on
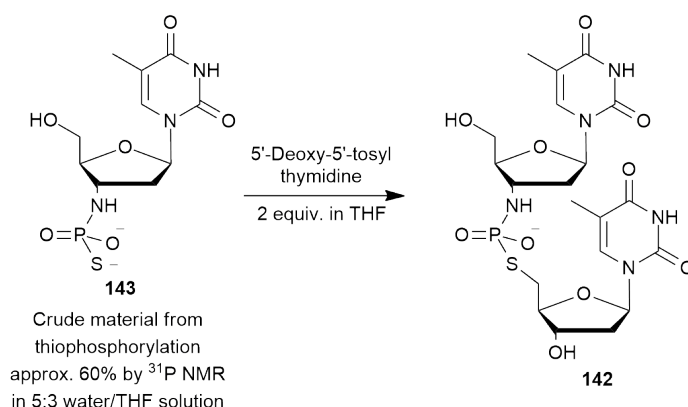
Scheme 3.4: The first attempt to alkylate the thiophosphoramidate used THF as the solvent to try to dissolve the alkylating agent.
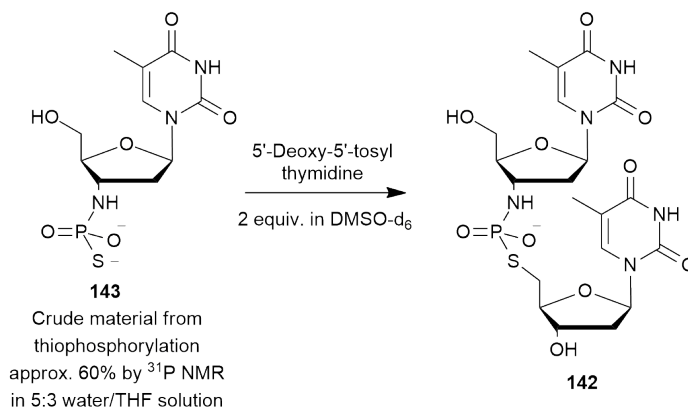
Scheme 3.5: The second attempt used DMSO-d_6 as the solvent, but was still unsuccessful.

this assumption, a fully aqueous solvent system should be an improvment. This would also have the advantage of simplifying purification by ion exchange chromatography. It was therefore decided to carry out the reaction in water, and to deprotonate the alkylating agent to force it into solution. The N-3 proton on thymidine has a pK_a of 9.93[117] (see Figure 3.2), and the pK_a of the tosylated analogue **145** could be expected to be similar, and so by using a reaction pH of approximately 12 the alkylating agent could be expected to be almost fully solubilised.
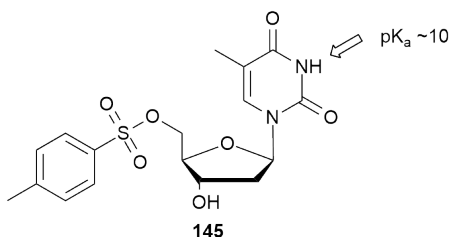
Figure 3.2: the pK_a of 5′-deoxy-5′-tosylthymidine **145** N-3 proton is
estimated to be approximately 10

Since there is no requirement for organic solvent in this new scheme of alkyla-
tion (and indeed its presence may decrease the solubility of the deprotonated
alkylating agent), the organic solvent was removed from the intermediate un-
alkylated thiophosphoramidate **143** under vacuum before its inclusion in the
reaction mixture. The aqueous residue was then lyophilised before being re-
dissolved in D_2O, to allow the reaction to be followed by NMR spectroscopy.
The alkylating agent was added, along with one equivalent of 1 M sodium
deuteroxide (to account for the hydroxide consumed in the deprotonation of
the alkylation agent). After heating for 18 hours at 80 °C, the pH of the
solution was found to have dropped to approximately 7. The solution was
analysed by ^{31}P NMR spectroscopy and found to contain mostly inorganic
phosphate (approximately 85% of phosphorus-containing species). However,
a small quantity of the desired product **142** (around 9% with a ^{31}P NMR
chemical shift of 22 ppm) along with some *S*-alkylated thiophosphate **149**
(chemical shift of 16 ppm) and the thiophosphoramidate starting material
143 (chemical shift of 41 ppm) were also evident within the mixture.

The production of inorganic phosphate indicates that hydrolysis had drasti-
cally affected the yield of product – whether this was due to the breakdown
of the product, the thiophosphoramidate intermediate, or both, is not clear.
The synthesis of the unalkylated thiophosphate has shown (in section 2.3.5 -
optimal pH for the thiophosphorylation is 12) to be relatively stable at high
pH, albeit at shorter reaction times and lower temperatures, and as a dianion
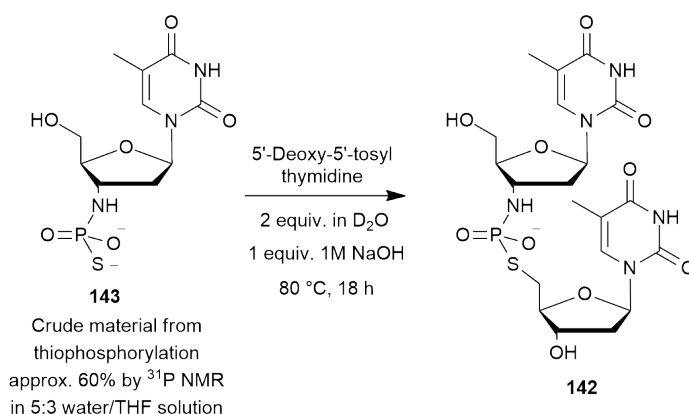
Scheme 3.6: The third attempt was performed using only water as the solvent, at a sufficiently high pH to deprotonate and thus solubilise the alkylating agent.

seems likely to be more stable than the monoanionic product due to repulsion of the negatively charged hydroxide ions. At lower pH, however (such as the pH of the reaction mixture at the end of the reaction), the product may be stable, whilst the unalkylated thiophosphoramidate decomposes.

Whilst the reaction was partially successful, the levels of conversion observed were very low. There were a number of improvements which could be made to the reaction; in order to minimise reaction time, a more reactive alkylating agent could be used. Increasing the solubility of the alkylating agent would increase its effective concentration in solution, and thus decrease the reaction time. Greater control of pH would also be advantageous, as it could minimse the decomposition of starting material and product. A smaller number of equivalents of thiophosphoryl chloride could be used in the thiophosphorylation step; the excess, rather than increasing the conversion levels of the thiophosphorylation appears just to generate inorganic thiophosphate which then consumes the alkylating agent.

With these objectives in mind, 5′-deoxy-5′-tosylthymidine **145** was replaced with 5′-deoxy-5′-iodothymidine **148** as a more reactive alkylating agent. It was hypothesised that the relatively small iodide would be less hydrophilic than the large, organic tosyl group. The number of equivalents of thiophos-

phoryl chloride **99** was reduced to 1.2. The unalkylated thiophosphorami-
date **143** was again lyophilised and redissolved in water, and the pH was
raised to 12 using an autotitrator to add 1 M potassium hydroxide solution
as required. After addition of the alkylating agent, pH control was main-
tained, with potassium hydroxide solution being added automatically as the
5′-deoxy-5′-iodothymidine **148** was deprotonated and solubilised. After the
pH stabilised and the rate of addition of potassium hydroxide was negligible,
the solution was heated at 80 °C in a sealed flask for eighteen hours. Analysis
by ^{31}P NMR spectroscopy showed several peaks in the expected region for
the product, the largest of which integrated to 21% of the total of all peaks.
Purification by anion exchange chromatography was attempted, however,
two peaks were present which were very difficult to separate. The crudely
purified material, analysed by ^{31}P NMR spectroscopy, contained two species
in the thiophosphoramidate region. The mixture was purified by preparative
reversed-phase HPLC and a quantity of the thiophosphoramidate product
was isolated as the triethylammonium salt, with a total yield of 8%.
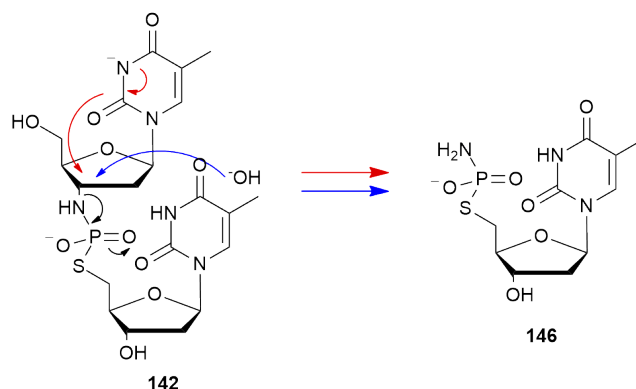
Scheme 3.7: Two possible mechanisms for the formation of the
S-linked thiophosphoramidate.

Interestingly, the other thiophosphoramidate species was also isolated, char-
acterised, and found to be the *S*-linked, *N*-nonbridging thiophosphoramidate.

Two possible mechanisms for the formation of nonbridged thiophosphorami-
date **146** are attack at the 3′- position by hydroxide, or the intramolecular
attack by the nucleobase, catalysed by hydroxide (Scheme 3.7). The produc-
tion of this compound shows that a balance must be achieved in the reaction
pH; if the pH is too low, the alkylating will not be solubilised, while if it is
too high, it was believed that the product could decompose (however, later
hydrolytic studies indicated that the thiophosphoramidate linkage is stable
even to very high pH, see chapter 4).
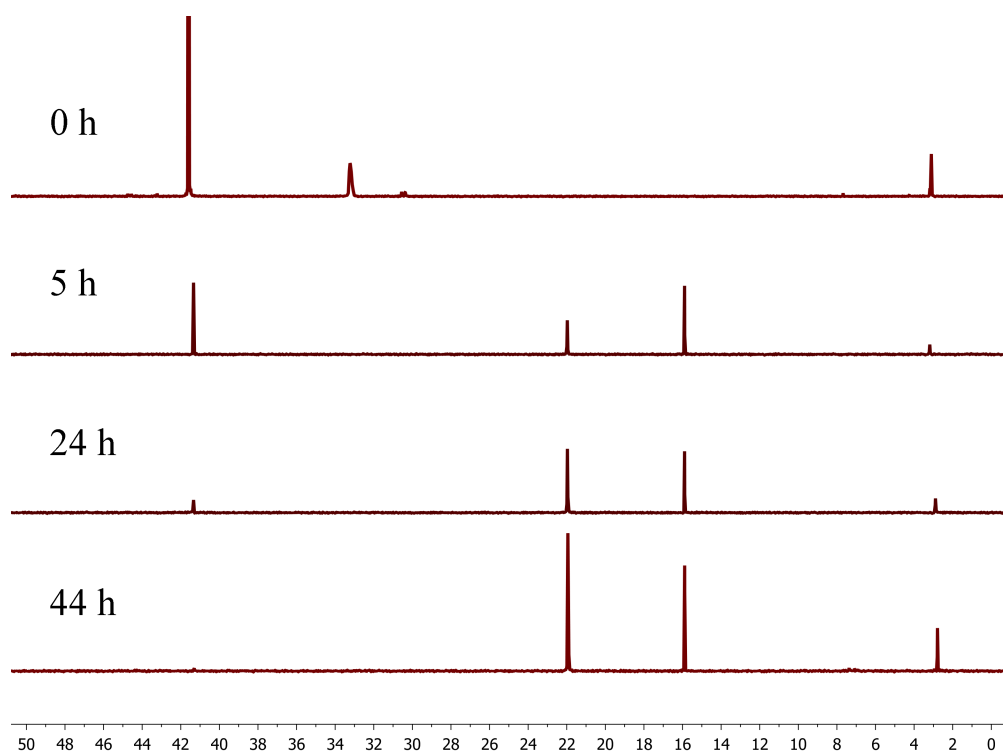
Figure 3.3: The alkylation of 3′-amino-3′-deoxythymidine
N-thiophosphate. The identities of the signals are as follows:
unalkylated thiophosphoramidate **143**, 41 ppm; inorganic thiophosphate
147, 33 ppm; alkylated thiophosphoramidate **142**, 22 ppm;
5′-deoxy-5′-thiothymidine S-phosphate **149**, 16 ppm; inorganic
phosphate **118**, 3 ppm.

Whilst the levels of conversion had increased, there was a lot of room for improvement. By this time, the thiophosphorylation procedure had been optimised for 3′-amino-3′-deoxythymidine **55**, as described in section 2.3.5. The solvents were removed from the resulting unalkylated thiophosphoramidate **143**, and the residue was then redissolved in 5 ml of water maintained at pH 12 with 1 M potassium hydroxide solution, as before. 5′-Deoxy-5′-iodothymidine **148** was added to the solution, and the pH maintained until complete dissolution had taken place. The reaction was then sealed and heated to 50 °C. A lower temperature was used this time, in the hope that it would reduce hydrolysis of both the alkylated and unalkylated thiophosphoramidates. The pH was not controlled after the heating began, and was allowed to drop as the reaction continued. The reaction was monitored by ^{31}P NMR spectroscopy at intervals, and the heating was continued until all the signal for the unalkylated thiophosphoramidate **143** had disappeared. This took two days to complete, after which the pH had dropped to 10.45. Close to complete conversion of the unalkylated thiophosphoramidate **143** to the product **142** was observed, with no side products apart from inorganic phosphate and 5′-deoxy-5′-thiothymidine *S*-phosphate **149** visible by ^{31}P NMR spectroscopy (this was performed upon aliquots of reaction mixture containing non-deuterated solvent and as such is inexact. However, it is useful for determining when all the starting mixture has been consumed.)

It can be seen from Figure 3.4 that the inorganic thiophosphate reacts very rapidly with 5′-deoxy-5′-iodothymidine **148** to form 5′-deoxy-5′-thiothymidine *S*-phosphate **149**.

The reaction mixture was again purified by anion exchange chromatography. The lack of side products greatly aided the purification procedure, as the *S*-linked, *N*-nonbridging thiophosphoramidate **146** appears to have similar ionisation characteristics to the product, and is quite difficult to separate by anion exchange chromatography. The only other side products - the *S*-alkylated thiophosphate **149** and inorganic phosphate - are multiply charged, and were thus easily separable from the singly charged product. The product was isolated as the triethylammonium salt, with a yield of 64% in terms of
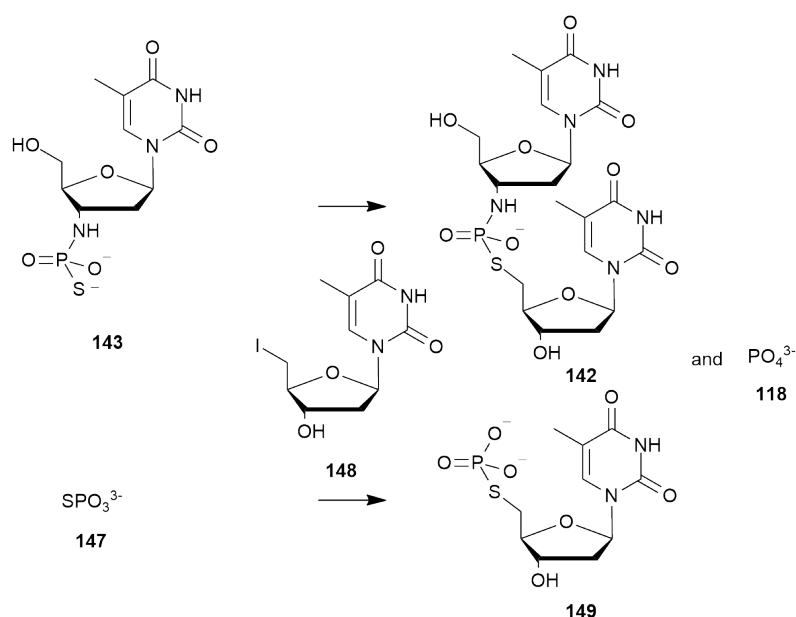
Scheme 3.8: The starting materials, products, and byproducts observed in the alkylation of 3′-deoxythymidine 3′-*S*-thiophosphoramidate **143**.

the 3′-amino-3′-deoxythymidine **55** as the starting material, or 98% in terms of the thiophosphoramidate **143** (although this might be overstated as the ^{1}H NMR spectroscopy integrals for the triethylammonium counter ion are larger than expected, so there may be residual salt present). This is a reasonable yield and a very large improvement over previous attempts to synthesise this compound.

3.3 Conformation of Dinucleoside 142

As described in section 1.3.1, the conformation of the ribose rings in an oligonucleotide significantly affects the ability of the oligonucleotide to form duplexes with complementary strands.[42,43] Investigation of the effect that modification of the phosphate group has on conformation is therefore important.

Many of the important signals in the ^{1}H NMR spectrum of the thiophospho-
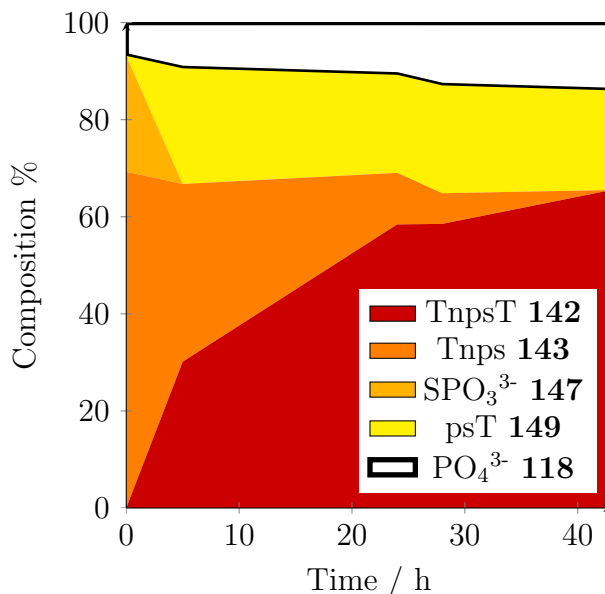
Figure 3.4: A plot of the composition of the reaction mixture with time. The legend refers to the following compounds: TnpsT, alkylated thiophosphoramidate **142**; Tnps, unalkylated thiophosphoramidate **143**; psT, 5′-deoxy-5′-thiothymidine S-phosphate **149**.

ramidate system appear at similar chemical shifts, and second-order coupling makes it difficult to extract the required J coupling values for many of the ribose protons. The shifts for the C1′- protons, however, are well separated, and the $J_{1'\text{-}2'}$ and $J_{1'\text{-}2''}$ coupling values are found to be 7.50 and 4.00 Hz, respectively for the 3′-amino-3′-deoxythymidine residue (Tnp). The C1′-H signal for the 5′-deoxy-5′-thiothymidine fragment (psT) presents as an apparent triplet with a coupling constant of 6.7 Hz (see Figure 3.5).

Rinkel and Altona[76] have found that the sum of the $J_{1'\text{-}2'}$ and $J_{1'\text{-}2''}$ coupling constants, $\Sigma H1'$, is linearly correlated with the proportion of the south conformer through the equation:

$$P_S = \frac{\Sigma H1' - 9.8}{5.9} \tag{3.1}$$

Where P_S is the proportion of the 'south' conformer.

6.30 6.29 6.28 6.27 6.26 6.25 6.24 6.23 6.22 6.21 6.20 6.19 6.18 6.17 6.16
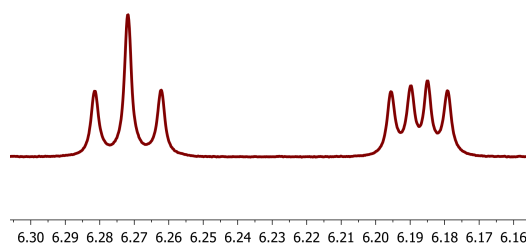
Figure 3.5: The signals corresponding to the C1′- protons in the dinucleoside system; to the left, the signal corresponding to the 5′-linked nucleoside, on the right, the signal corresponding to the 3′-linked nucleoside

The equation yields approximate values of 29% south for the Tnp part and 61% south for the psT part. Comparison with the natural TpT system[75,77] indicates that the substitution of nitrogen for oxygen has brought about a change in conformation of the Tnp ribose ring to become more 'north', C3′-endo, or 'RNA-like', while the psT part has retained its 'DNA-like' conformation. This is not surprising, as the conformation of the furanose ring is largely dictated by the anomeric and gauche effects, the lower electronegativity of nitrogen as compared to oxygen will reduce the gauche effect. The thiophosphoramidate group is not linked directly to the ribose ring of the psT fragment and so has no influence through the gauche or anomeric effect, and thus the conformational shifts can be expected to be smaller.

The conformational change is similar to that observed by Beevers *et al.* in the dideoxynucleoside 3′-phosphorothiolate analogue[75] (section 1.3.1).

3.4 Conclusions

3′-Amino-3′-deoxythymidylyl(3′→5′)-5′-deoxy-5′-thiothymidine **142** was successfully synthesised. The yield was moderate, due chiefly to low conversion in the thiophosphorylation of 3′-amino-3′-deoxythymidine **55** step. The conversion for the alkylation step (98%) was very high, and compares favourably with the alkylations reported by Delley (see section 2.1.2) although elevated temperature and relatively long reaction times were required.
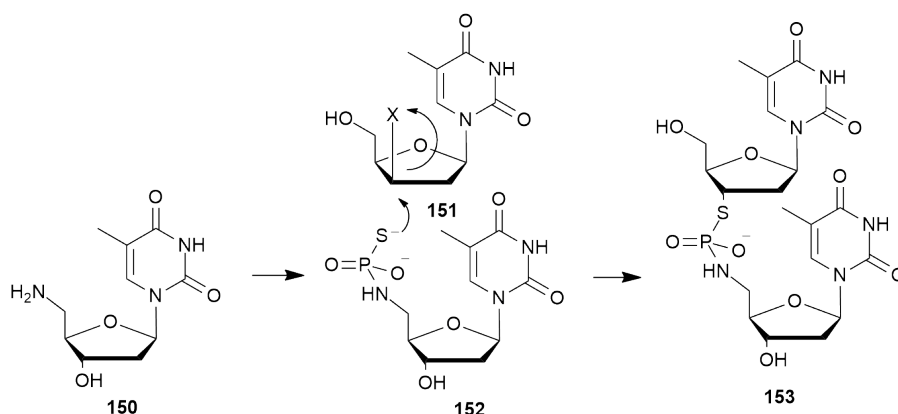
Scheme 3.9: A conjectured synthesis of
3′-deoxy-3′-thiothymidylyl(3′→5′)-5′-amino-5′-deoxythymidine **153**

As has been shown in section 2.3.5, the levels of conversion for the oxyphor-
sphorylation and thiophosphorylation of 3′-amino-3′-deoxythymidine **55** is
generally lower than those of the 5′-amino-5′-deoxynucleosides. It may there-
fore be possile to synthesise the 'reversed' thiophosphoramidate analogue,
i.e. 3′-deoxy-3′-thiothymidylyl(3′→5′)-5′-amino-5′-deoxythymidine **153** with
improved yield.

While the thiophosphorylation of the 5′- amine may be expected to be more
efficient, the alkylation step, which involves attack at a secondary centre,
may be more difficult. The preparation of the reagents, in particular the
alkylating agent, would also appear to be more synthetically challenging.

The approach to the synthesis of thiophosphoramidate compounds devel-
oped here may in the future be applied to the synthesis of other biologically
relevent molecules, such as analogues of nucleoside phosphate sugars **154** and
155 (see Figure 3.6).
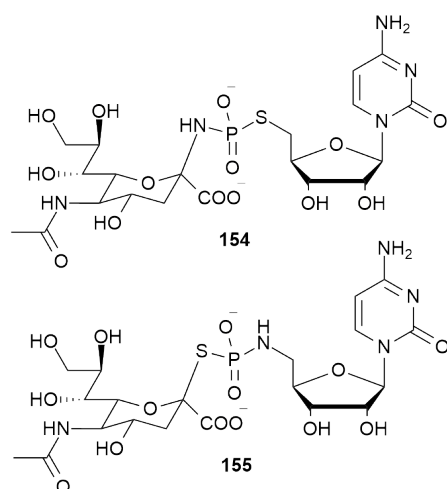
Figure 3.6: Two thiophosphoramidate analogues of
CMP-N-acylneuraminate. Using the methodology developed in this
chapter may allow the synthesis of compounds such as these.

Due to the efficiency of the alkylation reaction, this methodology shows
promise as a strategy for the ligation of nucleic acid strands, in a similar
manner to the techniques described in section 1.2.4. The use of a template
to bring the reactive moieties together may also accelerate the reaction and
allow it to be performed at a lower temperature.

Chapter 4

Hydrolysis Kinetics of the Thiophosphoramidate Group

4.1 Introduction
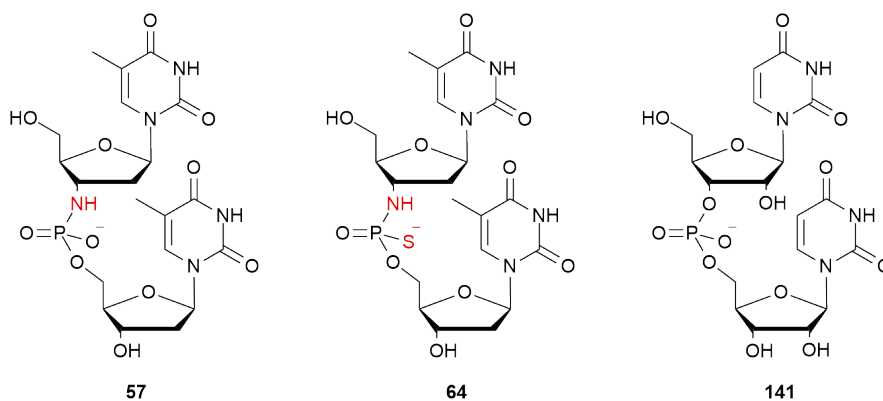
Figure 4.1: The phosphoramidate **57** and thiophosphoramidate **64** systems investigated by Ora *et al.*[46] and uridylyl(3′,5′)uridine, the hydrolysis of which was investigated by Järvinen *et al.*[5]

To further optimise the synthesis of the thiophosphoramidate linkage and determine what synthetic condtions it could withstand, and to investigate whether these compounds were stable under physiological conditions it was necessary to study how the hydrolytical stability of the thiophosphoramidate group is related to pH.

The hydrolytic properties of *N*- and *S*-linked thiophosphoramidates have not, to our knowledge, been studied before. Ora *et al.* have produced detailed pH - 'rate' profiles for the hydrolysis of 3′-*N* phosphoramidate **57** and *S*-nonbridging thiophosphoramidate **64** dinucleosides and the intermediates along the hydrolytic pathway.
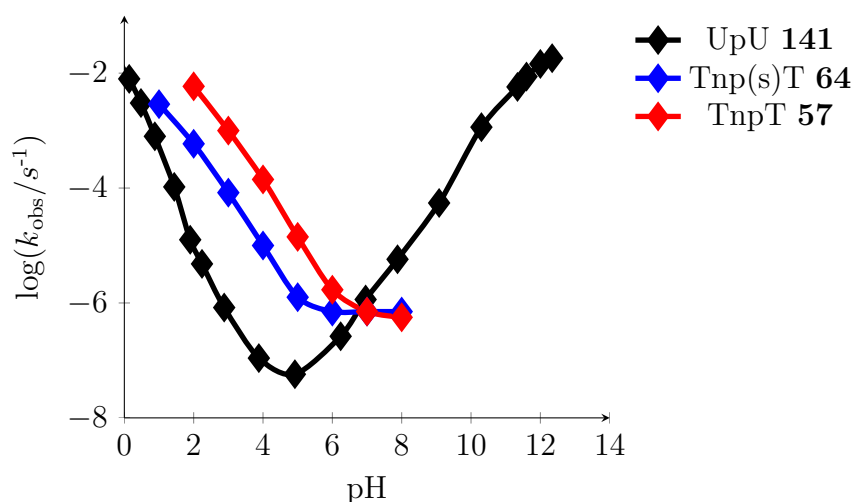
Figure 4.2: The pH-rate profiles determined by Ora *et al.* (Tnp(s)T and TnpT) and Järvinen *et al.* (uridylyl(3′,5′)uridine) at 90 °C.

They found that the thiophosphoramidates **64** (both R_P and S_P were studied) were more stable than the phosphoramidate **57**. Comparing with the pH-rate profile of uridylyl(3′,5′)uridine **141** (with a 'natural' phosphodiester bond, using the data determined by Järvinen *et al.*[5]), it can be seen that below approximately pH 7, the natural phosphodiester **141** is much more

stable than the thiophosphoramidate **64** and phosphoramidate **57** mimics. At higher pH values, the hydrolysis of the UpU system **141** is much more rapid, due to the presence of the 2′-hydroxyl group, which, catalysed by hydroxide, can intramolecularly attack the phosphodiester linkage.[136]

Despite this, the analogues are relatively stable, with half lives of approximately 11 days under these harsh (90 °C) conditions.
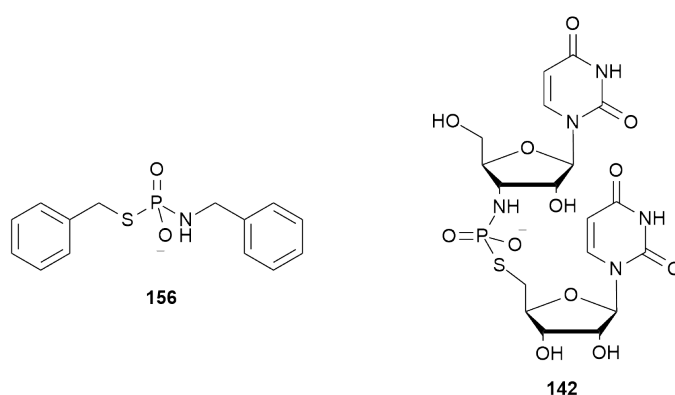
Figure 4.3: The model substrates used for the study of the hydrolysis of the thiophosphoramidate linkage; *N*-,*S*-dibenzyl thiophosphoramidate **156** and 3′-Amino-3′-deoxythymidylyl(3′→5′)-5′-deoxy-5′-thiothymidine **142**.

This chapter describes how the hydrolytic properties of the thiophosphoramidate group were investigated, first using an *N*-,*S*-dibenzyl thiophosphoramidate **156** for preliminary studies, then using the *N*,*S*-linked thiophosphoramidate **142** synthesised in chapter 3 as a model substrate to construct a complete pH-rate profile for the hydrolysis.

4.2   Experimental Work

4.2.1   Preliminary Investigations

The initial kinetic experiments were performed using *N*-,*S*-dibenzyl thio-phosphoramidate **156** as a substrate (Figure 4.4), which was synthesised according to the method developed by Milena Trmčić.[49] To find the conditions under which the compound would decompose over a reasonable timescale, the material was placed in an NMR tube with a buffer solution prepared from undeuterated solvent, and the decomposition of the material was monitored by ^{31}P NMR spectroscopy.
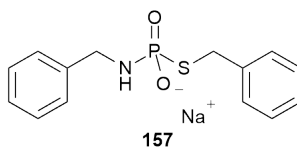
Figure 4.4: *N*-,*S*-dibenzyl thiophosphoramidate **156**, the initial substrate for the hydrolysis experiments.

The buffer solution and the temperature were changed until finally the material was found to decompose over several hours, using an acetate buffer at pH 4.64 and a temperature of 80 °C. At higher pH values (MES buffer at pH 6.54, and above), no appreciable hydrolysis was observed over several days.

Plotting the natural logarithms of the integrals (relative to the sum of all integrals) corresponding to the substrate against time provided pseudo-first-order rate constants for the decay of the substrate **157** (Figure 4.5). Hydrolysis experiments were repeated with different buffer concentrations to yield a crude, buffer-free rate constant for the hydrolysis of the thiophosphorami-date (Figure 4.6), and a half-life of approximately seven hours at 80 °C, pH 4.64.
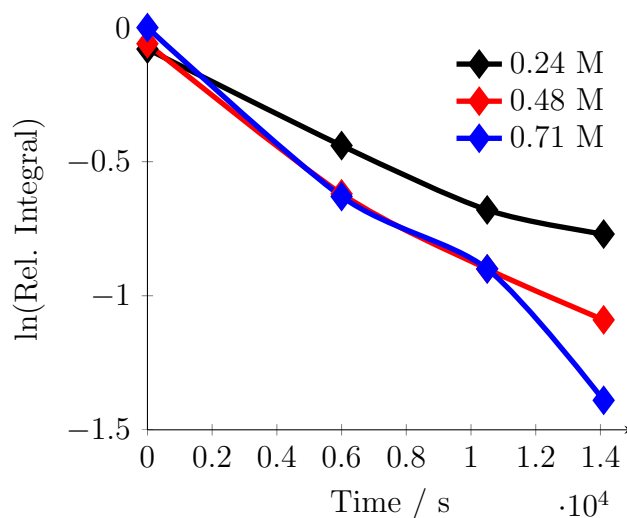
Figure 4.5: Plots of the natural logarithms of the relative integrals of the substrate against time. Buffer concentrations are denoted in the legend.

These results are crude; the quantities of substrate required for ^{31}P NMR spectroscopy are large and this in turn limits the concentration of buffer which can be used. In these experiments, the buffer concentrations ranged from 0.24 to 0.71 M, which corresponds to $5\times$ - $15\times$ the concentration of the substrate - ideally the buffer concentration should be in much greater excess to minimise perturbation to the pH as the reaction proceeds. A more sensitive technique would allow a smaller quantity of the substrate, and a greater relative concentration of buffer to be used. The next step was therefore to attempt analysis of the hydrolytic process by high performance liquid chromatography (HPLC).

Possible hydrolysis products were synthesised (*N*- benzyl phosphoramidate **158** and *S*- benzyl thiophosphate **159**, respectively, in addition to benzylthiol **161**) or acquired commercially (benzylamine **160**) and attempts were made to measure the retention times of these species and the starting material. The results, however, were unsatisfactory, with the compounds giving poor UV responses. The benzyl groups were poor choromophores and so an alternative susbstrate was sought, with more detectable chromophores.
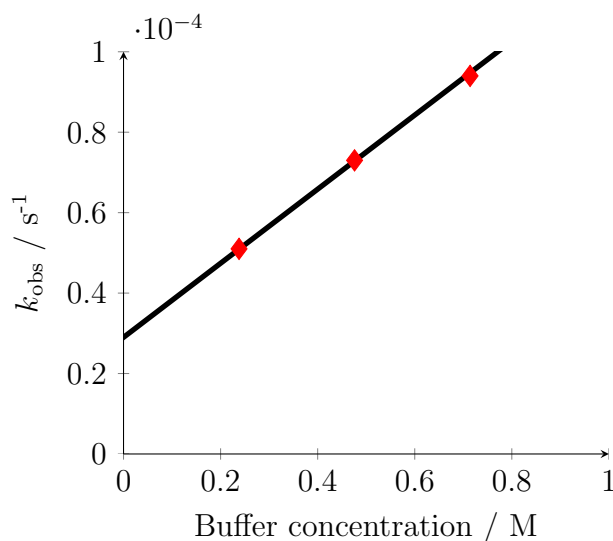
Figure 4.6: Plotting the observed rate constant against the buffer concentration and extrapolating to zero buffer provides a buffer-free rate constant.

4.2.2   Kinetic Experiments Using TnpsT as a Substrate

The thiophosphoramidate analogue **142** of thymidylyl-3′,5′-thymidine presents an attractive susbtrate for these hydrolysis studies; an excellent chromophore, in the form of the thymine nucleobase, is present on both 'ends' of the thiophosphoramidate group. Whilst the quantities available were smaller, and the material more difficult to synthesise than the dibenzyl thiophosphoramidate **156** (as described in chapter 3), the greater sensitivity of HPLC over ^{31}P NMR spectroscopy offers the possibility that the kinetic experiments to be performed on a smaller quantity of material.

The preliminary ^{31}P NMR experiments performed on the dibenzyl thiophosphoramidate **156** also provided a starting point for kinetic studies on the thymidylyl-3′,5′-thymidine analogue **142**; under the same conditions, the observed rate constants for the hydrolysis of both thiophosphoramidate species were expected to be similar.

Several possible hydrolysis products (3′-amino-3′-deoxythymidine *N*-phosphate **162**, 5′-deoxy-5′-thiothymidine *S*-phosphate **149**, 5′-deoxy-5′-thiothy-
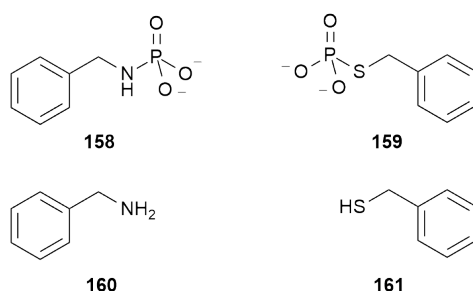
Figure 4.7: Possible products of hydrolysis were synthesised or
acquired commercially.

midine S phosphoramidate **146**, 3′-amino-3′-deoxythymidine **55**, and 5′-de-
oxy-5′-thiothymidine **163**, see Figure 4.8) were prepared or were commer-
cially available (thymidine **144**) and were used, alongside the thiophospho-
ramidate substrate **142**, to develop a HPLC protocol which would allow all
the possible product peaks to be sufficiently resolved. A number of unreac-
tive standards (Figure 4.9), against which the integrals of other peaks could
be integrated were also tested to ensure that they did not occlude any of
the other peaks which might appear in chromatograms of hydrolysis product
mixtures.

The experiments were typically carried out by preparing twenty sealed am-
poules, each containing one millilitre of a solution containing 0.1 mM sub-
strate and 0.1 mM of the standard. Ten of the ampoules contained one hun-
dred equivalents of buffer, *i.e.* 10 mM, while the remainder contained one
thousand (100 mM), so that buffer catalysis could be detected. The buffers
were chosen so that their pK_as were approximately one unit apart at 90 °C
(see section 4.3.1), and comprised formate, acetate, MES, phosphate, bicine,
and borate where each was used in 50% free acid form. At the extremes of
pH, solutions of hydrochloric acid or potassium hydroxide were used.

The ampoules were placed in a water bath maintained at 90 °C, and at
intervals two ampoules (one containing 100× buffer, one containing 1000×),
were removed and analysed by HPLC. For most experiments, cooling to room
temperature was sufficient to quench the reaction, but for faster reactions
a quench solution of two to twenty equivalents (relative to the buffer) of
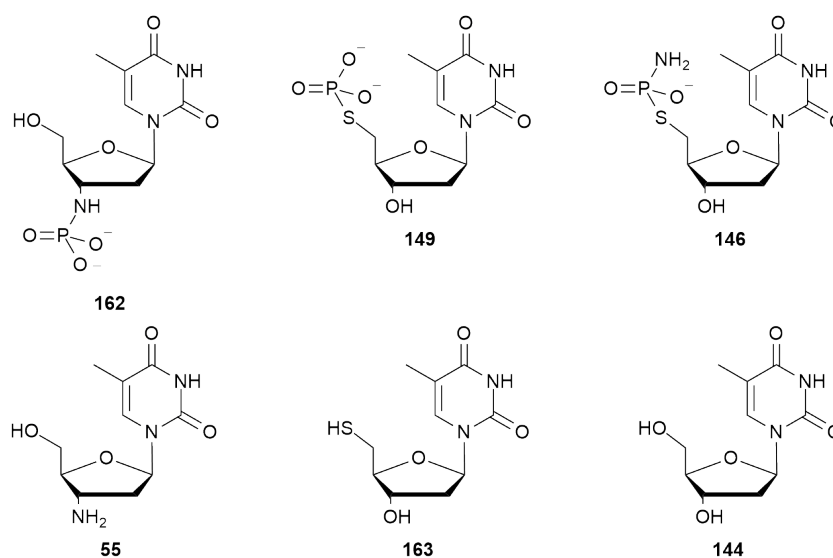
Figure 4.8: A number of possible hydrolysis products were commercially available, or were synthesised.
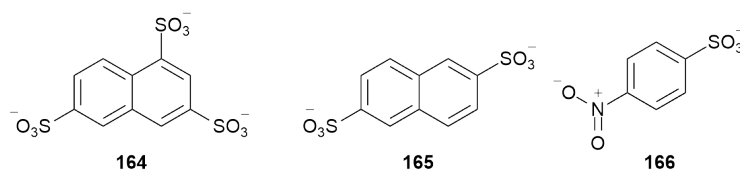
Figure 4.9: The compounds investigated as HPLC integration standards; 1,3,(6,7)-naphthalenetrisulphonate **164**, 2,6-naphthalenedisulphonate **165**, and *p*-nitrobenzenesulphonate **166** salts.

monopotassium phosphate (for basic solutions) or dipotassium phosphate (for acidic solutions) was used. Very rapid reactions were performed in open ampoules, in a heating block, as described in the experimental section 8.4. The processing and analysis of the results are described in the following section.

4.3 Results and Analysis

4.3.1 Buffer pH and Temperature

The pH values of the buffer solutions are measured at 25 °C. However, since the hydrolysis experiments are being carried out at 90 °C, the change in pH of a buffer solution between these temperatures must be determined.

The dependence of the pH of a buffer composed of a weak acid and its salt with temperature is described by the equation:[137]

$$\frac{\partial pH}{\partial T} \approx -\frac{\partial log K}{\partial T} - (2z + 1)\frac{\partial log \gamma}{\partial T} \tag{4.1}$$

Where pH is the negative common logarithm of the activity of the hydronium ion, T is the absolute temperature, K is the acid dissociation constant of the buffer species, z describes the ionisation of the acid (see Table 4.1), and γ is the activity coefficient of an average univalent ion.

Table 4.1: The values of z for equation 4.1 depend on the ionisation characteristics of the buffer system[137]

Acid:	Base:	z
HB^{2+}	B^+	+1
HB^+	B	0
HB	B^-	-1
HB^-	B^{2-}	-2
HB^{2-}	B^{3-}	-3

The $\partial log \gamma / \partial T$ term is typically small and can be neglected, and so our equation becomes:

$$\frac{\partial pH}{\partial T} \approx -\frac{\partial logK}{\partial T} \tag{4.2}$$

The relationship between the acid dissociation constant and temperature is described by the van't Hoff equation:

$$\frac{\partial lnK}{\partial T} = \frac{\Delta H^\circ}{RT^2} \tag{4.3}$$

Where ΔH° is the molar enthalpy change for the dissociation of the acid and R is the gas constant.

In order to get the equation into the $\partial logK/\partial T$ form, the identity $ln(x) = ln(10)log(x)$ must be substituted to give:

$$\frac{\partial logK}{\partial T} = \frac{\Delta H^\circ}{ln(10)RT^2} \tag{4.4}$$

Thus, if ΔH° can be found in the literature, it may be used directly. Alternatively, values for $\partial logK/\partial T$ for a number of electrolytes have been determined, in the form of $\Delta pH/^\circ C$ at 20 or 25 °C, and by substituting these into equation 4.5, ΔH° may be determined.

Combining equations 4.2 and 4.4, we arrive at:

$$\frac{\partial pH}{\partial T} \approx -\frac{\Delta H^\circ}{ln(10)RT^2} \tag{4.5}$$

Integrating this (and assuming that ΔH° is independent of temperature):

$$\int_{pH_1}^{pH_2} \partial pH \approx -\int_{T_1}^{T_2} \frac{\Delta H^\circ}{ln(10)RT^2} \partial T \tag{4.6}$$

$$\Delta pH \approx \frac{\Delta H^\circ}{ln(10)R} \left(\frac{1}{T_2} - \frac{1}{T_1} \right) \tag{4.7}$$

As an example, the value of $\partial logK/\partial T$ at 25°C (298.15 K) for acetic acid

is reported to be $-0.0002\ K^{-1}$. By substituting these values into equation 4.4, the value of $\Delta H°/ln(10)R$ is found to be -18 K. The change in pH of an acetate buffer between 25 °C (298.15 K) and 90 °C (363.15 K) can then be calculated to be 0.011, indicating that acetate is relatively insensitive to temperature. Performing the same series of calculations with the $\partial logK/\partial T$ reported for the second ionisation of phosphate $(0.0024\ K^{-1})$ yields a pH change of -0.13, a more significant difference.
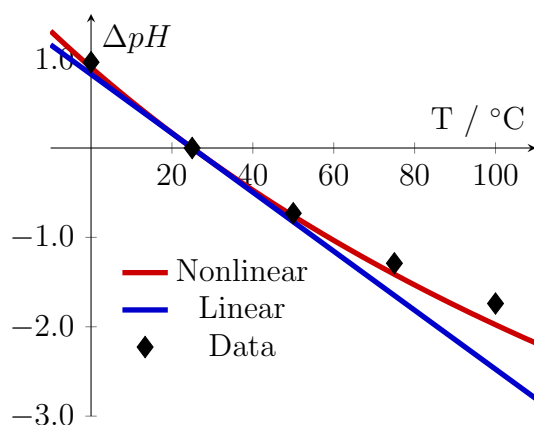
Figure 4.10: The linear (blue) and nonlinear (red) extrapolated relationships between temperature and ΔpH. It can be seen that there is a significant difference between the two at higher temperatures. The nonlinear equation more closely follows the measured values.

Equation 4.7 can be plotted alongside the linear extrapolation, using the autoionisation of water as an example ($\partial logK/\partial T$ of 0.033 at 25 °C), and this illustrates that while at temperatures close to 25 °C the approximation is quite good, at higher temperatures, there is a significant divergence.

The measured values[138] do deviate from equation 4.7 at higher temperatures, probably due to $\Delta H°$ itself having a dependence on temperature.

At low pH values, solutions of hydrochloric acid are used, in a great enough excess over the substrate that the change in pH is negligible over the course
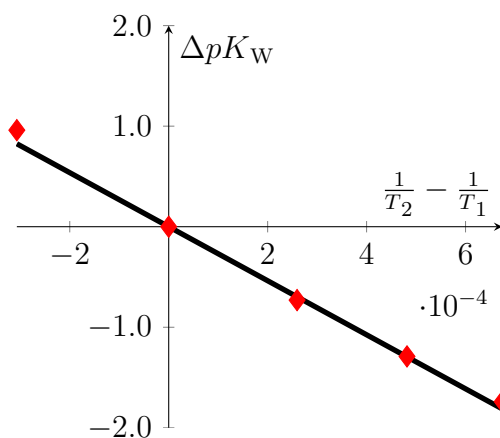
Figure 4.11: The literature values for the equilibrium constant for the autoionisation of water can be fitted to equation 4.7 and interpolated to determine the change in pK_W at any temperature in the liquid range of water at standard pressure. ΔpK_W is relative to the pK_W at T_2, 298.15 K

of the reaction. Neglecting the thermal expansion of the solvent, there should be no change in pH when the solution is heated to 90 °C since the acid is effectively fully dissociated; the concentration of protons will be the same in both cases. At high pH values, when potassium hydroxide is used, the concentration of hydroxide is constant, but the concentration of protons will be dependent on the equilibrium constant for the autoionisation of water (K_W), which is temperature dependent. The values of the equilibrium constant at several temperatures can be found in the literature;[138] these can be fitted to equation 4.7 (see Figure 4.11) and the value of ΔH° can thus be determined.

The value of ΔH° is found to be -51 kJ mol^{-1}, and the change in the equilibrium constant can now be estimated for any temperature required.

The buffer pH values for the kinetic experiments were measured at 25 °C and the hydrolyses were performed at a temperature of 90 °C. The changes in pH for the various buffers used in the study, calculated as above, are tabulated in Table 4.2.

Table 4.2: The change in pH from from 25 to 90 °C calculated for the various buffers used in the hydrolysis experiments

Buffer:	$\partial \mathbf{logK}/\partial \mathbf{T}$	$\mathbf{\Delta pH}$
Formate	-0.0001 (25 °C)[137]	0.01
Acetate	-0.0002 (25 °C)[137]	0.01
MES	0.011 (20 °C)[139]	-0.62
Phosphate (K_{2a})	0.0024 (25 °C)[137]	-0.13
Bicine	0.018 (20 °C)[139]	-0.93
Borate	0.0082 (25 °C)[137]	-0.44
K_W	[138]	-1.65

4.3.2 TnpsT Hydrolysis Results
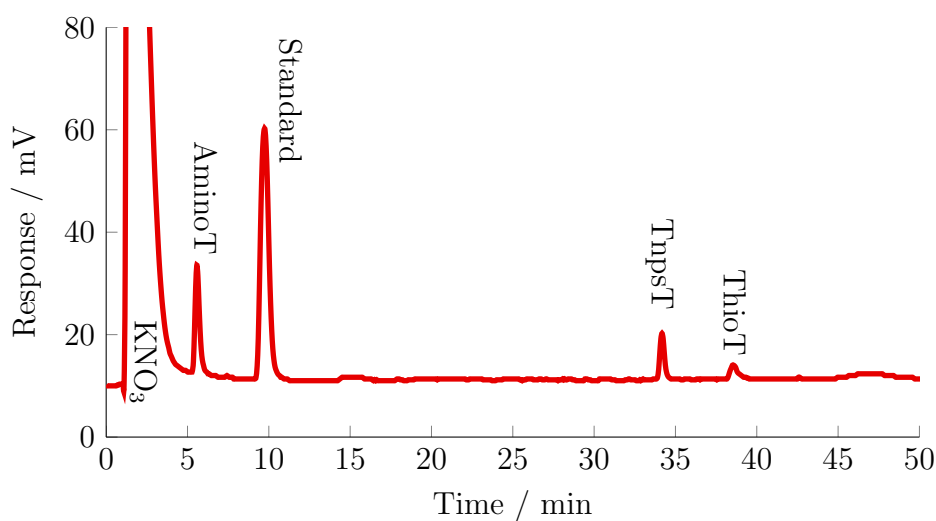
Figure 4.12: An example of a chromatogram: 5mM HCl solution after 3.5 min heating at 90°C. The very large peak at the solvent front is due to potassium nitrate. The other peaks are: 3′-amino-3′-deoxythymidine **55** (6 min), *p*-nitrobenzenesulphonate **166** (10 min), TnpsT **142** (34 min), and 5′-deoxy-5′-thiothymidine **163** (39 min).

A typical chromatogram is shown in Figure 4.12. The peaks were integrated, and the ratios of each peak area to the peak area corresponding to the standard were determined. Plotting the natural logarithm of the relative integrals against time showed a linear relationship (Figure 4.14) in all cases, indicating that the hydrolysis was pseudo-first-order.
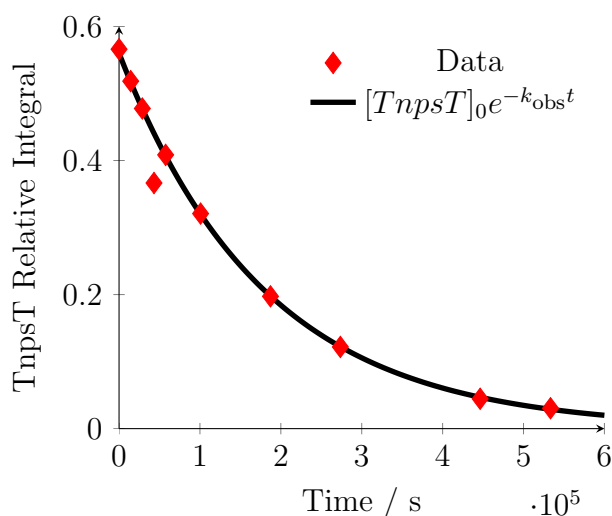
Figure 4.13: A plot of TnpsT **142** against time in 100 mM MES buffer (pH 5.68 at 90 °C). The hydrolysis is pseudo-first-order, as shown by the close fit to the exponential decay.

For each buffer, the observed rate constant was determined at both 10 mM and 100 mM buffer concentrations. In most cases, there was no significant difference in the observed rate constants, however, for formate and acetate buffers there was approximately an order of magnitude change on increasing from 10 mM to 100 mM buffer concentration. Additional experiments were performed with 40 mM and 70 mM concentrations of each buffer. A linear plot was then used to determine the buffer-free observed rate constants and the second-order buffer-catalysed rate constants (see Figure 4.15 for an example).
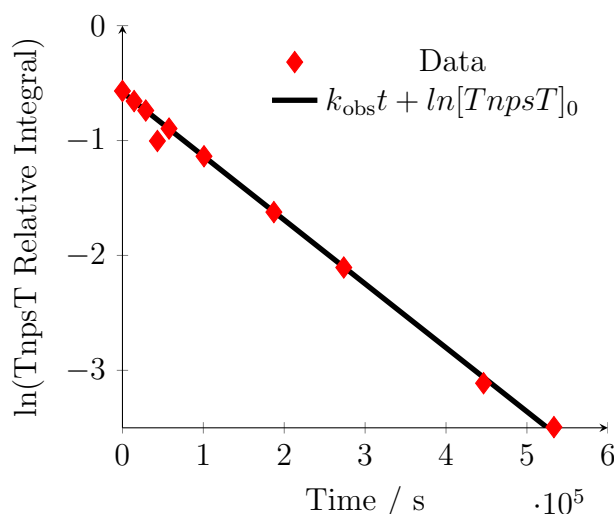
Figure 4.14: A plot of the natural logarithm of the relative integral of TnpsT against time in 100 mM MES buffer (pH 5.68 at 90 °C). The close fit to the linear equation shows that the hydrolysis is pseudo-first-order.

The kinetic data for the breakdown of TnpsT are plotted in Figure 4.16. The measurements were performed at pH values ranging from 1.32 to 10.91. At lower pH values, the hydrolysis was too quick to permit accurate measurement; at pH 1.32 the half-life for the hydrolysis was measured to be nine seconds, and at a pH one unit lower, the half-life could be as low as one second. Under strongly alkaline conditions, the glass ampoules containing the reaction mixtures showed visible signs of hydroxide etching; these factors therefore put physical limits on the pH range which could be readily investigated.

It can be seen that under acidic conditions (below approximately pH 6) there is a linear relationship between pH and the logarithm of the rate constant, with a gradient of -1. This is followed by a plateau in the observed rate constant around neutral pH. At higher pH values, there appears to be a deceleration in the rate of hydrolysis, where an acceleration due to attack by increasing concentrations of hydroxide might have been expected. This downturn is effectively based upon a single data point, and so it is difficult to draw conclusions with a great degree of certainty. The change may be due
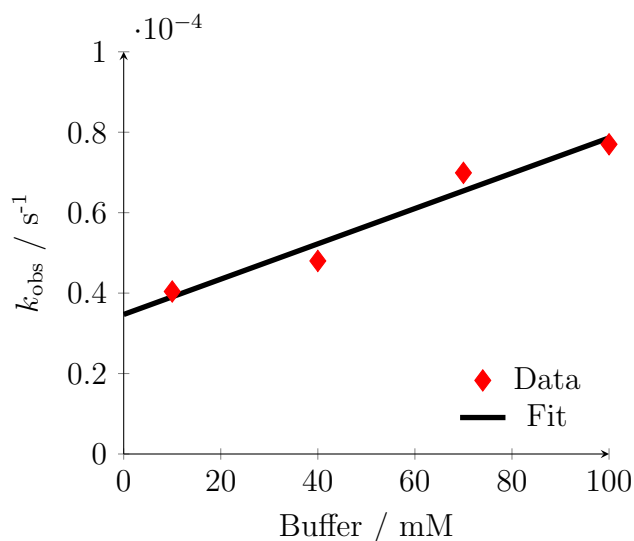
Figure 4.15: A plot of the observed rate constant against acetate buffer
concentration at pH 4.61. The y-intercept provides the buffer-free rate
constant, while the gradient is the second-order buffer-catalysed rate
constant.

to a change in mechanism of the hydrolysis, for example, by a deprotonation
of the thiophosphoramidate group to create a species which is less readily
hydrolysed, or deprotonation of the thymine nucleobase (which, as stated
before, has a pK_a of *circa* 10)[117] and thus increased repulsion of the hydroxide
anion.

Note also the deviation from the fitted line near the point of positive curva-
ture, *i.e.* between pH 5 and 8. The deviation of these points appears to be
systematic rather than due to random error, and an explanation for this will
be advanced in the following section.

4.3.3   Analysis

The hydrolysis of the thiophosphoramidate system was observed to be pseudo-
first-order, and so the rate equation is simply:
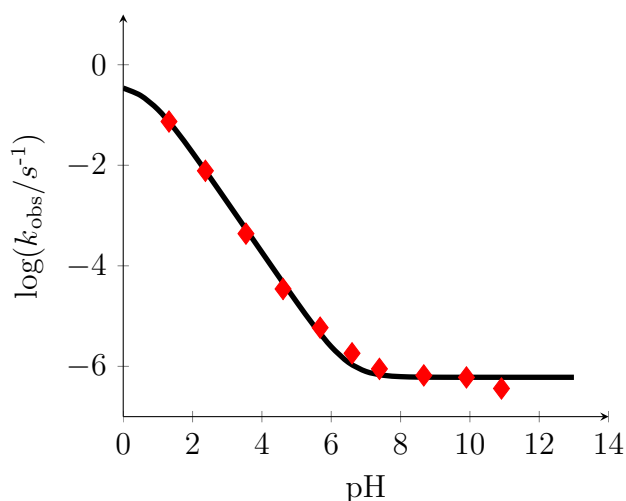
Figure 4.16: A plot of the common logarithm of the observed rate of hydrolysis against pH. Experimental values are represented by red diamonds, and the fitted equation 4.16 by the solid black line. The *x*-axis pH values are those calculated using equation 4.7 with $T_2 = 90\ °C$

$$-\frac{\mathrm{d}[TnpsT]}{\mathrm{d}t} = k_{\mathrm{obs}}[TnpsT] \tag{4.8}$$

At different pH values, the rate of hydrolysis includes contributions from the hydrolysis of different species, which exist in equilibria with each other.

At low pH values, both the thiophosphoramidate oxygen and thiophosphoramidate nitrogen could be protonated. The pK_a of the nitrogen in an *N*-alkyl phosphoramidate has been shown to be in the 7 to 10 region,[140] and the corresponding pK_a of the TnpsT system might be expected to be similar. The first and second ionisations of phosphoric acid have pK_a values of 2.12 and 7.21 respectively, and substitution of one of the oxygen atoms for sulphur has been shown to lower the pK_as to 2.05 and 5.6.[141, 142] As the pH rises, the oxygen is expected to be deprotonated, followed by the nitrogen.

The overall rate equation is composed of terms for the contribution of each species, each with its individual rate constant:
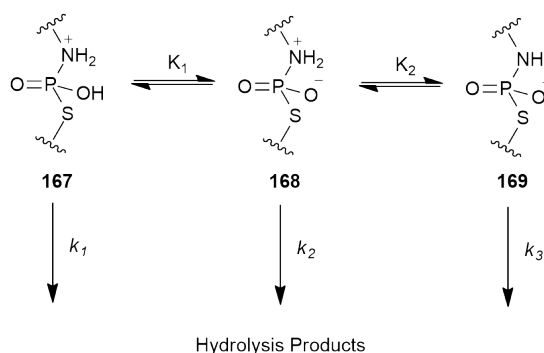
Scheme 4.1: The species hypothesised to contribute to the overall observed rate constant

$$-\frac{\mathrm{d}[TnpsT]}{\mathrm{d}t} = k_1[sub_1] + k_2[sub_2] + k_3[sub_3] \tag{4.9}$$

Where k_1, k_2, and k_3 are the rate coefficients for each species (denoted by $[sub_n]$, see Scheme 4.1). The proposed relationship of the proportion of each species to the concentration of acid is described by the following equations:

$$x_1 = \frac{[H^+]^2}{K_1K_2 + K_1[H^+] + [H^+]^2} \tag{4.10}$$

$$x_2 = \frac{K_1[H^+]}{K_1K_2 + K_1[H^+] + [H^+]^2} \tag{4.11}$$

$$x_3 = \frac{K_1K_2}{K_1K_2 + K_1[H^+] + [H^+]^2} \tag{4.12}$$

Where K_1 and K_2 are the acid equilibrium constants for the deprotonations of OH and N^+H_2P. The proportions of each species as a function of pH are illustrated in Figure 4.17

Therefore, taking $[TnpsT]$ to refer to the overall concentration of thiophosphoramidate **142** in all its ionisation states, the equation describing the rate of hydrolysis in terms of these three species is described by:
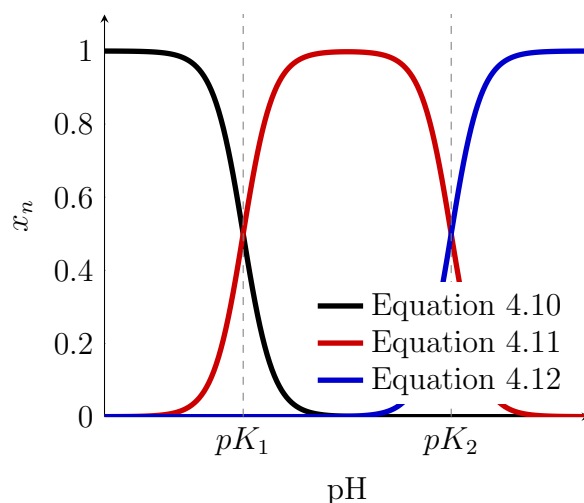
Figure 4.17: A plot of equations 4.10, 4.11, 4.12 where K_1 and K_2 are well separated

$$-\frac{\mathrm{d}[TnpsT]}{\mathrm{d}t} = [TnpsT]\frac{k_1[H^+]^2 + k_2K_1[H^+] + k_3K_1K_2}{K_1K_2 + K_1[H^+] + [H^+]^2} \tag{4.13}$$

k_{obs} therefore becomes:

$$k_{\mathrm{obs}} = \frac{k_1[H^+]^2 + k_2K_1[H^+] + k_3K_1K_2}{K_1K_2 + K_1[H^+] + [H^+]^2} \tag{4.14}$$

A logarithmic plot of this equation, with coefficients chosen so that the points of inflection and turning may be clearly seen, is shown in Figure 4.18.

This equation should describe the hydrolysis of the thiophosphoramidate **142** over most of the pH range for which measurements have been made. At higher pH values, hydrolysis due to attack by hydroxide may occur, but this has not been observed at the measured pH values.

In order to fit this equation to the observed rate constants, the values for five constants (the two equilibrium constants and three rate constants) must be found. However, there is not information in the data collected to make this fitting with a great degree of confidence. Comparing Figure 4.18 with Figure 4.16 it can be seen that the $log(k_1)$ plateau has not been reached,
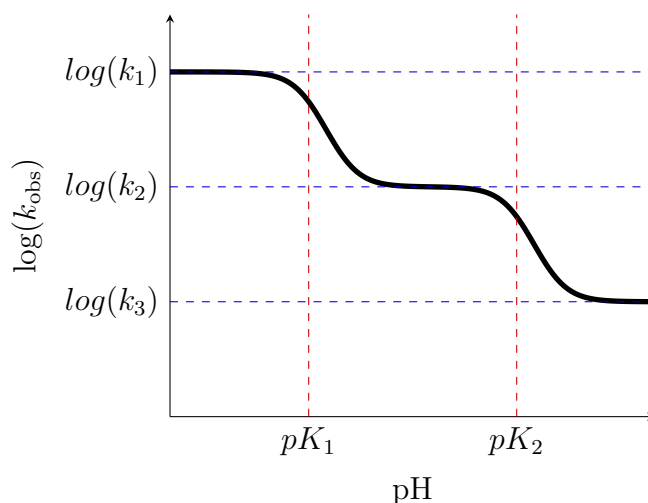
Figure 4.18: A logarithmic plot of equation 4.14 where pK$_1$ and pK$_2$ are well separated, and log(k_1), log(k_2), and log(k_3) are equally spaced.

which makes it difficult to fit values to k_1 and K_1. The curvature at pK_2 is also indistinct. In order to produce a reasonable fitting, experiments would have to be carried out at lower pH values, however, as previously stated, this would be practically difficult given the rapidity of the hydrolysis at low pH.

The lack of an clear additional pH plateau (see Figure 4.18) indicates that the major contributions to the overall observed rate constant are from two species in equilibrium with each other. Making this assumption, the equation is then:

$$-\frac{\mathrm{d}[TnpsT]}{\mathrm{d}t} = [TnpsT]\frac{k_1[H^+] + k_2K_a}{[H^+] + K_a} \tag{4.15}$$

and the observed rate constant is:

$$k_{\mathrm{obs}} = \frac{k_1[H^+] + k_2K_a}{[H^+] + K_a} \tag{4.16}$$

In making this approximation, the fit to the observed data will not be as good, as the simplified equation does not fully explain the hydrolytic process. It may be for this reason that the deviation of the data points from the fitted

curve is observed in Figure 4.16; there may be two species with differing contributions to the rate constant (zwitterion **168** and the deprotonated form **169**) which in equation 4.16 are treated as a single species.

The value of k_2 is simply the rate constant for uncatalysed hydrolysis, *i.e.* the rate on the plateau ($6.30 \times 10^{-7} s^{-1}$), and so there are only two unknown constants to fit to the measured data. However, to do this more data points at low pH are needed, as the equation predicts a second plateau in this region (when $[H^+] >> K_a$, the expression for k_{obs} becomes $k_{obs} = k_1$). Therefore the K_a can not be determined with confidence, but limits can be put on what values K_a can take. By constraining K_a to certain values, then performing the fitting on the remaining free variable, k_1, it can be seen that only a pK_a value less than 1 is consistent with the measured data, as shown in Figure 4.19.
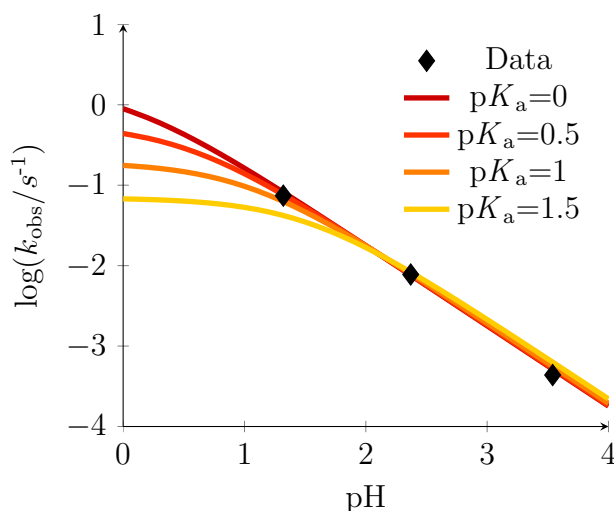
Figure 4.19: By constraining the value of the pK_a to various values and fitting k_1, it can be seen that the pK_a must be lower than approximately 1 in order to be consistent with the measured data.

This is lower than the estimate given by Ora *et al.* of pH 1-2 for their

phosphoramidate **57** and S-unlinked thiophosphoramidate **64** dinucleosides (Figure 4.1).[46]

Our measurements appear to have been performed in the region where $[H^+]$ $<< K_a$, and if the approximation that the concentration of protons is negligible compared to the K_a is made, the expression for the observed rate constant can be simplified to:

$$k_{\mathrm{obs}} = \frac{k_1}{K_a}[H^+] + k_2 \tag{4.17}$$

or:

$$k_{\mathrm{obs}} = k_H[H^+] + k_2 \tag{4.18}$$

And so it can be determined that k_H is 1.53 s^{-1}, pK_a < 1, and thus k_1 < $0.1 \times k_H$.

Given the low value of the pK_a, it seems reasonable to assume that it is that of the thiophosphoramidate oxygen or sulphur. The 'bump' at around pH 7 may be due to the zwitterionic form of the thiophosphoramidate **168** and the species on the plateau, since the plateau extends up to high pH values, is then likely to be the thiophosphoramidate in its deprotonated form (**169**).

4.3.4   Hydrolysis Products

Over the majority of the pH range studied, the only hydrolysis products observed were 3′-amino-3′-deoxythymidine **55** and, less frequently, 5′-deoxy-5′-thiothymidine **163**. The thiol appears to either have a lower absorbance than the amine, or to present as a broader peak on the HPLC chromatogram, rendering its detection more difficult.

At very low pH values (1.32 and 2.37), disappearance of the amine **55** is also observed, either by attack by water on the protonated amine **170** with inversion of stereochemistry, or through a two step process in which oxygen on
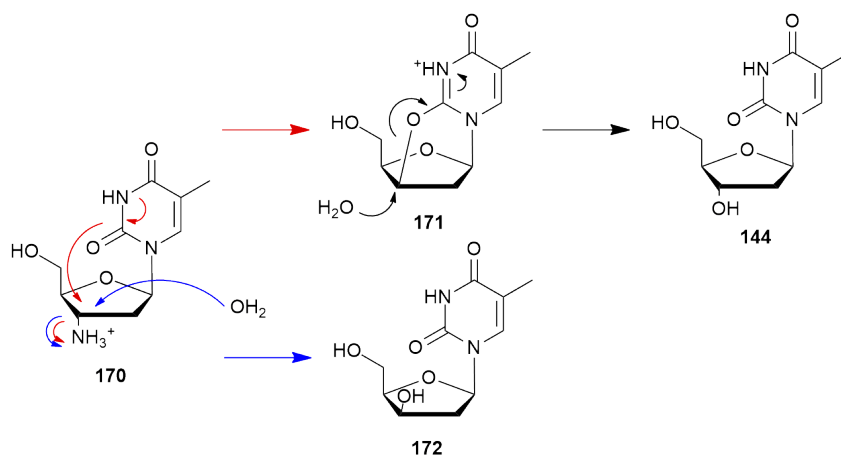
Scheme 4.2: Possible hydrolytic pathways for
3′-amino-3′-deoxythymidine **55**

the nucleobase attacks the amine, followed by an acid-catalysed ring opening
by water (Scheme 4.2). The two hydrolysis products should, in principle, be
distinguishable, however, neither is observed by HPLC, which is not entirely
surprising. Even in the most acidic experiments, the decomposition of the
amine was slow and thus relatively small quantities of the decomposition
products were formed.

The rate equation for a hydrolysis product of TnpsT **142**, x, which can itself
hydrolyse is:

$$\frac{\mathrm{d}[x]}{\mathrm{d}t} = k_{\mathrm{acc}}[TnpsT] - k_{\mathrm{dec}}[x] \tag{4.19}$$

Where k_{acc} and k_{dec} are rate constants for the accumulation and decompo-
sition of x, respectively. As the concentration of TnpsT follows pseudo-first-
order kinetics, [TnpsT] can be substituted for $[TnpsT]_0 e^{-k_{\mathrm{obs}}t}$ to give the
equation:

$$\frac{\mathrm{d}[x]}{\mathrm{d}t} = k_{\mathrm{acc}}[TnpsT]_0 e^{-k_{\mathrm{obs}}t} - k_{\mathrm{dec}}[x] \tag{4.20}$$

The solution to this equation is:
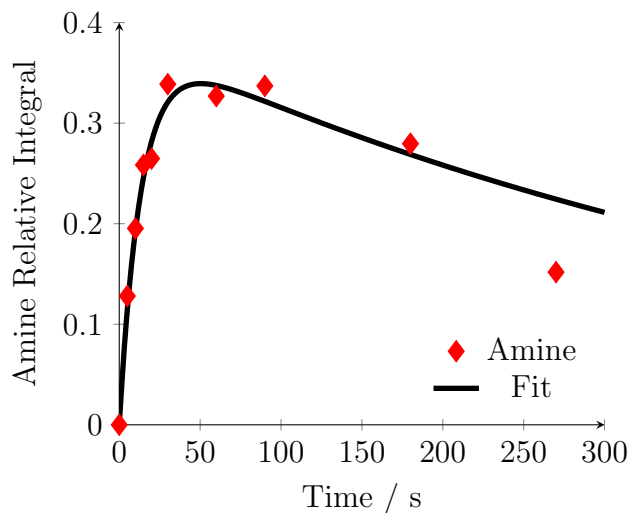
Figure 4.20: The change in the relative integral of
3′-amino-3′-deoxythymidine **55** with time in hydrochloric acid solution
at pH 1.32, with equation 4.21 fitted.

$$[x] = \frac{k_{\mathrm{acc}}[TnpsT]_0}{k_{\mathrm{dec}} - k_{\mathrm{obs}}}(e^{-k_{\mathrm{obs}}t} - e^{-k_{\mathrm{dec}}t}) \qquad (4.21)$$

The values for k_{obs} and $[Tnpst]_0$ are of course known from the analysis of
the hydrolysis of TnpsT **142**, which leaves only k_{acc} and k_{dec} to be fitted.
This was done for the pH 1.32 and 2.37 experiments (see Figure 4.20 for an
example), the only ones in which decomposition of the amine is evident, and
the results are shown in Figure 4.21.

When the decomposition of the amine is negligibile, as it is for higher pH
values, the data can be fitted to the equation:

$$[x] = A(1 - e^{-k_{\mathrm{obs}}t}) \qquad (4.22)$$

Performing this fitting can provide another way of measuring k_{obs}. This was
done over the entire pH range, and the results are shown in Figure 4.21,
alongside the results derived from studying the decay of TnpsT **142** directly.

The results agree closely, as can be seen from the graph. Puzzlingly, at the
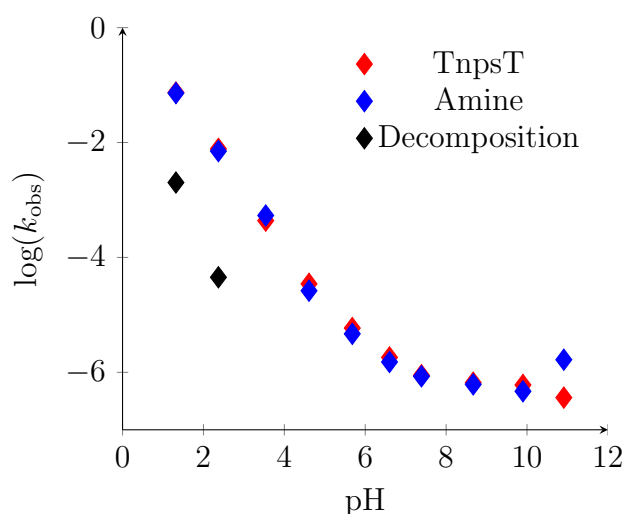
Figure 4.21: The values for k_{obs} derived from the direct observation of the decay of TnpsT **142** overlaid with those derived from the appearance of 3′-amino-3′-deoxythymidine **55**. The rates for the decomposition of the amine at high pH are also shown.

highest pH values, the results from analysis of the amine report a rise in k_{obs}, instead of the drop seen in those derived from analysis of the loss of TnpsT, and it is not clear why this should be the case. The change in the rate constant for the decomposition of the amine with pH is surprisingly large, if it were to follow the kinetics of equation 4.16, as one might expect, the rate of change of $log(k_{\mathrm{obs}})$ with pH should be between -1 and 0. A simple linear interpolation of the data provides a rate of change of -1.64; this is probably due to the small effect of decomposition at pH 2.37 and thus the difficulty in extracting the rate constant accurately.
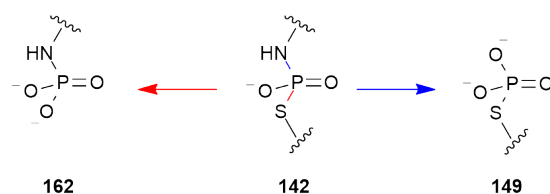
Scheme 4.3: The thiophosphoramidate appears to be cleaved at either the N-P or P-S bond at almost equal rates at high pH

At high pH values, it appears that the phosphorylated hydrolysis products are sufficiently stable that they can accumulate enough to be detectable. Both 3′-amino-3′-deoxythymidine N-phosphate **162** and 5′-deoxy-5′-thiothymidine S-phosphate **149** are observed at pH 10.91.
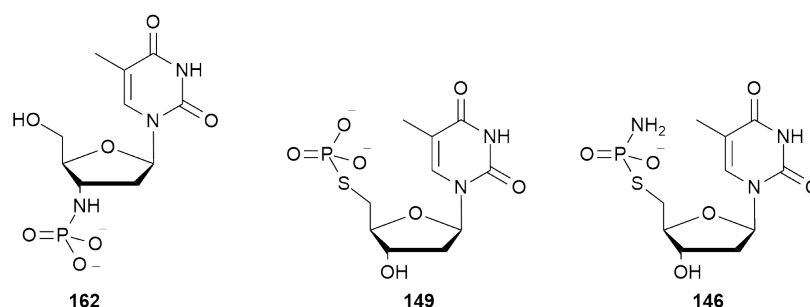
Figure 4.22: Some partially hydrolysed products of the reaction; 3′-amino-3′-deoxythymidine N-phosphate **162**, 5′-deoxy-5′-thiothymidine S-phosphate **149**, and 5′-S-thiophosphoramidato-5′-deoxythymidine **146**.

Surprisingly, no 5′-S-thiophosphoramidato-5′-deoxythymidine **146** is observed, which has been seen to be significant side product when TnpsT **142** is synthesised at high pH values. This may be due to the differing temperatures at which the reactions were carried out; the synthesis was performed at 50 °C while the hydrolysis took place at 90 °C. The value of pK_W drops significantly with increasing temperature, and so it may be that higher pH values were achieved during the synthesis and under these conditions, the different mechanism of hydrolysis becomes dominant, in which the N-nonbridging thiophosphoramidate **146** is formed.

The appearance and disappearance of these intermediates can also be fitted to equation 4.21 in the case of the Tnp intermediate, this is shown in Figure 4.23. The fit is not perfect for either of the intermediates and this is probably due to the fact that only small quantities of the intermediates are observed, and the associated errors are therefore large. The fitting provides values of
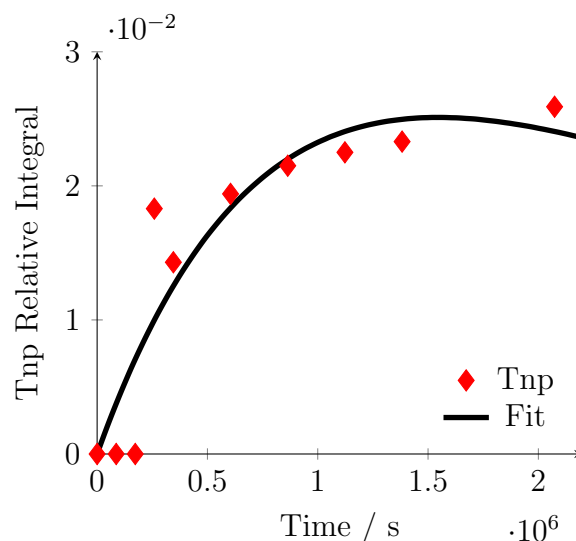
Figure 4.23: The change in the relative integral of
3′-amino-3′-deoxythymidine N-phosphate **162** with time in pH 10.91
potassium hydroxide solution

$k_{\mathrm{acc}} = 9 \times 10^{-8}$ and $k_{\mathrm{dec}} = 1 \times 10^{-6}$ for Tnp, and $k_{\mathrm{acc}} = 1 \times 10^{-7}$ and $k_{\mathrm{dec}} = 2 \times 10^{-6}$ for psT.

4.4 Conclusions

The hydrolytic stability of a model thiophosphoramidate compound has been studied over a wide pH range. The compound has been shown to be highly stable, with a half-life of approximately two weeks on the pH-independent plateau (Figure 4.16, pH 7-10) at 90 °C. Unfortunately, data for the hydrolysis of the natural thymidylyl-3′,5′-thymidine system **141** under the same conditions could not be found for comparison. However, as stated in section 1.1.1, the observed rate constant for hydrolysis of the deoxyribonucleoside TpT **141** system at 80 °C in 1 M potassium hydroxide solution has been found to be $6 \times 10^{-7} s^{-1}$[2] - this is approximately the same as the observed rate constant for the TnpsT system **142**, albeit under conditions more basic and 10 °C. The pH-'rate' profile for uridylyl-3′,5′-uridine (Figure 4.2) can be expected to be similar to thymidylyl-3′,5′-thymidine, at least at lower pH

values where the base catalysed contribution to the observed rate constant is small. These data indicate that while the thiophosphoramidate N-, S-diester is relatively stable, it is still two orders of magnitude less stable than the natural phosphodiester linkage.
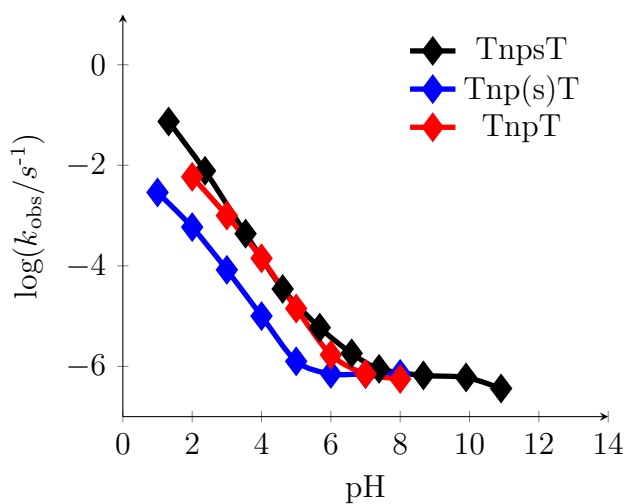
Figure 4.24: A plot of the observed rate constants for the hydrolysis of the TnpsT system, alongside the results obtained for similar systems by Ora, Murtola, Aho, and Oivanen[46]

When compared to the hydrolytic profiles obtained for the Tnp(s)T **64** and TnpT **57** systems by Ora *et al.*, it can be seen that there is great similarity. In particular, the profiles for TnpsT **142** and TnpT **57** are very similar and were both less stable at low pH than the Tnp(s)T system **64**. This could be due to the steric bulk of the negatively charged sulphur atom. Equation 4.16 predicts a levelling off at low pH, and the beginnings of this can be seen in the pH-rate profiles of TnpT **57** and Tnp(s)T **64**. Fitting of the equation to these curves provides pK_a values of 2.1 and 1.3 respectively. In the case of TnpsT **142**, the relationship appears linear even at the lowest pH which could be measured, and so the pK_a can not be determined accurately, however, it appears that it must be below 1.

Some hydrolysis products have been observed, however, they are only seen at high pH, and in very small quantities. There is therefore not enough information to draw any strong conclusions regarding the mechanism of hydrolysis, other than that at high pH both the N-P and S-P bonds appear to be approximately equally labile. The synthesis of the TnpsT **142** system indicates that it is possible for the C3′-N bond to be broken, however, the product of this reaction is not observed under the kinetic experiment conditions; possibly due to the higher temperatures employed. The kinetic information determined in this chapter may be of use in optimising the synthesis of thiophosphoramidate compounds. Future work in this area could include studying the hydrolytic stability of the intermediates in the synthesis, *i.e.* the unalkylated thiophosphoramidate **143**, and the dependence of the thymine imide pK_a on temperature.

The data indicate that thiophosphoramidate compounds are highly stable under medium to high pH values even at elevated temperatures and thus may have use in the synthesis of analogues of biological phosphate systems. These properties would also be beneficial if the thiophosphormaidate synthetic methodology were to be applied to the ligation of nucleic acid strands, as described in section 1.2.4. The resistance of these compounds to phosphodiesterases in unknown and further study could be performed in this area.

4.5 Future Work

The end of this chapter draws to a close the work performed on the thiophosphorylation of aminonucleosides. Future work in this area could include the application of the methodology developed here to the synthesis of biologically relevant molecules, such as templated oligonucleotide ligations for the production of circularised nucleic acids, which may have applications in gene interference. In the case of oligonucleotide analogues, the stability of the thiophosphoramidate linkage towards enzymatic degradation could also be studied. Thiophosphoramidate analogues of nucleotide sugar systems are

another potential target, as described in section 3.4. Acting as substrates or inhibitors of enzymes, these may have biological and therapeutic uses.

Chapter 5

Aqueous Reduction of Organic Azides with Thiophosphate Ion

This chapter describes the development of an convenient, aqueous method of reducing azides with sodium thiophosphate.

5.1 Introduction

5.1.1 Azide Reduction

Primary amines are common functional groups in synthetic organic chemistry, and methods for their formation are therefore valuable. There are broadly two methods for synthesising these compounds from alkyl halides or tosylates - substitution by protected ammonia followed by deprotection, as in the Gabriel synthesis (Scheme 5.1, or substitution by the azide anion and subsequent reduction. Direct alkylation of ammonia is generally avoided, due to the primary amine products' tendency to continue to react with the alkylating agent and so producing undesired secondary, tertiary, and quaternary amines.[143]

While the Gabriel synthesis works well with primary alkyl halides, it is less
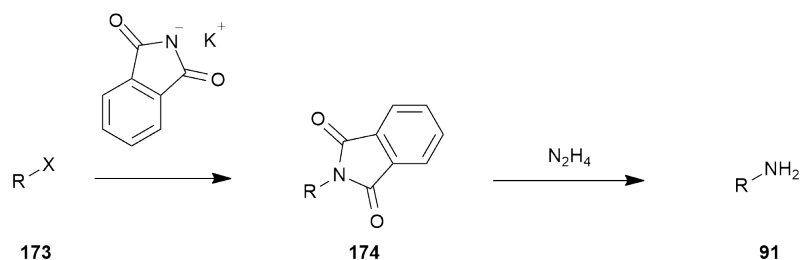
Scheme 5.1: The Gabriel synthesis

effective for secondary substrates, as the elimination products tend to be formed.[144]

Many routes to primary amines have been developed using azides. Azide substituted compounds can easily be created by nucleophilic substitution of a good leaving group (e.g. halide, tosyl) by the azide anion. This precludes the problematic multiple substitutions which arise when the primary amine is directly introduced by substitution with ammonia. The reduction step can be accomplished using a variety of methods. The usual methods for reducing azides to amines include reaction with triphenylphosphine in the Staudinger reaction,[145] hydrogenation,[146] metal hydride reducing agents,[147] or, less commonly, reaction with hydrogen sulphide (see Scheme 5.2).[148]
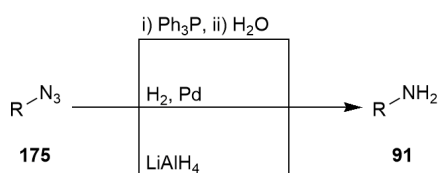
Scheme 5.2: The most common methods for reducing azides

Computational studies[149] have indicated that the Staudinger reaction begins with the attack of triphenylphosphine on the azide. This phospazide intermediate **176** rapidly rearranges to form an iminophosphorane **177** and expel nitrogen gas. Hydrolysis of the iminophosphorane **177** affords the amine **91**

and triphenylphosphine oxide. The Staudinger reaction presents a very mild method for reducing azides to primary amines, however, the triphenylphosphine oxide produced as a by-product can be exceedingly difficult to separate from the product.
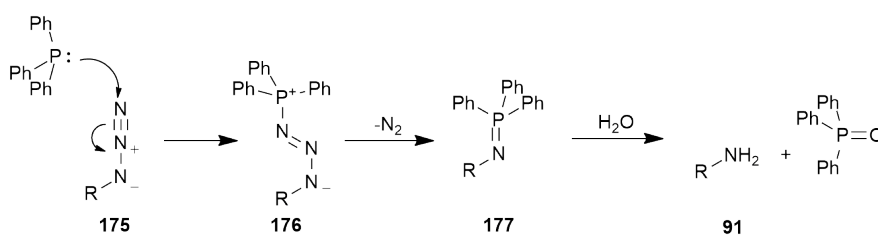
Scheme 5.3: The mechanism of the Staudinger reaction

Hydrogenation with palladium on carbon is frequently used to effect the reduction of azides. The advantage of this approach is that upon completion, the reaction mixture can simply be filtered to remove the catalyst. Conversion of the substrate is often high, rendering further purification unnecessary. The disadvantages of this approach are difficulties in carrying out small scale reactions, and a lack of selectivity.[150]

Lithium aluminium hydride and sodium borohydride have been used to reduce azides to amines, however, the reactive and unselective nature of these compounds makes their use impractical for substrates possessing other reducible or otherwise sensitive functional groups.[151] Another drawback is the difficulty in handling lithium aluminium hydride, and the poor yields afforded by sodium borohydride.
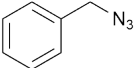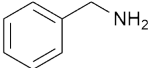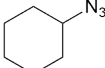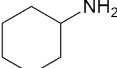
A milder route uses hydrogen sulphide and triethylamine to carry out the reduction.[152] Hydrogen sulphide, however, is of course unpleasant to work with and still presents handling difficulties.

5.1.2   Discovery

The project was a continuation of work begun David Hodgson in 2007 and followed up by Gemma Freeman, Milena Trmčić, and Jennifer Norcliffe. In an attempt to form a phosphoramidate linkage by reaction of an azide with sodium thiophosphate, the corresponding amine was instead found to be produced.

Table 5.1: Results of reduction of several substrates. The reaction with azido ethyl acetate was carried out in D_2O and followed by ^1H NMR spectroscopy. 100% conversion to glycine was observed, but the product was not isolated.

$$R-N_3 \xrightarrow[\substack{H_2O \text{ or } 2:1 \\ H_2O/iPrOH, \text{ reflux}}]{3\text{-}10 \text{ equiv. } Na_3SPO_3} R-NH_2$$
$$\mathbf{175} \qquad\qquad\qquad \mathbf{91}$$
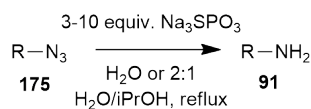
Substrate:	Product:	Time / h	Yield %
178	**179**	3	93
$CH_3(CH_2)_7N_3$ **180**	$CH_3(CH_2)_7NH_2$ **181**	16	54
$MeO_2CCH_2N_3$ **182**	$^-O_2CCH_2NH_2$ **183**	1	–
184	**185**	16	87

My role in the project was to apply the protocol to additional substrates (see Figure 5.1), and to investigate the kinetics of the reaction.
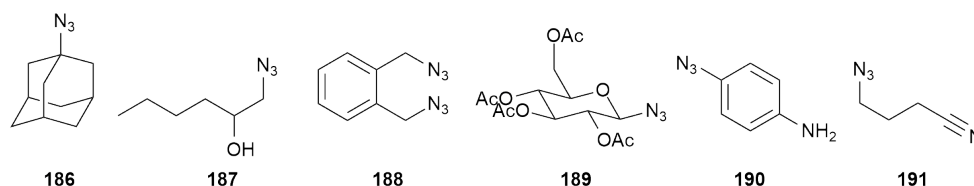
Figure 5.1: The substrates we planned to test under the optimised procedure, from left to right: 1-azidoadamantane **186**, 1-azido-2-hexanol **187**, *a,a′*-diazido-o-xylene **188**, *β*-D-Glucopyranosyl azide, 2,3,4,6-tetraacetate **189**, *p*-azidoaniline **190**, and 1-azido-3-cyanopropane **191**

The substrates which we intended to test were chosen because they were commercially available (in the case of 1-azidoadamantane **186** and 4-azidoaniline **190**), were readily synthesised from reagents we already possessed in the lab, or, in the case of 1-azidooctane **180**, had already been synthesised by Jennifer Norcliffe for use in preliminary experiments. The reduction of 1-azidooctane **180** was also to be investigated, as the yield determined by Norclife was unexpectedly low.
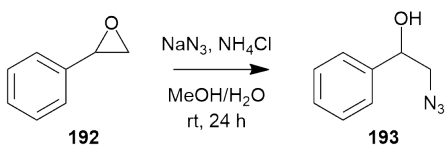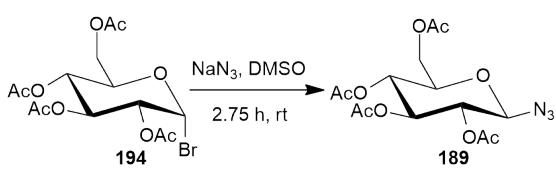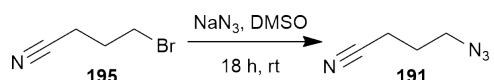
5.2 Synthesis and Results

The commercially available sodium thiophosphate was found to be relatively expensive and did not appear to be completely dry or indeed pure; a significant proportion was found to be sodium phosphate. Instead, a quantity was synthesised from thiophosphoryl chloride according to a literature procedure.[153] After purification by recrystallisation and drying, the sodium thiophosphate so produced was found by thermogravimetric analysis (TGA) to contain no water, and analysis by ^{31}P NMR spectroscopy determined that no phosphate was present.

5.2.1   Synthesis of Azides

Some azides which were not commercially available were synthesised following literature procedures (see Table 5.2).

Table 5.2: Literature procedures were followed to create some organic azide susbtrates for the reactions.

Reaction:	Yield %:	Citation:
	72	154
	76	155
	49	156

5.2.2   Reduction of Azides

Standard Procedure

The standard conditions, developed by Jennifer Norcliffe, under which the reductions were performed were 1 mmol of substrate and three equivalents of sodium thiophosphate in 10 ml of a 2:1 water / isopropanol solution. The solution was heated at reflux for three hours. Upon completion of the reaction, the solution was extracted with chloroform.

The products of the reaction were analysed by ^{1}H and ^{13}C NMR spectroscopy, and their identities confirmed by 'spiking' the sample with the authentic material.

Results

The results of the thiophosphate reduction reaction are shown in Table 5.3. The standard reaction conditions were followed, unless otherwise stated. The cases in which deviation does occur from the standard conditions are discussed below.
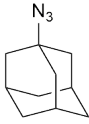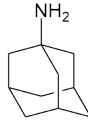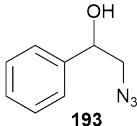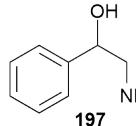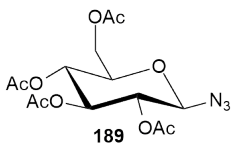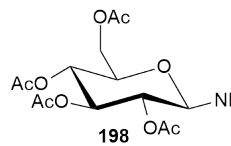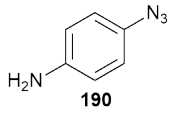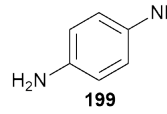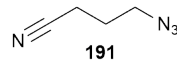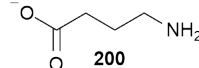
1-Azidoadamantane

1-azidoadamantane **186** had been investigated previously as a substrate for these reductions by Jennifer Norcliffe, and been found to be problematic. The reaction of this tertiary azide was very slow, and even after 24 hours was incomplete. The reaction time was therefore extended, and ten equivalents of thiophosphate were used; five equivalents initially, followed after 24 hours by a further five equivalents and a further 24 hours of heating. Despite these modifications to the standard procedure, a yield of only 43% was achieved. The material recovered is fully reduced to the amine, and so the problem appears to be one of mass recovery, however, repeated extractions failed to significantly improve the yield.

1-Azidooctane

There was no improvement over the yield previously reported by Jennifer Norcliffe. To ensure that protonation of the amine **181** was not occurring, and thus keeping it in the aqueous solution, the aqueous layer was made more alkaline through the addition of sodium hydroxide, before extraction into chloroform was again attempted. This, however, did not appreciably improve the yield.

Table 5.3: Results of reduction of several substrates. The non-standard reaction conditions are **a**: 5 equiv. Na_3SPO_3 initially, 5 equiv. after 24 h, total reaction time 48 h; **b**: 3.5 equiv. Na_3SPO_3 in an NMR tube with D_2O, heated to 90 °C for 5 h. NaOD added and heated for a further 18 h. Complete conversion to product obseved, but not isolated.

Substrate:	Product:	Conditions:	Yield %
186	196	a	43
$CH_3(CH_2)_7N_3$ 180	$CH_3(CH_2)_7NH_2$ 181	Standard	54
193	197	Standard	72
189	198	Standard	0
190	199	Standard	56
191	200	b	-

One side reaction which could have been responsible for reducing the quantity of product recovered would be the formation of a phosphoramidate

(Scheme 5.5), which would be highly water soluble. To determine whether this had occurred, the aqueous layer remaining from the extraction was analysed by ^{31}P NMR spectroscopy, then spiked with some commercial sodium orthophosphate and analysed again. Only a single peak was visible in both cases, indicating that the only phosphorus containing species present was inorganic phosphate.

Another possible side reaction that was considered was elimination to form an alkene. To investigate this, a smaller scale reduction was attempted in an NMR tube using D_2O and D_3OD rather than the water / isopropanol used in the standard protocol). Reaction progress was monitored by ^{1}H and ^{31}P NMR spectroscopy to look for any signs of alkene or phosphoramidate formation. The only signals observed, however, were those belonging to the expected amine **181**.

No improvement over the originally reported yield of 54% could be achieved. Again the source of the difficulty appears to be the recovery of the product, but it is not clear why this is so problematic.

β-D-Glucopyranosyl azide, 2,3,4,6-tetraacetate

The standard procedure for reduction was applied to the newly formed azide **189**, but a brown precipitate appeared soon after the reaction began, suggesting that the basic conditions of the reduction had caused decomposition of the sugar derivative. The precipitate (possibly carbon) was soluble in neither chloroform nor water, and so no NMR spectroscopy was possible. For this reason, no yield was recorded for this substrate.

p-Azidoaniline

Preliminary experiments carried out in D_2O to follow the progress of the reaction (see section 5.3) had shown that the substrate **190** was fully reduced after around 3 h at 70 °C. Despite NMR spectroscopy experiments showing complete conversion of the azide, work-up of the reaction gave only a 54%

isolated yield. This may be attributable to the hydrophilicity and poor partitioning of the diamine product between chloroform and the aqueous solvent in the presence of isopropanol.

1-Azido-3-cyanopropane
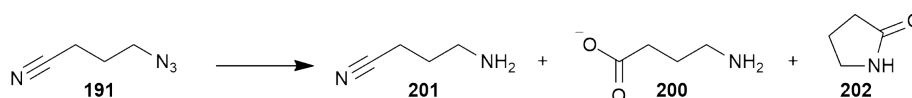
Scheme 5.4: The various products of the reduction of
1-azido-cyanopropane under the reaction conditions

Under the reaction conditions, it was hypothesised that side reactions such as hydrolysis, or cyclisation to form a lactam **202** could occur. To observe the evolution of these species, a small scale reaction was first carried out at 90 °C using D$_2$O as the solvent. This experiment showed that a mixture of species is indeed formed (see Scheme 5.4), and that even after more than 36 h of heating, no single product was formed. Dividing the reaction mixture and 'spiking' one with γ-aminobutyric acid **200** (GABA) and one with 2-pyrrolidone **202** showed that these were both present, in an approximately 30:70 ratio.

Pushing the reaction all the way to form GABA **200** was deemed to be the most expedient way of producing a single product. Therefore, upon completion of the reduction, 20 equivalents of sodium deuteroxide were added, and the NMR tube heated overnight to fully hydrolyse the products. After 18 h of heating, the susbtrate was found to have been completely converted to GABA, and confirmed by an authentic GABA 'spike'. Due to its water solubility, we did not attempt to extract the product, thus a yield was not recorded.
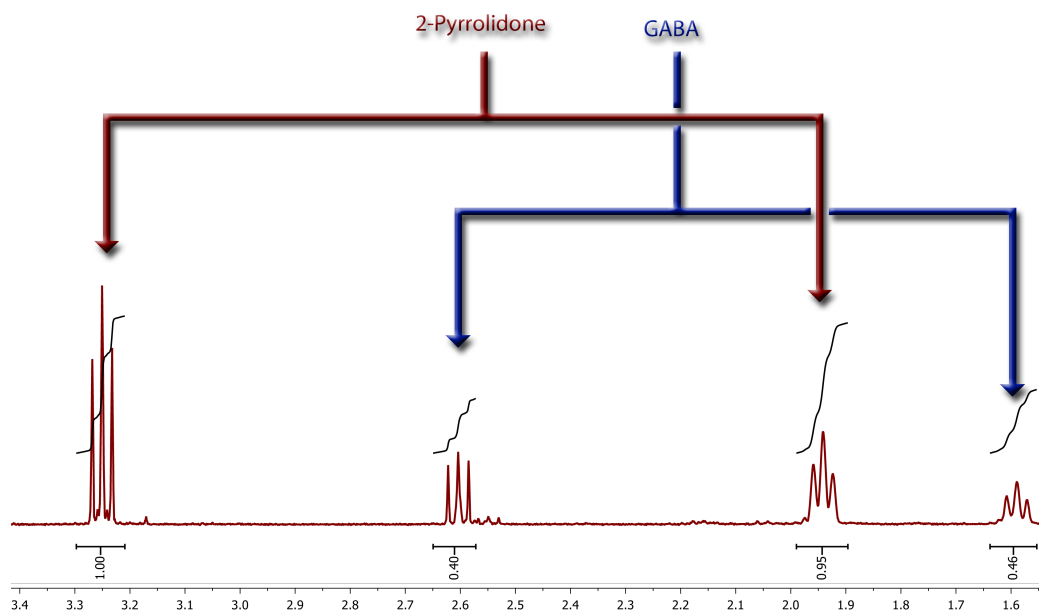
Figure 5.2: The azide **191** was reduced, however hydrolysis also
occurred, leading to multiple products.

5.3 Mechanism

Three mechanisms were proposed for the reduction of azides using thiophos-
phate; the thiophosphate anion may first attack the azide and then hydrolyse,
or form a cyclic intermediate which hydrolyses to yield the amine. Alterna-
tively, the thiophosphate may hydrolyse first to form hydrosulphide anions
which can then attack the azide to produce the amine.

In order to help resolve this question, two identical small scale reactions
were carried out in NMR spectroscopy tubes using deuterated solvent. This
allowed the progress of the reduction (^{1}H NMR spectroscopy) and the propor-
tions of phosphorus species involved in the reaction (^{31}P NMR spectroscopy)
to be monitored. Two experiments were necessary in order to monitor the
reaction by both ^{1}H NMR and ^{31}P NMR spectrometry. *p*-Azidoaniline **190**
was used as the substrate, owing to the simple NMR spectra both of it, and
the product of the reaction, *p*-diaminobenzene **199**. The data from the ex-
periments were combined to produce a graph of the concentration of reagents

Pathway A
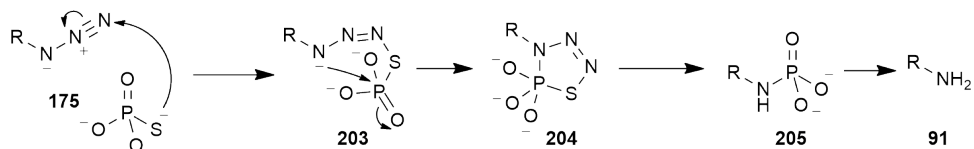
Pathway B
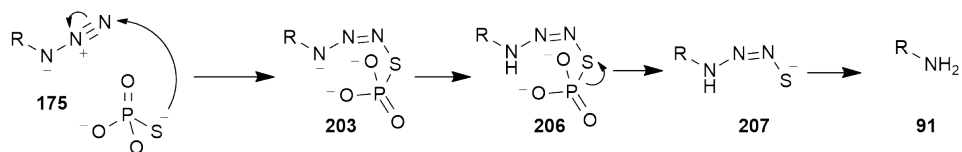
Pathway C
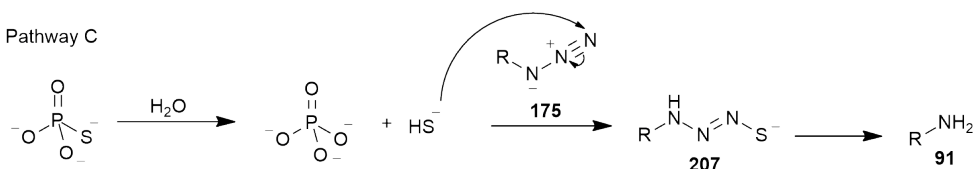
Scheme 5.5: Some proposed mechanisms for the reduction

and products over time (Figure 5.3).

There is a clear lag in the formation of the product, indicating that some time is required for an intermediate to build up. This supports pathway C as the mechanism of reduction, as the rate of formation of product will depend upon the concentration of thiolate, which in turn is produced via the hydrolysis of thiophosphate. Interestingly, the concentration of thiophosphate appears to decrease almost linearly, suggesting zero order kinetics. However, this is probably due to the pH of the solution decreasing from 11 to 9 as thiophosphate is converted to phosphate, accelerating the process of hydrolysis. The rate acceleration due to the increase in acidity appears to counter the retardation caused by the decrease in thiophosphate concentration, so that the overall rate of decay seems almost constant.

Carrying out the reduction under more or less basic conditions has shown that reducing the pH of the reaction mixture greatly accelerates the hydrolysis of thiophosphate, while increasing the pH effectively brings it to a halt. In
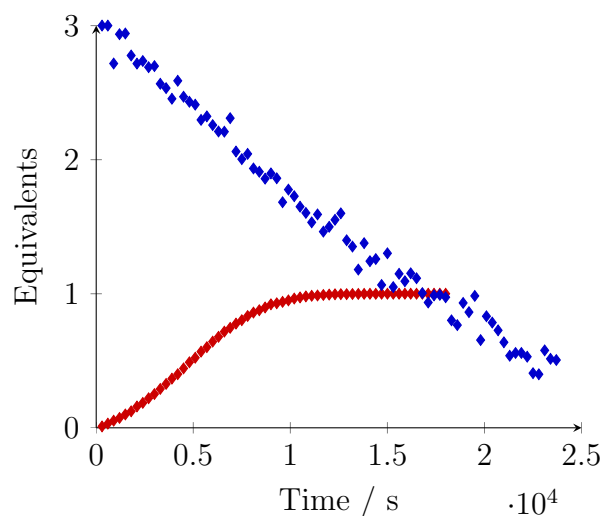
Figure 5.3: The change in concentration of thiophosphate (blue) and
4-aminoaniline **199** (red) with time.

both cases, the reduction of the substrate is adversely affected, which is
consistent with the proposed mechanism. Further studies could be performed
to investigate the effect pH has on the consumption of thiophosphate and
reduction of the substrate. This could be done by systematically changing
the starting pH of the reaction, or performing the reaction in a buffered
solution.

5.4 Conclusion

In contrast to the alternative methods, using sodium thiophosphate is conve-
nient, and generates byproducts which are easily separated from the product.
The byproducts themselves (aqueous polysulphides and hydrosulphide) are
easily disposed of; oxidation to sulphate with bleach renders them innocu-
ous. Typically three equivalents of sodium thiophosphate are used, and the
reaction is allowed to continue for 3 h. Sodium thiophosphate can be bought
commercially or synthesised cheaply and quickly from thiophosphoryl chlo-
ride, as was the case for the majority of our experiments.[153]

We have shown that trisodium thiophosphate is an effective reagent for the reduction of alkyl and aryl azides to amines on a range of substrates, although some, such as the azido adamantane **186**, required more forcing conditions. Full conversion to the amine is observed on the substrates which we have followed by NMR spectroscopy; the low yields of some of the reactions would appear to be due poor recovery of the product from the aqueous reaction mixture.

The most likely mechanism for this reaction appears to be hydrolysis of the thiophosphate to produce thiolate ions. It is then this species which actually attacks the azide to produce the amine. This mechanism is consistent with the observed requirement that the pH of the reaction mixture is high enough to deprotonate hydrogen suphide, but not so high that hydrolysis of thiophosphate comes to a halt.

This work has been published in Tetrahedron Letters.[157]

Chapter 6

Appendix A: The Synthesis of Guanosine Monophosphate Analogues for Use in G-Quadruplex Studies

6.1 Introduction

As part of a collaboration with the Wu group in Queen's University at Kingston, Canada, the Hodgson group synthesised several derivatives of guanosine monophosphate (GMP). The Wu group would then use solid state NMR techniques to investigate the ability of these compounds to form G-quadruplex structures (Figure 6.1) in solution.

A G-quadruplex structure occurs when four guanosine nucleotides arrange themselves in tetramers. This arrangement is stabilised by the presence of alkali metal cations, which are bound in the central channel.

Sodium GSMP **209** – the sodium salt derivative of S-linked guanosine monothiophosphate - had already been synthesised by a member of the Hodgson group using our own procedure and used in initial studies.[158,159]
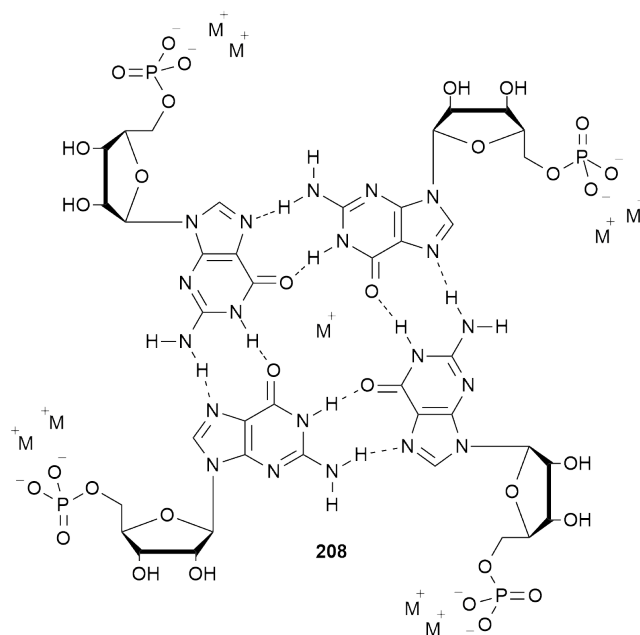
Figure 6.1: A G-quadruplex

The thiophosphate analogue **209** had been found to gelate much more readily than natural GMP, which is a physical manifestation of aggregation of the tetramers. It was hypothesised that the change in length (*i.e.* the O-P-S versus the O-P-O bond length) of the phosphate group has a role to play in the aggregation of these tetramers into helices. The cations were found to inhabit three different environments, from solid state NMR studies. These corresponded to being bound in the central channel of the helix, in association with the pendant phosphate groups, or being free in solution. This interaction with the phosphate group indicates that the identity of the alkali metal may be of significance. The aim of this project was therefore to investigate the properties of a range of guanosine monophosphate analogues in the form of salts of several alkali metal cations.
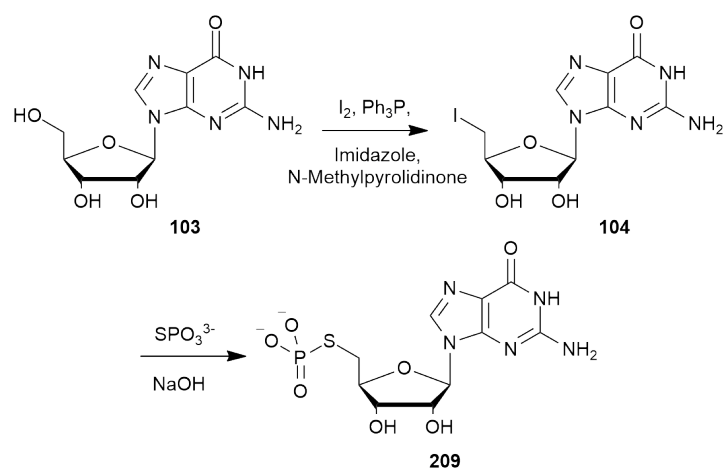
Scheme 6.1: The synthesis of GSMP **209**
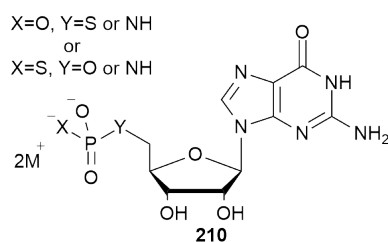
Figure 6.2: The general form of the derivatives to be synthesised

My role was to synthesise some more derivatives in which phosphate groups were replaced by sulphur and nitrogen-containing derivatives, and where the sodium used in the initial studies was replaced by other counter ions (Figure 6.2.

6.2   Synthesis

Having studied the *S*-linked thiophosphate **209** already, the next logical step
was to synthesise the *O*-linked thiophosphate **212** (GMPS).
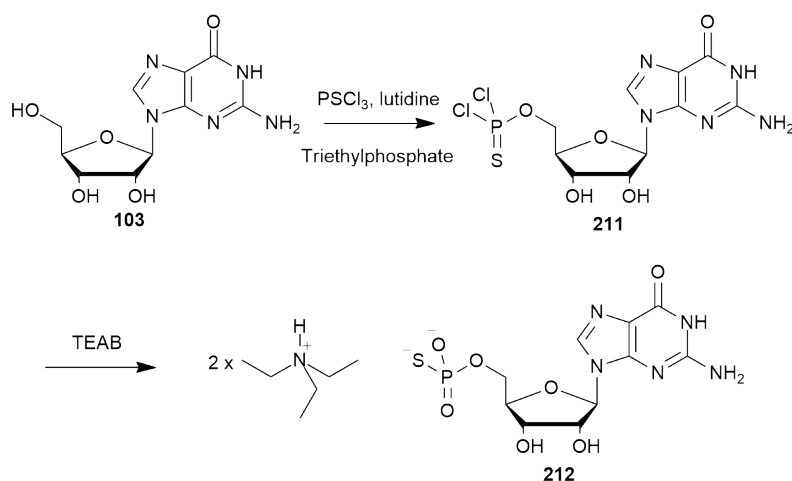
Scheme 6.2: The synthesis of GMPS **212**

This proved more difficult to accomplish; while GSMP **209** is formed in high
yield from the aqueous reaction of sodium thiophosphate and 5′-iodoguanosine
104, without the need for laborious purification, GMPS **212** requires the re-
action of guanosine with thiophosphoryl chloride under very dry conditions
in a Yoshikawa-type phosphorylation (see chapter 1). Guanosine is known
to be insoluble in most common solvents; the aqueous deprotonation used to
solubilise it in the GSMP synthesis cannot be used here. The reaction there-
fore gave a poor yield of product, which was then purified by ion exchange
chromatography to produce the triethylammonium GMPS salt. The salt was
then codissolved with sodium iodide, and the sodium salt precipitated by the
addition of acetone.

The lithium salt of GSMP **214** was also synthesised, simply by dissolving

the sodium salt in water with several equivalents of the lithium salt, followed by precipitation through the addition of acetone. This was repeated several times until 99% of the product was in the form of the lithium salt as determined through ICP-AES.
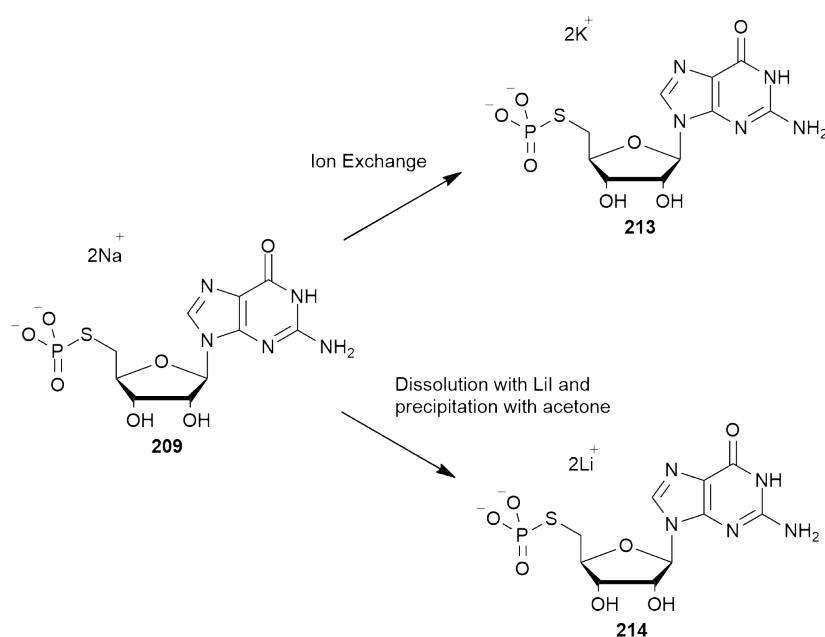
Scheme 6.3: The formation of different salts of GSMP

This method could also be used to produce the lithium salt of GMPS, using the sodium salt mentioned earlier. The analytical techniques performed on the compound are non destructive, and so the sodium salt could potentially be recovered and the cation exchanged for lithium to give another compound for testing.

The potassium salt of GSMP **213** was another target for synthesis. The method of cation exchange (codissolution in water with the metal iodide and precipitation with acetone) could not be applied here due to the insolubility of potassium iodide in acetone. Instead, we attempted to use ion exchange

chromatography to produce the desired salt. A cation exchange resin was first loaded with potassium ions by passing a potassium chloride solution over it. The sample of sodium GSMP **209** was then injected and passed over the resin. It was hoped that the large excess of potassium ions versus the sodium ions present in the sample would result in a product which was almost entirely in the form of the potassium salt. However, analysis of the product found that it still had significant sodium impurities, and so several repetitions would be necessary. Upon attempting the ion exchange again, however, the very property that we were investigating began to work against us. The potassium salt **213** appears to be an effective gelator, as the maximum flow rate of the column dropped until it was effectively unusable. This approach was therefore abandoned as being too time consuming.

6.3   Conclusions

We have synthesised several GMP derivatives for use in ssNMR studies. Problems were encountered in the synthesis of the potassium salts, which could possibly be obviated, in the case of GSMP, by using potassium thiophosphate in the beginning of the synthesis, rather than creating the sodium salt and exchanging the metal. This would be a promising route should further derivatives be required in the future. If the sodium salt is accessible, then we have shown that it is trivial to produce the lithium version, and this method could be applied to a number of derivatives to produce further diversity in this group of compounds.

Chapter 7

Appendix B: The Fluorescent Labelling of 5′-Hydrazino-5′-deoxyguanosine for Use in RNA Labelling Studies

7.1   Introduction
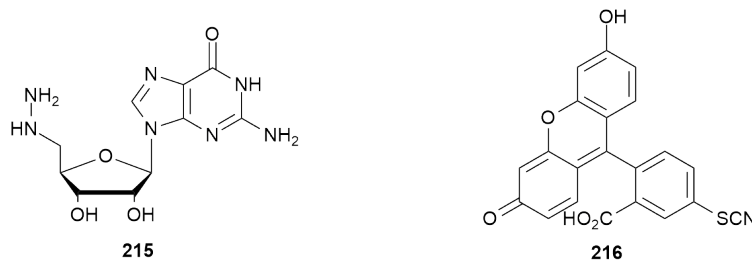
Figure 7.1: 5′-Deoxy-5′-hydrazinoguanosine **215** (GNN) and fluorescein isothiocyanate **216** (FITC)

131

The work described in this appendix was carried out in support of a project to incorporate 5'-hydrazino-5'-deoxyguanosine (GNN) **215** into the 5'- terminus of an RNA strand, and subsequently label it with fluorescein isothiocyanate (FITC) **216** (Scheme 7.2).

Fluorescent labelling of RNA is well studied and a number of different approaches have been developed. A common strategy is to incorporate nucleosides modified to possess a reactive functionality either chemically or enzymatically. An example of this, using 5'-deoxy-5'-*N*-phosphoramidatoguanosine **90** which is later unmasked as the 5'-amine **89**, is described in section 2.1.1. A few examples of other functional groups which have been incorporated include nucleoside monophosphates with amine, disulphide, or alkyne groups, which provide a useful handle for conjugation. An amidation, thiol–disulphide exchange, or Huisgen cycloaddition may then be performed to conjugate a fluorophore.[160]

Different functionalites can be included in the same RNA strand, allowing selective labelling of each terminus. Such a strategy has been employed by Yi, Xi, *et al.*,[161] where a fluorophore and a quencher are placed at either end of an RNA strand; hairpin formation can then be detected by the quenching of the fluorescence.
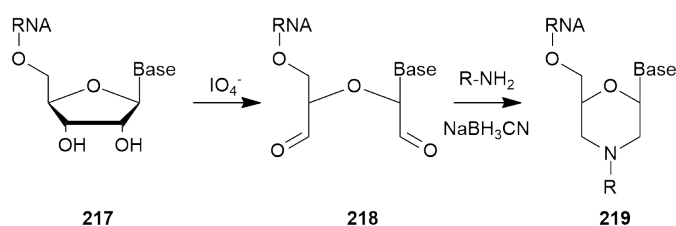
Scheme 7.1: The post-synthetic 3'- labelling of an RNA strand.

The RNA can also be modified post-synthetically; a common technique for labelling the 3'-terminus is periodate diol cleavage of the 2'-/3'- positions

followed by reductive amination provides a strategy for the stable ligation of a fluorophore (see Scheme 7.1).[160, 162]
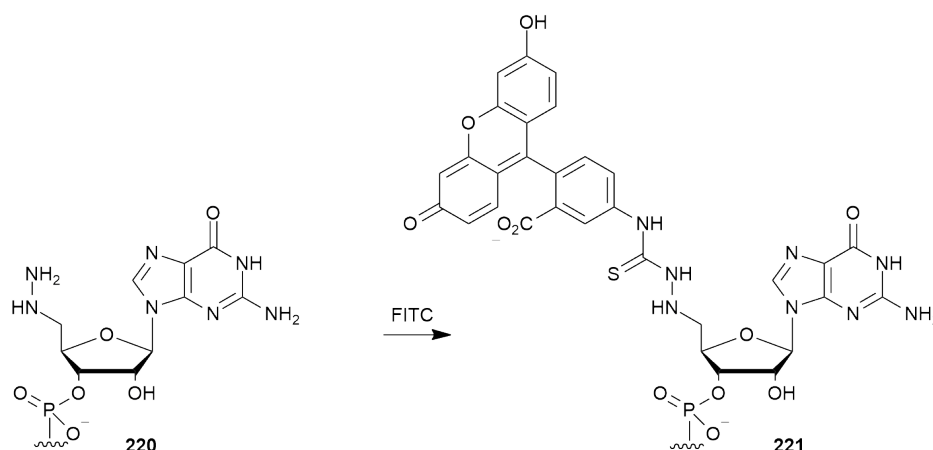
Scheme 7.2: The labelling of the 5′-terminal hydrazine of 5′-deoxy-5′-hydrazinoguanosine-incorporated RNA **220** with fluorescein isothiocyanate **216**

The aim of this project was to establish how many FITC adducts could be bound to the hydrazine group. To do this, 5′-hydrazino-5′-deoxyguanosine **215** was synthesised, following a literature procedure,[159] and was used as a model for 5′-hydrazino terminally labelled RNA **220**.

7.2 FITC Labelling

To label the GNN **215** with FITC **216**, the hydrazine was dissolved in triethylammonium bicarbonate (TEAB) buffer, and a solution of FITC in DMF was added dropwise to the solution. The reaction mixture was then stirred in a water-ice bath for four hours.

The reaction rates of amines with a range of conjugated isothiocyanates have

been measured by Martvon and Sura[163] with the slowest reaction having a bimolecular rate constant of 9.81 M^{-1} min^{-1}. If we assume the reaction of an amine with FITC to be, in the worst case, approximately this order of magnitude, then we can calculate a pseudo-first-order rate constant for the reaction: Our concentration of FITC is 10.8 mM (an approx. five fold excess), which gives us a pseudo-first-order rate constant of 0.106 min^{-1} (0.0108 M × 9.81 M^{-1} min^{-1}), and a half-life of 6.54 min (ln(2) / (0.106 min^{-1})) if the concentration of FITC is assumed to be constant. Hydrazine can be expected be an order of magnitude more reactive than an amine, to give us a pseudo-first order rate constant of approximately 1 min^{-1}, and while the isothiocyanates measured by Martvon and Sura do not include FITC, it seems reasonable to assume that the majority of the GNN will be consumed within a matter of minutes, and certainly within the timescale of the reaction.

After the four hours had elapsed, the solution was then lyophilised, and the residue was redissolved in concentrated ammonia solution and stirred for a further four hours, to ensure that all the isothiocyanate had been consumed. The solution was diluted with water, and again lyophilised. The components of the reaction mixtre were separated by ion exchange chromatography, over an anion exchange resin with a gradient of TEAB buffer, as shown in Figure 7.2. Each peak was analysed using mass spectrometry to search for any GNN-FITC adducts. The results of the analysis are tabulated in Table 7.1.

Table 7.1: The principal peaks observed by mass spectrometry in each collected peak and their identity for the labelling of GNN **215** with FITC **216**.

Peak:	Fractions:	Mass:	Assignment:
1a	23-27	346.0719 (ES−)	Hydrolysed FITC
1b	27-31	348.0861 (ES+)	Hydrolysed FITC
2a	34-36	718.1446 (ES−)	Unknown
2b	39-44	687.1613 (ES+)	Hydrazine - FITC Mono-adduct
3	46-51	371.0669 (ES−)	FITC − $2H_2O$ + NH_3 (tentative)
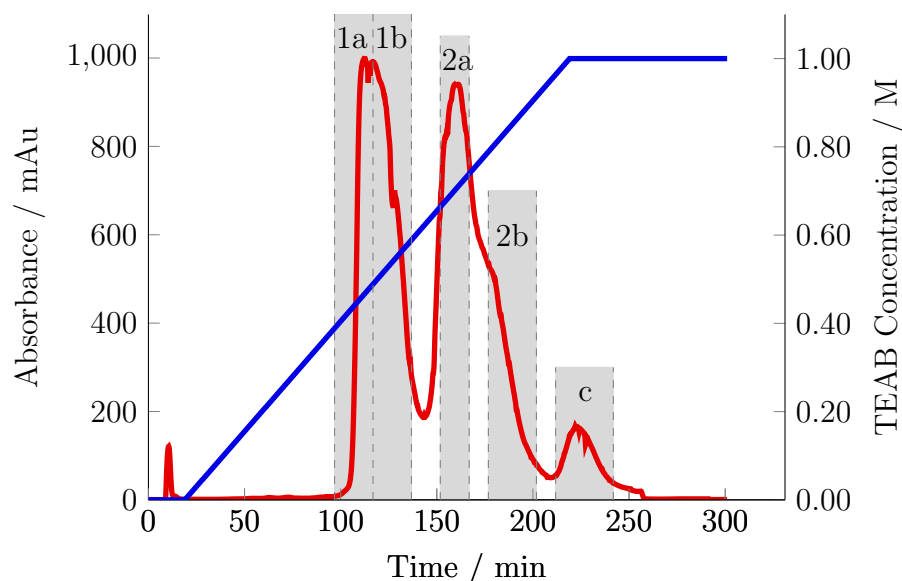
Figure 7.2: The ion exchange chromatogram of the reaction mixture resulting from the FITC labelling of GNN. The dashed lines denote the fractions which were collected.

An m/z peak corresponding to the mass of the GNN-FITC mono-adduct can be detected in the 'shoulder' of the second major peak to be eluted by ion exchange chromatography, marked **2b** in Figure 7.2. No other m/z peaks which could correspond to further conjugation to additional molecules of FITC **216** were detected, implying that the reaction proceeds no further than the mono-adduct.

The labelling experiment was repeated without the presence of GNN **215** to provide further evidence that the observed mass peak belongs to a GNN-FITC adduct. Analysis by ion exchange chromatography produces a chromatogram similar to that of the experiment including GNN, but lacking the 'shoulder' on the side of the second major peak (Figure 7.3). Mass spectrometric analysis of each of the eluted peaks showed no signs of the mass observed in the previous labelling experiment, lending further strength to the argument that the 'shoulder' is due to the presence of the GNN-FITC monoadduct.

Additionally, the collected peaks from the chromatographic separation were
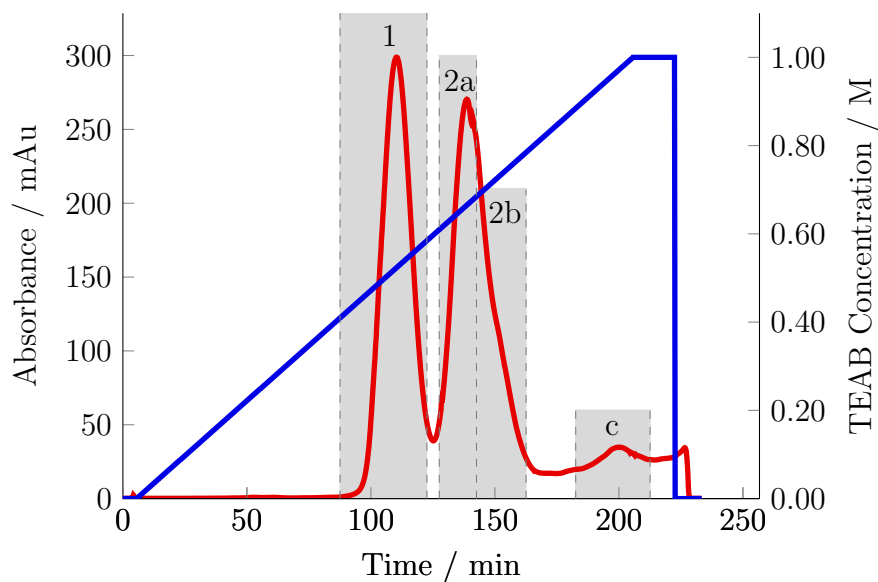
Figure 7.3: The ion exchange chromatogram of the labelling reaction in the absence of GNN **215**. The dashed lines denote the fractions which were collected.

Table 7.2: The principal peaks observed by mass spectrometry in each collected peak and their identity for the labelling reaction in the absence of GNN **215**.

Peak:	Fractions:	Mass:	Assignment:
1	20-26	346.0724 (ES−)	Hydrolysed FITC
2a	28-30	371.0672 (ES−)	$FITC - 2H_2O + NH_3$ (tentative)
2b	31-35	371.0670 (ES−)	$FITC - 2H_2O + NH_3$ (tentative)
3	39-44	371.0686 (ES−)	$FITC - 2H_2O + NH_3$ (tentative)
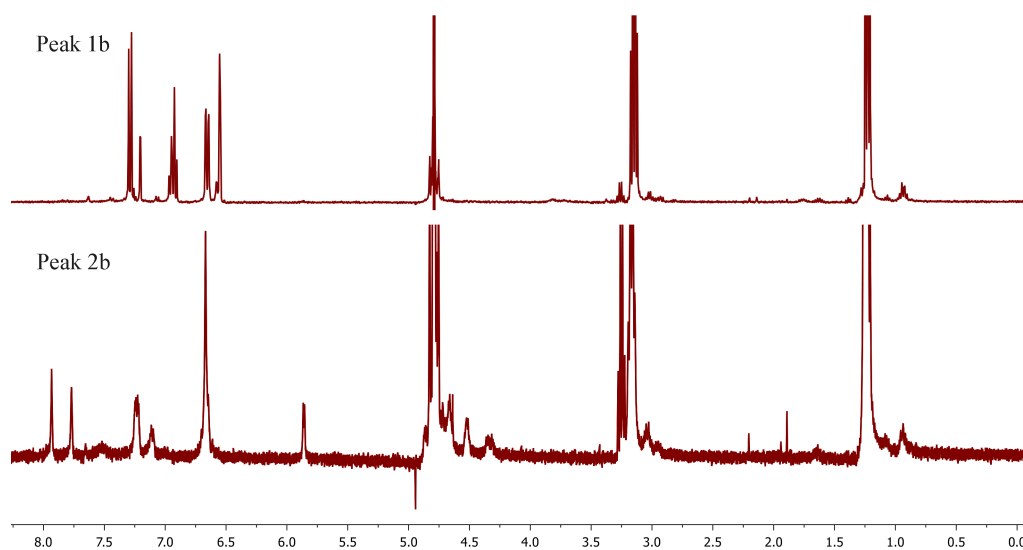
Figure 7.4: A comparison of the ^{1}H NMR spectra of peaks 1b and 2b from the chromatographic separation of the reaction mixture (*cf.* Figure 7.2).

analysed by ^{1}H NMR spectroscopy. A comparison of a non-adduct-containing peak (peak **1b**), and an adduct-containing peak (peak **2b**) from the GNN labelling experiment is shown in Figure 7.4. It can be seen that while the spectrum corresponding to peak **1b** shows only signals in the aromatic region (apart from those for the ethyl groups on the triethylammonium cation) corresponding to hydrolysed FITC, the spectrum corresponding to peak **2b** indicates the presence of both aromatic protons and those belonging to a nucleoside. this further confirms the evidence for the presence of a GNN-FITC adduct.

7.3   Conclusion

We have shown that when FITC **216** reacts in the presence of GNN **215**, a compound is formed which has an accurate mass spectrometry m/z value corresponding to that expected for a GNN-FITC adduct. Conversely, in the absence of GNN, no such m/z peak is observed. ^{1}H NMR analysis of

the products of the reaction indicates the presence of both nucleoside and aromatic protons characteristic of FITC. No evidence for any higher adducts has been found. Taken together, these findings strongly indicate that the GNN-FITC mono-adduct is formed, and the quantities of any higher adducts formed are negligible. The same conclusions can be expected to be true when RNA incorporating GNN at the 5′-terminus is labelled with FITC.

Chapter 8

Experimental

8.1 Materials and Equipment

NMR spectra were recorded on a Varian 700, Varian 500, Bruker 400, or Varian 400 spectrometer. Spectra were analysed using the MestReNova software package from Mestrelab Research S. L. on Microsoft® Windows® 7 and referenced using residual solvent peaks. All *J*-coupling values are given in Hz. Mass spectra were recorded on Thermo-Finnigan LTQ FT and Micromass LCT spectrometers. HPLC chormatograms were processed using the TotalChrom™ Chromatography Data System from PerkinElmer on Microsoft® Windows® XP. Nucleosides were dried overnight in a Büchi B-585 oven under vacuum, heated to 80 °C before being used in any reactions. Liquid amines were distilled before being used.

Nucleosides and nucleoside derivatives (with the exception of guanosine) were purchased from Carbosynth Limited. Other chemicals were purchased from Sigma-Aldrich®.

Solvents were dried prior to use, either using 3 or 4Å molecular sieves, as appropriate, which had been prepared by heating to 140 °C in a Büchi B-585 oven under vacuum, or using an Innovative Technology Inc. solvent purification system. Phosphoryl and thiophosphoryl chloride were distilled before

use. Pyridine was distilled over calcium hydride to ensure the absence of
moisture. Triethylammonium bicarbonate (TEAB) buffer was prepared by
bubbling carbon dioxide through a mixture of triethylamine (140 ml, 1.00
mol) made up to 1 l with high purity water. The triethylamine was, like
other liquid amines, distilled before use. For the constant-pH experiments,
a Radiometer TIM-856 instrument with a pHC4000 calomel combined pH
electrode was used. The probe was calibrated at 25 °C using a pH 7 stan-
dard solution, and a saturated calcium hydroxide solution for the pH 12.454
standard. Lyophilisation was performed via a Jouan high vacuum system.

8.2   Phosphorylation of Aminonucleosides

8.2.1   Miscellaneous Compounds

Lithium Azide[164]

Following a literature procedure,[164] sodium azide (6.52 g, 100 mmol) and
lithium sulphate (6.90 g, 62.8 mmol) were co-dissolved in water (35 ml) and
stirred for 10 min. Ethanol (175 ml) was added slowly, and the mixture was
stirred for a further 10 min. The precipitate was removed by filtration, and
the solvent was removed from the filtrate under vacuum. The solid residue
was dried on the high vacuum line to yield the product (4.82 g, 98%).

8.2.2 Synthesis of Adenosine Derivatives

5′-Deoxy-5′-(1,3-Dihydro-1,3-dioxo-2H-isoindol-2-yl)-2′,3′-*O*-isopropylideneadenosine (120)[124]
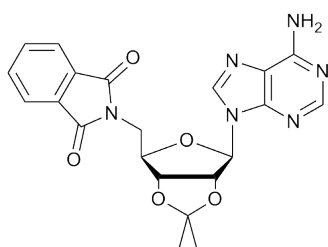
Following a literature procedure,[124] 2′,3′-*O*-isopropylideneadenosine (2.00 g, 6.51 mmol), phthalimide (958 mg, 6.51 mmol), and triphenylphosphine (1.71 g, 6.51 mmol) were placed in a round bottomed flask with dry THF (22 ml) under an atmosphere of nitrogen. Diethyl azodicarboxylate (1.13 g, 6.51 mmol) was added dropwise to the suspension. The reaction was stirred at room temperature for 2 h 15 min before being placed in the fridge overnight. The reaction mixture was then filtered, and the residue washed with diethyl ether (2 × 17 ml) before being dried in a vacuum desiccator over P_2O_5 overnight to yield the 5′-phthalimide **120** (2.02 g, 71%); ν_{max}/cm^{-1} 1769, 1710, 1661, 1597; δ_H (400 MHz, CDCl$_3$) 1.37 (3H, s, C(C*H$_3$*)$_a$(CH$_3$)$_b$), 1.58 (3H, s, C(CH$_3$)$_a$(C*H$_3$*)$_b$), 3.97 (1H, dd, *J* 14.0, 6.0, C5′*H$_a$*), 4.05 (1H, dd, *J* 14.0, 6.0, C5′*H$_b$*), 4.54 (1H, dt, *J* 6.0, 3.5, C4′*H*), 5.25 (1H, dd, *J* 6.4, 3.5, C3′*H*), 5.53 (1H, dd, *J* 6.4, 1.9, C2′*H*), 5.57 (2H, br s, N*H$_2$*), 6.02 (1H, d, *J* 1.9, C1′*H*), 7.70 (2H, dd, *J* 5.6, 2.8, phthalimide), 7.79 (2H, dd, *J* 5.6, 3.2, phthalimide), 7.86 (1H, s, C4*H*), 8.06 (1H, s, C1*H*); δ_C (100.6 MHz, CDCl$_3$) 25.6, 27.3, 39.6, 82.6, 84.2, 85.2, 90.8, 114.6, 120.5, 123.5, 132.1, 134.1, 140.5, 149.4, 153.1, 155.5, 168.3; *m/z* 437.15585 ([M+H]$^+$, 100%) requires 437.15679

5′-Deoxy-5′-amino-2′,3′-O-isopropylideneadenosine (121)[124]
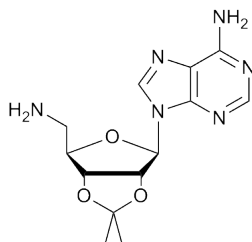
Following a literature procedure,[124] 5′-deoxy-5′-(1,3-dihydro-1,3-dioxo-2H-isoindol-2-yl)-2′,3′-O-isopropylideneadenosine (1.81 g, 4.14 mmol) was placed in a round bottomed flask with hydrazine hydrate (80% purity, 51% hydrazine, 71 ml) and ethanol (127 ml), and the mixture was heated at reflux for 18 h. The solution was then allowed to cool to room temperature, and the solvents were removed under reduced pressure. The residue was dissolved in water (19 ml) and acidified to pH 4 with acetic acid. The mixture was filtered and the pH of the filtrate was raised to 11 with sodium hydroxide solution (5 M). The solution was extracted with chloroform (3 × 35 ml) and the combined chloroform extracts were dried over $MgSO_4$, filtered, and the solvent removed to yield the amine **121** (803 mg, 64%); ν_{max}/cm^{-1} 1708, 1674, 1603; δ_H (400 MHz, CDCl$_3$) 1.38 (3H, s, C(CH_3)$_a$(CH$_3$)$_b$), 1.61 (3H, s, C(CH$_3$)$_a$(CH_3)$_b$), 2.94 (1H, dd, J 13.4, 6.0, C5′H_a), 3.02 (1H, dd, J 13.4, 4.8, C5′H_b), 4.22-4.27 (1H, m, C4′H), 5.01 (1H, dd, J 6.5, 3.5, C3′H), 5.46 (1H, dd, J 6.5, 3.0, C2′H), 5.98 (2H, br s, NH_2), 6.02 (1H, d, J 3.0, C1′H), 7.92 (1H, s, C4H), 8.32 (1H, s, C1H); δ_C (100.6 MHz, CDCl$_3$) 25.5, 27.4, 44.0, 82.0, 83.8, 87.7, 90.8, 114.7, 120.5, 140.0, 149.6, 153.3, 155.8; m/z 307.15086 ([M+H]$^+$, 100%) requires 307.15131

5′-Deoxy-5′-aminoadenosine, hydrochloride salt (122)[124]
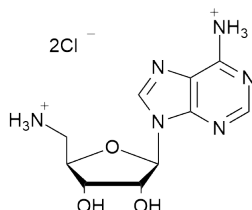
Following a literature procedure,[124] 5′-deoxy-5′-amino-2′,3′-O-isopropylidene-adenosine (645 mg, 2.10 mmol) was placed in a round bottomed flask with formic acid solution (1:1 HCOOH:H_2O, v/v, 8 ml) and the mixture was stirred at room temperature for 24 h. The solvents were then removed under reduced pressure by azeotropic coevaporation with absolute ethanol (4 × 20 ml). The residue was dissolved in ethanol (26 ml) and hydrogen chloride gas was bubbled through the solution until the hydrochloride salt precipitated. The crude product was isolated by filtration, and recrystallised from ethanol to yield the amine as the hydrochloride salt (492 mg, 68%); ν_{max}/cm^{-1} 1705, 1627; δ_H (400 MHz, D_2O) 3.41-3.54 (2H, m, C5′H_2), 4.38 (1H, dt, J 8.8, 4.2, C4′H), 4.46 (1H, dd, J 4.8, 4.2, C3′H), 4.84 (1H, app. t, J 5.4, C2′H), 6.13 (1H, d, J 5.0, C1′H), 8.42 (1H, s, C4H), 8.43 (1H, s, C1H); δ_C (100.6 MHz, D_2O) 40.2, 70.2, 72.5, 79.5, 88.7, 118.4, 142.4, 143.8, 147.1, 149.3; m/z 267.1210 ([M−HCl$_2$]$^+$, 100%) requires 267.1206

8.2.3   Synthesis of Cytidine Derivatives

*N*4-Benzoylcytidine (124)[165]
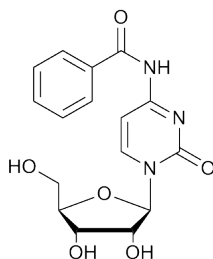
Based on a literature procedure,[165] cytidine (2.78 g, 11.4 mmol) and benzoic anhydride (2.82 g, 12.5 mmol) were placed in a round bottomed flask with dry methanol (300 ml) and the mixture was heated at reflux with stirring. After 1 h, additional benzoic anhydride (2.77 g, 12.3 mmol) was added, followed by further additions (2.79 g, 12.3 mmol after 2 h, 2.79 g, 12.4 mmol after 3 h). Heating was maintained for a total of 5 h. After allowing the reaction mixture to cool for 18 h, the precipitate was collected by vacuum filtration and dried over P_2O_5 under vacuum to yield the benzoylated nucleoside **124** (2.79 g, 70%), mp 236-238 °C (from methanol, lit.,[166] 238-240 °C); ν_{max}/cm^{-1} 3421, 3307, 3161, 1644 (CO); δ_H (400 MHz, $(CD_3)_2SO$) 3.61 (1H, ddd, *J* 12.3, 5.2, 2.9, C5′-H_a), 3.76 (1H, ddd, *J* 12.3, 5.2, 2.9, C5′-H_b), 3.92 (1H, dt, *J* 5.9, 2.9, C4′-*H*), 3.95-4.05 (2H, m, C2′-*H*, C3′-*H*), 5.05 (1H, d, *J* 5.7, C3′-O*H*), 5.18 (1H, app. t, *J* 5.2, C5′-O*H*), 5.51 (1H, d, *J* 4.8, C2′-O*H*), 5.81 (1H, d, *J* 2.9, C1′-*H*), 7.34 (1H, d, *J* 7.5, C5-*H*), 7.52 (2H, dd, *J* 8.4, 7.1, *m*-Ph), 7.63 (1H, t, *J* 7.4, *p*-Ph), 8.00 (2H, d, *J* 7.5, *o*-Ph), 8.51 (1H, d, *J* 7.5, C6-*H*), 11.25 (1H, s, N*H*); δ_C (100.6 MHz, $(CD_3)_2SO$) 60.6, 69.3, 75.3, 84.9, 90.9, 96.6, 110.0, 129.2, 133.5, 133.8, 146.1, 155.4, 163.8, 168.0; *m/z* 346.2 ([M−H]⁻, 100%) 347.2 (26) 693 (22).

N4-Benzoyl-2′,3′-O-isopropylidenecytidine (125)
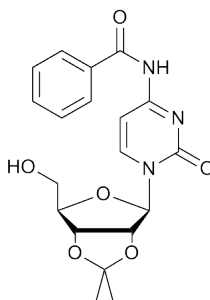
In an adapted literature procedure,[131] N4-benzoylcytidine (2.79 g, 8.03 mmol), 2,2-dimethoxypropane (11 ml), 4 Å molecular sieves, and p-toluenesulphonic acid monohydrate (0.45 g, 2.37 mmol) were placed in a round-bottomed flask with DMF (44 ml). The mixture was heated at 40 °C for 2.5 h, before Amberlyst® A-21 anion exchanger (1.19 g) was added and heating was continued for a further 30 min. The mixture was filtered through Celite®, the solvent was then removed under reduced pressure from the filtrate, and the residue was recrystallised from water to yield the acetonide **125** (2.375 g, 76%); ν_{max}/cm^{-1} 1652 (CO), 1482, 1303; δ_H (400 MHz, CDCl$_3$) 1.37 (3H, s, C(CH_3)$_a$(CH$_3$)$_b$), 1.63 (3H, s, C(CH$_3$)$_a$(CH_3)$_b$), 3.54 (1H, br s, C5′-OH), 3.84 (1H, app. d, J 12.3, C5′-H_a), 3.97 (1H, dd, J 12.3, 2.3, C5′-H_b), 4.40 (1H, app.q, J 3.0, C4′-H), 5.09 (1H, dd, J 6.4, 3.2, C3′-H), 5.25 (1H, dd, J 6.4, 2.7, C2′-H), 5.55 (1H, d, J 2.7, C1′-H), 7.52 (2H, d, J 7.8, m-Ph), 7.63 (1H, t, J 7.4, p-Ph), 7.81 (1H, d, J 7.4, C6-H), 7.89 (2H, d, J 7.5, o-Ph), 8.77 (1H, s, NH); δ_C (126 MHz, CDCl$_3$) 25.2 ((CH$_3$)$_a$), 27.3 ((CH$_3$)$_b$), 62.9 (C3′), 80.5 (C2′), 83.6 (C4′), 88.1 (C1′), 99.0 (C5), 100.0 (C(CH$_3$)$_a$(CH$_3$)$_b$), 112.8 (C5′), 114.1 (C2), 127.3, 127.6 (Arom. Bz), 128.6 (Arom. Bz), 129.1 (Arom. Bz), 133.4 (Arom. Bz), 143.3 (C6), 166.1 (C4); m/z 388.1500 ([M+H]$^+$, 20%), requires 388.1509, 410.1325 ([M+Na]$^+$, 100).

*N*4-Benzoyl-2′,3′-*O*-isopropylidene-5′-*O*-toluenesulphonylcytidine (126)
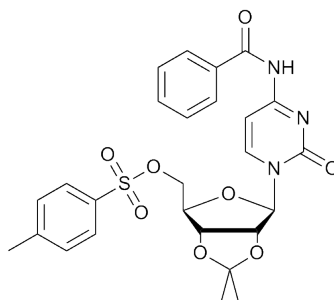
*N*4-Benzoyl-2′,3′-*O*-isopropylidenecytidine (2.10 g, 5.42 mmol), 4-toluene-sulphonyl chloride (2.44 g, 12.9 mmol), pyridine (20 ml) and DCM (40 ml) were placed in a round-bottomed flask and heated at reflux for 2.5 h. The solution was then diluted with chloroform (120 ml) and washed with hydrochloric acid (0.5 M, 5 × 50 ml) and saturated sodium hydrogencarbonate solution (2 × 50 ml). The organic layer was dried over MgSO$_4$, filtered, and the solvent was removed under reduced pressure to yield the crude tosylate **126**, which was used in the next reaction without further purification. (1.53 g).

5′-Azido-5′-deoxy-*N*4-benzoyl-2′,3′-*O*-isopropylidenecytidine (127)
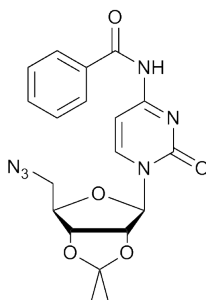
*N*4-Benzoyl-2′,3′-*O*-isopropylidene-5′-*O*-toluenesulphonylcytidine (1.08 g, 1.99 mmol) and sodium azide (579 mg, 8.91 mmol) were placed in a flask with DMSO (10 ml) and heated at 70 °C for 2 h 20 min. The solution was then added to H_2O (550 ml) and the mixture was stirred for 18 h at room temperature. The precipitated protected azide **127** was then isolated by vacuum filtration and washed with water. (430 mg, 52%); mp 163-165 °C; ν_{max}/cm^{-1} 3354, 1640 (CO), 1485; δ_H (400 MHz, CDCl$_3$) 1.37 (3H, s, C(C*H$_3$*)$_a$(CH$_3$)$_b$), 1.60 (3H, s, C(CH$_3$)$_a$(C*H$_3$*)$_b$), 3.65 (1H, dd, *J* 12.8, 4.4, C5′-*H$_a$*), 3.76, (1H, dd, *J* 12.8, 6.8, C5′-*H$_b$*) 4.31-4.36 (1H, m, C4′-*H*), 4.90 (1H, dd, *J* 6.4, 4.0, C2′-*H*), 5.11-5.15 (1H, m, C3′-*H*), 5.70 (1H, d, *J* 1.5, C1′-*H*), 7.53 (2H, t, *J* 7.6, *m*-Ph), 7.63 (1H, t, *J* 7.4, *p*-Ph), 7.77 (1H, d, *J* 7.4, C6-*H*), 7.89 (2H, d, *J* 7.2, *o*-Ph), 8.67 (1H, s, N*H*); δ_H (100 MHz, CDCl$_3$) 25.2 ((CH$_3$)$_a$), 27.3 ((CH$_3$)$_b$), 62.8 (C3′), 77.2 (C5′), 80.5 (C2′), 83.8 (C4′), 88.1 (C1′), 97.0 (C5), 98.7 (C(CH$_3$)$_a$(CH$_3$)$_b$), 114.1 (C2), 127.7 (Arom. Bz), 129.1 (Arom. Bz), 132.7 (Arom. Bz), 133.4 (Arom. Bz), 147.8 (C6), 163.1 (C4); *m/z* 413.1585 ([M+H]$^+$, 100%), requires 413.1573, 435.1406 ([M+Na]$^+$, 40%).

5′-Azido-5′-deoxycytidine (128)
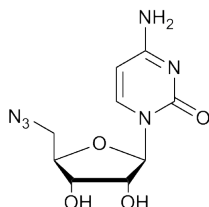
5′-Azido-5′-deoxy-N4-benzoyl-2′,3′-O-isopropylidenecytidine (732 mg, 1.78 mmol) was placed in a round-bottomed flask with a 1:1 mixture of methanol and ammonia solution (90 ml, 35% w/w) and the mixture was stirred at room temperature for 18 h. The solvents were removed under reduced pressure, and the residue was stirred in a 9:1 mixture of trifluoroacetic acid and H_2O for 3 h at room temperature before the solvents were removed under reduced pressure. The residue was dissolved in H_2O and introduced to a protonated SP Sepharose® Fast Flow cation exchange column (1.6 cm i.d. × 22 cm, 5 ml/min flow rate). The nucleoside was eluted with a 3% ammonium hydroxide solution (diluted from 35% (w/w) ammonia solution) and the eluted fractions were freeze-dried. The residue was then dissolved in methanol and filtered, and the solvent was removed from the filtrate under vacuum to give the deprotected azide **128**. (334 mg, 70%); ν_{max}/cm⁻¹ 2104 (N_3),1645 (CO), 1438; δ_H (400 MHz, D_2O) 3.64 (1H, dd, J 13.7, 5.0, C5′-H_a), 3.78 (1H, dd, J 13.7, 3.1, C5′-H_b), 4.14-4.19 (1H, m, C4′-H), 4.21 (1H, dd, J 6.2, 5.3, C3′-H), 4.34 (1H, dd, J 5.3, 4.0, C2′-H), 5.87 (1H, d, J 4.0, C1′-H), 6.03 (1H, d, J 7.6, C5-H), 7.74 (1H, d, J 7.6, C6-H); δ_C (100 MHz, D_2O) 51.2 (C5′), 69.9 (C3′), 73.3 (C2′), 81.5 (C4′), 90.5 (C1′), 96.3 (C5), 141.6 (C4), 157.4 (C6), 163.8 (C2); m/z 267.2 ([M−H]⁻, 100%) 268.3 (15).

5′-Amino-5′-deoxycytidine (129), dihydrochloride salt
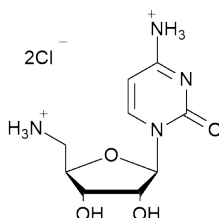
5′-Azido-5′-deoxycytidine (400 mg, 1.49 mmol) was placed in a flask with triphenylphosphine (790 mg, 3.01 mmol) and pyridine (6 ml). The solution was stirred at room temperature for 3 h before further triphenylphosphine (791 mg, 3.02) and pyridine (6 ml) were added. The solution was stirred for an additional 3 h at room temperature before ammonia solution (50 ml, 35% w/w) was added, whereupon immediate precipitation was observed. The mixture was stirred overnight before being diluted with water (100 ml) and extracted with chloroform (3 × 100 ml). Residual chloroform was removed from the aqueous layer under vacuum, and the aqueous extracts were lyophilised. The resulting solid was dissolved in ethanol (60 ml) and hydrogen chloride gas was bubbled through the solution. The addition of diethyl ether (300 ml) precipitated the dihydrochloride salt, which was isolated by filtration, washed with a small quantity of diethyl ether, and dried under vacuum overnight over P_2O_5 (382 mg, 81%); mp 190-191 °C (decomp., from ethanol); ν_{max}/cm^{-1} 3118, 3046, 1715, 1673, 1404; δ_H (400 MHz, D_2O) 3.34 (1H, dd, J 13.6, 9.4, C5′-H_a), 3.47 (1H, dd, J 13.6, 3.0, C5′-H_b), 4.18-4.31 (2H, m, C3′-H, C4′-H) 4.51 (1H, dd, J 5.5, 3.4, C2′-H), 5.77 (1H, d, J 3.4, C1′-H), 6.24 (1H, d, J 7.9, C5-H), 7.87 (1H, d, J 7.9, C6-H); δ_C (100 MHz, D_2O) 41.9 (C5′), 71.4 (C3′), 73.5 (C2′), 80.2 (C4′), 94.1 (C1′), 95.8 (C5), 137.8 (C4), 145.9 (C6), 160.9 (C2); m/z 243.1095 ([M+H]$^+$, 50%), requires 243.1093, 265.0907 ([M+Na]$^+$, 100).

8.2.4 Synthesis of Guanosine Derivatives

5′-deoxy-5′-iodoguanosine (104)[120]
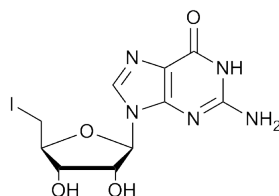
Following a literature procedure,[120] guanosine (10.0 g, 35.3 mmol), *N*-methyl-pyrrolidinone (136 ml), imidazole (15.0 g, 221 mmol), and triphenylphosphine (29.2 g, 111 mmol) were placed in a flask with a drying tube ($CaCl_2$). While the mixture was being stirred, iodine (26.7 g, 104 mmol) was slowly added. The mixture was stirred at room temperature for 3 h before being poured into DCM (1.34 l) and water (400 ml). The mixture was left overnight to precipitate before the crude product was collected by filtration. The crude product was refluxed with DCM (400 ml), then filtered and refluxed in water (400 ml) before being again filtered to yield the product (4.57 g, 33%); δ_H (400 MHz, $(CD_3)_2SO$) 3.42 (1H, dd, *J* 10.4, 6.7, C5′-H_a) 3.56 (1H, dd, *J* 10.5, 6.2, C5′-H_a) 3.90-3.96 (1H, m, C4′-*H*) 4.03-4.09 (1H, m, C3′-*H*), 4.63 (1H, q, *J* 5.8, C2′-*H*), 5.40 (1H, d, *J* 4.8, C3′-O*H*), 5.56 (1H, d, *J* 6.1, C2′-O*H*), 5.71 (1H, d, *J* 6.2, C1′-O*H*), 6.50 (2H, s, N*H₂*), 7.93 (1H, s, C6-*H*), 10.65 (1H, s, N*H*)); δ_C (101 MHz, $(CD_3)_2SO$) 8.0, 72.7, 73.1, 83.8, 86.5, 100.5, 116.7, 135.8, 151.4, 153.7, 156.7

5′-Azido-5′-deoxyguanosine (105)[120]
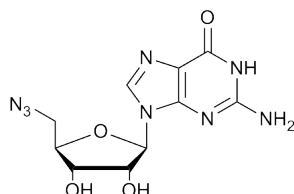
Following a literature procedure,[120] 5′-deoxy-5′-iodoguanosine (3.00 g, 7.63 mmol) and sodium azide (1.15 g, 17.8 mmol) were stirred in DMF (24 ml) under nitrogen for 20 h. The DMF was then removed under reduced pressure, and the residue was stirred in water for 30 min. The precipitate was collected by filtration and washed with cold water (2 × 20 ml), ethanol (14 ml), and finally diethyl ether (10 ml). The product was dried overnight under vacuum over phosphorus pentoxide to yield the azide **105** (2.05 g, 87%); δ_H (400 MHz, $(CD_3)_2SO$) 3.52 (1H, dd, J 13.1, 3.9, C5′-H_a) 3.67 (1H, dd, J 13.1, 7.1, C5′-H_b) 3.90-3.96 (1H, app. dt, J 7.4, 3.8, C4′-H) 4.06 (1H, dd, J 5.1, 3.6, C3′-H), 4.58 (1H, app. t, J 5.5, C2′-H), 5.72 (1H, d, J 5.8, C1′-OH), 6.55 (2H, s, NH_2), 7.91 (1H, s, C8-H), 10.78 (1H, s, NH)); δ_C (101 MHz, $(CD_3)_2SO$) 51.8, 71.0, 72.7, 82.8, 86.8, 116.9, 135.8, 151.4, 153.9, 157.1

5′-Amino-5′-deoxyguanosine (89)[120]
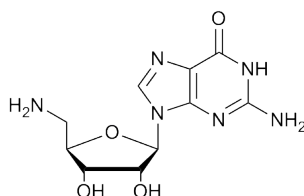
Following a literature procedure,[120] 5′-azido-5′-deoxyguanosine (2.00 g, 6.49 mmol) and triphenylphosphine (3.40 g, 13.0 mmol) were stirred in pyridine (32 ml) at 0 °C for 3 h. After this time, a cold solution of ammonia (10 ml 35% ammonia solution in 34 ml water) was added and the mixture was stirred for a further 18 h. The solvents were then removed under reduced pressure, and the residue was stirred in ethyl acetate (200 ml) for 15 min. The mixture was then filtered and the solid was washed with cold ethyl acetate (36 ml) and methanol / ethyl acetate solution (50:50 *v:v*, 36 ml). The retained solid was recrystallised from water to yield the amine **89** (1.34 g, 73%); δ_H (400 MHz, $(CD_3)_2SO$) 2.71 (1H, dd, *J* 13.4, 5.4, C5′-H_a) 2.78 (1H, dd, *J* 13.4, 5.0, C5′-H_b) 3.75-3.82 (1H, m, C4′-*H*) 4.05-4.10 (1H, m, C3′-*H*), 4.44 (1H, br s, C2′-*H*), 5.50 (1H, br s, C3′-O*H*), 5.38 (1H, br s, C2′-O*H*), 5.66 (1H, d, *J* 5.9, C1′-O*H*), 6.47 (2H, s, N*H₂*), 7.94 (1H, s, C6-*H*); δ_C (101 MHz, $(CD_3)_2SO$) 43.7, 70.7, 73.2, 85.7, 86.3, 116.8, 135.8, 151.4, 153.7, 156.8

8.2.5 Synthesis of Thymidine Derivatives

3′-Amino-3′-deoxythymidine (130), hydrochloride salt[125]
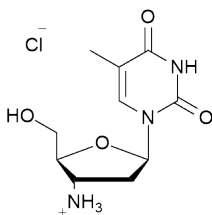
Adapting a literature procedure,[125] 3′-amino-3′-deoxythymidine (1.00 g, 3.74 mmol) and triphenylphosphine (1.54 g, 5.87 mmol) were dissolved in pyridine (8 ml) and the mixture was stirred at room temperature for 1 h. Ammonia solution (30 ml, 35%) was then added, and the mixture was stirred overnight. The suspension was diluted with water (30 ml) and extracted with chloroform

$(3 \times 30$ ml) before being lyophilised. The solid residue was dissolved in ethanol (100 ml) and hydrogen chloride gas was bubbled through the solution until precipitation was observed. The precipitate was isolated by filtration, and washed with a small quantity of diethyl ether. Additional product was obtained by adding diethyl ether (500 ml) to the filtrate, and again filtering and washing the precipitate. The isolated solids were combined and dried under vacuum overnight yielding a total of 846 mg, 81%; mp 253-255 °C (decomp., from ethanol); ν_{max}/cm^{-1} 3392, 3032, 1694, 1644, 1470. δ_H (400 MHz, (D$_2$O) 1.86 (3H, s, C5-CH_3), 2.54-2.70 (2H, m, C2′-H_2), 3.81 (1H, dd, J 12.6, 4.6, C5′-H_a), 3.89 (1H, dd, J 12.6, 3.4, C5′-H_b), 4.06 (1H, dt, J 8.1, 5.5, C3′-H), 4.19-4.28 (1H, m, C4′-H), 6.25-6.32 (1H, t, J 6.8, C1′-H), 7.62 (1H, d, J 1.1, C6-H); δ_C (100 MHz, (D$_2$O) 10.5 (CH$_3$), 33.8 (C2′), 49.1 (C3′), 59.7 (C5′), 81.5 (C4′), 84.1 (C1′), 110.5 (C5), 136.6 (C6), 150.5 (C2), 165.4 (C4); m/z 242.1142 ([M+H]$^+$, 100%), requires 242.1141, 264.0961 ([M+Na]$^+$, 90).

8.2.6   Synthesis of Uridine Derivatives

5′-Azido-5′-deoxyuridine (134)[132]
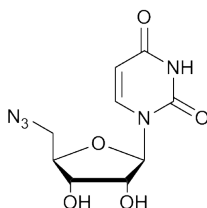
With some modifications, a literature procedure was followed.[132] Uridine (5.00 g, 20.5 mmol), triphenylphosphine (8.05 g, 30.5 mmol), tetrabromomethane (10.2 g, 30.5 mmol), and lithium azide (3.70 g, 75.5 mmol) were stirred together in DMF (100 ml) for 4 h at room temperature. As much

solvent as possible was removed under reduced pressure, and the residue was extracted with chloroform (100 ml) and water (100 ml), with the aqueous layer being retained. The aqueous layer was washed again with chloroform (2 × 100 ml) before being lyophilised. The viscous lyophilised residue was purified by column chromatography on silica, using an isocratic 5:1 mixture of chloroform and methanol. The resulting liquid (due to residual DMF) was dissolved in 5:1 chloroform/methanol and adsorbed on to a plug of silica, which was washed with 100% chloroform to remove residual DMF, then released using the 5:1 chloroform/methanol solution to yield the purified product. (3.70 g, 67%); ν_{max}/cm^{-1} 2102 (N$_3$), 1667 (CO), 1462, 1386, 1100 (R$_2$COH); δ_H (500 MHz, (D$_2$O) 3.69 (1H, dd, J 13.7, 5.0, C5'-H_a), 3.82 (1H, dd, J 13.7, 3.2, C5'-H_b), 4.18-4.23 (1H, m, C4'-H), 4.27 (1H, app. t, J 5.5, C'3-H), 4.42 (1H, dd, J 5.5, 4.5, C2'-H), 5.89 (1H, d, J 4.5, C1'-H), 5.93 (1H, d, J 8.1, C5-H), 7.80 (1H, d, J 8.1, C6-H); δ_H (126 MHz, (D$_2$O) 51.6 (C5'), 70.2 (C3'), 73.3 (C2'), 82.3 (C4'), 90.1 (C1'), 102.6 (C5), 142.2 (C6), 151.7 (C2), 166.2 (C4); m/z 268.0676 ([M−H]$^-$, 30%), requires 268.0682, 304.0408 (100).

5'-Amino-5'-deoxyuridine (135), Hydrochloride Salt
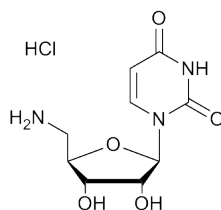
5'-Azido-5'-deoxyuridine (404 mg, 1.50 mmol) and triphenylphosphine were (1.66 g, 6.33 mmol) were dissolved in pyridine (1.6 ml) and stirred for 2 h. Ammonia solution (35%, 12 ml) was added, and the mixture was stirred

overnight. The mixture was diluted with water (40 ml) and extracted with chloroform (3 × 40 ml). Residual chloroform was then removed from the aqueous layer under vacuum, and the remaining aqueous solution was lyophilised. The resulting powder was then dissolved in ethanol (20 ml) and heated at reflux until dissolved. Hydrogen chloride gas was bubbled through the solution until precipitation occurred, and the hydrochloride salt **138**·HCl was isolated by filtration and washing with a small quantity of ethanol. (329 mg, 78%); mp 210-215 °C (decomp., from ethanol); ν_{max}/cm^{-1} 3040, 1666 (CO), 1464, 1042; δ_H (700 MHz, (D$_2$O) 3.29-3.36 (1H, m, C5'-H_a), 3.44-3.49 (1H, m, C5'-H_b), 4.22-4.26 (2H, m, C'3-H, C4'-H), 4.52 (1H, dd, J 5.2, 4.0, C2'-H), 5.77 (1H, d, J 4.0, C1'-H), 5.89 (1H, d, J 8.1, C5-H), 7.66 (1H, d, J 8.1, C6-H); δ_C (126 MHz, (D$_2$O) 41.8 (C5'), 71.4 (C3'), 73.2 (C2'), 80.0 (C4'), 93.3 (C1'), 102.8 (C5), 143.9 (C6), 152.0 (C2), 166.9 (C4); m/z 244.0934 ([M−H]$^-$, 100%), requires 244.0933.

8.2.7 Synthesis of Phosphorylating Agents

Potassium phosphodichloridate and potassium thiophosphodichloridate were synthesised according to literature methods.[118,121]

Potassium Phosphodichloridate (98), 0.333 M Solution in Acetonitrile

Phosphoryl chloride (1.275 g, 8.315 mmol) was weighed into a volumetric flask and made up to 25 ml with dried acetonitrile. The solution was then stirred with potassium hydrogen carbonate (1.675 g, 16.73 mmol) for 15 min before being filtered under a stream of N$_2$ gas.

Potassium Thiophosphodichloridate (100), 0.333 M Solution in Acetonitrile

Thiophosphoryl chloride (1.410 g, 8.323 mmol) was weighed into a volumetric flask and made up to 25 ml with dried acetonitrile. The solution was then stirred with potassium hydrogen carbonate (1.675 g, 16.73 mmol) overnight before being filtered under a stream of N_2 gas.

8.2.8   Aminonucleoside Phosphorylation Procedure

This section describes the method used to phosphorylate the 5′-amino-5′-deoxynucleosides and 3′-amino-3′-deoxythymidine, and the procedures for analysis of the products.

Phosphorylation

The aminonucleoside (0.500 mmol) was placed in a flask with a solution (5 ml) of water made up to the desired pH with potassium hydroxide solution (1.000 M). The phosphorylating agent (1.50 ml, 0.333 M in MeCN) was added using a Hamilton® microlitre syringe. The addition took place slowly, with vigorous stirring, and with the tip of the syringe below the surface of the reaction mixture. Throughout the experiment, the pH was kept constant using a 1.000 M solution of potassium hydroxide, added by the autotitrator system described in the Materials and Equipment section (8.1). The experiment was considered to be complete when the autotitrator needed to add negligible quantites of potassium hydroxide solution to the reaction mixture in order to maintain pH.

Analysis

After the completion of the reaction, the pH of the reaction mixture was raised to 12, and the organic solvent was removed under reduced pressure.

The aqueous remainder was then lyophilised. The resulting solid was dissolved in the minimum volume of D_2O, and analysed using a Varian 400 MHz NMR spectrometer to determine conversion. A ^{1}H NMR analysis was performed with 128 transients to estimate conversions. For ^{31}P NMR spectra, a relaxation time of 10 s, acquisition time of 1.28 s, and 128 transients were used. The ^{1}H NMR estimations of conversion were obtained by comparing the signals corresponding to the 5'- protons of the various reaction products. The ^{31}P NMR conversions were estimated using all the signals visible in each ^{31}P NMR spectrum.

8.2.9 Results of Phosphorylations

Oxyphosphorylation Optimisations

5'-Amino-5'-deoxyguanosine
Oxyphosphoryl chloride

pH	Product Fractions / %			
	11.0	**11.5**	**12.0**	**12.5**
Product	72	77	80	77
Phosphorodiamidate	6	2	2	1
Inorganic Phosphate	22	21	18	17
Other	0	0	0	5

5'-Amino-5'-deoxyguanosine
Potassium phosphodichloridate

pH	Product Fractions / %			
	11.0	**11.5**	**12.0**	**12.5**
Phosphoramidate	72	77	80	77
Phosphorodiamidate	6	2	2	1
Inorganic phosphate	22	21	18	17
Other	0	0	0	5

Oxyphosphorylations

The oxyphosphorylations were carried out at pH 12 with oxyphosphoryl chloride and potassium phosphodichloridate.

5′-Amino-5′-deoxyadenosine

	Product Fractions / %	
pH	**$POCl_3$**	**$KOPOCl_2$**
Phosphoramidate	74	73
Phosphorodiamidate	8	1
Inorganic phosphate	16	25
Other	3	1

3′-Amino-3′-deoxythymidine

	Product Fractions / %	
pH	**$POCl_3$**	**$KOPOCl_2$**
Phosphoramidate	44	51
Phosphorodiamidate	0	0
Inorganic phosphate	44	49
Other	12	0

Thiophosphorylations

The thiophosphorylations were carried out at pH 12 with thiophosphoryl chloride and potassium thiophosphodichloridate.

5′-Amino-5′-deoxyadenosine

	Product Fractions / %	
pH	**$PSCl_3$**	**$KOPSCl_2$**
Thiophosphoramidate	99	90
Inorganic thiophosphate	0	10
Inorganic phosphate	1	0
Other	0	0

5′-Amino-5′-deoxycytidine

pH	Product Fractions / %	
	PSCl$_3$	KOPSCl$_2$
Thiophosphoramidate	92	80
Inorganic thiophosphate	6	20
Other	3	0

3′-Amino-3′-deoxythymidine

pH	Product Fractions / %	
	PSCl$_3$	KOPSCl$_2$
Thiophosphoramidate	65	48
Thiophosphorodiamidate	1	0
Inorganic thiophosphate	22	45
Inorganic Phosphate	6	4
Other	6	3

5′-Amino-5′-deoxyuridine

pH	Product Fractions / %	
	PSCl$_3$	KOPSCl$_2$
Thiophosphoramidate	91	82
Thiophosphorodiamidate	1	0
Inorganic thiophosphate	5	18
Inorganic Phosphate	2	1

8.3   3′-Amino-3′-deoxythymidylyl(3′→5′)-5′-de-oxy-5′-thiothymidine Synthesis

8.3.1   Synthesis

5′-Deoxy-5′-(4-toluenesulphonyl)thymidine (145)[134]
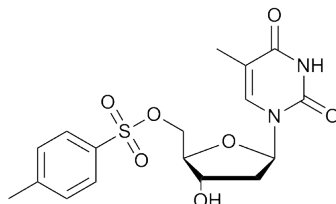
Thymidine (3.92 g, 16.2 mmol) was dissolved in pyridine (20 ml) in a round-bottomed flask, and placed in an water-ice bath. 4-Toluenesulphonyl chloride (3.83 g, 20.2 mmol), dissolved in pyridine (20 ml) was added dropwise over 10 min. Stirring was continued for a further 24 h. The solution was then poured into ice water (100 ml) and the mixture was extracted with ethyl acetate (2 × 60 ml). The organic extracts were washed with saturated sodium bicarbonate solution (40 ml), and water (40 ml) before being dried. The solvent was then removed under reduced pressure, and the residue recrystallised from water to give the tosylated nucleoside **145**, 5′-Deoxy-5′-(4-toluenesulphonyl)thymidine (1.57g, 24%). δ_H (400 MHz, $(CD_3)_2SO$) 1.76 (3H, s, C5-CH_3) 2.02-2.09 (1H, m, C2′-H_aH$_b$) 2.11-2.19 (1H, m, C2′-H$_a$$H_b$) 2.41 (3H, s, C$H_3$-Ph) 3.83-3.88 (1H, m, C3′-H), 4.12-4.20 (2H, m, C4′-H and C5′-H_aH$_b$) 4.25 (1H, dd, J 7.2, 3.4, C5′-H$_a$$H_b$) 5.44 (1H, d, J 4.4, OH) 6.14 (1H, app. t, J 7.2, C1′-H) 7.38 (1H, d, J 1.8, C6-H) 7.47 (2H, d, J 8.3, m-OSO$_2$Ph) 7.79 (2H, d, J 8.3, o-OSO$_2$Ph) 11.33 (1H, s, NH) δ_H (400 MHz, $(CD_3)_2SO$) 12.1, 21.1, 38.3, 69.9, 70.1, 83.1, 84.0, 109.8, 127.6, 130.2, 132.1,

135.9, 145.1, 150.3, 163.6.

5′-Deoxy-5′-iodothymidine (148)[25]
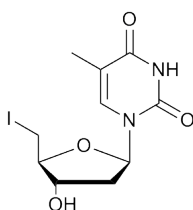
5′-Deoxy-5′-tosylthymidine (1.57 g, 3.96 mmol) and sodium iodide (2.97 g, 19.8 mmol) were placed in a round-bottomed flask and dissolved in the minimum volume of acetone. The solution was heated at reflux for 24 h, before the solvent was removed under reduced pressure. The residue was recrystallised from water to yield the product (1.20 g, 86%). δ_H (400 MHz, $(CD_3)_2SO$) 1.79 (3H, s, C5-CH_3) 2.07 (1H, ddd, J 13.5, 6.2, 3.1, C2′-H_aH$_b$) 2.29 (1H, ddd, J 13.5, 8.1, 6.2, C2′-H$_a$$H_b$) 3.39 (1H, dd, J 10.4, 6.3, C5′-H_aH$_b$) 3.52 (1H, dd, J 10.4, 6.3, C5′-H$_a$$H_b$) 3.80 (1H, dt, J 6.2, 2.8, C3′-H), 4.15-4.21 (1H, m, C4′-H), 5.49 (1H, d, J 4.3, OH) 6.22 (1H, dd, J 8.0, 6.2, C1′-H) 7.53 (1H, d, J 1.5, C6-H) 11.35 (1H, s, NH)

3′-Amino-3′-deoxythymidylyl-(3′ →5′)-5′-deoxy-5′-thiothymidine (142), Triethylammonium Salt - First Attempt
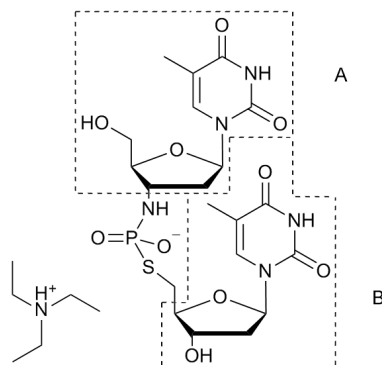
3′Amino-3′-deoxythymidine (50 mg, 0.21 mmol) was placed in a round-bottomed flask with sodium hydroxide solution (1 M, 1 ml) and stirred. To this was added thiophosphoryl chloride (0.02 ml, 0.21 mmol) in THF (0.6 ml) dropwise. Stirring was continued for 1 h, before the THF was removed under reduced pressure, and the aqueous residue lyophilised. To the remainder was added 2 ml D_2O, 5′-deoxy-5′-tosylthymidine (164 mg, 0.414 mmol) and NaOD solution (0.4 ml of a 40% *w/w* solution in D_2O)). This solution was heated at 80 °C for 16 h with stirring. The product was purified by ion exchange chromatography on a DEAE Sepharose™ Fast Flow column using freshly prepared TEAB buffer (1 M) with the buffer concentration increasing from 10 mM to 150 mM over 2 h, and a flow rate of 5 ml/min. The purification was then repeated on the product-containing fractions using a smaller column packed with the same resin, and a gradient rising from 10 mM to 100 mM over 2 h. The product-containing fractions were lyophilised to give the pure 3′-*N*-5′-*S* thiophosphoramidate analogue of thymidylyl-3′,5′-thymidine, triethylammonium salt (6 mg, 4%) δ_P (162 MHz, D_2O) 22.8 (1P, q, *J* 9.9, HN*P*O_2^-S), *m/z* 560.1216 ([M – HNEt$_3$]$^-$, 80%) requires 560.1216.

3′-Amino-3′-deoxythymidylyl-(3′ →5′)-5′-deoxy-5′-thiothymidine (142), Triethylammonium Salt - Second Attempt
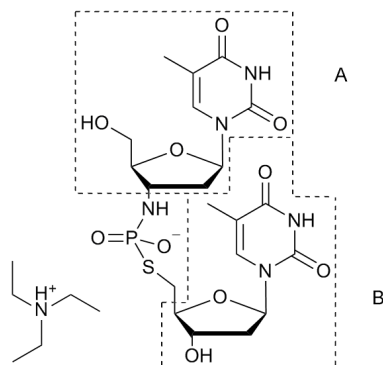
3′-Amino-3′-deoxythymidine (200 mg, 0.828 mmol) was placed in a round-bottomed flask with sodium hydroxide solution (1 M, 4 ml) and D_2O (512 µl), and stirred. To this was added thiophosphoryl chloride (97 µl, 0.99 mmol) in THF (2.9 ml) dropwise and the mixture was stirred for 1 h. To this mixture was added 5′-deoxy-5′-iodo-thymidine (584 mg, 1.66 mmol) and sodium hydroxide solution (1 M, 2.4 ml). The reaction was heated to 80 °C for 18 h. A crude purification was performed by ion exchange chromatography, with a TEAB buffer rising from an initial concentration of 1 mM to 10 mM over the course of 1 h. The collected fractions were lyophilised and purified by preparative reverse phase HPLC using a methanol/water gradient to yield the product. δ_H (700 MHz, D_2O) 1.29 (9H, t, *J* 7.3, $HN^+CH_2CH_3$) 1.88 (3H, d, *J* 1.2, A- or B- $C5CH_3$) 1.89 (3H, d, *J* 1.2, A- or B- $C5CH_3$), 2.36-2.45 (3H, m, A-C2′H_a and B-C2′H_2) 2.49 (1H, ddd, *J* 14.0, 8.1, 3.9, A-C2′H_b), 3.04-3.11 (2H, m, B-C5′H_2), 3.21 (6H, q, *J* 7.0, $HN^+CH_2CH_3$), 3.78-3.85 (2H, m, A-C3′H and A-C5′H_a) 3.86-3.89 (1H, m, A-C5′H_b), 4.14-4.20 (2H, m, A- and B-C4′H), 4.46-4.49 (1H, m, B-C3′H), 6.16 (1H, dd, *J* 7.4, 4.0, A-C1′H), 6.25 (1H, app. t, *J* 6.7, B-C1′H), 7.67 (1H, d, *J* 1.2, A- or B-C6H), 7.71 (1H, d,

J 1.2, A- or B-C6H); δ_C (151 MHz, D$_2$O) 8.2 (HN$^+$CH$_2$$CH_3$), 11.5 (A- and B-C5$CH_3$), 32.0, (B-$C$5′), 38.0 (B-$C$2′), 38.5 (A-$C$2′), 46.6 (HN$^+$$CH_2CH_3$), 58.9 (A-$C$3′), 60.2, (A-$C$5′), 72.0 (B-$C$3′), 84.5 (A-$C$1′), 84.7 (B-$C$1′), 84.9 (B-$C$4′), 85.5 (A-$C$4′), 111.1 (A- or B-$C$5), 111.3 (A- or B-$C$5), 137.4 (A- or B-$C$6), 137.5 (A- or B-$C$6), 151.4 (A- and B-$C$2), 166.1 (A- or B-$C$4), 166.3 (A- or B-$C$4); δ_P (162 MHz, D$_2$O) 21.57 (1P, app. q, J 9.7, HNPO$_2^-$S); m/z 560.1233 ([M − H$^+$NEt$_3$]$^-$, 80%) requires 560.1216

3′-Amino-3′-deoxythymidylyl-(3′ →5′)-5′-deoxy-5′-thiothymidine (142), Triethylammonium Salt - Third Attempt
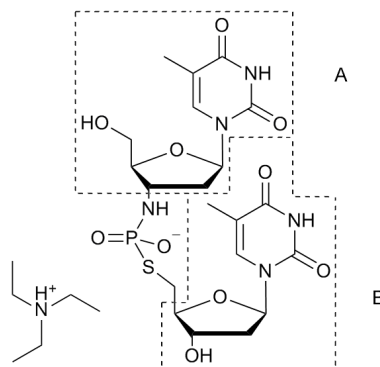
3′-Amino-3′-deoxythymidine-N-thiophosphoramidate **143** was prepared according to the standard phosphorylation procedure, beginning from 3′-amino-3′-deoxythymidine, hydrochloride salt **131** (139 mg, 0.500 mmol). The lyophilised thiophosphoramidate was redissolved in water (5 ml at pH 12 with 1 M potassium hydroxide solution) with stirring. 5′-deoxy-5′-iodothymidine (352 mg, 1.00 mmol) was added to the solution, while the pH was maintained at 12 with potassium hydroxide solution (1 M) by an autotitrator. Once the 5′-deoxy-5′-iodothymidine had fully dissolved and no further addition of potassium hydroxide was required to maintain the pH, The solution

was sealed to prevent losses to evaporation and heated to 50 °C. At intervals, aliquots were removed from the reaction vessel and analysed by ^{31}P NMR spectroscopy. The reaction was continued until the thiophosphoramidate starting material had been completely consumed; the solution was then allowed to cool to room temerature. The pH of the reaction mixture was measured and found to be 10.45. The solution was lyophilised and redissolved in 1 M TEAB buffer, then purified by anion exchange chromatography with a flow rate of 5 ml/min over a DEAE-Sepharose® resin. Triethylammonium bicarbonate buffer was applied in a 0 to 0.15 M gradient over 3 h.
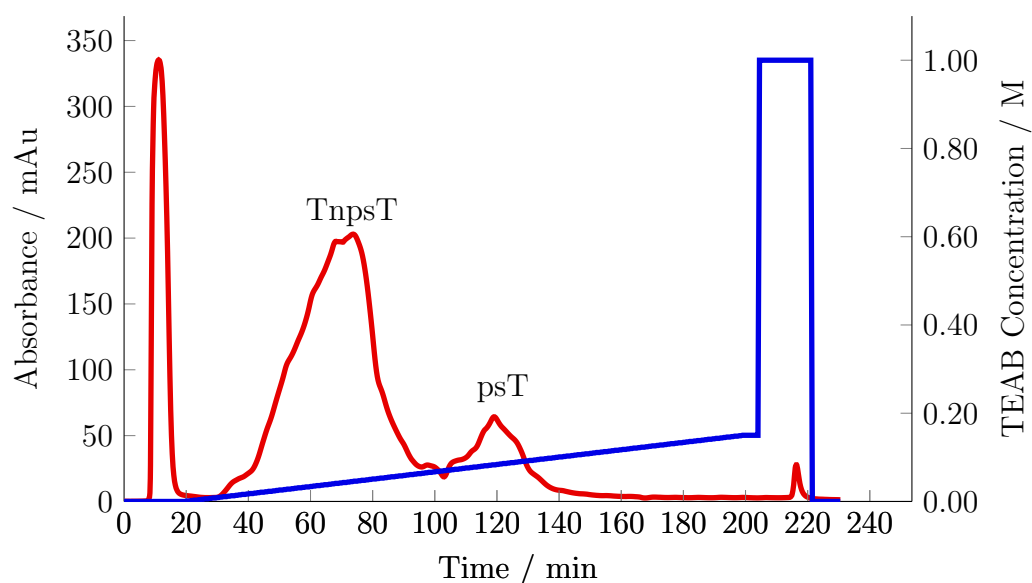
A second chromatographic purification using the same method was required to remove all impurities, primarily 5′-deoxy-5′-thiothymidine S-phosphate (psT) and inorganic phosphate (invisible to the UV detector).
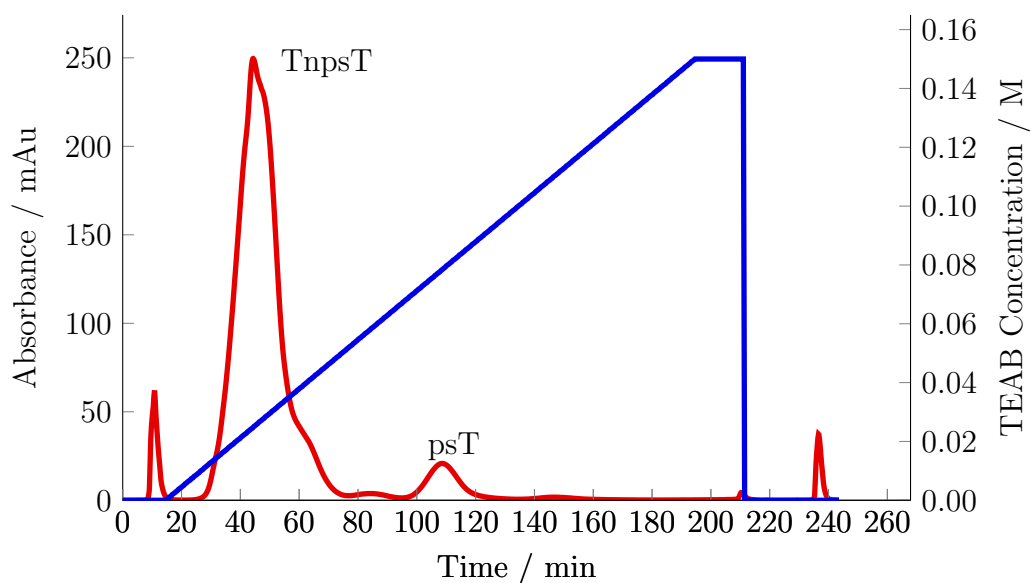
This process gave a yield of 212 mg (64% overall, 98% of available thiophosphoramidate alkylated), however the triethylammonium ^{1}H NMR signals were larger than expected, indicating that some residual triethylammonium salts may be present. δ_H (700 MHz, D_2O) 1.29 (9H, t, J 7.3, HN$^+$CH$_2$CH_3) 1.88 (3H, d, J 1.2, A- or B- C5CH$_3$) 1.89 (3H, d, J 1.2, A- or B- C5CH_3), 2.36-2.45 (3H, m, A-C2$'H_a$ and B-C2$'H_2$) 2.49 (1H, ddd, J 14.0, 8.1, 3.9, A-C2$'H_b$), 3.04-3.11 (2H, m, B-C5$'H_2$), 3.21 (6H, q, J 7.0, HN$^+$CH_2CH$_3$), 3.78-3.85 (2H, m, A-C3$'H$ and A-C5$'H_a$) 3.86-3.89 (1H, m, A-C5$'H_b$), 4.14-4.20 (2H, m, A- and B-C4$'H$), 4.46-4.49 (1H, m, B-C3$'H$), 6.16 (1H, dd, J 7.4, 4.0, A-C1$'H$), 6.25 (1H, app. t, J 6.7, B-C1$'H$), 7.67 (1H, d, J 1.2, A- or B-C6H), 7.71 (1H, d, J 1.2, A- or B-C6H); δ_C (151 MHz, D_2O) 8.2 (HN$^+$CH$_2$$CH_3$), 11.5 (A- and B-C5$CH_3$), 32.0, (B-$C5'$), 38.0 (B-$C2'$), 38.5 (A-$C2'$), 46.6 (HN$^+$$CH_2CH_3$), 58.9 (A-$C3'$), 60.2, (A-$C5'$), 72.0 (B-$C3'$), 84.5 (A-$C1'$), 84.7 (B-$C1'$), 84.9 (B-$C4'$), 85.5 (A-$C4'$), 111.1 (A- or B-$C$5), 111.3 (A- or B-$C$5), 137.4 (A- or B-$C$6), 137.5 (A- or B-$C$6), 151.4 (A- and B-$C$2), 166.1 (A- or B-$C$4), 166.3 (A- or B-$C$4); δ_P (162 MHz, D_2O) 21.57 (1P, app. q, J 9.7, HNPO_2^-S); m/z 560.1207 ([M – HNEt3]$^-$, 100%) requires 560.1216, 279.5541 ([M – H$_2$NEt$_3$]$^{2-}$).

8.4 Hydrolysis Kinetics of a Thiophosphoramidate System

8.4.1 Synthesis

N,S-Dibenzyl thiophosphoramidate (156)[49]
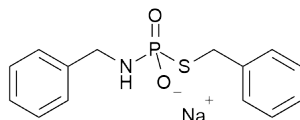
N,S-Dibenzyl thiophosphoramidate was synthesised according to the method developed by Milena Trmčić.[49] Benzylamine (0.50 ml, 0.49 g, 4.6 mmol) was placed in an indented round bottomed flask with sodium hydroxide solution (19 ml, 1 M) and water (2.45 ml). Thiophosphoryl chloride (0.386 ml, 0.645 g, 3.81 mmol) dissolved in THF (11.6 ml) was added dropwise over 10 min. The solution was allowed to stir for 15 min before benzyl chloride (0.877 ml, 0.965 g, 7.62 mmol) was added dropwise over 10 min. The solution was stirred for 22 h before being extracted with diethyl ether (3 × 50 ml). The aqueous layer was then lyophilised to yield the product, along with residual salt and sodium hydroxide. (2.27 g) δ_H (400 MHz, (D$_2$O)) 3.65-3.86 (4H, m, SCH_2 and NHCH_2), 7.05-7.45 (10H, m, phenyl); δ_C (100 MHz, (D$_2$O)) 34.1 (CH$_2$S), 45.4 (CH$_2$N), 127.2 (Arom. Bn), 127.3 (Arom. Bn), 127.7 (Arom. Bn), 128.6 (Arom. Bn), 128.7 (Arom. Bn), 128.9 (Arom. Bn), 139.1 (Arom. Bn), 139.1 (Arom. Bn), 140.4 (Arom. Bn), 140.5 (Arom. Bn); δ_P (100 MHz, (D$_2$O)) 24.6 (1P, dd, *J* 8.9, 8.3, NHPO$_2^-$S).

3′-Amino-3′-deoxythymidylyl-(3′ →5′)-5′-deoxy-5′-thiothymidine (142), Potassium Salt
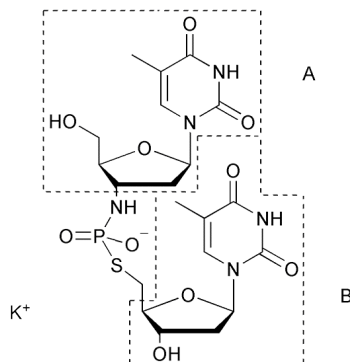
The dinucleoside was isolated as the potassium salt according to the following procedure; an SP-Sepharose resin® was exchanged with potassium ions by passing a solution of potassium chloride (100 mM) over it. The triethylammonium salt of the dinucleoside (100 mg) was then dissolved in water (4 ml) and passed over the resin. The UV-active fractions were collected and lyophilised to yield the dinucleoside as its potassium salt (60 mg, 66%) δ_H (700 MHz, D_2O) 1.88 (3H, d, J 1.2, A- or B- C5CH_3) 1.89 (3H, d, J 1.2, A- or B- C5CH_3), 2.35-2.46 (3H, m, A-C2′H_a and B-C2′H_2) 2.49 (1H, ddd, J 14.0, 8.1, 4.0, A-C2′H_b), 3.02-3.11 (2H, m, B-C5′H_2), 3.78-3.85 (2H, m, A-C3′H and A-C5′H_a) 3.88 (1H, ddd, J 7.3, 4.5, 2.5, A-C4′H), 3.94 (1H, dd, J 12.6, 2.5, A-C5′H_b), 4.18 (1H, app.q, J 5.1, B-C4′H), 4.48 (1H, app. dt, J 6.5, 4.6, B-C3′H), 6.17 (1H, dd, J 7.5, 4.0, A-C1′H), 6.25 (1H, app. t, J 6.7, B-C1′H), 7.68 (1H, d, J 1.4, A- or B-C6H), 7.71 (1H, d, J 1.2, A- or B-C6H); δ_C (151 MHz, D_2O) 11.5, 11.5, 32.0, 38.0, 38.5, 50.4, 60.2, 72.0, 84.5, 84.7, 84.8, 84.8, 85.5, 85.6, 111.1, 111.3, 137.4, 137.5, 151.4, 151.4, 166.1, 166.3, 171.1; δ_P (162 MHz, D_2O) 21.64 (1P, app. q, J 10.0, HNPO_2^-S); m/z

560.1208 ([M-K]⁻, 100%) requires 560.1216, 1121.2450 ([2M – 2K+H]⁻).

HPLC Standard - Potassium *p*-nitrobenzenesulphonate (166)
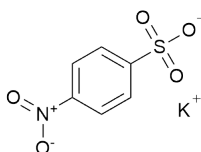
p-Nitrobenzenesulphonyl chloride (222 mg, 1.00 mmol) was placed in a flask with potassium hydroxide solution (2 ml, 1.000 M) and water (20 ml). The solution was heated at reflux for 3 h before being lyophilised to yield a mixture of the desired product and potassium chloride in a 1:1 molar ratio. (231 mg, 98%) δ_H (400 MHz, (D$_2$O) 8.00 (2H, d, *J* 8.9, ^{1}H *m*- to sulphonate), 8.35 (2H, d, *J* 8.9, ^{1}H *o*- to sulphonate); δ_C (101 MHz, (D$_2$O) 124.3, 126.9, 148.1, 149.1.

8.4.2   Initial Experiments With *N,S*-Dibenzyl Thiophosphoramidate

Three NMR tubes were prepared at the same pH in order to check for buffer catalysis; *N,S*-dibenzylthiophosphoramidate (14 mg of a 1:3:1 mixture of thiophosphoramidate/NaCl/NaOH, approx. 25 µmol) was placed in each NMR tube with 0.952 M acetate buffer (pH measured to be 4.64) and 1 M KCl solution (1 ml total of a 1:3, 1:1, and 3:1 ratio of buffer/KCl solution in each NMR tube) The NMR tubes were heated to 80 °C and their contents were analysed by ^{31}P NMR spectroscopy at intervals (in undeuterated solvent - no locking or shimming).

238 mM Buffer

Time / s:	Integral		Fraction	
	Substrate:	Phosphate:	Substrate:	Phosphate:
0	1.00	0.08	0.926	0.074
6000	0.97	0.54	0.642	0.358
10500	1.00	0.97	0.508	0.492
14100	1.00	1.17	0.461	0.539

476 mM Buffer

Time / s:	Integral		Fraction	
	Substrate:	Phosphate:	Substrate:	Phosphate:
0	1.00	0.06	0.943	0.057
6000	1.00	0.86	0.538	0.462
10500	1.00	1.46	0.407	0.593
14100	1.00	1.96	0.338	0.662

714 mM Buffer

Time / s:	Integral		Fraction	
	Substrate:	Phosphate:	Substrate:	Phosphate:
0	1.00	0.00	1.000	0.000
6000	1.00	0.88	0.532	0.468
10500	1.00	1.47	0.405	0.595
14100	1.00	3.00	0.250	0.750

Analysis

Time / s:	ln(Substrate Fraction)		
	238 mM	**476 mM**	**714 mM**
0	-0.077	-0.058	0.000
6000	-0.443	-0.621	-0.631
10500	-0.678	-0.900	-0.904
14100	-0.775	-1.085	-1.386

	Buffer Concentration		
	238 mM	**476 mM**	**714 mM**
k_{obs} / s^{-1}	5.1×10^{-5}	7.3×10^{-5}	9.4×10^{-5}
Standard error / s^{-1}	5×10^{-6}	7×10^{-6}	8×10^{-6}
R^2	0.981	0.981	0.986
Half-life / s	14000	9500	7300
Half-life / h	3.8	2.6	2.0

General Catalysis Analysis

	Value:	Standard Error:
k_0 / s^{-1}	2.88×10^{-5}	6×10^{-7}
k_{buff} / $M^{-1}s^{-1}$	9.2×10^{-5}	1×10^{-6}
R^2	0.9998	
Half-life / s	24100	
Half-life / h	6.69	

$$k_{\mathrm{obs}} = k_0 + k_{\mathrm{buff}}[\text{buffer}]$$

HPLC analysis of the kinetics of hydrolysis of *N,S*-dibenzyl thiophosphoramidate failed due to the benzyl groups being poor chromophores. Instead, the analysis was performed upon 3′-amino-3′-deoxythymidylyl-(3′ →5′)-5′-deoxy-5′-thiothymidine, potassium salt.

8.4.3   Substrate HPLC Calibration Curves

Samples of the substrate and some of the expected hydrolysis products were analysed by HPLC and the relationships between the UV/vis response and the concentration of the sample were investigated to ensure that they were linear.

Concentration	Integral		
/ μM	Amine:	Thymidine:	TnpsT:
0	0.0000	0.0000	0.0000
20	0.4945		0.2573
40	0.9994	1.1036	0.5213
60	1.5470		0.7726
80	2.1858	2.0874	1.0539
100	2.7688		1.3082
120		3.2613	
160		4.3562	
200		5.4954	

Analysis

$$concentration = m \times integral$$
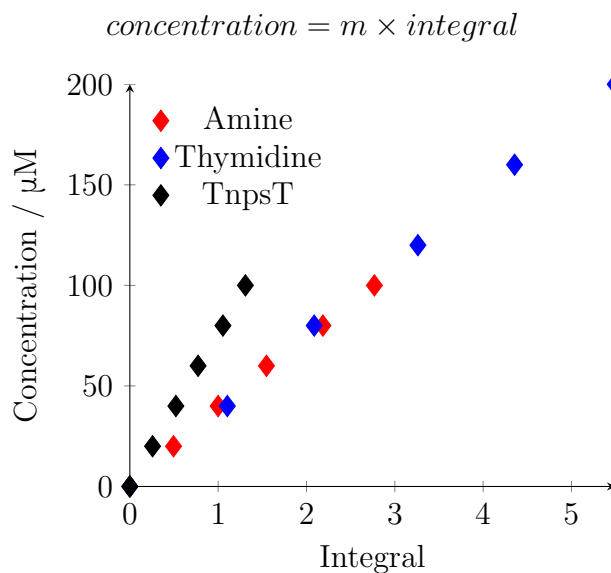
	Amine:	Thymidine:	TnpsT:
Flow rate / ml min^{-1} :	0.9	0.9	1.0
m / μM:	37.0	36.7	76.5
Standard error / μM:	0.6	0.3	0.3
R^2:	0.9988	0.9998	0.99994

Intercept forced to be zero. The R^2 values very close to unity indicate that the relationships can be considered to be linear over this range of concentrations.

8.4.4   HPLC Conditions and Retention Times

The parameters and elution method recorded below were used for all the kinetic experiments analysed through HPLC. A PerkinElmer Series 200 HPLC system was used, with a Phenomenex Hyperclone 5 μC18 column measuring 250 mm in length and 3.2 mm in diameter. Chromatograms were processed using the TotalChrom™ Chromatography Data System from PerkinElmer on Microsoft® Windows® XP.

Parameter:	Value:	Unit:
Sampling Rate:	2.2727	s^{-1}
Injection Volume:	50	μl
Detector A:	254	nm
Detector B:	280	nm

Step:	Time / min:	Flow / ml min^{-1}:	Acetate %	MeCN %	Curve
0	0.5	1.00	100.0	0.0	0.0
1	10.0	1.00	100.0	0.0	0.0
2	32.0	1.00	90.0	10.0	1.0
3	12.0	1.00	90.0	10.0	0.0
4	2.0	1.00	100.0	0.0	1.0
5	3.0	1.00	100.0	0.0	0.0

Chromatogram of Possible Hydrolysis Products
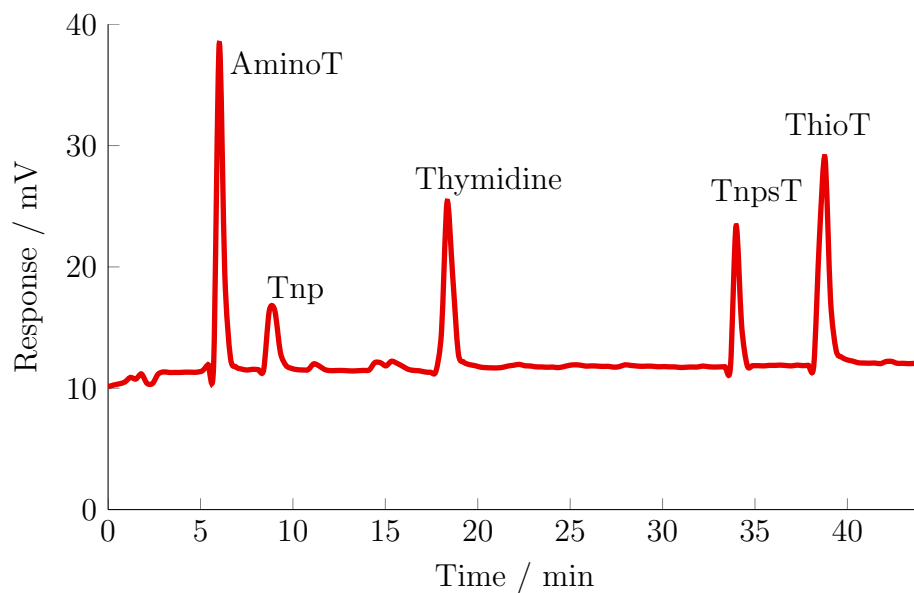
Chromatogram of p-Nitrobenzenesulphonate Standard
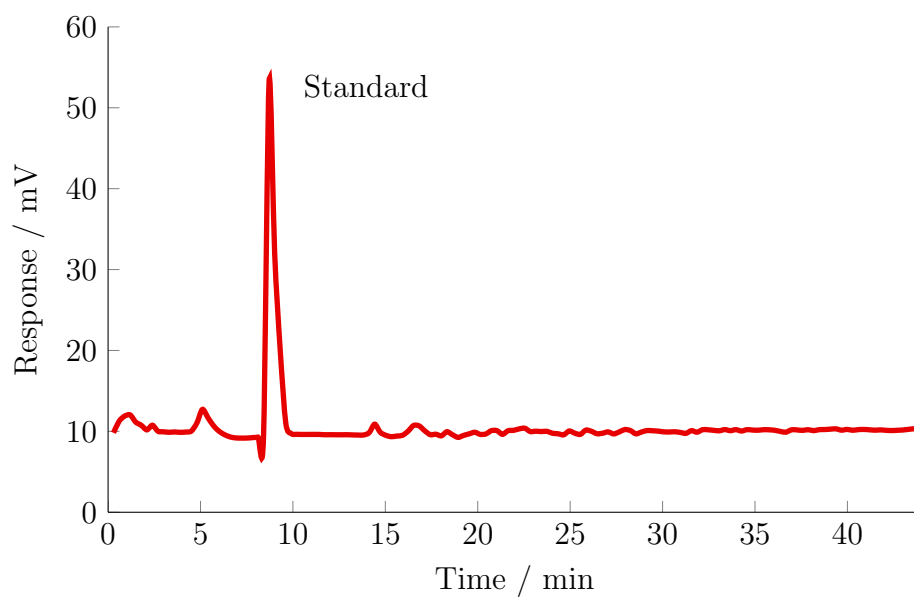
Compound:	Retention Time / min:
3′-Amino-3′-deoxythymidine	5.7
Tnp	6.6
spT	7.4
Potassium *p*-nitrobenzenesulphonate	9.8
Thymidine	18.3
TnpsT	34.5
5′-Deoxy-5′-thiothymidine	38.7

8.4.5 Sample Preparation

In this section, the procedures for the preparation of the hydrolytic experiments using TnpsT as a substrate are described. The pH of each buffer, hydrochloric acid, or potassium hydroxide solution prepared according to the following protocols was measured at 25 °C and the corresponding pH at 90 °C was calculated according to the method described in section 4.3.1.

General Procedure for pH 3.54 - 8.67 (At 90 °C)

For the hydrolytic reactions taking place in buffered solutions, the general procedure was as follows: a solution of buffer was prepared with a concentration double that required for the experiment and an ionic strength made up to 1 M with potassium nitrate. A 1 mM solution of the standard (potassium *p*-nitrobenzenesulphonate) was also prepared and again made up to IS = 1 M with potassium nitrate. In a 10 ml volumetric flask, the standard solution (1 ml), the buffer solution (5 ml), and a solution of the TnpsT substrate (100 μl of a 10 mM solution) were combined, and the volume was made up to 10 ml with potassium nitrate solution (1 M). The solution was divided between ten ampoules, which were then sealed. The ampoules were submerged in a covered water bath, maintained at a temperature of 90.0 °C ± 0.1 (determined by an accurate mercury thermometer). After the required time had

elapsed, the ampoule was removed from the bath, the neck broken, and the solution transferred to a HPLC vial.

In the case of the formate buffered solutions, 200 µl of a quench solution of dipotassium phosphate (at 10 × the concentration of the buffer solution in the ampoule) was added. For the other buffer solutions, cooling to ambient temperature was sufficient to quench the reaction.

For each buffer, this procedure was carried out twice once each with 10 and 100 mM concentrations of buffer. If the results of these experiments indicated general catalysis was taking place, the experiment was repeated with 40 and 70 mM concentrations of buffer. These results were then extrapolated to a buffer concentration of zero in order to determine the non-buffer catalysed rate constant.

Reactions at pH > 8.67 and < 3.54 (At 90 °C)

At high or low pH values, solutions of potassium hydroxide or hydrochloric acid were used, respectively. 1:1 *mol:mol* Potassium *p*-nitrobenzenesulphonate / potassium chloride (1.6 mg, 5 µmol) was placed in a volumetric flask (50 ml) with a quantity of potassium nitrate sufficient to make the IS of the final solution 1 M. The required volume of 1 M hydrochloric acid or potassium hydroxide solution was then measured into the volumetric flask using a pipette, and water was added to make up the volume.

In the case of the potassium hydroxide solutions, 10 ml of the solution was then transferred to a 10 ml volumetric flask, and the substrate solution (100 µl, 10 mM) was added (for the procedure with HCl solutions, see the following section (8.4.5)). The solution was then divided between ten ampoules which were sealed and placed in the water bath and handled from this point onwards according to the general procedure.

For each solution of this type a HCl or KOH concentration of at least 5 mM ($\geq$ 50 equivalents compared to the TnpsT substrate) was used.

Rapid Reactions (pH $<$ 3.54 At 90 °C)

For rapid reactions (*i.e.* those carried out in HCl solutions) the short time-scales involved rendered the use of a water bath impractical. Instead, an aluminium heating block was used. One well within the block was filled with silicone oil and held a thermometer, enabling the temperature of the block to be adjusted until 90.0 °C $\pm$ 0.1 was maintained. Into an adjacent well was placed a small quantity of silicone oil to aid heat conduction, and a broken-necked ampoule containing hydrochloric acid solution (1 ml), the preparation of which is described in the previous section.

The solution was allowed to equilibrate for 5 min, after which time TnpsT solution (10 μl, 10 mM) was added by micropipette. After the required time had elapsed, quench solution (200 μl of dipotassium phosphate solution at 10 $\times$ the concentration of the HCl solution, with the exception of the 1 M HCl solution, which required 150 μl 8 M NaOH solution) was added, and the mixture was transferred to a HPLC vial.

8.4.6 Kinetic Data for HCl Solutions

Linear regression was performed using Microsoft® Excel® 2010, on Microsoft® Windows® 7.

Time points marked with an asterisk (*) have been neglected in the analysis.

Integrals for 50 mM HCl, pH 1.32

Time / s:	Amine:	Standard:	TnpsT:	Thiol:
0		1668725	842016	0
5	222437	1736711	699473	0
10	351465	1799685	467513	68978
15	441637	1708811	320593	169838
20	454743	1717293	221233	204705
30	581509	1716614	94343	250085
60	562742	1721351	0	281536
90	579303	1718788	0	308643
180	485071	1734882	0	225346
270	270435	1780902	364761	69309

Relative Integrals for 50 mM HCl, pH 1.32

Time / s:	Amine:	TnpsT:	ln(TnpsT):
0		0.505	-0.684
5	0.128	0.403	-0.909
10	0.195	0.260	-1.348
15	0.258	0.188	-1.673
20	0.265	0.129	-2.049
30	0.339	0.055	-2.901
60	0.327	0.000	
90	0.337	0.000	
180	0.280	0.000	
*270	0.152	0.205	-1.586

Analysis for 50 mM HCl, pH 1.32

	Value:	Standard Error:
$\ln([\text{Tnpst}]_0)$	-6.0×10^{-1}	5×10^{-2}
k_{obs} / s^{-1}	7.5×10^{-2}	3×10^{-3}
R^2	0.994	
Half-life / s	9.3	

Integrals for 5 mM HCl, pH 2.37

Time / s:	Amine:	Standard:	TnpsT:	Thiol:
0		2063195	1020409	0
30	176618	2112442	851018	0
60	271715	2120004	688949	0
90	284949	2107044	542938	0
120	376500	2120180	405840	70260
150	425299	2169817	351470	89970
180	525191	2126879	259863	79903
210	585470	2138014	215083	109019
240	540219	2125079	168982	102285
480	672987	2175757	27515	145162

Relative Integrals for 5 mM HCl, pH 2.37

Time / s:	Amine:	TnpsT:	ln(TnpsT):
0		0.495	-0.704
30	0.084	0.403	-0.909
60	0.128	0.325	-1.124
90	0.135	0.258	-1.356
120	0.178	0.191	-1.653
150	0.196	0.162	-1.820
180	0.247	0.122	-2.102
210	0.274	0.101	-2.297
240	0.254	0.080	-2.532
480	0.309	0.013	-4.370

Analysis for 5 mM HCl, pH 2.37

	Value:	Standard Error:
$\ln([\text{Tnpst}]_0)$	-7.0×10^{-1}	1×10^{-2}
k_{obs} / s^{-1}	7.68×10^{-3}	6×10^{-5}
R^2	0.9995	
Half-life / s	90.2	

8.4.7 Kinetic Data for pH 3.54 Formate Buffer

Integrals for 10 mM Formate Buffer

Time / s:	Amine:	Standard:	TnpsT:
0		1863002	1038372
600	158766	1811382	735585
1200	270427	1853054	558248
1800	352222	1847398	406960
2400	387760	1837817	334182
3000	432438	1806502	229673
3600	505999	1868529	194648
4200	502423	1884936	159793
4800	513653	1854381	114813
7200	567234	1879317	26923

Relative Integrals for 10 mM Formate Buffer

Time / s:	Amine:	TnpsT:	ln(TnpsT):
0		0.557	-0.585
600	0.088	0.406	-0.901
1200	0.146	0.301	-1.200
1800	0.191	0.220	-1.513
2400	0.211	0.182	-1.705
3000	0.239	0.127	-2.062
3600	0.271	0.104	-2.262
4200	0.267	0.085	-2.468
4800	0.277	0.062	-2.782
7200	0.302	0.014	-4.246

Analysis for 10 mM Formate Buffer

	Value:	Standard Error:
$\ln([\text{Tnpst}]_0)$	-6.4×10^{-1}	3×10^{-2}
k_{obs} / s^{-1}	4.5×10^{-4}	1×10^{-5}
R^2	0.996	
Half-life / s	1500	
Half-life / h	0.42	

Integrals for 40 mM Formate Buffer

Time / s:	Amine:	Standard:	TnpsT:
0	27454	1877886	1027287
600	283445	1894847	627732
1200	363439	1810505	317365
1800	417673	1865756	285476
2400	460377	1861908	186338
3000	444225	1761668	139665
3600	590644	1894533	80160
4200	599375	1903955	72573
4800	606714	1875177	47718
7200	622338	1871291	0

Relative Integrals for 40 mM Formate Buffer

Time / s:	Amine:	TnpsT:	ln(TnpsT):
0	0.015	0.547	-0.603
600	0.150	0.331	-1.105
1200	0.201	0.175	-1.741
1800	0.224	0.153	-1.877
2400	0.247	0.100	-2.302
3000	0.252	0.079	-2.535
3600	0.312	0.042	-3.163
4200	0.271	0.038	-3.267
4800	0.324	0.025	-3.671
7200	0.333	0.000	

Analysis for 40 mM Formate Buffer

	Value:	Standard Error:
$\ln([\text{Tnpst}]_0)$	-7.7×10^{-1}	9×10^{-2}
k_{obs} / s^{-1}	6.2×10^{-4}	3×10^{-5}
R^2	0.984	
Half-life / s	1100	
Half-life / h	0.31	

Integrals for 70 mM Formate Buffer

Time / s:	Amine:	Standard:	TnpsT:
0	42210	1803395	948497
600	275106	1834177	524305
1200	360450	1810752	345338
1800	441468	1831797	227687
2400	478595	1828492	141365
3000	501626	1865159	96130
3600	528873	1858092	69903
4200	614538	1873930	26856
4800	621640	1878338	21844
7200	623469	1867325	0

Relative Integrals for 70 mM Formate Buffer

Time / s:	Amine:	TnpsT:	ln(TnpsT):
0	0.023	0.526	-0.643
600	0.150	0.286	-1.252
1200	0.199	0.191	-1.657
1800	0.241	0.124	-2.085
2400	0.262	0.077	-2.560
3000	0.269	0.052	-2.965
3600	0.285	0.038	-3.280
4200	0.328	0.014	-4.245
4800	0.331	0.012	-4.454
7200	0.334	0.000	

Analysis for 70 mM Formate Buffer

	Value:	Standard Error:
$\ln([\text{Tnpst}]_0)$	-6.8×10^{-1}	9×10^{-2}
k_{obs} / s^{-1}	7.9×10^{-4}	3×10^{-5}
R^2	0.990	
Half-life / s	880	
Half-life / h	0.24	

Integrals for 100 mM Formate Buffer

Time / s:	Amine:	Standard:	TnpsT:
0	136088	1835852	862826
600	367776	1855558	466413
1200	408697	1820854	302063
1800	482957	1836787	165026
2400	536739	1802089	115643
3000	534078	1867048	75302
3600	592037	1880597	47813
4200	614862	1880102	0
4800	633340	1912330	0

Relative Integrals for 100 mM Formate Buffer

Time / s:	Amine:	TnpsT:	ln(TnpsT):
0	0.074	0.470	-0.755
600	0.198	0.251	-1.381
1200	0.224	0.166	-1.796
1800	0.263	0.090	-2.410
2400	0.298	0.064	-2.746
3000	0.286	0.040	-3.211
3600	0.315	0.025	-3.672
4200	0.285	0.000	
4800	0.331	0.000	

Analysis for 100 mM Formate Buffer

	Value:	Standard Error:
$\ln([\text{Tnpst}]_0)$	-8.5×10^{-1}	5×10^{-2}
k_{obs} / s^{-1}	8.0×10^{-4}	2×10^{-5}
R^2	0.995	
Half-life / s	870	
Half-life / h	0.24	

General Catalysis Analysis for Formate Buffer

Buffer Concentration / mM:	k_{obs} / s^{-1}
10	4.5×10^{-4}
40	6.2×10^{-4}
70	7.9×10^{-4}
100	8.0×10^{-4}

	Value:	Standard Error:
k_0 / s^{-1}	4.4×10^{-4}	6×10^{-5}
k_{buff} / $M^{-1}s^{-1}$	4.0×10^{-6}	9×10^{-7}
R^2	0.903	
Half-life / s	1600	
Half-life / h	0.44	

8.4.8 Kinetic Data for pH 4.61 Acetate Buffer

Integrals for 10 mM Acetate Buffer

Time / s:	Amine:	Standard:	TnpsT:	Thiol:
0		8397616	1621528	0
3515	163529	8376815	1374020	0
7370	343582	8484302	1179757	104466
10675	422916	8513861	1016781	183900
13595	420923	8504952	833894	236256
18995	446484	6348309	740416	261372
24395	903533	8552437	186005	195374
29795	758384	8274768	471698	298874
34775	705388	8436376	391363	313518
97655	1009816	8278421	0	196920

Relative Integrals for 10 mM Acetate Buffer

Time / s:	Amine:	TnpsT:	ln(TnpsT):
0		0.193	-1.645
3515	0.020	0.164	-1.808
7370	0.040	0.139	-1.973
10675	0.050	0.119	-2.125
13595	0.049	0.098	-2.322
*18995	0.070	0.117	-2.149
*24395	0.106	0.022	-3.828
29795	0.092	0.057	-2.865
34775	0.084	0.046	-3.071
97655	0.122	0	

Analysis for 10 mM Acetate Buffer

	Value:	Standard Error:
$\ln([\text{Tnpst}]_0)$	-1.68	3×10^{-2}
k_{obs} / s^{-1}	4.0×10^{-5}	1×10^{-6}
R^2	0.994	
Half-life / s	17000	
Half-life / h	4.8	

Integrals for 40 mM Acetate Buffer

Time / s:	Amine:	Standard:	TnpsT:
0	154949	8501649	1438272
1800	263650	8248089	1374904
3600	368523	8673931	1273517
5460	397356	8730098	1156327
7200	383899	8551222	1049075
10800	445593	8454592	944505
16440	825242	8506709	701764
21900	929792	8445133	107234
28800	847369	8698518	371920
86400	972620	8605404	0

Relative Integrals for 40 mM Acetate Buffer

Time / s:	Amine:	TnpsT:	ln(TnpsT):
0	0.018	0.169	-1.777
1800	0.032	0.167	-1.792
3600	0.042	0.147	-1.919
5460	0.046	0.132	-2.022
7200	0.045	0.123	-2.098
10800	0.053	0.112	-2.192
16440	0.097	0.082	-2.495
*21900	0.110	0.013	-4.366
28800	0.097	0.043	-3.152
86400	0.113	0.000	

Analysis for 40 mM Acetate Buffer

	Value:	Standard Error:
$\ln([\text{Tnpst}]_0)$	-1.74	2×10^{-2}
k_{obs} / s^{-1}	4.8×10^{-5}	2×10^{-6}
R^2	0.993	
Half-life / s	14000	
Half-life / h	4.0	

Integrals for 70 mM Acetate Buffer

Time / s:	Amine:	Standard:	TnpsT:
0	221836	9250739	1370111
1800	357870	8462860	1113800
3600	447075	8382452	1027973
5460	418478	8632344	885457
7200	583077	8807920	843788
10800	689137	8523983	619775
16440	776817	8229660	401528
21900	757797	8423038	293792
28800	819962	8617800	166829
86400	1025310	8384993	0

Relative Integrals for 70 mM Acetate Buffer

Time / s:	Amine:	TnpsT:	ln(TnpsT):
0	0.024	0.148	-1.910
1800	0.042	0.132	-2.028
3600	0.053	0.123	-2.099
5460	0.048	0.103	-2.277
7200	0.066	0.096	-2.346
10800	0.081	0.073	-2.621
16440	0.094	0.049	-3.020
21900	0.090	0.035	-3.356
28800	0.095	0.019	-3.945
86400	0.122	0.000	

Analysis for 70 mM Acetate Buffer

	Value:	Standard Error:
$\ln([\text{Tnpst}]_0)$	-1.88	2×10^{-2}
k_{obs} / s^{-1}	7.0×10^{-5}	1×10^{-6}
R^2	0.997	
Half-life / s	9900	
Half-life / h	2.8	

Integrals for 100 mM Acetate Buffer

Time / s:	Amine:	Standard:	TnpsT:	Thiol:
0		8504619	1500229	0
3515	391558	8406408	890909	138014
7370	554154	8522067	667638	207539
10675	670521	8494405	525229	237612
13595	759499	8421799	399498	241875
18995	858901	8433994	275297	255533
24395	881390	7837413	203051	262795
29795	954196	8334426	0	210901
34775	963061	8485922	0	167586
97655	887185	8239523	0	959124

Relative Integrals for 100 mM Acetate Buffer

Time / s:	Amine:	TnpsT:	ln(TnpsT):
0		0.176	-1.735
3515	0.047	0.106	-2.245
7370	0.065	0.078	-2.547
10675	0.079	0.062	-2.783
13595	0.090	0.047	-3.048
18995	0.102	0.033	-3.422
24395	0.112	0.026	-3.653
29795	0.114	0.000	
34775	0.113	0.000	
97655	0.108	0.000	

Analysis for 100 mM Acetate Buffer

	Value:	Standard Error:
$\ln([\mathrm{Tnpst}]_0)$	-1.91	8×10^{-2}
k_{obs} / s^{-1}	7.7×10^{-5}	6×10^{-6}
R^2	0.973	
Half-life / s	9000	
Half-life / h	2.5	

General Catalysis Analysis for Acetate Buffer

Buffer Concentration / mM:	$k_{\mathbf{obs}}$ / s^{-1}
10	4.0×10^{-5}
40	4.8×10^{-5}
70	7.0×10^{-5}
100	7.7×10^{-5}

	Value:	Standard Error:
k_0 / s^{-1}	3.5×10^{-5}	4×10^{-6}
k_{buff} / $M^{-1}s^{-1}$	4.4×10^{-7}	7×10^{-8}
R^2	0.953	
Half-life / s	20000	
Half-life / h	5.5	

8.4.9   Kinetic Data for pH 5.68 MES Buffer

Integrals for 10 mM MES Buffer

Time / s:	Amine:	Standard:	TnpsT:
0		3052158	1699478
14400		3042009	1569030
28800	104994	3075507	1416279
43200	295546	3036299	1350318
57600	348030	3175283	1121011
100800	490947	3126050	914473
187200	707079	3086310	527249
273600	841728	3099233	309101
446400	1231040	3122664	107307
533400	1173325	3381350	69145

Relative Integrals for 10 mM MES Buffer

Time / s:	Amine:	TnpsT:	ln(TnpsT):
0		0.557	-0.586
14400		0.516	-0.662
28800	0.034	0.461	-0.775
43200	0.097	0.445	-0.810
57600	0.110	0.353	-1.041
100800	0.157	0.293	-1.229
187200	0.229	0.171	-1.767
273600	0.272	0.100	-2.305
446400	0.394	0.034	-3.371
533400	0.347	0.020	-3.890

Analysis for 10 mM MES Buffer

	Value:	Standard Error:
$\ln([\mathrm{Tnpst}]_0)$	-0.593	7×10^{-3}
k_{obs} / s^{-1}	6.21×10^{-6}	3×10^{-8}
R^2	0.9999	
Half-life / s	112000	
Half-life / h	31.0	
Half-life / day	1.29	

Integrals for 100 mM MES Buffer

Time / s:	Amine:	Standard:	TnpsT:
0		3015608	1706954
14400		3077453	1595214
28800		3176581	1517047
43200		3060482	1121410
57600	338848	3171542	1295226
100800	419325	3449446	1106546
187200	693082	3276010	646507
273600	857438	3036560	370006
446400	1010046	3311320	147441
533400	1186327	3179948	96592

Relative Integrals for 100 mM MES Buffer

Time / s:	Amine:	TnpsT:	ln(TnpsT):
0		0.566	-0.569
14400		0.518	-0.657
28800		0.478	-0.739
*43200		0.366	-1.004
57600	0.107	0.408	-0.896
100800	0.122	0.321	-1.137
187200	0.212	0.197	-1.623
273600	0.282	0.122	-2.105
446400	0.305	0.045	-3.112
533400	0.373	0.030	-3.494

Analysis for 100 mM MES Buffer

	Value:	Standard Error:
$\ln([\text{Tnpst}]_0)$	-5.8×10^{-1}	1×10^{-2}
k_{obs} / s^{-1}	5.56×10^{-6}	5×10^{-8}
R^2	0.9994	
Half-life / s	125000	
Half-life / h	34.7	
Half-life / day	1.44	

Average of 100 mM and 10 mM MES buffer k_{obs} values: 5.88×10^{-6} s^{-1}

8.4.10   Kinetic Data for pH 6.60 Phosphate Buffer

Integrals for 10 mM Phosphate Buffer

Time / s:	Amine:	Standard:	TnpsT:
0		3012915	1686985
86400		3090826	1471150
259200	342439	2968220	1021488
604800	552355	3038786	458631
777600	690532	3565864	471385
941400	770991	3243316	293507
1114200	769013	3097616	211586
1287000	811945	3071116	174762

Relative Integrals for 10 mM Phosphate Buffer

Time / s:	Amine:	TnpsT:	ln(TnpsT):
0		0.560	-0.580
86400		0.476	-0.742
259200	0.115	0.344	-1.067
604800	0.182	0.151	-1.891
777600	0.194	0.132	-2.023
941400	0.238	0.090	-2.402
1114200	0.248	0.068	-2.684
1287000	0.264	0.057	-2.866

Analysis for 10 mM Phosphate Buffer

	Value:	Standard Error:
$\ln([\text{Tnpst}]_0)$	-6.2×10^{-1}	5×10^{-2}
k_{obs} / s^{-1}	1.83×10^{-6}	7×10^{-8}
R^2	0.9914	
Half-life / s	378000	
Half-life / h	105	
Half-life / day	4.37	

Integrals for 100 mM Phosphate Buffer

Time / s:	Amine:	Standard:	TnpsT:
0		3091195	1693658
86400		3136620	1440037
259200	369892	3160139	999850
604800	624089	3112808	548636
777600	688447	3026656	396416
941400	807564	3264554	337415
1114200	800326	3096372	219028
1287000	847382	3237171	161483

Relative Integrals for 100 mM Phosphate Buffer

Time / s:	Amine:	TnpsT:	ln(TnpsT):
0		0.548	-0.602
86400		0.459	-0.778
259200	0.117	0.316	-1.151
604800	0.200	0.176	-1.736
777600	0.227	0.131	-2.033
941400	0.247	0.103	-2.270
1114200	0.258	0.071	-2.649
1287000	0.262	0.050	-2.998

Analysis for 100 mM Phosphate Buffer

	Value:	Standard Error:
$\ln([\text{Tnpst}]_0)$	-6.3×10^{-1}	2×10^{-2}
k_{obs} / s^{-1}	1.82×10^{-6}	3×10^{-8}
R^2	0.9983	
Half-life / s	382000	
Half-life / h	106	
Half-life / day	4.42	

Average of 100 mM and 10 mM phosphate buffer k_{obs} values: 1.83×10^{-6} s^{-1}

8.4.11   Kinetic Data for pH 7.39 Bicine Buffer

Integrals for 10 mM Bicine Buffer

Time / s:	Amine:	Standard:	TnpsT:
0		2148300	1307292
86400	104238	2199756	1237154
172800	162265	2172812	1131429
259200	177073	2115830	1053357
345600	265377	2147877	984923
518400	326853	2175006	847496
691200	411425	2178048	735849
864000	525665	2157935	627924
1036800	552963	2167248	540634
1209600	644530	2218031	440499

Relative Integrals for 10 mM Bicine Buffer

Time / s:	Amine:	TnpsT:	ln(TnpsT):
0		0.609	-0.497
86400	0.047	0.562	-0.576
172800	0.075	0.521	-0.653
259200	0.084	0.498	-0.697
345600	0.084	0.459	-0.780
518400	0.150	0.390	-0.943
691200	0.189	0.338	-1.085
864000	0.244	0.291	-1.234
1036800	0.255	0.249	-1.388
1209600	0.291	0.199	-1.616

Analysis for 10 mM Bicine Buffer

	Value:	Standard Error:
$\ln([\text{Tnpst}]_0)$	-4.8×10^{-1}	1×10^{-2}
k_{obs} / s^{-1}	9.0×10^{-7}	2×10^{-8}
R^2	0.996	
Half-life / s	770000	
Half-life / h	210	
Half-life / day	9.0	

Integrals for 100 mM Bicine Buffer

Time / s:	Amine:	Standard:	TnpsT:
0		2160962	1324508
86400	83216	2180873	1241694
172800	172561	2159787	1139773
259200	231624	2151164	1066353
345600	242326	2168983	989034
518400	390714	2172934	856892
691200	440459	2156941	736468
864000	560255	2153378	631954
1036800	585301	2134569	545087
1209600	651485	2208360	464536

Relative Integrals for 100 mM Bicine Buffer

Time / s:	Amine:	TnpsT:	ln(TnpsT):
0		0.613	-0.490
86400	0.038	0.569	-0.563
172800	0.080	0.528	-0.639
259200	0.108	0.496	-0.702
345600	0.108	0.456	-0.785
518400	0.180	0.394	-0.931
691200	0.204	0.341	-1.075
864000	0.260	0.293	-1.226
1036800	0.274	0.255	-1.365
1209600	0.295	0.210	-1.559

Analysis for 100 mM Bicine Buffer

	Value:	Standard Error:
$\ln([\text{Tnpst}]_0)$	-4.84×10^{-1}	7×10^{-3}
k_{obs} / s^{-1}	8.7×10^{-7}	1×10^{-8}
R^2	0.9989	
Half-life / s	800000	
Half-life / h	220	
Half-life / day	9.3	

Average of 100 mM and 10 mM bicine buffer k_{obs} values: 8.8×10^{-7} s^{-1}

8.4.12   Kinetic Data for pH 8.67 Borate Buffer

Integrals for 10 mM Borate Buffer

Time / s:	Amine:	Standard:	TnpsT:
0		2028390	1284514
86400	50498	1960392	1240312
172800	155490	1981424	1142461
259200	170913	1966629	1087065
345600	236837	1954921	1019262
864000	410757	2021553	707156
1382400	565758	1993645	497993
1900800	672018	1989387	338960
2419200	729964	1854456	212817
2592000	755514	1981444	202675

Relative Integrals for 10 mM Borate Buffer

Time / s:	Amine:	TnpsT:	ln(TnpsT):
0		0.633	-0.457
86400	0.026	0.633	-0.458
172800	0.078	0.577	-0.551
259200	0.087	0.553	-0.593
345600	0.087	0.521	-0.651
864000	0.203	0.350	-1.050
1382400	0.284	0.250	-1.387
1900800	0.338	0.170	-1.770
2419200	0.394	0.115	-2.165
2592000	0.381	0.102	-2.280

Analysis for 10 mM Borate Buffer

	Value:	Standard Error:
$\ln([\text{Tnpst}]_0)$	-4.18×10^{-1}	9×10^{-3}
k_{obs} / s^{-1}	7.16×10^{-7}	7×10^{-9}
R^2	0.9993	
Half-life / s	968000	
Half-life / h	269	
Half-life / day	11.2	

Integrals for 100 mM Borate Buffer

Time / s:	Amine:	Standard:	TnpsT:
0		1992483	1300266
86400	42378	1969394	1245993
172800	95656	2033986	1187240
259200	165481	2025699	1121865
345600	184571	2024400	1061050
864000	389585	2034419	768034
1382400	538873	2019683	567425
1900800	655180	2023361	409904
2419200	693175	1963368	292018
2592000	791713	1981763	271846

Relative Integrals for 100 mM Borate Buffer

Time / s:	Amine:	TnpsT:	ln(TnpsT):
0		0.653	-0.427
86400	0.022	0.633	-0.458
172800	0.048	0.584	-0.538
259200	0.082	0.554	-0.591
345600	0.082	0.524	-0.646
864000	0.191	0.378	-0.974
1382400	0.267	0.281	-1.270
1900800	0.324	0.203	-1.597
2419200	0.353	0.149	-1.906
2592000	0.399	0.137	-1.987

Analysis for 100 mM Borate Buffer

	Value:	Standard Error:
$\ln([\text{Tnpst}]_0)$	-4.30×10^{-1}	6×10^{-3}
k_{obs} / s^{-1}	6.08×10^{-7}	5×10^{-9}
R^2	0.9995	
Half-life / s	1140000	
Half-life / h	317	
Half-life / day	13.2	

Average of 100 mM and 10 mM borate buffer k_{obs} values: 6.62×10^{-7} s^{-1}

8.4.13   Kinetic Data for pH KOH Solutions

Integrals for 5 mM KOH, pH 9.90

Time / s:	Amine:	Standard:	TnpsT:
0		2101459	1302862
345600	154000	2060733	1065851
691200	286624	2067771	862236
1036800	349486	2104794	688079
1382400	542729	2027073	559721
1728000	588032	2059645	461009
2073600	635070	2076066	374792
*2246400	640072	1988955	284602

Relative Integrals for 5 mM KOH, pH 9.90

Time / s:	Amine:	TnpsT:	ln(TnpsT):
0		0.620	-0.478
345600	0.075	0.517	-0.659
691200	0.139	0.417	-0.875
1036800	0.166	0.327	-1.118
1382400	0.268	0.276	-1.287
1728000	0.286	0.224	-1.497
2073600	0.306	0.181	-1.712
*2246400	0.322	0.143	-1.944

Analysis for 5 mM KOH, pH 9.90

	Value:	Standard Error:
$\ln([\text{Tnpst}]_0)$	-4.7×10^{-1}	1×10^{-2}
k_{obs} / s^{-1}	5.98×10^{-7}	9×10^{-9}
R^2	0.9989	
Half-life / s	1160000	
Half-life / h	322	
Half-life / day	13.4	

Integrals for 50 mM KOH, pH 10.91

Time / s:	Amine:	Standard:	TnpsT:
*0	20487	2239815	1243620
86400	88042	2172057	1086538
172800	137060	2147684	1028657
259200	267019	2158397	987880
345600	272411	2144063	948256
604800	334815	2109071	854148
864000	377634	2130542	779238
1123200	439685	2079998	695064
1382400	471280	2084791	630095
2073600	565757	2025894	489438

Relative Integrals for 50 mM KOH, pH 10.91

Time / s:	Amine:	TnpsT:	ln(TnpsT):
* 0	0.009	0.555	-0.588
86400	0.041	0.500	-0.693
172800	0.064	0.479	-0.736
259200	0.124	0.458	-0.782
345600	0.127	0.442	-0.816
604800	0.159	0.405	-0.904
864000	0.177	0.366	-1.006
1123200	0.211	0.334	-1.096
1382400	0.226	0.302	-1.197
2073600	0.279	0.242	-1.421

Analysis for 50 mM KOH, pH 10.91

	Value:	Standard Error:
$\ln([\text{Tnpst}]_0)$	-6.81×10^{-1}	7×10^{-3}
k_{obs} / s^{-1}	3.64×10^{-7}	7×10^{-9}
R^2	0.9976	
Half-life / s	1900000	
Half-life / h	528	
Half-life / day	22.0	

Integrals for 50 mM KOH, pH 10.91 Monophosphate Species

Time / s:	Tnp:	psT:	Standard:
0			2239815
86400		22633	2172057
172800			2147684
259200	39571	43340	2158397
345600	30643	34383	2144063
604800	40939	48563	2109071
864000	45701	49828	2130542
1123200	46750	60188	2079998
1382400	48601	57041	2084791
2073600	52452	59039	2025894

Relative Integrals for 50 mM KOH, pH 10.91 Monophosphate Species

Time / s:	Tnp:	psT:
0		
86400		0.0104
172800		
259200	0.0183	0.0201
345600	0.0143	0.0160
604800	0.0194	0.0230
864000	0.0215	0.0234
1123200	0.0225	0.0289
1382400	0.0233	0.0274
2073600	0.0259	0.0291

Analysis for 50 mM KOH, pH 10.91 Monophosphate Species

A least squares fitting to the equation:

$$[Mono] = \frac{k_{\mathrm{acc}}[TnpsT]_0}{k_{\mathrm{dec}} - k_{\mathrm{obs}}} \left(e^{-k_{\mathrm{obs}}t} - e^{-k_{\mathrm{dec}}t} \right)$$

was performed, where $[Mono]$ is the concentration of the monophosphate species, and k_{acc} and k_{dec} are the rate constants for the accumulation and decomposition, respectively, of the monophosphate species. k_{obs} and $[TnpsT]_0$ have already been determined from the hydrolysis of TnpsT.

	Tnp:	psT:
$[Tnpst]_0$	5.1×10^{-1}	5.1×10^{-1}
k_{obs}/s^{-1}	3.64×10^{-7}	3.64×10^{-7}
k_{acc}/s^{-1}	9×10^{-8}	1×10^{-7}
k_{dec}/s^{-1}	1×10^{-6}	1×10^{-6}

8.4.14   Collected TnpsT Hydrolysis Results

Buffer:	pH at 25 °C:	pH at 90 °C:	Rate / s⁻¹:	log(Rate):
HCl	1.32	1.32	7.35×10^{-2}	-1.13
HCl	2.37	2.37	7.68×10^{-3}	-2.11
Formate	3.53	3.54	4.41×10^{-4}	-3.36
Acetate	4.60	4.61	3.46×10^{-5}	-4.46
MES	6.25	5.68	5.88×10^{-6}	-5.23
Phosphate	6.47	6.60	1.82×10^{-6}	-5.74
Bicine	8.32	7.39	8.81×10^{-7}	-6.05
Borate	9.11	8.67	6.62×10^{-7}	-6.18
KOH	11.55	9.90	5.98×10^{-7}	-6.22
KOH	12.56	10.91	3.64×10^{-7}	-6.44

8.5   Azide Reduction

8.5.1   Synthetic Work

Trisodium Thiophosphate

Following the procedure of Yasuda and Lambert,[153] water (100 ml) and thiophosphoryl chloride (17.5 ml, 29.2 g, 173 mmol) were added to a solution of sodium hydroxide (200 ml, 5 M). The solution was heated at reflux for 15 min, then cooled in an water-ice bath to precipitate the crude product. The solid material was collected by filtration and dissolved in the minimum amount of warm water (125 ml at 45 °C). Methanol was added to precipitate the crude trisodium thiophosphate, the resulting solid was collected by filtration and the precipitation procedure was repeated. The isolated material was suspended in anhydrous methanol for 1 h with stirring, before being filtered and dried in an oven at 95 °C for 1 h to yield the product (15.5 g, 50%). δ_P (162 MHz, D_2O) 32.8; TGA shows negligible mass loss up to 200 °C.

1-Aminoadamantane (196)[167]

NH$_2$
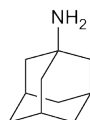
1-Azidoadamantane (168 mg, 0.948 mmol) and trisodium thiophosphate (870 mg, 4.83 mmol) were placed in a 50 ml round bottomed flask with a 2:1 water / isopropanol mixture (10 ml). The flask was fitted with a condenser and heated at reflux for 24 h. Additional trisodium thiophosphate (670 mg 3.72 mmol) was added, and reflux was continued for a further 24 h. The standard work-up procedure was followed and a 'spike' confirmed the identity of the product as 1-aminoadamantane. (65 mg, 43%). δ_H (400 MHz, CDCl$_3$) 1.55-2.15 (15H, m); δ_C (100 MHz, CDCl$_3$) 29.9 (CH), 36.4 (CH$_2$ δ to NH$_2$), 46.3 (CH$_2$ β to NH$_2$), 47.6 (C-NH$_2$).

1-Aminooctane (181)[168]

NH$_2$
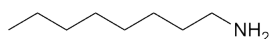
1-azidooctane (150 mg, 0.968 mmol) was placed in a round bottomed flask with trisodium thiophosphate (539 mg, 2.99 mmol) and of a 2:1 water / isopropanol mixture (6 ml). The flask was fitted with a condenser and heated at reflux for 24 h. The standard work-up procedure was then followed to yield the product, which was confirmed by a 'spike' to be 1-aminooctane (67 mg,

54%); δ_H (400 MHz, CDCl$_3$) 0.81 (3H, t, J 5.4, CH_3), 1.13-1.30 (12H, br s, (CH_2)$_6$), 1.32-1.41 (2H, m, NH_2), 2.61 (2H, t, J 6.8, CH_2NH$_2$); δ_C (100 MHz, CDCl$_3$) 14.0, 22.6, 26.8, 29.3, 29.4, 31.8, 33.8, 42.2.

2-Azido-1-phenylethanol (193)[154]
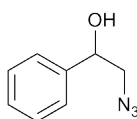
Following a literature procedure,[154] styrene oxide (1.19 g, 9.86 mmol), ammonium chloride (1.07 g, 20.0 mmol), and sodium azide (5.18 g, 79.7 mmol) were placed in a flask with an 8:1 mixture of methanol and water (100 ml). The solution was stirred at room temperature for 24 h before the methanol was removed under reduced pressure. The remaining liquid was diluted with water (50 ml), extracted with ethyl acetate (3 × 30 ml), and washed with brine (40 ml). The organic extract was over MgSO$_4$ and the solvent removed under reduced pressure. The major isomer was isolated by silica gel chromatography (1:2 EtOAc/Hexane) (664 mg, 41%) δ_H (400 MHz, CDCl$_3$) 1.92-2.04 (1H, br s, OH), 3.71-3.82 (2H, m, CH_2N$_3$), 4.70 (1H, dd, J 7.0, 5.8, CHOH) 7.32-7.46 (5H, m, Ph); δ_C (100 MHz, CDCl$_3$) 66.5, 67.9, 127.2, 128.8, 129.0, 136.

2-Amino-1-phenylethanol (197)[169]

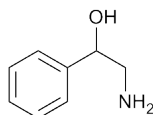2-Azido-1-phenylethanol (168 mg, 1.03 mmol) and trisodium thiophosphate (560 mg, 3.11 mmol) were placed in a round bottomed flask with a 1:2 mixture of isopropanol and water (10 ml). The flask was fitted with a condenser was heated at reflux for 3 h. The standard work up was followed, with several additional extractions with chloroform to yield the crude product. (101 mg, 72%) δ_H (400 MHz, CDCl$_3$) 2.60-2.90 (3H, br s, NH_2, OH), 3.55 (1H, dd, J 10.9, 8.4, CH_aH$_b$NH$_2$), 3.72 (1H, dd, J 10.9, 4.2, CH$_a$$H_bNH_2$), 4.03 (1H, dd, J 8.4, 4.2, CHOH), 7.23-7.40 (5H, m, Ph); δ_C (100 MHz, CDCl$_3$) 57.4, 67.9, 126.6, 127.5, 128.6, 142.5.

β-D-Glucopyranosyl azide, 2,3,4,6-tetraacetate (189)[155]

Following a literature procedure,[155] α-D-glucopyranosyl bromide, 2,3,4,6-tetra-acetate (97 mg, 0.24 mmol) was placed in a round bottomed flask with sodium azide (20 mg, 0.31 mmol) with DMSO (5 ml). The solution was stirred

for 2 h 45 min at room temperature. On completion, the reaction mixture was diluted with water (20 ml), extracted with ethyl acetate (20 ml), and washed with more water (2 × 20 ml). The organic extract was then dried over MgSO$_4$ and the solvent removed under reduced pressure to afford the product, β-D-glucopyranosyl azide, 2,3,4,6-tetraacetate (68 mg, 76%) δ$_H$ (400 MHz, CDCl$_3$) 2.01 (3H, s, (CO)CH$_3$), 2.04 (3H, s, (CO)CH$_3$), 2.08 (3H, s, (CO)CH$_3$), 2.11 (3H, s, (CO)CH$_3$), 3.80 (1H, ddd, *J* 10.0, 4.8, 2.3, C5-H), 4.17 (1H, dd, *J* 12.5, 2.3, C6-*H$_a$*H$_b$), 4.28 (1H, dd, *J* 12.5, 4.8, C6-$_a$*H$_b$*), 4.65, (1H, d, *J* 8.9, C1-H), 4.96, (1H, dd, *J* 9.5, 8.8, C2-H), 5.11 (1 H, app. t, *J* 9.8, C3-H), 5.22 (1 H, app. t, *J* 9.5, C4-H); δ$_C$ (100 MHz, CDCl$_3$) 20.6, 20.7, 61.6, 67.9, 70.6, 72.6, 74.0, 87.9, 169.2, 169.3, 170.1, 170.6

1,4-Diaminobenzene (199)[170]

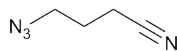*p*-Azidoaniline hydrochloride (170 mg, 0.996 mmol), sodium hydroxide (0.2 ml of a 5M solution), and trisodium thiophosphate (544 mg, 3.02 mmol) were placed in a round bottomed flask with a 1:2 mixture of isopropanol and water (10 ml). The mixture was heated at reflux for 3 h before the product was isolated via the standard work-up procedure and 'spiked' to confirm its identity. (60 mg, 56%) δ$_H$ (400 MHz, CDCl$_3$) 3.33 (4H, s, N*H$_2$*), 6.58 (4H, s, C*H*); δ$_C$ (100 MHz, CDCl$_3$) 116.7, 138.6

1-Azido-3-cyanopropane (191)^{156}

Following a literature procedure,[156] 1-bromo-3-cyanopropane (875 mg, 5.91 mmol), sodium azide (605 mg, 9.31 mmol) and DMSO (10 ml) were placed in a round bottomed flask and stirred at room temperature for 18 h. On completion of the reaction, water (20 ml) was added to the vessel, the reaction mixture was extracted with diethyl ether (20 ml) and the organic extract was washed with water (3 × 20 ml). The organic layer was dried over $MgSO_4$ and the solvent was removed under reduced pressure to afford the product, 1-azido-3-cyanopropane (322 mg, 49%) δ_H (400 MHz, CDCl$_3$) 1.92 (2H, app.quintet, *J* 6.7, CH$_2$C*H$_2$*CH$_2$), 2.48 (2H, t, *J* 7.1, C*H$_2$*CN) 3.50 (2H, t, *J* 6.3, C*H$_2$*N$_3$); δ_C (100 MHz, CDCl$_3$) 14.6, 25.0, 49.5, 118.6

γ-Aminobutyric acid (200)^{171}

1-Azido-3-cyanopropane (5 mg, 5 μmol) and trisodium thiophosphate (28 mg, 160 μmol) were placed in an NMR tube with D$_2$O as the solvent (0.7 ml). The reaction mixture was heated for 5 h at 90 °C. Sodium deuteroxide (0.1 ml of 40% *w/w* solution in D$_2$O) was added to the NMR tube, and the mixture was heated at 90°C for 18 h. The reaction mixture was then

analysed by NMR spectroscopy and complete conversion to the GABA salt
was observed. The reaction mixture was 'spiked' with a sample of authentic
GABA to confirm the identity of the product. δ_H (400 MHz, CDCl$_3$) 1.46-1.56
(2H, m, CH$_2$CH_2CH$_2$), 2.42 (2H, t, J 7.2 CH_2NH$_2$) *N.B.* An additional peak
(2.04 (2H, t, J 7.6, HO(CO)CH_2) appears in the GABA-spiked spectrum
which is not visible in the original. This is presumably due to rapid exchange
of the acidic protons α- to the nitrile group; δ_C (100 MHz, CDCl$_3$) 29.0, 35.1,
40.5, 183.4

8.5.2   Work-up and Analysis for Azide Reductions

On completion of each azide reduction, unless otherwise stated, the mixture
was filtered before being extracted with chloroform (3 × 8 ml). The organic
extracts were combined and washed with water (3 × 10 ml), then dried over
MgSO$_4$. Finally, the solvent was removed under reduced pressure to give
the crude product. The isolated material was analysed by ^{1}H and ^{13}C NMR
spectroscopy, then 'spiked' with the authentic amine, apart from the 1-azido-
2-hydroxyl substrate, which was not commercially available, to confirm that
the correct product had been formed.

8.5.3   NMR Kinetic Studies

As the NMR spectrometer could only be set up to monitor one nucleus at
a time, two identical small scale reactions were carried out in NMR spec-
troscopy tubes, one to be monitored by ^{1}H, the other by ^{31}P NMR spec-
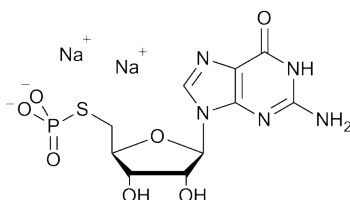troscopy, both under the same conditions.

Sample Preparation

p-Azidoaniline hydrochloride (2.2 mg, 13 μmol) was placed in an NMR tube
with sodium thiophosphate (6.8 mg, 38 μmol), NaOD solution (15 μl, 1 M),
and D$_2$O (800 μl). Some of the solution was then removed until the liquid
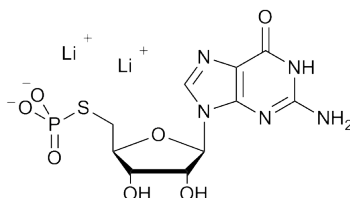
occupied the bottom two centimetres of the NMR tube. The tubes were heated to 70 °C within the NMR spectrometer and were analysed periodically, one by ^{1}H, the other by ^{31}P NMR spectroscopy.

8.6 The Synthesis of GMP Analogues

GSMP, Sodium Salt (209)[159]

Following a literature procedure,[159] 5′-deoxy-5′-iodoguanosine (487 mg, 1.24 mmol) and trisodium thiophosphate (2.36 g, 13.1 mmol) were placed in a round bottomed flask and a solution of sodium hydroxide (0.1 M, 13 ml) was added. The mixture was heated at 50 °C for 2h 30 min before being allowed to cool. The contents of the flask were divided into two centrifuge tubes, and methanol (10 ml) was added to each. The suspension was centrifuged at 4500 rpm for 15 min and the clear liquid was decanted and combined. Methanol was removed from the solution under vacuum, and the remainder was freeze-dried . The crude product was suspended in acetone with stirring for 30 min before it was filtered and dried in a vacuum desiccators over P_2O_5. Some product was lost to spillage (254 mg, 48%) δ_H (400 MHz, D_2O) 3.00-3.12 (2H, m, C5′-H_2), 4.30-4.35 (1H, m, C4′-H), 4.45 (1H, app. t, J 4.6 C3′-H), 4.75 (1H, app. t, J 5.7, C2′-H), 5.85 (1H, d, J 5.8, C1′-H), 7.97 (1H, s, C8-H); δ_P (162 MHz, D_2O) 2.72, (s, $PO_4{}^{3-}$), 16.20 (t, J 10.0, $CH_2SPO_3{}^{2-}$)

GSMP, Lithium Salt (214)

Guanosine monothiophosphate, sodium salt (455 mg, 1.08 mmol) and lithium iodide (1.65 g, 12.3 mmol) were dissolved in water (9 ml). After five minutes, acetone (45 ml) was added to the mixture, and the precipitate was collected by centrifugation at 4400 rpm for 5 min. The clear liquid was decanted to leave an off-white solid. The entire procedure repeated three times before the solid residue was finally collected and dried under vacuum over calcium chloride to give the lithium salt (250 mg, 0.639 mmol) 59%. δ_H (400 MHz, D$_2$O) 2.97-3.12 (2H, m, C5′-H_2), 4.29-4.36 (1H, m, C4′-H), 4.44 (1H, app. t, J 4.6 C3′-H), 4.73 (1H, app. t, J 4.8, C2′-H), 5.86 (1H, d, J 5.9, C1′-H), 7.96 (1H, s, C8-H); δ_P (162 MHz, D$_2$O) 17.20 (t, J 10.0, CH$_2$S$PO_3$$^{2-}$)

7-10-11

Louis Conway   5

Sodium & Lithium

LPC 130

14.74 mg

% Na = 0.14 %

% Li = 3.91 %

The ICP-AES analysis is calculated on a mass basis; for conversion to an atom basis, see equation 8.1.

$$100 \times \frac{3.91/6.941}{0.14/22.9898 + 3.91/6.941} = 99\% \text{ Lithium, atom basis.} \qquad (8.1)$$

GMPS, Sodium Salt[21]
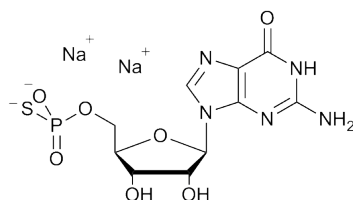
Dried guanosine (5.00 g, 17.7 mmol) was added to triethylphosphate (200 ml) and the mixture was heated to 160 °C until the guanosine had dissolved. The solution was allowed to cool to room temperature, and thiophosphoryl chloride (3.58 ml, 35.4 mmol) was added dropwise. The mixture was left at room temperature for 1.25 h before it was poured into petroleum ether (150 ml) and the precipitate was collected by filtration. The solid was washed with diethyl ether, then added to TEAB (150 ml, 2 M). The mixture was stirred for 1 h, filtered, and the filtrate was lyophilised. The crude product was then purified by anion exchange chromatography. A DEAE Sepharose™ Fast Flow column with a flow rate of 5 ml/min was used. High purity water and a 2M TEAB solution were used to generate the required gradients.
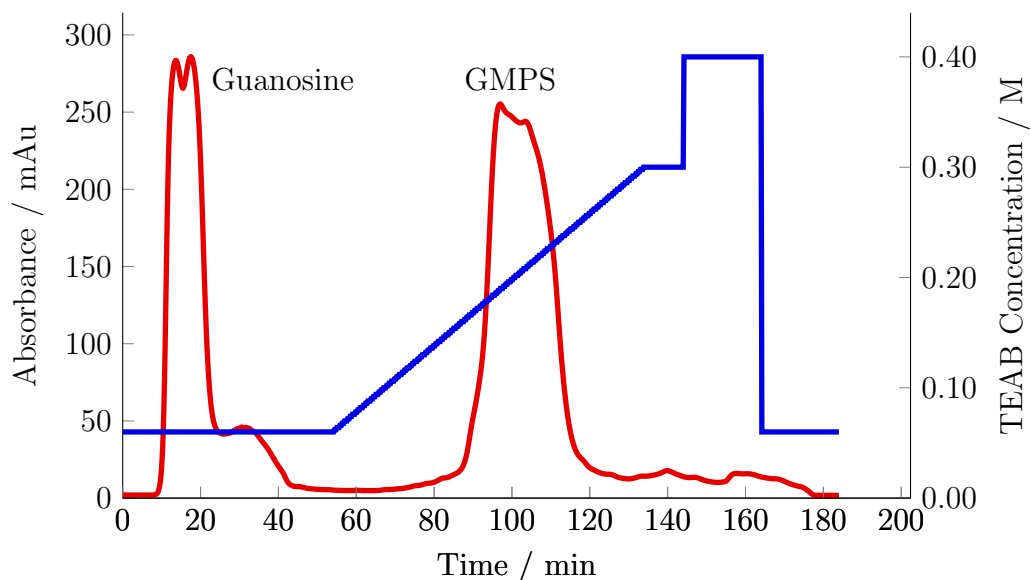
The purified product (242 mg, 0.416 mmol), was codissolved with sodium iodide (266 mg, 1.77 mmol) in water (3 ml), then precipitated with acetone (20 ml). The crude product was isolated as a solid by centrifugation (10 min at 3000 rpm). The procedure was repeated once again to produce the desired product (132 mg, 2.4%). δ_H (400 MHz, D_2O) 3.99-4.06 (2H, m, C5'-H_2), 4.29-4.35 (1H, m, C4'-H), 4.47-4.51 (1H, m, C3'-H), 5.87-5.92 (1H, m, C1'-H), 8.22 (1H, s, C8-H); δ_P (162 MHz, D_2O) 44.3, (s, PO_3S^{2-})

8.7 The Fluorescent Labelling of 5′-Hydrazino-5′-deoxyguanosine as a Model for 5′-hydrazinyl-RNA Labelling Studies

8.7.1 Synthesis

5′-Deoxy-5′-hydrazinoguanosine (215)[159]
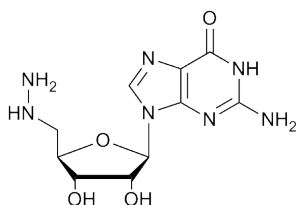
Following a literature procedure,[159] 5′-deoxy-5′-iodoguanosine (0.918 g, 2.30 mmol) was stirred in a solution of approx. 50% hydrazine hydrate (80% purity, 51% hydrazine, 9.2 ml) for 16 h at 40 °C. The solution was then divided between two centrifuge tubes and precipitated through the addition of methanol (23 ml). The solid was isolated by centrifugation (4000 rpm for 10 min), then refluxed in methanol (92 ml) until completely dissolved. The solution was allowed to cool and a precipitate formed, which was again isolated by centrifugation (4000 rpm for 10 min). The product was dried under vacuum over phosphorus pentoxide to give a yield of 205 mg (30%). δ_H (400 MHz, $(CD_3)_2SO$) 2.78-2.90 (2H, m, C5′-H_2), 3.96 (1H, app.q, J 5.2, C4′-H), 4.05 (1H, app. t, J 4.4, C3′-H), 4.47 (1H, app. t, J 5.6, C2′-H), 5.20 (3H, br s, NHNH_2), 5.64 (1H, d, J 6.0, C1′-H), 6.53 (2H, br s, C2′-OH and C3′-OH), 7.89 (1H, s, C6-H); δ_C (100.6 MHz, $(CD_3)_2SO$) 57.1, 71.7, 72.9, 82.7, 86.7, 116.9, 136.0, 151.2, 153.7, 159.5

8.7.2   Labelling Procedure

5′-Deoxy-5′-hydrazinylguanosine (15 mg, 50 μmol) was dissolved in triethy-lammonium bicarbonate (TEAB) solution (22.5 ml) and cooled in an water-ice bath. A solution of fluorescein isothiocyanate (FITC, from Sigma-Aldrich, 97 mg, 270 μmol) in dry DMF (2.5 ml) was added to the reaction vessel dropwise over the course of 10 min. The reaction mixture was stirred in the water-ice bath for 4 h before being lyophilised. The residue was then dissolved in ammonia solution (2.5 ml, 35% *w/w*), the mixture was stirred for 4 h at room temperature, diluted with water (10 ml) and lyophilised. The resulting solid residue was then purified by ion exchange chromatography on a DEAE Sepharose Fast Flow™ anion exchange resin (26 mm in diameter, 80 mm in height) with a TEAB buffer gradient rising from 0 M to 1 M over 200 min with a flow rate of 4 ml/min.

The procedure was also repeated without the presence of 5′-deoxy-5′-hy-drazinoguanosine, for comparison.

8.7.3   Analysis

The composition of the reaction mixtures were analysed by anion exchange chromatography with a DEAE-Sepharose® FastFlow resin.A gradient of 0 to 1 M TEAB buffer was applied over 200 min and the fractions corresponding to a UV response were collected and lyophilised. The residues were analysed by mass spectrometry and ^{1}H NMR spectroscopy.

Chapter 9

Bibliography

[1] R. Wolfenden, *Ann. Rev. Biochem.*, 2011, **80**, 645-667.

[2] N. Takeda, M. Shibata, N. Tajima, K. Hirao, M. Komiyama, *J. Org. Chem.*, 2000, **65**, 4391–4396.

[3] N. H. Williams, P. Wyman, *Chem. Commun.*, 2001, 1268-1269.

[4] G. K. Schroeder, C. Lad, P. Wyman, N. H. Williams, R. Wolfenden, *Proc. Nat. Acad. Sci. USA*, 2006, **103**, 4052-4055.

[5] P. Järvinen, M. Oivanen, H. Lönnberg, *J. Org. Chem.*, 1991, **56**, 5396-5401.

[6] B. Ramstedt, J. P. Slotte, *FEBS Lett.*, 30 October 2002, **531**, 33-37.

[7] L. L. Lairson, B. Henrissat, G. J. Davies, S. G. Withers, *Annu. Rev. Biochem.*, 2008, **77**, 521-555.

[8] T. Beddoe, Z. Fulton, A. McAlister, M. C. J. Wilce, R. Brammananth, L. Zaker-Tabrizi, M. A. Perugini, S. P. Bottomley, R. L. Coppel, P. K. Crellin, J. Rossjohn, *J. Biol. Chem.*, 2008, **283**, 27881-27890.

[9] C. Schaub, B. Muller, R. R. Schmidt, *Glycoconjugate J.*, 1998, **15**, 345-354.

[10] G. K. Wagner, T. Pesnot R. A. Field, *Nat. Prod. Rep.*, 2009, *26*, 1172-1194.

[11] J. R. Kouvaris, V. E. Kouloulias, L. J. Vlahos, *Oncologist*, 2007, **12**, 738-747.

[12] B. Zhang, Z. Cui, L. Sun, *Org. Lett.*, 2001, **3**, 275-278.

[13] L. Zhang, L. L. Sun, Z. Y. Cui, R. L. Gottlieb, B. L. Zhang, *Bioconj. Chem.*, 2001, **12**, 939-948.

[14] D. Williamson, M. J. Cann, D. R. W. Hodgson, *Chem. Commun.*, 2007, 5096-5098.

[15] D. Williamson, D. R. W. Hodgson, *Org. Biomol. Chem.*, 2008, **6**, 1056-1062.

[16] V. J. Davisson, D. R. Davis, V. M. Dixit, C. D. Poulter, *J. Org. Chem.*, 1987, **52**, 1794-1801.

[17] A. B. Woodside, Z. Huang, C. D. Poulter, *Org. Synth.*, 1988, **66**, 211-219

[18] E. Espinosa, C. Belmant, F. Pont, B. Luciani, R. Poupot, F. Romagné, H. Brailly, M. Bonneville, J.-J. Fournié, *J. Biol. Chem.*, 2001, **276**, 18337-18344.

[19] M. Yoshikawa, T. Kato, T. Takenishi, *Bull. Chem. Soc. Jpn.*, 1969, **42**, 3505-3508.

[20] J. Ludwig, *Acta Biochim. Biophys. Acad. Sci. Hung.*, 1981, **16**, 131-133.

[21] A. B. Burgin, N. R. Pace, *EMBO J.*, 1990, **9**, 4111-4118.

[22] A. Arabshahi, P. A. Frey, *Biochem. Biophys. Res. Commun.*, 1994, **204**, 150-155.

[23] V. Borsenberger, M. Kukwikila, S. Howorka, *Org. Biomol. Chem.*, 2009, **7**, 3826-3835.

[24] A. M. Michelson, A. R. Todd, *J. Chem. Soc.*, 1955, 2632-2638.

[25] P. J. Garegg, J. Stawinski, R. Strömberg, *J. Org. Chem.*, 1987, **52**, 284-287.

[26] P. T. Gilham, H. G. Khorana, *J. Am. Chem. Soc.*, 1958, **80**, 6212-6222.

[27] S. L. Beaucage, M. H. Caruthers, *Tetrahedron Lett.*, 1981, **22**, 1859–1862.

[28] E. Stirchak, J. Summerton, S. Weller, 1989, *Nuc. Acids Res.*, **17**, 6129-6141.

[29] J. Summerton, D. Weller, *Antisense & Nucleic Acid Drug Development*, 1997, **7**, 187-195.

[30] H. Kang, P. Chou, C. Johnson, D. Weller, S. Huang, J. Summerton, *Biopolymers*, 1992, **32**, 1351-1363.

[31] R. M. Hudziak, E. Barofsky, D. F. Barofsky, D. L. Weller, S. B. Huang, D. D Weller, *Antisense Nucleic Acid Drug Dev.*, 1996, **6**, 267-272.

[32] F. Eckstein, *Annu. Rev. Biochem.*, 1985, **54**, 367-402.

[33] N. S. Li, J. K. Frederiksen, J. A. Piccirilli, *Acc. Chem. Res.*, 2011, **44**, 1257-1269.

[34] T. A. Kunkel, F. Eckstein, A. S. Mildvan, R. M. Koplitz, L. Loeb, 1981, *Proc. Natl. Acad. Sci. USA* **78**, 6734-6738.

[35] A. M. Michelson, *J. Chem. Soc.*, 1962, 979-982.

[36] A. F. Cook, *J. Am. Chem. Soc.*, 1970, **92**, 190–195.

[37] S. Chladek, J. Nagyvary, *J. Am. Chem. Soc.*, 1972, **94**, 2079–2085.

[38] J. Wang, J. Zhou, G. P. Donaldson, S. Nakayama, L. Yan, Y. Lam, V. T. Lee, H. O. Sintim, *J. Am. Chem. Soc.*, 2011, **133**, 9320-9330.

[39] R. Cosstick, J. S. Vyle, *J. Chem. Soc., Chem. Commun.*, 1988, 992-993.

[40] R. Cosstick, J. S. Vyle, *Nuc. Acids Res.*, 1990, **18**, 829-835.

[41] R. Cosstick, J. S. Vyle, *Tetrahedron Lett.*, 1989, **30**, 4693-4696.

[42] S. Gryaznov, J.-K. Chen, *J. Am. Chem. Soc.*, 1994, **116**, 3143-3144.

[43] S. M. Gryaznov, D. H. Lloyd, J.-K. Chen, R. G. Schultz, L. A. DeDionisio, L. Ratmeyer, W. D. Wilson, *Proc. Nat. Acad. Sci. USA*, 1995, **92**, 5798-5802.

[44] J.-K. Chen, R. G. Schultz, D. H. Lloyd, S. M. Gryaznov, *Nuc. Acids Res.*, 1995, **23**, 2661-2668.

[45] M. Egli, S. M. Gryaznov, *Cell. Mol. Life Sci.*, 2000, **57**, 1440–1456.

[46] M. Ora, M. Murtola, S. Aho, M. Oivanen, *Org. Biomol. Chem.*, 2004, **2**, 593-600.

[47] M. Ora, K. Mattila, T. Lönnberg, M. Oivanen, H. Lönnberg, *J. Am. Chem. Soc.*, 2002, **124**, 14364-14372.

[48] J. S. Nelson, K. L. Fearon, M. Q. Nguyen, S. N. McCurdy, J. E. Frediani, M. F. Foy, B. L. Hirschbein, *J. Org. Chem.*, 1997, **62**, 7278–7287.

[49] M. Trmčić, D. R. W. Hodgson, *Chem. Commun.*, 2011, **47**, 6156-6158.

[50] K. Pongracz, S. Gryaznov, *Tetrahedron Lett.*, 1999, **40**, 7661-7664.

[51] J. Stawinski, M. Thelin, E. Westman, R. Zain, *J. Org. Chem.*, 1990, **55**, 3503–3506.

[52] M. J. Nemer, K. K. Ogilvie, *Tetrahedron Lett.*, 1980, **21**, 4149-4152.

[53] S. A. Noble, E. F. Fisher, M. H.Caruthers, *Nucl. Acids. Res.*, 1984, **12**, 3387-3404.

[54] N. Oka, T. Wada, *Chem. Soc. Rev.*, 2011, **40**, 5829–5843.

[55] E. M. Huie, M. R. Kirshenbaum, G. L. Trainor, *J. Org. Chem.*, 1992, **57**, 4569-4570.

[56] J. Micklefield, K. J. Fettes, *Tetrahedron*, 1998, **54**, 2129-2142.

[57] K. J. Fettes, N. Howard, D. T. Hickman, S. A. Adah, M. R. Player, P. F. Torrence, J. Micklefield, *Chem. Commun.*, 2000, 765-766.

[58] K. J. Fettes, N. Howard, D. T. Hickman, S. Adah, M. R. Player, P. F. Torrence, J. Micklefield, *J. Chem. Soc., Perkin Trans. 1*, 2002, 485-495.

59 P. Li, Z. A. Sergueeva, M. Dobrikov, B. R. Shaw, *Chem. Rev.*, 2007, **107**, 4746-4796.

60 A. J. A. Cobb, *Org. Biomol. Chem.*, 2007, **5**, 3260-3275.

61 S. Shakeel, S. Karim, A. Ali, *J. Chem. Technol. Biotechnol.*, 2006, **81**, 892-899.

62 A. P. Silverman, E. T. Kool, *Chem. Rev.*, 2006, **106**, 3775-3789.

63 Z. A. Shabarova, O. A. Fedorova, N. G. Dolinnaya, M. B. Gottikh, *Origins Life and Evolution of the Biosphere*, 1997, **27**, 555-566.

64 S. H. Wang, E. T. Kool, *Nucl. Acids Res.*, 1994, **22**, 2326-2333.

65 E. Rubin, S. Rumney, S. H. Wang, E. T. Kool, *Nucl. Acids Res.*, 1995, **23**, 3547-3553.

66 J. T. Goodwin, D. G. Lynn, *J. Am. Chem. Soc.*, 1992, **114**, 9197-9198

67 M. K. Herrlein, R. L. Letsinger, *Nucl. Acids Res.*, 1994, **22**, 5076-

68 Y. Xu, E. T. Kool, *Nucl. Acids Res.*, 1999, **27**, 875-881.

69 S. Sando, E. T. Kool, *J. Am. Chem. Soc.*, 2002, **124**, 2096-2097.

70 H. Abe, E. T. Kool, *J. Am. Chem. Soc.*, 2004, **126**, 13980-13986.

71 W. Saenger, *Principles of Nucleic Acid Structure*, Springer-Verlag, New York, 1984, 220

72 Zephyris at the English language Wikipedia licensed under the Creative Commons Attribution-Share Alike 3.0 Unported license.

73 C. Altona, M. Sundaralingam, *J. Am. Chem. Soc.*, 1972, **94**, 8205–8212.

74 C. Altona, M. Sundaralingam, *J. Am. Chem. Soc.*, 1973, **95**, 2333–2344.

75 A. P. G. Beevers, E. M. Witch, B. C. N. M. Jones, R. Cosstick, J. R. P. Arnold, J. Fisher, *Mag. Reson. Chem.*, 1999, **37**, 814-820.

76 L. J. Rinkel, C. Altona, *J. Biomol. Struct. Dynam.*, 1987, **4**, 621-649.

[77] C. Glemarec, A. Nyilas, C. Sund, J. Chattopadhyaya, *J. Biochem. Biophys. Meth.*, 1990, **21**, 311-332.

[78] E. M. Nottoli, J. B. Lambert, R L. Letsinger, *J. Am. Chem. Soc.*, 1977, **99**, 3486–3491.

[79] V.N. Rybakov, M.I. Rivkin, V.P. Kumarev, *Nuc. Acids Res.*, 1981, **9**, 189–201.

[80] S. Verma, F. Eckstein, *Ann. Rev. Biochem.*, 1998, **67**, 99-134.

[81] L. C. S. Vortler, F. Eckstein, *RNA-Ligand Interactions Pt. A*, 2000, **317**, 74-91.

[82] F. Eckstein, *Biochimie*, 2002, **84**, 841-848.

[83] S. Verma, S. Jager, O. Thum, M. Famulok, *Chem. Rec.*, 2003, **3**, 51-60.

[84] K. H. Jung, A. Marx, *Cell. Mol. Life Sci.*, 2005, **62**, 2080-2091.

[85] P. Guga, M. Koziolkiewicz, *Chem. Biodiv.*, 2011, **8**, 1642-1681.

[86] W. P. Zheng, *Curr. Med. Chem.*, 2013, **20**, 3743-3758.

[87] C. Liang, L.C. Allen, *J. Am. Chem. Soc.*, 1987, **109**, 6449–6453.

[88] K. Mizuuchi, T. J. Nobbs, S. E. Halford, K. Adzuma, J. Qin, *Biochemistry*, 1999, **38**, 4640-4648.

[89] A. K. Kennedy, D. B. Haniford, K. Mizuuchi, *Cell*, 2000, **101**, 295-305.

[90] B. Nawrot, K. Widera, M. Wojcik, B. Rebowska, G. Nowak, W. J. Stec, *Febs J.*, 2007, **274**, 1062-1072.

[91] J. L. Hougland, A. V. Kravchuk, D. Herschlag, J. A. Piccirilli, *Plos Biology*, 2005, **3**, 1536-1548.

[92] Y. G. Ren, L. A. Kirsebom, A. Virtanen, *J. Biol. Chem.*, 2004, **279**, 48702-48706.

[93] S. Shan, A. V. Kravchuk, J. A. Piccirilli, D. Herschlag, *Biochem.*, 2001, **40**, 5161-5171.

[94] A. Yoshida, S. G. Sun, J. A. Piccirilli, *Nat. Struc. Biol.*, 1999, **6**, 318-321.

[95] J. A. Piccirilli, J. S. Vyle, M. H. Caruthers, T. R. Cech, *Nature*, 1993, **361**, 85-88.

[96] R. G. Kuimelis, L. W. Mclaughlin, *J. Am. Chem. Soc.*, 1995, **117**, 11019-11020.

[97] P. M. Gordon, R. Fong, J. A. Piccirilli, *Chem. Biol.*, 2007, **14**, 607-612.

[98] J. E. Deweese, A. B. Burgin, N. Osheroff, *Nuc. Acids Res.*, 2008, **36**, 4883-4893.

[99] S. L. Elliott, J. Brazier, R. Cosstick, B. A. Connolly, *J. Mol. Biol.*, 2005, **353**, 692-703.

[100] J. Lu, N. S. Li, R. N. Sengupta, J. A. Piccirilli, *Bioorg. Med. Chem.*, 2008, **16**, 5754-5760.

[101] A. M. Popova, P. Z. Qin, *Biophys. J.*, 2010, **99**, 2180-2189.

[102] P. Z. Qin, S. E. Butcher, J. Feigon, W. L. Hubbell, *Biochem.*, 2001, **40**, 6929-6936.

[103] J. B. Thomson, B. K. Patel, V. Jimenez, K. Eckart, F. Eckstein, *J. Org. Chem.*, 1996, **61**, 6273-6281.

[104] E. J. Sontheimer, S. G. Sun, J. A. Piccirilli, *Nature*, 1997, **388**, 801-805.

[105] S. O. Shan, A. Yoshida, S. G. Sun, J. A. Piccirilli, D. Herschlag, *Proc. Nat. Acad. Sci. USA*, 1999, **96**, 12299-12304.

[106] S. A. Williams, S. E. Halford, *J. Mol. Biol.*, 2002, **318**, 387-394.

[107] T. J. Wilson, N. S. Li, J. Lu, J. K. Frederiksen, J. A. Piccirilli, D. M. J. Lilley, *Proc. Nat. Acad. Sci. USA*, 2010, **107**, 11751-11756.

[108] S. R. Das, J. A. Piccirilli, *Nat. Chem. Biol.*, 2005, **1**, 45-52.

[109] A. V. Korennykh, M. J. Plantinga, C. C. Correll, J. A. Piccirilli, *Biochem.*, 2007, **46**, 12744-12756.

[110] H. Suga, J. A. Cowan, J. W. Szostak, *Biochemistry*, 1998, **37**, 10118-10125.

[111] Nucleic Acids in Chemistry, Biology, 2 edn., Oxford University Press, New York, 1996.

[112] C. Schotten, *Berichte der deutschen chemischen Gesellschaft*, 1884, **17**, 2544-2547.

[113] E. Baumann, *Berichte der deutschen chemischen Gesellschaft*, 1886, **19**, 3218-3222.

[114] R. F. Hudson, G. Moss, *J. Chem. Soc.*, 1962, 3599-3604.

[115] M. Trmčić, F. L. Chadbourne, P. M. Brear, P. W. Denny, S. L. Cobb, D. R. W. Hodgson, *Org. Biomol. Chem.*, 2013, **11**, 2660-2675.

[116] M. Trmčić, PhD Thesis, University of Durham, 2009.

[117] G. M. Blackburn, M. J. Gait, *Nucleic Acids in Chemistry and Biology*, 2nd ed., OUP, 1996, ch. 2, pp. 18.

[118] R. J. Delley, A. C. Donoghue, D. R. W. Hodgson, *J. Org. Chem.*, 2012, **77**, 5829-5831.

[119] H. K. Hall, *J. Am. Chem. Soc.*, 1957, **79**, 5441-5444.

[120] D. K. Dean, *Synthetic Commun.*, 2002, **32**, 1517-1521.

[121] Y. Segall, *J. Agric. Food. Chem.*, 2011, **59**, 2845-2856.

[122] P. S. Traylor, F. H. Westheimer, *J. Am. Chem. Soc.*, 1965, **87**, 553–559.

[123] E. W. Crunden, R. F. Hudson, *J. Chem. Soc.*, 1962, 3591-3599.

[124] M. Kolb, C. Danzin, J. Barth, N. Claverie, *J. Med. Chem.*, 1982, **25**, 550-556.

[125] P. Cano-Soldado, M. Molina-Arcas, B. Alguero, I. Larrayoz, M. P. Lostao, A. Grandas, F. J. Casado, M. Pastor-Anglada, *Biochem. Pharmacol.*, 2008, **75**, 639-648.

[126] G. V. M. Sharma, S. Chandrasekhar, *Synth. Commun.*, 1989, **19**, 3289-3293

[127] T. V. Goud, A.-M. Aubertin, J.-F. Biellmann, *Nucleosides, Nucleotides and Nucleic Acids*, 2008, **27**, 495-505.

[128] M. Saneyoshi, T. Fujii, T. Kawaguchi, K. Sawai, S. Kimura, *Nucleic Acid Chem.*, 1991, **4**, 67-72.

[129] T. P. Dang, A. J. Sobczak, A. M. Mebel, C. Chatgilialoglu, S. F. Wnuk, *Tetrahedron*, 2012, **68**, 5655-5667.

[130] A. Postigo, S. Kopsov, C. Ferreri, C. Chatgilialoglu, *Org. Lett.*, 2007, **9**, 5159-5162.

[131] K. A. Winans, C. R. Bertozzi, *Chem. Biol.*, 2002, **9**, 113-129.

[132] I. Yamamoto, M. Sekine, T. Hata, *J. Chem. Soc., Perk. Trans. 1*, 1980, 306-310.

[133] J. Park, S. Bhuniya, H. Lee, Y.-W. Noh, Y. T. Lim, J. H. Jung, K. S. Hong, J. S. Kim, *Chem. Commun.*, 2012, **48**, 3218-3220

[134] D. M. Williams, V. H. Harris, *Practical Approach in Chemistry: Organophosphorus Reagents*, 1st ed., OUP, 2004, ch. 9, pp. 259.

[135] J. D. Chanley, E. Feageson, *J. Am. Chem. Soc.*, 1958, **80**, 2686–2691.

[136] M. E. Harris, Q. Dai, H. Gu, D. L. Kellerman, J. A. Piccirilli, V. E. Anderson, *J. Am. Chem. Soc.*, 2010, **132** 11613-11621.

[137] Determination of pH: Theory and Practice, Roger Gordon Bates, Wiley, 1964

[138] A. V. Bandura, S. N. Lvov, *J. Phys. Chem. Ref. Data*, 2006, **35**, 15-30.

[139] N. E. Good, G. D. Winget, W. Winter, T. N. Connolly, S. Izawa, R. M. M. Singh, *Biochemistry*, 1966, **5**, 467-477.

[140] S. J. Benkovic, E. J. Sampson, *J. Am. Chem. Soc.*, 1971, **93**, 4009-4016.

[141] D. C. Dittmer, O. B. Ramsay, *J. Org. Chem.*, 1963, **28**, 1268-1272.

[142] *Ionization Constants of Inorganic Acids and Bases in Aqueous Solution. IUPAC Chemical Data Series*, No. 29, ed. D. D. Perrin, 2nd edn., Pergamon, Oxford, 1982.

[143] J. March, *Advanced Organic Chemistry*, John Wiley & Sons, New York, 1992.

[144] M. S. Gibson, R. W. Bradshaw, *Angew. Chem. Int. Edit.*, 1968, **7**, 919-930.

[145] H. Staudinger, J. Meyer, *Helv. Chim. Acta*, 1919, **2**, 635-646.

[146] E. J. Corey, J. O. Link, *J. Am. Chem. Soc.*, 1992, **114**, 1906-1908.

[147] V. Rawat, P. V. Chouthaiwale, V. B. Chavan, G. Suryavanshi, A. Sudalai, *Tetrahedron Lett.*, 2010, **51**, 6565-6567.

[148] S. Kulstad, L. A. Malmsten, *Acta Chem. Scand. B*, 1979, **33**, 469-474.

[149] W. Q. Tian, Y. A. Wang, *J. Org. Chem.*, 2004, **69**, 4299-4308.

[150] R. Jones, L. Godorhazy, D. Szalay, J. Gerencser, G. Dorman, L. Urge, F. Darvas, *Qsar Comb. Sci.*, 2005, **24**, 722-727.

[151] E. F. V. Scriven, K. Turnbull, *Chem. Rev.*, 1988, **88**, 297-368.

[152] A. K. Bose, M. S. Manhas, J. E. Vincent, K. Gala, I. F. Fernandez, *J. Org. Chem.*, 1982, **47**, 4075-4081.

[153] S. K. Yasuda, J. L. Lambert, *J. Am. Chem. Soc.*, 1954, **76**, 5356-5356.

[154] G. Acquaah-Harrison, S. Zhou, J. V. Hines, S. C. Bergmeier, *J. Comb. Chem.*, 2010, **12**, 491-496.

[155] R. Kumar, P. R. Maulik, A. K. Misra, *Glycoconjugate J.*, 2008, **25**, 595-602.

[156] H. Yuan, R. B. Silverman, *Bioorgan. Med. Chem.*, 2006, **14**, 1331-1338.

[157] J. L. Norcliffe, L. P. Conway, D. R. W. Hodgson, *Tetrahedron Lett.*, 2011, **52**, 2730-2732.

[158] I. C. M. Kwan, R. J. Delley, D. R. W. Hodgson, G. Wu, *Chem. Commun.*, 2011, **47**, 3882-3884.

[159] P. Brear, G. R. Freeman, M. C. Shankey, M. Trmčić, D. R. W. Hodgson, *Chem. Commun.*, 2009, 4980–4981.

[160] E. Paredes, M. Evans, S. R. Das, *Methods*, 2011, **54**, 251–259.

[161] S Li, D. Ma, L. Yi, S. Mei, D. Ouyanga, Z. Xia, *Bioorg. Med. Chem. Lett.*, 2013, **23**, 6304–6306.

[162] D. Proudnikov, A. Mirzabekov, *Nucl. Acids Res.*, 1996, **24**, 4535-4542.

[163] A. Martvon, J. Sura, *Chemicke Zvesti*, 1973, **27**, 811-815.

[164] *Handbuch der Präparativen Anorganischen Chemie*, 3 edn., Ferdinand Enke Verlag, Stuttgart, 1975.

[165] K. A. Watanabe, J. J. Fox, *Angew. Chem. Int. Edit.*, 1966, **5**, 579-580.

[166] P. S. Ludwig, R. A. Schwendener, H. Schott, *Synthesis*, 2002, 2387-2392.

[167] P. Kovacic, P. D. Roskos, *Tetrahedron Lett.*, 1968, **9**, 5833–5835.

[168] L. H. Amundsen, L. S. Nelson, *J. Am. Chem. Soc.*, 1951, **73**, 242-244.

[169] R. F. Nystrom, F. Robert, W. G. Brown, *J. Am. Chem. Soc.*, 1948, **70**, 3738-3740.

[170] G. P. Boldrini, G. Cainelli, A. Umani-Ronchi, *J. Organometallic Chem.*, 1983, **243**, 195-198.

[171] G. Talbot, R. Gaudry, L. Berlinguet *Can. J. Chem.*, 1958, **36**, 593-596.